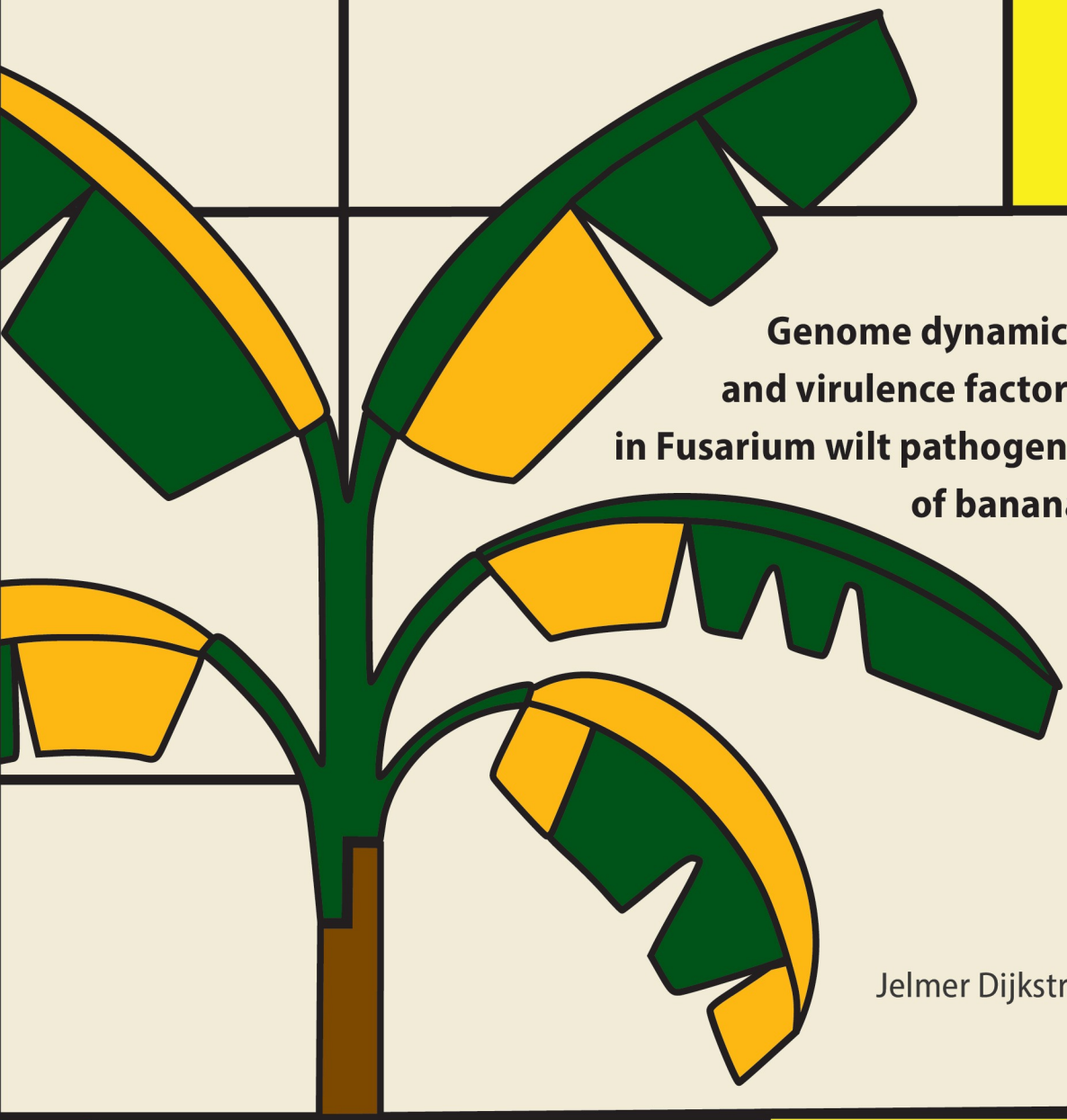
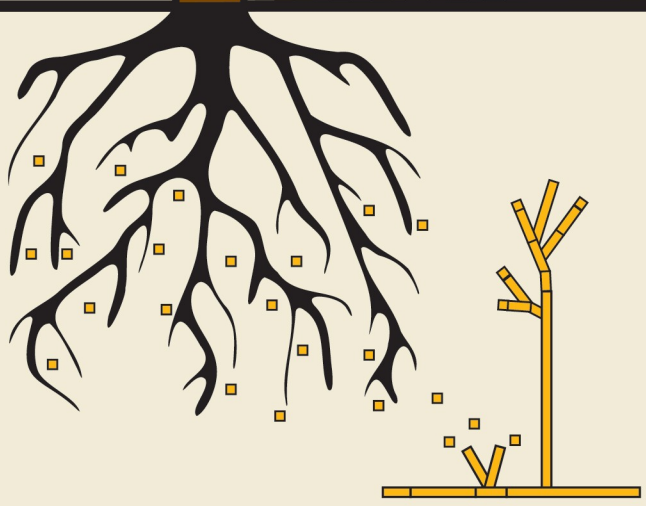
Genome dynamics and virulence factors in Fusarium wilt pathogens of banana

Jelmer Dijkstra





Propositions

1. Genome compartmentalization in fungal plant pathogens greatly enhances effector research.
   (this thesis)

2. Transposable elements are major drivers for genetic variation in a clonally reproducing fungus.
   (this thesis)

3. Without open access publication no knowledge was generated.

4. Phage therapy will be crucial in combating antibiotic resistant bacteria.

5. The Western outlook on GMO crops is based on a position of luxury.

6. Publication fees are an inappropriate expenditure of public funds.

Propositions belonging to the thesis, entitled
Genome dynamics and virulence factors
in Fusarium wilt pathogens of banana

Jelmer Dijkstra
Wageningen, 8 July 2025

Genome dynamics and virulence factors in Fusarium wilt pathogens of banana

Jelmer Dijkstra

Thesis committee

Promotor
Prof. Dr G. H. J. Kema
Professor of Phytopathology
Wageningen University & Research

Co-promotors
Dr C. Aguilera-Galvez
Postdoctoral researcher, Área Sistemas Naturales y Sostenibilidad
Escuela de Ciencias Aplicadas e Ingeniería
Universidad EAFIT, Medellín, Colombia

Dr H. C. van der Does
Lecturer, Laboratory of Phytopathology
Wageningen University & Research

Other members
Prof. Dr D. K. Aanen, Wageningen University & Research
Prof. Dr M. Rep, University of Amsterdam
Dr T. A. J. van der Lee, Wageningen University & Research
Prof. Dr E. H. Stukenbrock, Christian-Albrechts University of Kiel, Germany

This research was conducted under the auspices of the Graduate School Experimental Plant Sciences.

Genome dynamics and virulence factors in Fusarium wilt pathogens of banana

Jelmer Dijkstra

Thesis

submitted in fulfilment of the requirements for the degree of doctor
at Wageningen University
by the authority of the Rector Magnificus,
Prof. Dr C. Kroeze,
in the presence of the
Thesis Committee appointed by the Academic Board
to be defended in public
on Tuesday 8 July 2025
at 10:30 a.m. in the Omnia Auditorium.

Jelmer Dijkstra

Genome dynamics and virulence factors in Fusarium wilt pathogens of banana, 158 pages.

PhD thesis, Wageningen University, Wageningen, the Netherlands (2025)
With references, with summary in English

DOI: https://doi.org/10.18174/681345

Table of contents

Chapter 1	General introduction	**7**
Chapter 2	Effector identification in Tropical Race 4, the Fusarium wilt pathogen of banana	**27**
Chapter 3	Extensive intrachromosomal duplications in a virulence-associated fungal accessory chromosome	**53**
Chapter 4	Helitron activity in a plant pathogenic fungus caused large-scale deletions affecting secondary metabolism without attenuating pathogenicity	**83**
Chapter 5	General discussion	**111**

References **129**

Summary **151**

Acknowledgements **153**

About the author **155**

List of publications **156**

Chapter 1

General introduction

Introduction

Agriculture is a relatively young practice on an evolutionary scale (Balter, 2007), albeit with profound subsequent effects on food production (Godfray *et al.*, 2010; Rajaram, 2011; Pingali, 2012), the global population rise (Godfray *et al.*, 2010; Pingali, 2012) and the environment (Yang *et al.*, 2024). Agricultural production is confronted by a multitude of steep challenges, especially in the face of global population increases (Godfray *et al.*, 2010; Yang *et al.*, 2024).

One of the challenges that has likely plagued agriculture since its origin are the losses due to pests and diseases (Stewart & Robertson, 1968; van Zeist & Palfenier-Vegter, 1981; Kislev, 1982; Dark & Gent, 2002; Iriti & Faoro, 2008; Zadoks, 2008). Although exact numbers are often lacking, and effects are heavily crop and location dependent, estimates of crop losses due to pests and diseases typically range around 25%, which can occur both before and after harvest, with considerably higher and lower yield losses (Flood, 2010; Savary *et al.*, 2019). Moreover, crop losses due to pathogens and pests tend to be higher in regions that have lower food security (Savary *et al.*, 2019). Despite already significant crop losses, climate change (Fisher *et al.*, 2012; Chaloner *et al.*, 2021; Yang *et al.*, 2024), as well as a demand for reduced pesticide use (Schebesta *et al.*, 2020) are likely to exacerbate the effects of pests and diseases. The emergence and spread of many devastating plant pathogens are facilitated by anthropogenic factors, especially the vast monocultures of high yielding but often susceptible crop cultivars. Such monocultures pose a strong selection pressure on the pathogen (Marshall *et al.*, 2009; Sommerhalder *et al.*, 2011; Zhan *et al.*, 2015), and subsequently provide a very fertile ecosystem for emergence and spread of highly aggressive plant pathogens (Stukenbrock & McDonald, 2008; Fones *et al.*, 2020). Similarly, overreliance on fungicides has instead led to the quick buildup of fungicide insensitive populations in several plant pathogens (McDonald *et al.*, 2019; Chong *et al.*, 2021).

Banana: a crop of major importance

Banana is a major crop, at times considered the 4th most important (Pillay & Tripathi, 2007), and the number one produced fruit in the world (FAO, 2020). The vast majority of edible banana cultivars comprise diploid or triploid hybrids consisting of variations of *Musa acuminata* (A-genome) or hybridizations between *M. acuminata* and *M. balbisiana* (B-genome) (Perrier *et al.*, 2011). The history of banana diversification and domestication is very complex, but fossil evidence suggests that banana cultivation occurred as early as 6,500 years ago in the highlands of New Guinea (Perrier *et al.*, 2011). In line with this, the wild diploid ancestors of almost all modern banana cultivars

originate from Southeast Asia (De Langhe *et al.*, 2009; Rouard *et al.*, 2018). Subsequent spread and further diversification have seen the rise of several areas of high banana cultivar variation, including some outside the center of origin in Southeast Asia, such as the East African Highland bananas (De Langhe *et al.*, 2009).

Although there is a certain degree of genetic variation in cultivated bananas, and a large degree of genetic variation in wild diploid subspecies, banana cultivation is dominated by very few cultivars with a genetically narrow basis (Ploetz *et al.*, 2015). More than 40% of the worldwide banana production comprises a single cultivar called Cavendish, mostly produced in large monocultures, and another 20% consists of genetically closely related cultivars (Drenth & Kema, 2021). The export trade of banana is dominated by Cavendish, accounting for roughly 95% of all exported bananas (García-Bastidas *et al.*, 2022), but this represents only 15% of the global production (Drenth & Kema, 2021). The other 85% of the global banana production ends up at local markets, most of which is derived from smallholder farms (Ordóñez *et al.*, 2015). The majority production by smallholders for local markets means banana is important for the livelihoods of millions (>400) of people in the tropics and sub-tropics (Drenth & Kema, 2021) (Fig. 1), especially in the Great Lakes region of Africa, the area with the highest per capita consumption of bananas (Karamura, 1998; Karangwa *et al.*, 2016). This region is dominated by banana cultivars that serve to produce the local staple of East African Highland bananas (AAA-EAHB) that are generally used as cooking bananas (Karamura, 1998) (Fig. 1), in contrast to the export-oriented dessert bananas. Countries in this region could become net importers of food in the absence of banana production (Kubiriba *et al.*, 2016). In contrast to the large Cavendish monocultures, banana production in this region is often based on different intercropping systems (Karangwa *et al.*, 2016). Besides direct fruit consumption, this region also produces bananas for use in beer production and fiber-based products (Karamura, 1998).

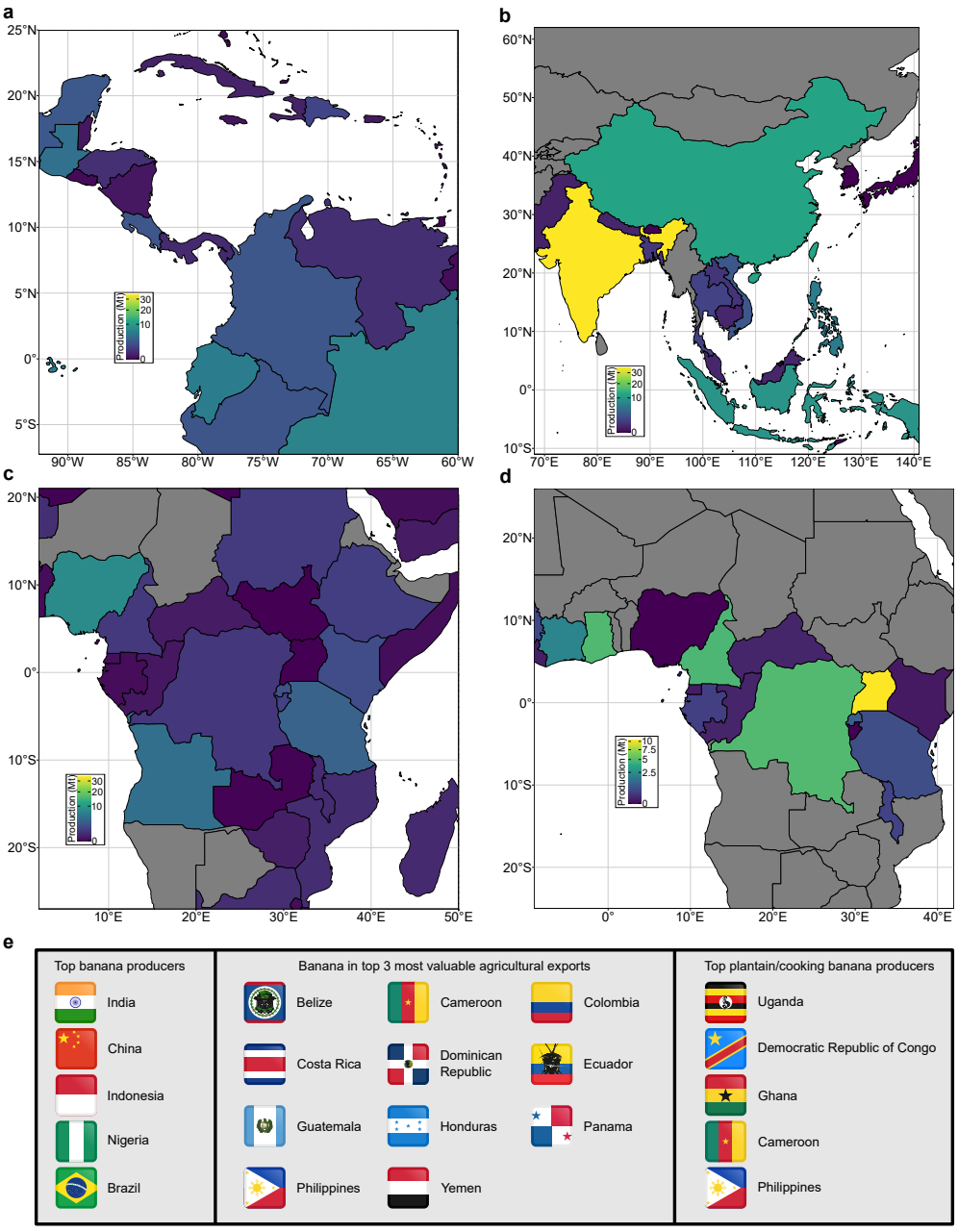


FIGURE 1 | Regional importance of banana production and export. a) Production of banana in million tons (Mt) for the major production areas of Latin America. **b**) Production of banana in Mt for the major production areas of East Asia. **c**) Production of banana in Mt for the major production areas of Central and Eastern Africa. **d**) Production of plantain/cooking banana in Mt for the major production areas of Central and Eastern Africa. Plantain refers to cooking bananas of AAB genome composition. **e**) Table displaying top five producing countries of banana (left), plantain/cooking banana (right), and countries with banana among the top three most valuable agricultural export products (middle). All data obtained from FAOSTAT for the year 2023.

Banana: a troubled history

A background on the broader importance and impact of banana cultivation, beyond its role in the West as the most popular fruit, is not complete without at least briefly addressing the troubled recent history of intense large-scale banana production. This problematic history is most apparent throughout events in 20th century Latin America, still the contemporary dominant region of global banana export. The ramping export of bananas from Latin America, especially from the Central American countries Costa Rica, Guatemala, Honduras and Nicaragua was essentially an entirely foreign endeavor starting in the late 19th century (Langley & Schoonover, 1995). This trade was quickly controlled by three major companies: United Fruit Company (UFCO), Vaccaro Brothers Company, and Cuyamel Fruit Company operating from ports in the United States such as Mobile and New Orleans (Fig. 2). Later, in 1929 UFCO and Cuyamel Fruit Company would merge, further consolidating the domineering role of UFCO (Langley & Schoonover, 1995). This merged company exists to this day as Chiquita Brands International, while the Vaccaro Brothers Company, in part, continued as Dole Food Company and is now known as Dole plc.



FIGURE 2 | Historical photos unloading of banana steamers. a) Photo of the unloading of a banana steamer in Mobile circa 1906. Library of Congress code: LC-DIG-det-4a31461. **b**) Photo of the unloading of a banana steamer in New Orleans taken between 1900 and 1910. Library of Congress code: LC-DIG-det-4a22772.

The rise and dominance of the banana companies was based on an all-encompassing control of land, transport, communication, finances and politics. This was achieved through extremely favorable land subsidies, private railroad construction projects, radio towers, ports and banks (Langley & Schoonover, 1995; Merril, 1995). As such, several of the northern ports of the Central American countries essentially operated as enclaves of company towns for the banana companies (Langley & Schoonover, 1995; Merril, 1995; Langley, 2002). This level of control led to the banana companies

holding a lot of political sway in the Central American isthmus. For example, taxes from UFCO amounted to 50% of government revenue in Honduras and Costa Rica in the 1930s (Langley & Schoonover, 1995). Moreover, the banana companies increased their political power using bribes and loans for desperate governments which led to the frequent perception that company managers were more powerful than elected officials (Langley & Schoonover, 1995; Merril, 1995; Langley, 2002). In the most extreme cases the banana companies were even involved in direct regime change such as the Honduran Coup of 1910-1911 and the Guatemalan Coup of 1954 (Langley & Schoonover, 1995; Merril, 1995). The troubled history of the banana companies, most prominently UFCO, is passionately displayed in a poem by Nobel laureate Pablo Neruda (Neruda, 1966).

The history of intense large scale banana production and export is further intertwined with the role of two major plant pathogenic fungi. Soon after the rapid expansion of intense banana cultivation in the 1890s, plantations started to suffer from a severe plant disease. First, this occurred in plantations in Panama and Costa Rica, as such the epidemic was referred to as 'Panama Disease', nowadays commonly called 'Fusarium wilt' of banana (FWB), caused by the soilborne pathogen *Fusarium oxysporum* f. sp. *cubense* (Marquardt, 2001; Drenth & Kema, 2021). The vast Central American monoculture plantations of the genetically uniform and export-friendly banana cultivar Gros Michel proved to be a fertile environment for the rapid spread of FWB (Marquardt, 2001; Drenth & Kema, 2021). At first, declining production and abandonment of plantations were supplemented by a steady pace of newly exploited plantations (Marquardt, 2001; Marquardt, 2002; Drenth & Kema, 2021). However, this was an altogether unsustainable solution, and the spread of FWB caused the average effective lifespan of banana plantations to go from between fifteen and twenty years to less than five (Marquardt, 2001). Scattered efforts to combat the pathogen through chemical measures, soil amendments, flood-fallowing, adapted agricultural practices, and selective breeding proved futile in stopping the spread of FWB, which was causing the abandonment of huge swathes of land (Marquardt, 2001; Drenth & Kema, 2021). In the end, the only viable solution was found in the use of the less desired Cavendish cultivars that proved to be resistant to the ongoing FWB epidemic (Marquardt, 2001; Drenth & Kema, 2021). Importantly, Cavendish was not a product from intentional resistance breeding, but, rather simply, a clone originally obtained from southern China by British colonial botanists (Drenth & Kema, 2021). Cavendish was, compared to Gros Michel, considered to be less tasteful and not suitable for export due to its easy bruising. Therefore, it was only after successful trials in disease resistance and the development of a boxing procedure to prevent bruising during transport by the much smaller company Standard Fruit (formerly Vaccaro Brothers Company) that Cavendish cultivars quickly became the new all dominant banana

crops from the 1960s onwards (Marquardt, 2001; Drenth & Kema, 2021).

The impact of FWB is also noted in Anton de Kom's historical account of slavery in the former Dutch colony Suriname. Banana was seen as a potentially profitable alternative to cacao cultivation, which had rapidly declined from 1895 onwards because of the fungus *Moniliophtora perniciosa,* the causal agent of Witches broom disease of cacao (Kom, 1971). In turn, banana cultivation was started based on a governmental initiative in 1905, but this quickly turned into a disaster in part due to the quick invasion of FWB. As a consequence, the initiative was already liquidated again by 1911 (Kom, 1971).

During the period in which the banana companies were still heavily struggling in their battle with FWB, another fungal plant pathogen was about to spread from its South Pacific confinement. In 1934 'Sigatoka leaf spot disease', caused by *Pseudocercospora musae* (formerly known as *Mycosphaerella musicola*), causing the disease generally referred to as 'yellow Sigatoka', was first discovered in Trinidad (Marquardt, 2002). Within three years yellow Sigatoka had spread around the entire Central American isthmus and was considered an equal or even greater threat than FWB (Marquardt, 2002). In contrast to the soilborne nature of FWB, it was quickly discovered that the foliar pathogen *P. musae* could be controlled using the commonly used fungicide copper sulfate (Marquardt, 2002). Subsequently, banana plantations were hand sprayed on an immense scale from 1938 to 1962, using 'Bordeaux mixture', a mixture of copper sulfate, water and lime to control the pathogen (Marquardt, 2001; Marquardt, 2002). The hand spraying was so pervasive that banana plantation workers applying the fungicide were often called 'parakeets' for the blue-green stain left on their clothes and skin (Marquardt, 2001; Marquardt, 2002). The yellow Sigatoka control program took on an unprecedented scale applying fifty to seventy thousand liters of Bordeaux mixture per hectare annually in twenty to thirty applications. A full quarter of the UFCO farm labor force was involved in the control of yellow Sigatoka (Marquardt, 2002). Only following several labor struggles and due to the development of alternative refined petroleum oils (later combined with different fungicide cocktails) that could be applied by planes or helicopters, the use of hand-sprayed Bordeaux mixture was finally abandoned, albeit leaving thousands of hand sprayers with significant respiratory health problems (Marquardt, 2001; Marquardt, 2002).

History repeats itself

With the use of the FWB resistant Cavendish cultivar and the spraying of fungicide mixtures the two existential threats to banana production were seemingly solved from the 1960s onwards. Nevertheless, for both fungal threats, especially FWB, history was to repeat itself. Cavendish plants with FWB symptoms were first detected in Taiwan in

1967 (Su *et al.*, 1986). The disease in Cavendish quickly spread further in Southeast Asia and the causal agent was soon designated as *Fusarium oxysporum* f. sp. *cubense* Tropical Race 4 (TR4), contrasting the epidemic on Gros Michel caused by Race 1 strains (Ploetz, R. C., 2015; Drenth & Kema, 2021). Since its initial discovery in 1967, TR4 has since spread to all major banana-producing continents, driven by the vast susceptible Cavendish monocultures, as Race 1 strains once did for Gros Michel (Ordóñez *et al.*, 2015; Drenth & Kema, 2021; van Westerhoven *et al.*, 2022). With the presence of TR4 in Colombia, Peru, and most recently Venezuela (van Westerhoven *et al.*, 2022; Mejías Herrera *et al.*, 2023), FWB is once again threatening the major banana export countries. Moreover, its presence in Mozambique is threatening the food security of the Great Lakes region of Africa (van Westerhoven *et al.*, 2022; van Westerhoven *et al.*, 2023). Similarly, a new and more virulent sister species of *P. musae*, *Pseudocercospora fijiensis* causal agent of black leaf streak disease, more commonly referred to as black Sigatoka, has spread globally since the 1970s often displacing *P. musae* (Drenth & Kema, 2021). In contrast to TR4, for which there are still no reliable control perspectives besides the development of novel resistant germplasm (Ploetz, Randy C., 2015), black Sigatoka can, at a great financial and environmental cost, still be managed through extensive fungicide use (Chong *et al.*, 2021; Drenth & Kema, 2021). Regions with the heaviest fungicide use are, however, confronted with significant reductions in sensitivity in *P. fijiensis* populations due to the enormous selection pressure exerted by the frequency of fungicide applications (Chong *et al.*, 2021). Clearly, the increasing reliance on fungicides is unsustainable and only too reminiscent of the environmental and health problems caused previously by Bordeaux mixture and DBCP (Marquardt, 2001; Marquardt, 2002).

With the vast susceptible Cavendish monocultures and the rapid spread of these two devastating fungal pathogens, it seems that the Cavendish era is over, mimicking the earlier period of Gros Michel dominance (Drenth & Kema, 2021). Despite the importance of banana as a cash crop, source of nutrition, and the dire need for new resistant germplasm, modern public genomic resources are severely lacking. High-quality chromosome level assemblies of the dominant Cavendish cultivar have only been generated recently (Huang, HR *et al.*, 2023; Li, X *et al.*, 2024). As such, insights into the genetic basis of FWB resistance are still rather limited (Dale *et al.*, 2017; Ahmad *et al.*, 2020; Li, X *et al.*, 2024). High quality genomic information of some other cultivars and wild (sub)species is available (D'Hont *et al.*, 2012; Wu *et al.*, 2016; Wang *et al.*, 2019; Belser *et al.*, 2021; Wang, ZF *et al.*, 2022; Martin *et al.*, 2025), but more will be required to sufficiently benefit breeding efforts for sustainable banana production. Some temporary respite might be found in the use of genetically modified resistant Cavendish plants (Dale *et al.*, 2017). However, in the end, a future with sustainable banana production and FWB control will require fundamental changes and not the search for a new 'silver bullet' cultivar, lest history be repeated once more.

The *Fusarium oxysporum* species complex

The *Fusarium oxysporum* species complex (FOSC) is a broad group of soilborne pathogens, part of the much larger *Fusarium* genus, most commonly divided into different *formae speciales* of polyphyletic origin depending on the host plant of a given strain (Michielse & Rep, 2009). More than 100 different *formae speciales* have been described for many important crops such as banana, tomato, oil palm, and cotton (Michielse & Rep, 2009; Dean *et al.*, 2012; Gordon, 2017). Next to infecting a large number of important crops, *F. oxysporum* is also an important opportunistic pathogen in humans (Zhang *et al.*, 2020; WHO, 2022). Although the FOSC as a whole has a large host range, a single strain can generally only infect one or in some cases a few related host species (Troisi *et al.*, 2010; Dean *et al.*, 2012; Li *et al.*, 2020b; Ayukawa *et al.*, 2021).

Besides the distinction in *formae speciales,* the FOSC is often subdivided into three recognized clades with strong genomic support (O'Donnell *et al.*, 1998; Brankovics *et al.*, 2017; van Westerhoven *et al.*, 2024b). Although there is a strong consensus on a species complex level grouping for the FOSC, the delineation of specific species level lineages within the species complex is a matter of strong debate, in contrast to other species complexes within the *Fusarium* genus (Aoki *et al.*, 2014; Maryani *et al.*, 2019; Geiser *et al.*, 2021; Torres Bedoya *et al.*, 2021; O'Donnell *et al.*, 2022). For example, *F. foetens*, *F. udum*, and *F. redolens* have all, at varying timepoints, been included or excluded from the FOSC (Aoki *et al.*, 2014; Geiser *et al.*, 2021). As mentioned earlier, the causal agent of FWB has been described as *Fusarium oxysporum* f. sp. *cubense*. Alternatively, some banana infecting lineages within the FOSC have been reclassified as species, with strains from the lineage encompassing TR4 being referred to as *F. odoratissimum* (Maryani et al., 2019).

Members of the FOSC are generally described as asexual fungi (Michielse & Rep, 2009) complicating species delineation. Despite the general description as an asexual fungus, some evidence suggests there might also be sexual recombination (Laurence *et al.*, 2014; McTaggart *et al.*, 2021; Fayyaz *et al.*, 2023). Whether or not these signs of recombination are signs of ongoing (para)sexual recombination, or signs of historic (para)sexual recombination is still up for debate, especially without direct observation of sexual reproduction (McTaggart *et al.*, 2021; Fayyaz *et al.*, 2023; Fokkens & Rep, 2023). Sampling biases seem to play a major role in resolving this longstanding question (Fokkens & Rep, 2023) where important pathogenic lineages still seem to evolve mostly clonally (McTaggart *et al.*, 2021; van Westerhoven *et al.*, 2024a). Moreover, niche adaptation due to the monocultural nature of modern agriculture and accumulation of mutations for female sterility in clonal lineages might have caused frequent loss of sexual reproduction capabilities (Gordon, 2017; Fokkens &

Rep, 2023). The lines of evidence for sexual reproduction in the absence of direct field or laboratory observation, are often referred to as 'cryptic sexuality' and many presumed asexual fungi were later proven to be capable of sexual reproduction after all (Dyer & Kück, 2017). Individual FOSC strains contain either one of two mating-type idiomorphs and as such would function as a heterothallic fungus in the case of sexual reproduction (Arie *et al.*, 2000; Fayyaz *et al.*, 2023). Despite their presence in strains belonging to the FOSC, the mating-type genes might serve other functions besides sexual reproduction as was observed in *Verticillium dahliae* (Zhang, YD *et al.*, 2024) another (presumably) asexual plant pathogen.

Reproduction and spread of FOSC members occur through the production of three different types of asexual spores: macroconidia, microconidia and chlamydospores (Ma *et al.*, 2013; Gordon, 2017). Although all play a role in the infection cycle of *F. oxysporum*, chlamydospores are generally considered to be more persistent and tolerant of harsh conditions (Ohara *et al.*, 2004; Gordon, 2017). Subsequent spore germination takes place in a density dependent manner and can be further affected by the effects of root exudates from host and non-host plants (Gordon, 2017; Vitale *et al.*, 2019). The process of root infection following spore germination has been investigated for multiple hosts in several studies (Lagopodi *et al.*, 2002; Czymmek *et al.*, 2007; Zhang *et al.*, 2015; Li *et al.*, 2017; Warman & Aitken, 2018; Dong *et al.*, 2019; Martínez-Soto *et al.*, 2023). Although some differences are observed depending on the used host plant, substrate and *Fusarium* strain, there are some general characteristics (Michielse & Rep, 2009). Spores initially adhere to the hosts root and progressively form a hyphal network (Lagopodi *et al.*, 2002; Olivain *et al.*, 2006; Zhang *et al.*, 2015; Li *et al.*, 2017). Subsequently, the epidermal cell layer is penetrated to allow for further colonization of the host (Lagopodi *et al.*, 2002; Zhang *et al.*, 2015; Li *et al.*, 2017; Martínez-Soto *et al.*, 2023). Conflicting observations have been made on preferential infection sites, but entry occurs both through direct penetration of epidermal cells as well as through intercellular growth at epidermal cell junctions (Lagopodi *et al.*, 2002; Gordon, 2017; Li *et al.*, 2017; Martínez-Soto *et al.*, 2023). The entry into the host plant is also facilitated by naturally occurring wounds (Li *et al.*, 2017). Although *F. oxysporum* does not make any clear infection structure such as an appressorium during infection, some forms of hyphal swelling are often observed at the infection site (Czymmek *et al.*, 2007; Li *et al.*, 2011; Fang *et al.*, 2012; Gordon, 2017; Martínez-Soto *et al.*, 2023). After penetration of the epidermal cell layer, the fungus further colonizes the root cortex moving towards the vasculature (Zhang *et al.*, 2015; Dong *et al.*, 2019; Martínez-Soto *et al.*, 2023). From there, the fungus will progressively infect the rest of a susceptible plant by colonizing and proliferating within the xylem vessels (Lagopodi *et al.*, 2002; Czymmek *et al.*, 2007; Zhang *et al.*, 2015; Dong *et al.*, 2019; Martínez-Soto *et al.*, 2023). Occlusion of the xylem vessels will cause the classic wilting symptoms caused by

pathogenic FOSC members (Gordon, 2017). Interestingly, resistant host plants are also colonized by avirulent strains, but the extent of colonization is different since avirulent strains show only limited colonization of the vascular system (Li *et al.*, 2017; van der Does *et al.*, 2018; Dong *et al.*, 2019). Following on plant colonization, several factors play a role in the further spread of FWB in agricultural systems. The local spread of FWB mainly occurs through short-medium distance movement of spores from wilted plant material, infested soil or water runoff (Summerell *et al.*, 2010; Dita *et al.*, 2018). Especially for long-distance movement, such as the transcontinental spread of TR4, anthropogenic factors play a major role in the dispersal of the pathogen. The use of infected plant material, the spread of infested soil, or the use of contaminated agricultural equipment can all contribute to local and long-distance movement of the pathogen (Summerell *et al.*, 2010; Dita *et al.*, 2018).

Due to their general importance, more than 800 strains belonging to the FOSC, both pathogenic and non-pathogenic, have been sequenced allowing for large scale genomic studies (Ma *et al.*, 2010; van Dam *et al.*, 2016; Zhang *et al.*, 2020; Fayyaz *et al.*, 2023; van Westerhoven *et al.*, 2024a; van Westerhoven *et al.*, 2024b). Specifically, the large number of sequenced strains provided important insights into both genome structure and virulence factors (Ma *et al.*, 2010; Ma *et al.*, 2013; van Dam *et al.*, 2017; Li *et al.*, 2020b; Ayukawa *et al.*, 2021; Redkar *et al.*, 2022; van Westerhoven *et al.*, 2024a). Albeit significant genome variation had previously been observed by electrophoretic karyotyping (Boehm, 1994), the first full genome sequence of an FOSC strain led to the discovery of the characteristically compartmentalized genome of FOSC members (Ma *et al.*, 2010; Ma, 2014).

Genome compartmentalization and accessory chromosomes

Compartmentalized genomes are a characteristic of many filamentous pathogens (Croll & McDonald, 2012; Dong *et al.*, 2015; Bertazzoni *et al.*, 2018; Sánchez-Vallet *et al.*, 2018; Torres *et al.*, 2020; Wacker *et al.*, 2023). In compartmentalized genomes a distinction is made between conserved core regions and adaptive, less conserved accessory regions (Bertazzoni *et al.*, 2018; Yang, H *et al.*, 2020). Accessory regions can make up entire accessory chromosomes or form parts of larger core chromosomes (Ma *et al.*, 2010; Bertazzoni *et al.*, 2018; van Westerhoven *et al.*, 2024a). Besides their low levels of conservation between related strains and species, accessory regions have several distinguishing features. Generally, accessory regions have a higher abundance of transposable elements (TEs), lower gene density, different codon usage, higher sequence variation and are enriched for facultative heterochromatin histone modifications (Coleman *et al.*, 2009; Connolly *et al.*, 2013; Schotanus *et al.*,

2015; Dutheil *et al.*, 2016; Seidl & Thomma, 2017; Bertazzoni *et al.*, 2018; Fokkens *et al.*, 2018; Cook *et al.*, 2020; Habig & Stukenbrock, 2020; Habig *et al.*, 2021; Habig *et al.*, 2024) (Fig. 3).

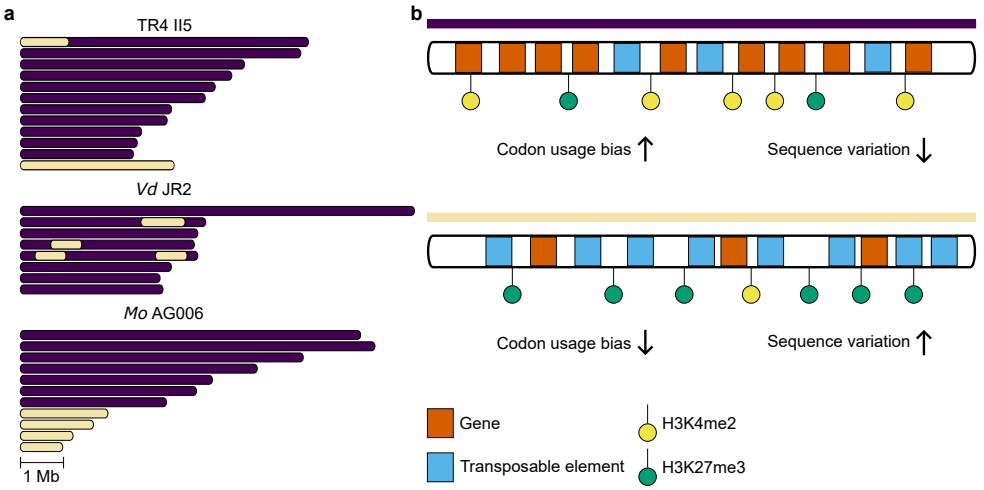


FIGURE 3 | Genome compartmentalization in fungi. a) Schematic of three fungal genomes with different forms of compartmentalized genomes. Top: *Fusarium oxysporum* TR4 strain II5 with one independent accessory chromosome and one accessory compartment as part of a larger core chromosome. Middle: *Verticillium dahliae* strain JR2. Accessory genome compartments are commonly referred to as lineage specific regions in *V. dahliae* (Faino et al., 2016). Bottom: *Magnaporthe oryzae* strain AG006. For *M. oryzae*, accessory genome compartments are often referred to as mini chromosomes (Barragan *et al.*, 2024). **b**) Schematic of key characteristics for core- (top) and accessory genome compartments (bottom). Core genome compartments generally have higher gene density, less transposable elements and have higher rates of H3K4me2 histone modification. Core genome compartments additionally have higher levels of codon usage bias and lower levels of sequence variation compared to accessory genome compartments.

For numerous fungi, including FOSC members, accessory regions have been shown to play an important role in virulence and host adaptation (Johnson *et al.*, 2001; Ma *et al.*, 2010; de Jonge *et al.*, 2013; van Dam *et al.*, 2017; Plaumann *et al.*, 2018; Ayukawa *et al.*, 2021). The role for accessory regions in virulence is generally ascribed to the (enriched) presence of effector genes within these regions (Ma *et al.*, 2010; Bertazzoni *et al.*, 2018; Sánchez-Vallet *et al.*, 2018; Ayukawa *et al.*, 2021), but can also include genes of other functions (Miao *et al.*, 1991; Rodriguez-Carres *et al.*, 2008; Witte *et al.*, 2021). The compartmentalization of the genome is also commonly referred to as the 'two-speed' genome model (Dong *et al.*, 2015; Sánchez-Vallet *et al.*, 2018; Torres *et al.*, 2020), although alternative nuanced descriptions highlight the various degrees and variations in genome compartmentalization (Fokkens *et al.*, 2018; Frantzeskakis *et al.*, 2019; Torres *et al.*, 2020). The association of virulence related genes and TEs in separate genomic compartments is thought to aid in increased adaptation rates for changing environments and host-pathogen interactions (Croll & McDonald, 2012;

Dong *et al.*, 2015; Torres *et al.*, 2020; Yu, Houlin *et al.*, 2023). Despite several clues into their origin (Croll & McDonald, 2012; Croll *et al.*, 2013; Sánchez-Vallet *et al.*, 2018; Habig & Stukenbrock, 2020; Torres *et al.*, 2020; Langner *et al.*, 2021; Fouché *et al.*, 2022), the exact evolutionary benefits and transitions that led to compartmentalized genomes in some fungi and their absence in others remains elusive (Torres *et al.*, 2020).

Genome compartmentalization is not only thought to aid in synchronizing transcriptional regulation and adaptability (Croll & McDonald, 2012; Sánchez-Vallet *et al.*, 2018; Fouché *et al.*, 2022), but the clustering of conditionally important genes could also facilitate their horizontal transfer as a functional unit (Dutheil *et al.*, 2016). Clustering, a form of compartmentalization, is also commonly observed in fungi for biosynthetic gene clusters and similarly thought to aid horizontal transfer of entire metabolic pathways (Wisecaver *et al.*, 2014). Horizontal transfer of accessory regions or chromosomes has been observed numerous times in natural fungal populations (Masel, 1996; Akagi *et al.*, 2009; Henry *et al.*, 2021; Barragan *et al.*, 2024; Habig *et al.*, 2024). Moreover, experimental horizontal chromosome transfer has also been achieved in several fungi (He *et al.*, 1998; Akagi *et al.*, 2009; Ma *et al.*, 2010; Habig *et al.*, 2024). Especially for members of the FOSC, experimental horizontal transfer of accessory chromosomes has been achieved relatively frequently (Ma *et al.*, 2010; Vlaardingerbroek *et al.*, 2016; van Dam *et al.*, 2017; Li *et al.*, 2020a; Li *et al.*, 2020b; Ayukawa *et al.*, 2021). Emphasizing the role of accessory chromosomes in host adaptation, the transfer of specific accessory chromosomes to the non-pathogenic *Fusarium* strain Fo47 allowed it to infect novel plant hosts (Ma *et al.*, 2010; Vlaardingerbroek *et al.*, 2016; van Dam *et al.*, 2017). As such, the formation of new pathogenic lineages seems to be the result of horizontal transfer of specific accessory chromosomes between lineages, in turn leading to the polyphyletic origin of different *formae speciales* (Fokkens & Rep, 2023). The exact mechanisms at play during horizontal transfer of accessory regions are still unknown, but genes involved in the facilitation of transfer might be directly encoded by the accessory regions themselves (Habig *et al.*, 2024). Analogous to this, the horizontal transfer of the extraordinarily large *Starship* transposable elements might be facilitated by *Starship* encoded genes (Gluck-Thaler *et al.*, 2022). The potential self-encoding of genes facilitating transfer is also reminiscent of bacterial plasmids encoding genes for their own transfer (Smillie *et al.*, 2010).

Lastly, the low gene density and lack of housekeeping genes indicates that accessory chromosomes are not required for axenic growth, hence are alternatively referred to as 'conditionally dispensable' (CD) chromosomes (Yu, Houlin *et al.*, 2023). The often-non-essential nature of accessory chromosomes is exemplified in the observed wide range of presence absence variation and (frequent) loss during reproduction (Miao *et al.*, 1991; Leclair *et al.*, 1996; Orbach, 1996; Wittenberg *et al.*, 2009; Balesdent *et al.*, 2013; Vlaardingerbroek *et al.*, 2016; Möller *et al.*, 2018; van Westerhoven *et al.*, 2024a).

Moreover, accessory chromosomes have been experimentally removed using mitosis disrupting chemicals in several fungi (VanEtten *et al.*, 1998; Habig *et al.*, 2017; van Dam *et al.*, 2017; Ayukawa *et al.*, 2021; Dijkstra *et al.*, 2024; Sakane *et al.*, 2024; Wei *et al.*, 2024). In some cases, the loss of an accessory chromosome causes unclear or minor effects (Habig *et al.*, 2017; Ayukawa *et al.*, 2021) while in others strongly affecting the interaction with the host (van Dam *et al.*, 2017; Ayukawa *et al.*, 2021; Dijkstra *et al.*, 2024; Habig *et al.*, 2024; Sakane *et al.*, 2024; Wei *et al.*, 2024). In contrast to loss of accessory chromosomes during propagation, several observations have been made of non-Mendelian inheritance of accessory chromosomes (Komluski *et al.*, 2022). In several of these cases accessory chromosomes increase in abundance, suggestive of drive (Tzeng *et al.*, 1992; Balesdent *et al.*, 2013; Habig *et al.*, 2018). Similar to the horizontal transfer, the presence of certain genes and epigenetic modifications might underlie these non-Mendelian inheritance patterns and cause accessory chromosomes to act as 'selfish' elements (Croll & McDonald, 2012; Vogan *et al.*, 2019; Komluski *et al.*, 2022; Habig *et al.*, 2024; Habig *et al.*, 2025).

Pathogen host interactions: a molecular battleground

In their interaction with the host, plant pathogens make use of a wide range of secreted molecules, so-called effectors, to aid in the colonization of the host (Stergiopoulos & de Wit, 2009; Pusztahelyi *et al.*, 2015; Toruño *et al.*, 2016; Collemare *et al.*, 2019; Rocafort *et al.*, 2020). The term effector generally refers to secreted proteins (Stergiopoulos & de Wit, 2009; Toruño *et al.*, 2016; Lovelace *et al.*, 2023), but in the broadest sense of the term, it refers to any secreted molecule that facilitates host colonization, including secondary metabolites and even small RNAs (Wang *et al.*, 2014; Collemare *et al.*, 2019). The molecular mechanisms by which effectors promote host colonization are extremely varied but often include disruption of protease activity, inhibiting plant immune receptors, or manipulating phytohormone levels (Lo Presti *et al.*, 2015; He *et al.*, 2020).

During host colonization all pathogens are recognized by the plant's immune system either through conserved factors from the pathogen, such as chitin fragments or by host-derived factors such as cutin monomers following cell damage (Lo Presti *et al.*, 2015). More specific pathogen detection can take place through effector recognition by either extracellular or intracellular receptors (Huang & Joosten, 2025). The recognition of the pathogen is required to mount a successful immune response, amongst others through the production of reactive oxygen species, callose deposition, transcriptional reprogramming and, in some cases, localized programmed cell death (Huang & Joosten, 2025). A relevant distinction for effector functioning and

the corresponding plant immune response, is the pathogen's lifestyle: necrotrophic, biotrophic, or hemi-biotrophic. Necrotrophic pathogens are those pathogens that rely on dead host tissue for proliferation and as such necrotrophic effectors tend to induce cell death by hijacking the plant cells programmed cell death for the benefit of the pathogen (Wang *et al.*, 2014; Lo Presti *et al.*, 2015). Biotrophic pathogens on the other hand, require living host cells for their proliferation. Because of this requirement, biotrophic pathogens need to secrete effectors that restrict the plants immune response and prevent recognition and programmed cell death (Lo Presti *et al.*, 2015). Finally, hemi-biotrophic pathogens have an initial biotrophic phase and a final necrotrophic phase during host colonization. Although many questions remain on the mechanisms behind the switch from biotrophy to necrotrophy for hemi-biotrophs, the switch seems to rely, in part, on close transcriptional regulation of specific effectors (Kelley *et al.*, 2010; Gan *et al.*, 2013). Although effectors are most commonly studied for pathogens, symbionts also employ them to allow for host colonization indicating their general role in the manipulation of host processes (Plett *et al.*, 2020; Teulet *et al.*, 2023).

The contrasting requirement of effectors for biotrophic or necrotrophic growth leads to two different models to describe their co-evolution in the arms race with the host. For biotrophic effectors, the gene-for-gene model applies, in which recognition of an effector by a receptor (R-gene) will lead to a fast plant immune response with localized cell death and, therefore, restriction of the pathogen's colonization (van der Burgh & Joosten, 2019). Following this model, the recognition of an effector by the appropriate receptor will impose a severe selection pressure on the pathogen for loss of recognition of the corresponding effector (Sánchez-Vallet *et al.*, 2018). For necrotrophic effectors, on the other hand, the inverse gene-for-gene model applies. In this model cell death is beneficially induced for the pathogen through necrotrophic effectors with specific host targets (Peters Haugrud *et al.*, 2019; Faris & Friesen, 2020). In contrast to the gene-for-gene model, this will impose the selection pressure on the host for the loss or modification of the effector target, often referred to as a susceptibility gene (S-gene) (Faris & Friesen, 2020). It should be noted that the term 'S-gene' does not necessarily only apply to necrotrophic effector targets, but also more generally refers to any gene of which the presence supports pathogen infection (van Schie & Takken, 2014; He *et al.*, 2020).

Besides directly affecting the host's cellular processes, effectors can also affect the host in more indirect manners. For example, recent studies in the plant pathogen *V. dahliae* have shown some proteinaceous effectors with strong effects on specific host-associated microbes (Snelders *et al.*, 2020; Snelders *et al.*, 2021). Similarly, *Zymoseptoria tritici* was shown to secrete a protein toxic to fungi (de Guillen *et al.*, 2024). Secreted proteins from *F. oxysporum* can also promote host colonization by manipulating the

microbiome (Chang *et al.*, 2021), as well as secondary metabolites (Jin *et al.*, 2024). Structural-based predictions indicate that antimicrobial properties might be common among fungal secretomes (Mesny & Thomma, 2024). The manipulation of the host microbiome could also occur more frequently as an indirect result of interference with the host's metabolism (Cai *et al.*, 2023). Together, these studies indicate that effectors also manipulate the microbiome to further facilitate host colonization and, hence, are likely a common component of the pathogen's colonization machinery (Snelders *et al.*, 2022; Mesny & Thomma, 2024) to create the optimal conditions for host colonization (Cai *et al.*, 2023).

Because of their prominent role in host-pathogen interactions, the reliable identification of effectors has seen considerable research (Lovelace *et al.*, 2023). Initial effector identification relies heavily on different bioinformatic prediction tools (Lovelace *et al.*, 2023). Comparatively, proteinaceous effector identification is relatively easy due to general sequence features and their secreted nature. Reliable bioinformatic tools allow for the prediction of targeting or secretion motifs (Almagro Armenteros *et al.*, 2019a; Teufel *et al.*, 2022). Besides a secretion motif, fungal effectors are generally smaller proteins and rich in cysteine residues compared to non-effectors enabling straightforward filtering (Lovelace *et al.*, 2023). Moreover, some fungal effectors can contain additional characteristic motifs (Godfrey *et al.*, 2010), but these are not as common or prominent, such as the RxLR motif found in many oomycete effectors (Morgan & Kamoun, 2007). Recent advances in protein structure prediction through tools such as AlphaFold2 (Jumper *et al.*, 2021) has caused an increasing number of effector studies utilizing structural data in effector prediction and characterization (Rocafort *et al.*, 2022; Seong & Krasileva, 2023; Yu *et al.*, 2024). Analysis of expression patterns during distinct infection stages is another common part of the bioinformatic toolbox for effector identification (Rocafort *et al.*, 2022; Yan *et al.*, 2023). In addition, genome compartmentalization and association with transposable elements can support effector identification in some fungi (Ma *et al.*, 2010; de Jonge *et al.*, 2013; Schmidt *et al.*, 2013). However, albeit these characteristic patterns helped to successfully identify and characterize many effectors, the aforementioned tools can also have blind spots for 'atypical' effectors such as those secreted by unconventional secretion pathways for which accurate prediction remains absent (Dulal & Wilson, 2024).

The prediction of non-proteinaceous effectors is much harder due to a lack of shared features and available tools. Although large numbers of biosynthetic gene clusters can reliably be predicted in fungal genomes using tools such as Antismash (Blin *et al.*, 2023), a function as effector can generally not be inferred from the predicted clusters. As such, the toxic function of secondary metabolites is generally tested using culture filtrate fractions or purified compounds (López-Díaz *et al.*, 2018; Kessler

et al., 2020). Roles as effectors for secondary metabolites with non-toxic functions are often inferred from expression data (Collemare *et al.*, 2008a; Dallery *et al.*, 2017), but subsequent characterization is difficult and, therefore, their exact function often remains unknown (Collemare *et al.*, 2019). For both proteinaceous and non-proteinaceous effectors, prediction is reliant on a high-quality genome assembly and annotation (Dallery *et al.*, 2017; Zhong *et al.*, 2017). Although together these bioinformatic tools enable the quick identification of large numbers of effector proteins, downstream characterization forms the bottleneck in effector research. Moreover, effector research in plant pathogens often suffers from functional redundancy and quantitative differences with a small effect (Kvitko *et al.*, 2009; Pliego *et al.*, 2013; Ali *et al.*, 2014; Brefort *et al.*, 2014; Collemare *et al.*, 2019). For the vast majority of effectors their function and contribution to virulence remain unknown (Kanja & Hammond-Kosack, 2020). In spite of this and due to their key role in plant immunity (Lovelace *et al.*, 2023), effector research is an essential component to support breeding crops for durable resistance to disease. Breeding for FWB resistant bananas is a case where the use of effector knowledge in the breeding process still has a world to gain.

Thesis outline

Despite the ongoing FWB epidemic, the lack of efficient control methods and the relative wealth of knowledge on FOSC strains infecting other host plants, there are still severe knowledge gaps for the interaction between banana and *Fusarium*. Especially at the molecular level, this interaction remains understudied, amplified by the genetic recalcitrance of the pathogen, but especially banana. Gaining further insight into this interaction and addressing these knowledge gaps is essential to aid in the development of sustainable FWB control methods and ensure future banana production. In this thesis, I describe the investigation of the interaction between banana and FOSC strains at a molecular level, focusing on genome dynamics and virulence factors to ultimately aid in rational information-driven resistance breeding in banana.

In **chapter 2**, I describe an RNA-seq study analyzing TR4 gene expression during banana infection. Manual genome annotation and expression analysis allowed for the identification of several novel effectors. Some of these effectors show conserved structural features with distantly related effectors, indicating potential shared functions. Additionally, analysis of several effector knockout mutants revealed their redundancy for virulence.

Genome compartmentalization and accessory chromosomes are key features in several plant pathogens. In **chapter 3**, I report on the newly discovered accessory

chromosome length polymorphisms within the TR4 lineage. Moreover, by generating a chromosome loss mutant, I show that the accessory chromosome in the TR4 lineage plays an important, but nonessential role in virulence during banana infection.

Transposable elements have significant effects on fungal genome dynamics, especially in clonal lineages. In **chapter 4**, I describe the effects of Helitron transposon activity on the genome of banana infecting *Fusarium* strains. Specifically, I highlight a TR4 strain, M1, that lost the conserved biosynthetic gene cluster for fusaric acid production because of Helitron activity. Metabolite analysis showcases the impact of the loss of fusaric acid production on the overall metabolite profile of the M1 strain. Further analysis of this strain and newly generated mutants show that despite the strong conservation of the fusaric acid biosynthetic gene cluster, its loss does not attenuate virulence on banana.

In **chapter 5**, I synthesize the different aspects of the interaction between *Fusarium* and banana that were studied in this thesis project. I then reflect on it and relate the new insights on genome dynamics and virulence factors to the knowledge of *Fusarium* strains infecting other hosts and of other plant pathogens. Moreover, I discuss the relevance of these studies for insights into fungal evolution and their use to aid in the development of future sustainable banana varieties.

Chapter 2

Effector identification in Tropical Race 4, the Fusarium wilt pathogen of banana

Jelmer Dijkstra[1]
Sebastien D. Garnier[1]
Giuliana Nakasato-Tagami[1]
Carolina Aguilera-Galvez[1,2]
Xiaoqian Shi-Kunne[1¶]
and Gert H.J. Kema[1¶]

[1]Laboratory of Phytopathology, Wageningen University and Research, Wageningen, the Netherlands.
[2]Área de Sistemas Naturales y Sostenibilidad, Escuela de Ciencias Aplicadas e Ingeniería, Universidad EAFIT, Medellín, Colombia.
¶These authors contributed equally to this work.

Abstract

Plant pathogenic fungi make use of a large repertoire of secreted effector molecules to aid infection of their hosts. In turn plant immunity is often reliant on recognition of secreted effectors to rapidly employ an immune response to pathogens. Effectors located on accessory compartments of the fungal genome often play an important role in host adaptation. However, the identification and characterization of effectors is, at least partly, dependent on a high-quality genome annotation. Here we use RNA-seq data to curate the genome annotation of the important banana pathogen *Fusarium oxysporum* Tropical Race 4 (TR4). By combining the improved genome annotation and expression analysis we pinpoint additional effectors of interest, focusing on those located on the adaptive accessory genome. We show-case a pair of effectors encoded by the accessory regions of TR4 strain II5 in a specific head-to-head orientation, which are part of a larger family of similarly structured and orientated effectors in other plant pathogens. Moreover, we demonstrate by knockouts that two other accessory effectors do not significantly affect the virulence of TR4 on Cavendish bananas, despite their high expression levels during infection. This suggests redundancy, but we also show their potential role in antimicrobial competition. Together, we generate a high-quality manual annotation of this major banana pathogen and provide further insights into the organization and functioning of effectors in TR4.

Introduction

Fungal plant pathogens are a major source of yield loss in agriculture (Dean *et al.*, 2012; Fones *et al.*, 2020; Mapuranga *et al.*, 2022). Moreover, the globalized market and modern agricultural practices are significant drivers in the emergence and spread of highly problematic plant pathogenic fungi (Fones *et al.*, 2020). Besides anthropogenic factors, the adaptability of a pathogen plays an important role in its ability to infect and spread (Huang, J *et al.*, 2023). Consequently, plant pathogenic fungi circumvent resistance of their respective hosts through many different infection strategies (Lo Presti *et al.*, 2015) and employ a wide range of secreted effector proteins that facilitate infection (Stergiopoulos & de Wit, 2009; Rocafort *et al.*, 2020). The functions of effectors are varied and include, amongst others the altering of host protein stability (Park *et al.*, 2016; Yang, Q *et al.*, 2020), inhibition of host proteases (Misas Villamil *et al.*, 2019), manipulation of the host microbiome (Snelders *et al.*, 2020; Snelders *et al.*, 2023) or activation of programmed cell death (Shi *et al.*, 2016). Especially, regulatory hubs of plant immunity are common effector targets to suppress the hosts' immune response and ultimately colonize the host (Lo Presti *et al.*, 2015; He *et al.*, 2020). These effectors are often located on accessory regions or chromosomes of the genome (Bertazzoni *et al.*, 2018). In the characterization of plant pathogen effectors, next to structural information, their temporal expression patterns are increasingly gaining attention (Rocafort *et al.*, 2022; Seong & Krasileva, 2023; Yan *et al.*, 2023; Yu *et al.*, 2024).

Similar to other crops, banana is threatened by a wide variety of pathogens and pests. One of the most important groups of pathogens that threaten global banana production, belong to the *Fusarium oxysporum* species complex (FOSC) (Michielse & Rep, 2009; Ploetz, 2009; Ploetz, R. C., 2015). Members of this species complex are the causal agents of Fusarium wilt of banana (FWB). Strains that belong to the Tropical Race 4 (TR4) lineage are the main threat due to their ability to infect and colonize, amongst others, the dominant banana cultivar Cavendish, which was in turn once adopted for its resistance to Race 1 strains (Ordóñez *et al.*, 2015; Ploetz, Randy C., 2015). Despite the immense threat posed by TR4 to global banana production, already being present in all major banana producing continents (Ordóñez *et al.*, 2015; van Westerhoven *et al.*, 2024a), efficient control methods are mostly absent (Ploetz, Randy C., 2015). Effective control can likely be best achieved through the development of resistant varieties (Drenth & Kema, 2021). Despite several efforts (Paul *et al.*, 2011; Ghag *et al.*, 2014; Dale *et al.*, 2017; Li, X *et al.*, 2024), however, resistant varieties are still not commercially available. Progress in this regard will also have to rely on improving the understanding of the interaction between banana and *Fusarium* spp.

FOSC members secrete a suite of different effectors to colonize their host (Srivastava *et al.*, 2024). Effector genes can be located on conserved core regions (Redkar *et al.*, 2022),

but also on lineage-specific accessory regions of the compartmentalized genome of *F. oxysporum* (Yang, H *et al.*, 2020). The latter frequently contain effectors important for adaptation to a specific host plant (Ma *et al.*, 2010; van Dam *et al.*, 2017; Yang, H *et al.*, 2020; Ayukawa *et al.*, 2021; Srivastava *et al.*, 2024). Although some individual effectors of TR4 strains have already been investigated (Widinugraheni *et al.*, 2018; An *et al.*, 2019; Zhang *et al.*, 2021; Guo *et al.*, 2022; Dijkstra *et al.*, 2024), (Chapter 3), the majority remains unknown, especially those restricted to banana-infecting FOSC lineages.

Since effector discovery can be significantly hindered by low-quality genome annotations resulting from automatic annotation tools (Zhong *et al.*, 2017), we decided to generate and use RNA-seq data of the TR4 reference strain II5 to manually curate its genome to facilitate the identification of novel effector candidates. We, therefore, assessed expression patterns during pathogenesis (early-mid stage, 4-8 days post inoculation (dpi), and late stage, 30 dpi) showing a general transcriptional shift for increased expression compared to vegetative growth. We identified several known conserved effectors as well as novel effectors among the strongly upregulated genes. The structural analysis of novel effector candidates revealed similarity with broader effector families despite limited sequence similarity. Lastly, functional analysis by CRISPR knock-outs shows that a novel ribosomally synthesized and post-translationally modified peptide (RiPP) precursor contributes to antimicrobial activity of culture filtrate. Knockouts of two effectors on the accessory genome does not affect the virulence of TR4 on banana.

Results

A transcriptional shift during banana colonization

We used RNA-seq data to manually reannotate and improve the genome annotation of TR4 reference strain II5. The expression data was used to correct many splicing sites, both the donor and acceptor site, as well as adding or removing exons/introns based on expression support (Fig. S1a). Sometimes there was strong support for unconventional splicing sites, which were generally missed by the automatic annotation. We also used the expression data to add new gene models that were missed by the automatic annotation pipeline (Fig. S1b). Subsequently, the newly manually curated genome was used to predict secreted proteins of TR4 II5. Out of the final 17,637 gene models, a total of 1,686 gene models were predicted to encode for a signal peptide-containing protein using SignalP 5.0 (Almagro Armenteros *et al.*, 2019b), of which 74 are located on the accessory region of chromosome 1 or accessory chromosome 12. Comparing genome-wide expression levels during pathogenesis and vegetative growth (mycelium and conidiospores) indicates a

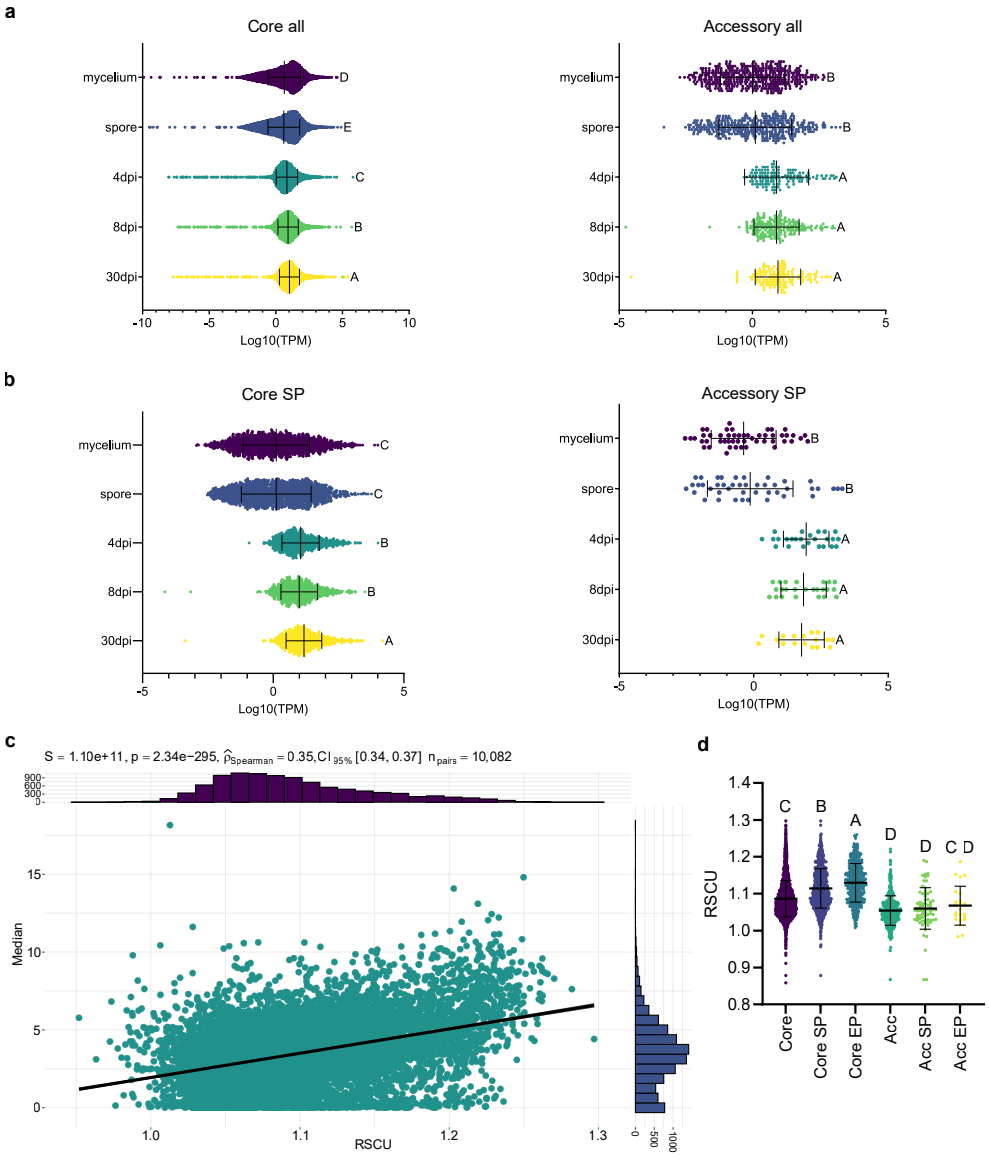


FIGURE 1 | Comparative *in-vitro* and *in-planta* transcriptional analysis of TR4. a) Scatterplot displaying average Log_{10}(TPM) expression levels of all core and accessory genes encoding non-secreted proteins for TR4 in mycelium, spores, and during pathogenesis (4-, 8- or 30-dpi) of Cavendish roots. Different letters indicate significant differences between treatments (Kruskal-Wallis test; P<0.05). Data are shown as mean ±SD. **b**) Scatterplot displaying average Log_{10}(TPM) expression levels of genes on the core and accessory regions that are predicted to encode secreted proteins (SP) in mycelium, spores and during pathogenesis (4-, 8- or 30-dpi) of Cavendish roots. Different letters indicate significant differences between treatments (Kruskal-Wallis test; P<0.05). Data are shown as mean ±SD. **c**) Spearman correlation analysis between gene-wide Relative Synonymous Codon Usage (RSCU) and median Log_2(TPM) expression across all samples for 10,082 expressed genes. **d**) Scatterplot of gene-wide RSCU for genes on the core genome or the accessory genome (Acc). Genes encoding a secreted protein (SP) or with a positive EffectorP (EP) score are shown

separately. Different letters indicate significant differences between treatments (Kruskal-Wallis test; P<0.05). Data are shown as mean ±SD.

strong transcriptional shift during the infection process (Fig. 1a), particularly for genes in the accessory regions and those encoding secreted proteins, both on the core and accessory regions of the genome (Fig. 1b).

A factor of significance in gene expression levels is the degree of codon optimization (LaBella *et al.*, 2021). We, therefore, calculated the genome-wide Relative Synonymous Codon Usage (RSCU) levels for all gene models in the curated II5 genome. Comparing the RSCU values to the median Log_2 Transcripts per Million (TPM) values for 10,082 expressed genes indicates a moderate positive correlation between RSCU and expression levels (Fig. 1c). Interestingly, genes with a predicted signal peptide and a positive EffectorP (Sperschneider & Dodds, 2022) score show significantly higher degrees of codon optimization compared to the other genes on the core genome. This same trend is observed, albeit not significantly, in the genes on the accessory regions (Fig. 1d). In general, core localized genes show significantly higher RSCU levels compared to accessory localized genes.

Known and novel effectors are strongly upregulated during infection

We used the temporal expression patterns of all genes to define clusters following similar patterns, which broadly resulted in eight clusters (Fig. 2a). The clusters for genes predominantly expressed during pathogenesis (4-, 8-, and 30 dpi) of the host are the smallest, accounting for roughly 19% of all genes (C2, C5, and C8). The biggest clusters are formed by genes expressed during vegetative growth. We further determined the top GO terms for each cluster. Those related to vegetative growth (C1, C3, C4, C6, and C7) are enriched for genes involved in basic cellular growth processes such as ribosome biogenesis, mRNA processing, and cellular transport. Early colonization (4-8 dpi), on the other hand, is dominated by genes involved in secondary metabolism, cellular detoxification, and degradation of host cell components (C2 and C5). The late colonization cluster (30 dpi, C8) is enriched for genes involved in cellular signaling. To identify novel effector candidates, we investigated the clustering of accessory genes containing a predicted signal peptide with a minimum average expression of >5 TPM across all samples. The vast majority of genes following these criteria, 23 in total, are in the infection-related clusters (C2, C5, and C8) (Fig. 2a) and are of extra interest for further investigation.

We also investigated the expression of the well-known Fusarium *SIX* effectors (Schmidt *et al.*, 2013) in our dataset. Their expression is generally *in planta* induced, but there are some significant differences (Fig. 2b). Most *SIX* effectors have low expression levels in spores except for *SIX1a* and *SIX6*. Moreover, despite being present, both *SIX8* and *SIX13*

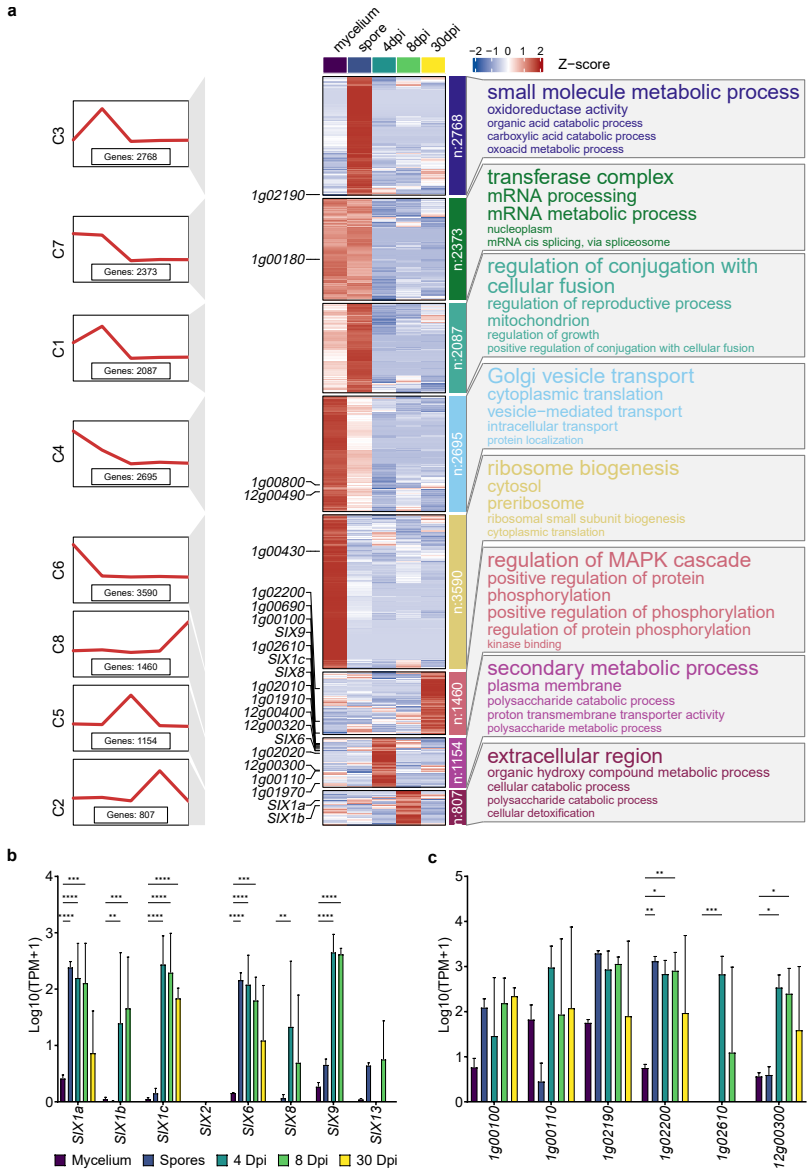


FIGURE 2 | Known and novel effectors are upregulated during pathogenesis of TR4 in susceptible Cavendish banana. a) Clustering of genes based on expression pattern using **ClusterGVis.** Marked genes, on the heatmap, are those genes located on the accessory regions with a predicted signal peptide and at least a minimum average expression of >5 TPM across all timepoints. **b**) Log_{10}(TPM+1) values for *SIX* genes of TR4 strain II5 during vegetative growth or infection. **c**) Log_{10}(TPM+1) values for differentially expressed core genome-encoded effector candidates of TR4 strain II5 during vegetative growth or infection. For both **b**) and **c**) Asterisks indicate significant p values following Dunnett's test using mycelium TPM values as control. Error bars indicate SD. For significance, * P≤0.05, ** P≤0.01, *** P≤0.001, **** P≤0.0001.

show relatively low expression levels during the different timepoints of pathogenesis. Furthermore, *SIX2* has no expression at any of the investigated timepoints, and it is the only *SIX* gene in TR4 that is not located on either of the accessory regions (van Westerhoven *et al.*, 2024a).

Besides the known *SIX* effectors, several novel accessory effector candidates show high expression levels in one or more stages of infection (Fig. 2c). Similar to the *SIX* effectors, these genes show varying degrees of expression during vegetative growth and are not exclusively *in planta* induced. Likewise, core regions of the genome contain effector candidates, some of which are differentially expressed. These core genes are either effectors lacking any known domains (Fig. S2a) or are predicted to be a CAZyme or CFEM protein (Fig. S2b). Two of these effectors have recently been noted to suppress BAX-triggered cell death during transient expression in *Nicotiana benthamiana* (*2g21270* and *5g00040* are FoSSP48 and FoSSP55, respectively) (Wang, T *et al.*, 2023). CFEM proteins are unique to fungi and have been implicated in several processes, including virulence (Wang *et al.,* 2022; Sabnam & Barman, 2017), and many are GPI anchored, such as the three differentially expressed CFEM encoding genes in II5 (Gíslason *et al.*, 2021). CAZymes are also expected to be upregulated during infection as they play an important role in the acquisition of nutrients and degradation of the plant cell wall during the infection process (Cantu *et al.*, 2008; Baroncelli *et al.*, 2016). In contrast, accessory genome-encoded secreted proteins mostly comprise small cysteine-rich proteins of which six are differentially expressed during at least one of the sampled time points. Surprisingly, the differentially expressed core effector candidate *2g20200* is the precursor protein in a conserved RiPP biosynthetic gene cluster present in several other *Fusarium* spp. (Fig. S3). Orthologs of *2g20200* are also upregulated during the infection of cabbage (FocnCong_v019494) (Ayukawa *et al.*, 2021) and tomato by their respective *Fusarium* pathogens (FOXG_11033) (van der Does *et al.*, 2016).

Several highly upregulated effectors associated with a transposon

Miniature impalas (*mimps*) are a family of Miniature inverted-repeat transposable elements (MITEs) that are non-autonomous Class II transposable elements (TEs). Previously, *mimps* have been shown to be associated with accessory regions and genes involved in pathogenicity in *Fusarium* spp. infecting several different hosts (Schmidt *et al.*, 2013; van Dam *et al.*, 2016). Although strain II5 contains considerably less *mimps* compared to other *Fusarium* strains (van Dam & Rep, 2017), they are still associated with the accessory regions. The accessory regions of strain II5 contain 52 *mimp* Terminal Inverted Repeats (TIRs), while the core regions contain only 10 *mimp* TIRs. Considering the differences in size of the core regions and the accessory regions of the genome, *mimps* are significantly associated with the accessory regions (Fisher's exact test $P<0.0001$). Moreover, the number of *mimp* TIRs on accessory chromosome 12

are underestimated due to the collapsed assembly of intrachromosomal duplications (Dijkstra *et al.*, 2024), (Chapter 3). In strain II5, several of the highly upregulated effector candidates contain *mimp* TIRs upstream (2.5 kb) of their coding regions. This includes the novel effector candidate *12g00300* as well as several of the *SIX* genes, similar to tomato infecting strain *Fol*4287 (Schmidt *et al.*, 2013). Moreover, the previously identified zinc-metalloproteinase *Foc1324* (*1g01910*) and effector candidate *Foc177* (*1g01900*) (Chang *et al.*, 2020), are also *mimp*-associated in II5, although, the latter has no detected expression during our sampled timepoints. Overall, the *mimp*-associated genes show the same earlier observed transcriptional shift during host infection (Fig. S4). Although *mimps* have been used previously to identify new effectors (Schmidt *et al.*, 2013; Chang *et al.*, 2020), *mimp*-based searches in strain II5 only provide *12g00300* as a novel highly expressed candidate with limited characterization (Dijkstra *et al.*, 2024), (Chapter 3).

Novel effector candidates are part of larger structural families

Some of the newly discovered effector candidates are present as two individual copies. In all cases, one copy is present in the accessory region of chromosome 1, while the other copy is located on accessory chromosome 12. In the case of one novel effector pair (*1g02190-1g02200/12g00400-12g00410*), they are located adjacent to each other in both locations in a head-to-head orientation. Interestingly, this effector pair is present in three additional copies, however these copies have undergone pseudogenization (Fig. S5). Similarly, the ortholog to the previously identified *SIX9* is present twice (van Westerhoven *et al.*, 2024a). These effector candidate copies mean that only a single novel identified effector (*12g00300*) is located exclusively on chromosome 12 (Dijkstra *et al.*, 2024), (Chapter 3).

The head-to-head orientation of effector candidates *1g02190* and *1g02200* is reminiscent of an increasing number of effector pairs with such a genomic organization (Ma *et al.*, 2015; Ayukawa *et al.*, 2021; Talbi *et al.*, 2023; Talbi *et al.*, 2024; Yu *et al.*, 2024). Closer sequence analysis shows that *1g02190* has some sequence similarity to *PSE1/PSL1* (Fig. 3a,b), an effector that is present in a head-to-head orientation with *SIX8* in *Fol*4287 (Ayukawa *et al.*, 2021; Yu *et al.*, 2024). Similar to the *SIX8-PSE1* pair, *1g02190* and *1g02200* appear as a pair in several other FOSC members infecting other hosts (Fig. 3a). Interestingly, a strongly conserved ortholog of *1g02200* was found in the more distantly related fungal species *Fusarium xylarioides* and *Verticillium dahliae* (Fig. 3a,c). In tomato-infecting *V. dahliae* strains this effector has been named TOM and is required for infection (Li *et al.*, 2022). The presence of this effector in *F. xylarioides* is likely a consequence of recently described horizontal transfers between FOSC members and *F. xylarioides* (Peck et al., 2024). In contrast to the FOSC strains, the effector is neither present as a pair in *F. xylarioides* nor in *V. dahliae*.

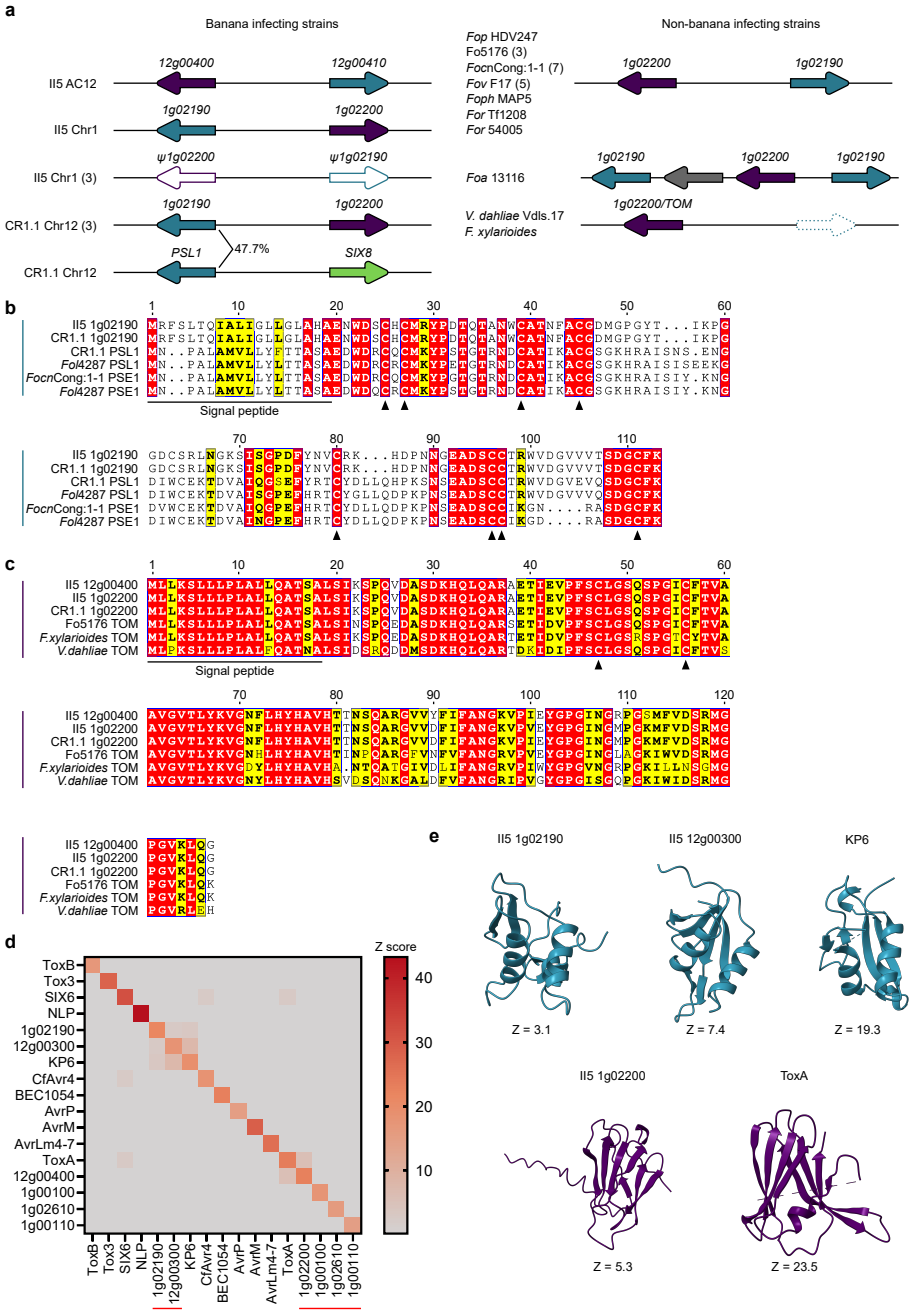


FIGURE 3 | A novel effector pair in TR4 is structurally similar to known effectors in other fungal pathogens. a) Schematic representation of the genomic organization of effector pair *1g02190* and *1g02200* and orthologous pairs. Left panel depicts orthologous pairs in banana infecting strains II5 (TR4) and CR1.1 (R1). Right panel depicts orthologous pairs in fungi infecting different hosts. AC12 stands for accessory chromosome 12. Additional copy numbers noted in brackets. *Fop*, *Fusarium oxysporum* f. sp. *pisi*; *Focn*

Fusarium oxysporum f. sp. *conglutinans; Fov Fusarium oxysporum* f. sp. *vasinfectum*; *Foph Fusarium oxysporum* f. sp. *physali; For Fusarium oxysporum* f. sp. *raphani; Foa Fusarium oxysporum* f. sp. *albedinis*. **b**) Amino acid alignment of II5 1g02190 and selected orthologs. The predicted signal peptide is underlined, and cysteine residues are indicated by black triangles. **c**) Amino acid alignment of II5 1g02200 and selected orthologs. The predicted signal peptide is underlined, and cysteine residues are indicated by black triangles. **d**) Heatmap depicting structural similarity between AlphaFold2 models of the novel effector candidates (red underlined) and crystal structures of characterized effectors using Dali pairwise comparison. **e**) AlphaFold2 structural models of the novel effectors and the crystal structures of their Dali search structural hits (KP6 or ToxA). Z scores of structural similarities to KP6 or ToxA are shown below the models.

We subsequently predicted the protein structures of the newly identified effector candidates using AlphaFold2. Generated protein structure models were used for structural similarity searches using Dali (Holm, 2022). Effectors 1g02190 and 12g00300 have structural similarity to the *Ustilago maydis* killer protein 6 (KP6) (Tao *et al.*, 1990), as do the effectors SIX5 and PSL1 (Fig. 3d, e) (Ayukawa *et al.*, 2021; Yu *et al.*, 2024). Effector 1g02200, on the other hand, showed structural similarity to ToxA, as was observed for Avr2 (Yu *et al.*, 2024). Thus, our newly identified effector pair is another novel pair of a KP6 structured effector in head-to-head orientation with a ToxA structured effector. Other effector candidates (1g00100, 1g00110 and 1g02610) did not provide any significant results during structural similarity searches on Dali. These effector candidates only show faint sequence similarities to proteins in very few other plant pathogens with little to no orthologs in other FOSC members (Fig. S6a-c). AlphaFold2 structural prediction of these proteins does, however, not indicate any further structural similarity (Fig S6d).

Novel effector candidates do not significantly affect virulence

To assess the role in virulence for newly identified effector candidates, we performed infection assays using knockout mutants of *1g00110, 1g02610,* and RiPP precursor *2g02200*. We compared the virulence level to wildtype II5, and an accessory chromosome loss mutant strain with reduced virulence (Dijkstra *et al.*, 2024), (Chapter 3). Infection assays showed no significant virulence differences between the individual effector knockouts and the wildtype strain, except for one of the two independently tested *Δ1g00110* mutants (Fig. 4a). This same mutant did, however, also show reduced growth on PDA plates, while other mutants showed similar growth to the wildtype strain (Fig. S7). External symptoms generally corresponded to internal corm necrosis with the mutants showing similar wilting symptoms as the wildtype strain, except *Δ1g00110* C5 and previously studied accessory chromosome loss mutant ΔAC12 6.4 (Fig. 4b).

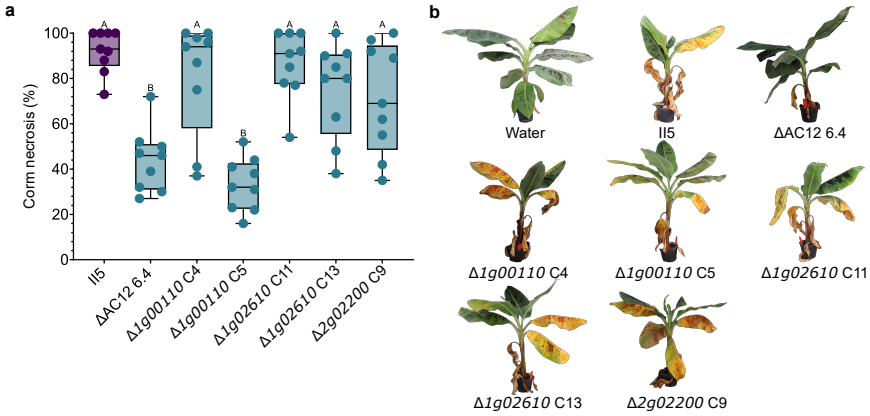


FIGURE 4 | Select effector candidates are not required for virulence on Cavendish banana. **a**) Percentage of corm necrosis of Cavendish 'Grand Naine' plants inoculated with wildtype strain II5, accessory chromosome mutant ΔAC12 6.4 or effector knockouts Δ*1g00110* (C4 regular growth, C5 slow growth), Δ*1g02610*, and Δ*2g20200*. Plants were scored at 10 weeks post-inoculation Corm necrosis was quantified using ImageJ (n=9). Letters indicate significant differences between treatments (Tukey-Kramer test; P<0.05). **b**) Photos of external symptoms following inoculation with strains and mutants from panel **a**. Enlarged photos are shown in Fig. S8.

Assessment of secretome antimicrobial activity

Several identified effectors have shown antimicrobial activity (Snelders *et al.*, 2022). Hence, we assessed the potential antimicrobial activity of selected accessory effectors by combining the AMAPEC tool (Mesny & Thomma, 2024) and the newly generated AlphaFold2 structural models. AMAPEC prediction indicates a high likelihood for antimicrobial activity for several accessory effectors (Table S1), particularly for effector candidates *1g00100*, *1g00110,* and *1g02610*. To further investigate potential antimicrobial activity, we tested the culture filtrates of wildtype and knockout mutants against a Gram-positive *Bacillus* spp. isolate and a Gram-negative *Acinetobacter* spp. isolate. The culture filtrate of the wildtype II5 showed strong antimicrobial activity against both bacteria in comparison to the control (Fig. S9). However, no clear differences were observed in the level of antimicrobial activity between the wildtype and the mutants except for the RiPP precursor mutant *Δ2g02200*. The culture filtrate of this mutant showed a clear, although not significant, trend for reduced antimicrobial activity against the *Bacillus* spp. isolate (Fig. 5a). This trend was most apparent at the last measured timepoint (Fig. 5b). The trend for reduced antimicrobial activity was not observed for the *Acinetobacter* spp. isolate (Fig. 5a-b). The difference in antimicrobial activity could be further observed by plating the mixture of the bacterial culture and culture filtrate following incubation (Fig. 5c). Plates of the *Bacillus* and *Δ2g02200* culture filtrate mixture showed more colony growth compared to the wildtype culture filtrate treatment. In contrast to the bacterial assays, knockout of the RiPP precursor did not visually affect competition with a *Trichoderma* spp. on PDA plates (Fig. S10).

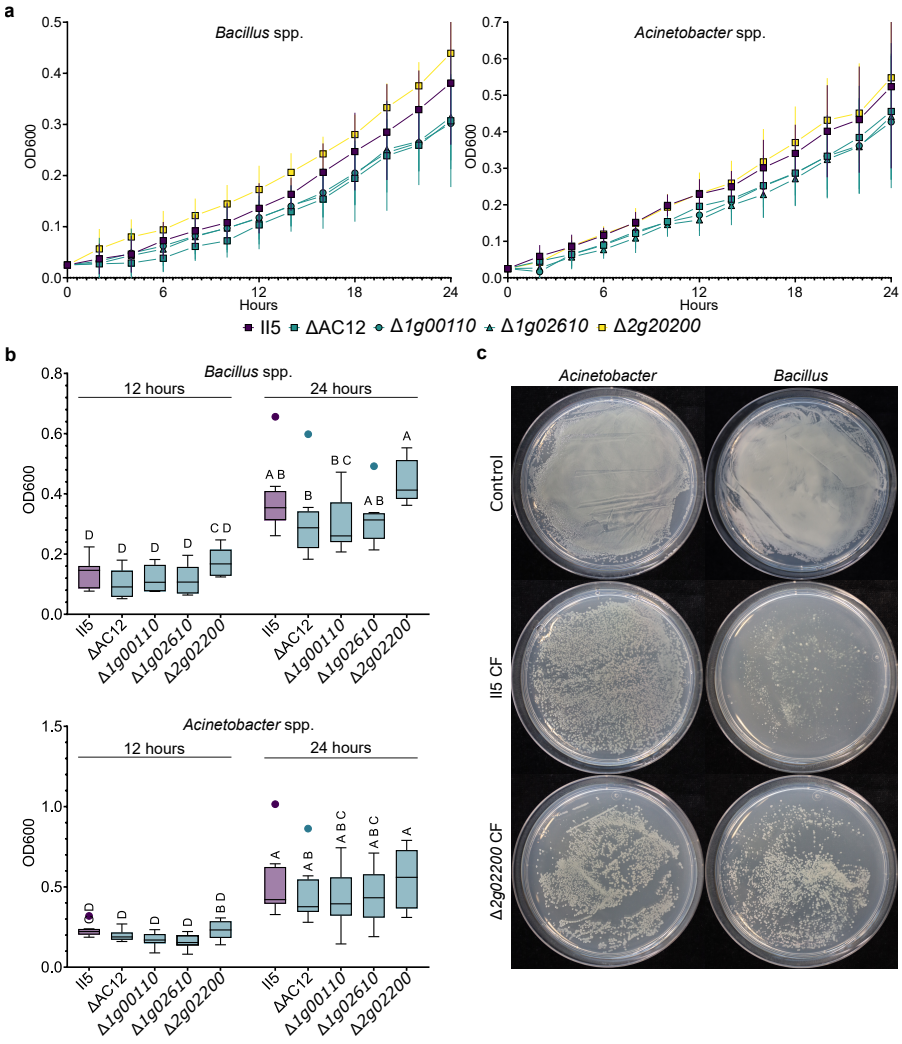


FIGURE 5 | Antimicrobial activity in culture filtrate of TR4 strain Il5. a) OD600 measurements along a 24-hour time course for a *Bacillus* spp. and *Acinetobacter* spp. isolate in medium supplemented with culture filtrate from wildtype strain Il5, accessory chromosome mutant ΔAC12 6.4 or effector knockouts Δ*1g00110*, Δ*1g02610*, and Δ*2g20200*. Bars represent ±SD (n=8). **d**) OD600 values following the treatment with culture filtrate from wildtype strain Il5 accessory chromosome mutant ΔAC12 6.4 or effector knockouts Δ*1g00110*, Δ*1g02610*, and Δ*2g20200*. Values after 12 hours of incubation are displayed on the left and values after 24 hours of incubation are displayed on the right. Letters indicate significant differences between treatments (Tukey-Kramer test; P<0.05). Boxplots are Tukey display (n=8). **e**) LB plates inoculated with *Acinetobacter* or *Bacillus* following 24 hours of incubation in LB supplemented with PDB (Control), culture filtrate from wildtype strain Il5 or RiPP precursor mutant Δ*2g20200*. Photos taken at 1 dpi.

Discussion

Effectors play a key role in facilitating host colonization by plant pathogenic fungi through targeted interference in a wide range of cellular processes (Stergiopoulos & de Wit, 2009; Toruño *et al.*, 2016; Rocafort *et al.*, 2020). In return plants have evolved mechanisms to detect effectors to mount an effective defense response (Cui *et al.*, 2015; Wang, Y *et al.*, 2022). Effector recognition and subsequent plant immunity cause severe selective pressure on a pathogen thus promoting the evasion of host recognition through effector mutation and modulation (Wang, Y *et al.*, 2022). Since effector recognition often provides full host immunity, the presence, absence or modification of a single effector gene can at times determine the entire outcome of the host pathogen interaction (Houterman *et al.*, 2009; de Jonge *et al.*, 2012; Mesarich *et al.*, 2014; Zhong *et al.*, 2017). As such, effector proteins form a focal point in host-pathogen coevolution and the overall interaction between plant pathogens and their hosts.

Here we investigated the effector repertoire in the TR4 reference strain II5. Using RNA-seq data we manually curated the full genome, identifying several new effector candidates and additional gene copies. We showcase a general transcriptional shift for upregulation during host colonization, especially for genes encoding secreted proteins and genes encoded by the two accessory regions. Although there is a strong upregulation of genes located on the accessory region of the genome, they have lower levels of codon optimization compared to genes on the core region. Similar codon usage observations were made in several other plant pathogenic fungi (Habig *et al.*, 2025). Through our analyses we highlight several known effectors as well as novel effector candidates for their expression, protein structure and potential role in virulence.

Manual genome curation often results in the discovery of previously unnoticed effectors and can lead to new insights (Zhong *et al.*, 2017; Amezrou *et al.*, 2023). Similarly, we discovered several new effector candidates as well as additional gene copies missed by automatic annotation pipelines. In addition to the exclusive use of temporal expression data, structural data analysis is gaining traction in the characterization and classification of effectors (de Guillen *et al.*, 2015; Seong & Krasileva, 2021; Rocafort *et al.*, 2022; Seong & Krasileva, 2023; Yu *et al.*, 2024). Among the newly discovered effector candidates, we uncover a specific head-to-head oriented pair which is present in several copies in the genome, some copies of which have undergone pseudogenization. Both the head-to-head orientation and the structural similarity suggests this effector pair is part of a larger family of similar effector pairs (Blekemolen *et al.*, 2022; Talbi *et al.*, 2023; Talbi *et al.*, 2024; Yu *et al.*, 2024). Interestingly, we find more distantly related fungal pathogens that only contain one

of the effectors of this pair. The phylogenetic distribution of this effector is highly suggestive of horizontal gene transfer. Several of these effector pairs function together through physical interactions and some can affect cell-to-cell movement (Cao *et al.*, 2018; Ayukawa *et al.*, 2021; Blekemolen *et al.*, 2022; Talbi *et al.*, 2024; Yu *et al.*, 2024). However, the absence of half of the pair in both *F. xylarioides* and *V. dahliae* raises questions on the functionality of this effector in these fungi. Moreover, the presence of several pseudogenized copies for this effector pair calls for further study into their evolutionary history. Whether or not this effector pair also physically interacts and has similar functions awaits further investigation.

In our experiments using several knockout mutants of effector gene candidates on the accessory region, no significant reduction in virulence was observed. This might be a consequence of effector redundancy or more subtle attenuation of the infection that we did not measure in this study. Effector redundancy has been previously observed in both fungal and bacterial plant pathogens (Kvitko *et al.*, 2009; Pliego *et al.*, 2013; Ali *et al.*, 2014; Brefort *et al.*, 2014). It was recently shown that loss of accessory chromosome 12 leads to a significant reduction in virulence, but not a complete loss of pathogenicity (Dijkstra *et al.*, 2024), (Chapter 3). This indicates that virulence might only be affected after larger changes affecting multiple effectors or virulence related genes. Study of double or multiple knockouts, as well as infection assays on resistant banana genotypes might shed more light on the function of these effectors. As single effector knockouts sometimes have little effect on the virulence level, another approach to determine important virulence factors could be to focus on shared regulators of genes likely involved in virulence. Accessory chromosomes also contain transcription factors that can regulate the expression of other (accessory) virulence related genes (Jonkers *et al.*, 2014; Niño-Sánchez *et al.*, 2016; van der Does *et al.*, 2016). Some transcription factor families have seen specific copy number expansions on accessory regions of the genome (Yu, H. *et al.*, 2023).

Next to direct virulence, our use of the AMAPEC prediction tool indicates that some of the accessory effectors might play a role in microbial competition, as has been shown previously for other plant pathogen effectors (Snelders *et al.*, 2020; Snelders *et al.*, 2021). Culture filtrate of strain II5 showed clear antimicrobial activity against both a Gram-positive and Gram-negative bacterium. The culture filtrate of the accessory effector knockouts did, however, not show significant difference compared to the wildtype. The antimicrobial potential of these effectors can be investigated more closely using heterologously produced protein to avoid differences in protein production and stability during cultivation. Furthermore, the antimicrobial effect can be limited to a narrow range of microbes (Snelders *et al.*, 2020; Snelders *et al.*, 2021). The structural similarity of effectors 1g02190 and 12g00300 to KP6 could further support their potential antimicrobial role as KP6 was originally discovered

as dsRNA encoded killer toxin in *U. maydis* (Tao et al., 1990). Homologs of KP6 were recently discovered in *Zymoseptoria tritici* and have antifungal properties (de Guillen *et al.*, 2024). However, in the same study, subgroups in KP6 proteins were detected separating those with known antifungal activity from those known to play a role in cell-cell movement which might indicate an evolutionary separation of these two functions. In contrast to the other knockout mutants, the culture filtrate of the RiPP mutant, did show reduced antimicrobial activity against the Gram-positive *Bacillus* spp., warranting further investigation into the exact product of this biosynthetic gene cluster. The upregulation of this RiPP precursor gene in other *Fusarium* pathogens during infection (van der Does *et al.*, 2016; Ayukawa *et al.*, 2021) might highlight a wider importance of the produced modified peptide. Identification of the exact peptide is crucial for further investigation.

Together, we used temporal expression data to improve the genome annotation of TR4 reference strain II5. The resulting curated genome was used to identify effector candidates important for infection of Cavendish bananas. We uncovered a highly expressed effector pair, part of a larger structural family of effector pairs. However, knockout of two individual accessory effectors did not lead to reduced virulence levels, suggesting potential effector redundancy or alternative roles, such as microbial competition. Further investigation of individual effectors, multiple knockouts and alternative roles besides virulence will be essential to understand the *Fusarium*-banana interaction.

Materials and methods

Fungal growth conditions and transformation

Fusarium oxysporum Tropical Race 4 (TR4) strains II5, ΔAC12 6.4 (Dijkstra *et al.*, 2024), (Chapter 3) and newly generated II5 mutant strains were routinely cultured on PDA plates at 25 °C. Conidial suspensions of all strains were stored as 15% glycerol stocks at –80 °C.

Effector knockout mutants were generated using CRISPR-Cas9 as previously described (Dijkstra *et al.*, 2024), (Chapter 3). Used primers are listed in Table S2.

RNA extraction and sampling

Cavendish 'Grand Naine' banana plants were grown in a greenhouse compartment (28 ± 2°C, 16 h light, and 85% relativity humidity). The roots of 2.5-month-old plants were dip-inoculated with 10^6 spores per ml. RNA was extracted from the roots of inoculated plants at 4 days post inoculation (dpi), 8 dpi, and 30 dpi. Additionally,

RNA was extracted from mycelium grown on potato dextrose agar (PDA) medium and filtered conidia after growth in potato dextrose broth (PDB) medium. Samples were taken in triplicate. After collection, samples were ground and RNA extraction was performed using the Maxwell Plant RNA kit (Promega, Madison, WI, USA) following the manufacturer's instructions. RNA sample quality was tested by agarose electrophoresis and quantified by Nanodrop (Thermo Fisher, Waltham, MA, USA). Subsequently, samples were sent to KeyGene (Wageningen, the Netherlands) for sequencing.

Expression analysis and genome curation

Mapping and quantifying gene transcripts from sequenced RNA-seq reads of all samples were performed using Kallisto (v0.44.0) (Bray *et al.*, 2016), with a 100-bootstrap value. Subsequently, an R package Sleuth (v0.30.0) was used for differentially expressed gene analyses (DEG) (Pimentel *et al.*, 2017). Gene expression clustering analysis was performed using an R package ClusterGVis (Zhang, 2022). Expression informed collaborative curation of the TR4 II5 genome was performed using Web Apollo (Lee *et al.*, 2013). Initial automatic annotation was performed using Funannotate (Palmer & Stajich, 2020).

Sequence analyses

Gene-wide Relative Synonymous Codon Usage (RSCU) values were calculated for all genes on the curated genome of TR4 II5 using BioKIT (Steenwyk *et al.*, 2022). The RSCU values were correlated to expression levels using the ggstats R package (Larmarange, 2025).

RiPP clusters orthologous to the *2g20200* containing cluster in TR4 strain II5 were obtained using cblaster (Gilchrist *et al.*, 2021), limited to *Fusarium* spp., and visualized using clinker (Gilchrist & Chooi, 2021).

Protein sequence and structure analysis

Protein sequence alignments were made using Clustal Omega (Sievers *et al.*, 2011) and visualized using ESPRipt 3.0 (Robert & Gouet, 2014).

Protein structures of novel effector candidates were predicted using AlphaFold2 (Jumper *et al.*, 2021). Newly generated protein structures were subsequently used as query structures against the PDB database with use of the Dali server (Holm, 2022). Newly generated AlphaFold2 models were also compared to known effector structures using Dali pairwise comparisons. Protein structures were visualized using ChimeraX (Meng *et al.*, 2023). Potential antimicrobial properties were predicted using AMAPEC with the newly generated AlphaFold2 models (Mesny & Thomma, 2024).

Plant growth conditions and infection assays

Cavendish 'Grand Naine' plants were grown in the greenhouse at a day/night temperature of 25/23 °C and a day length of 16 hours with 80% relative humidity.

Infection assays of Cavendish 'Grand Naine' banana plants were performed as described previously (García-Bastidas *et al.*, 2019).

In vitro antimicrobial assays

Antimicrobial assays using culture filtrate were performed as described previously (Snelders *et al.*, 2020) with slight modifications. TR4 strain II5 and effector knockout mutants were grown in PDB at 25 °C and 150 rpm. Cultures were filtered after 7 days through a 0.2 nm filter to obtain the culture filtrate. Culture filtrate was stored at –20 °C until use.

Overnight grown single colonies of *Bacillus* spp. and *Acinetobacter* spp. were picked from LBA plates and grown overnight in LB at 28 °C and 200 rpm. Overnight cultures were diluted to OD600=0.05 using LB and supplemented with culture filtrate to a final OD600=0.025. Lastly, 200 µl of the bacterial and culture filtrate mixture was incubated clear 96-well flat-bottom polystyrene tissue culture plates. The plates were incubated in a CLARIOstar plate reader at 25 °C with double orbital shaking every 15 minutes. The OD600 was measured every 15 minutes.

For colony growth formation tests the same procedure was used except the volumes were increased to 2 mL of LB and culture filtrate. Following the culture filtrate treatment, LB plates were inoculated with 10 µl of the mixture and incubated at 25 °C for 24 hours.

Acknowledgements

The authors would like to thank Anouk van Westerhoven, Maikel Steentjes, Harold Meijer, Einar Martínez de la Parte, Rahim Mehrabi, Sen Xie and Lisanne Kottenhagen for their contributions to the curation of the genome of TR4 strain II5. Sen Xie and Desalegn Etalo are thanked for providing the *Bacillus* and *Acinetobacter* isolates.

JD, CAG, GNT and GHJK were supported by the Bill and Melinda Gates Foundation, grant no.: AG – 4425. Banana research at Wageningen University has been supported by the Dutch Dioraphte Foundation, grant no.: 20 04 04 02.

Competing interests

None declared.

Author contributions

JD conducted experiments and performed analyses. SDG, CAG, and GNT conducted experiments. XSK performed analyses. JD wrote the manuscript with input from GHJK and XSK. All authors contributed to writing and editing the manuscript. GHJK conceived and supervised the project.

Data availability

All data are available in the main text or in the supporting information (Figs S1-S10; Table S1-2).

Supplementary materials

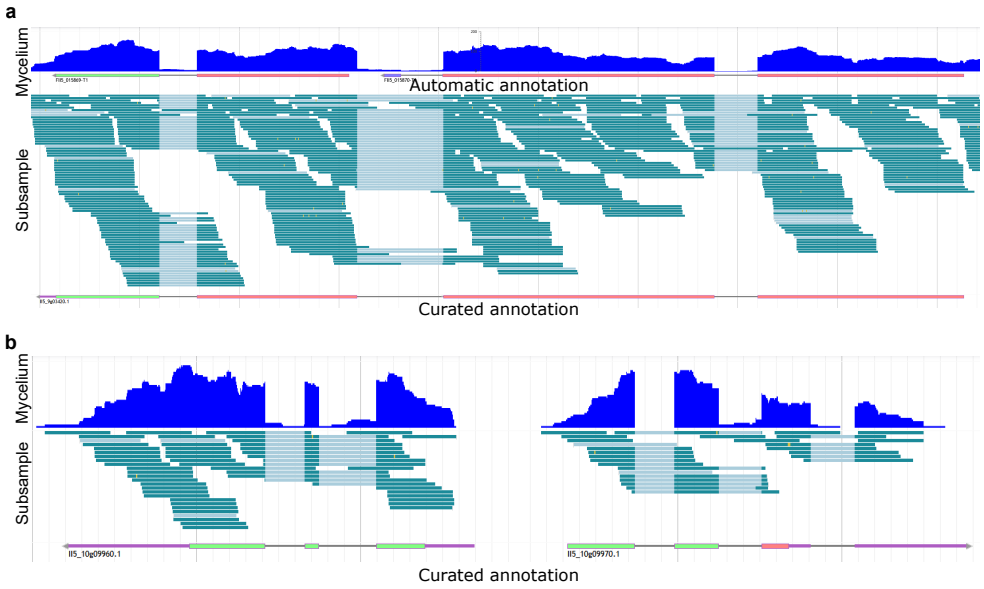


FIGURE S1 | Examples of adjusted gene models through curation of the genome of TR4 strain II5. **a**) Example of curated merger of two automatically annotated gene models to a single gene model based on expression evidence. **b**) Example of two newly added gene models based on expression evidence. Both newly added gene models encode effector candidates. For both **a**) and **b**) the aggregated expression from mycelium samples is shown as well as subsamples showing individually mapped reads. The new curated annotations are displayed below. View obtained from Web Apollo.

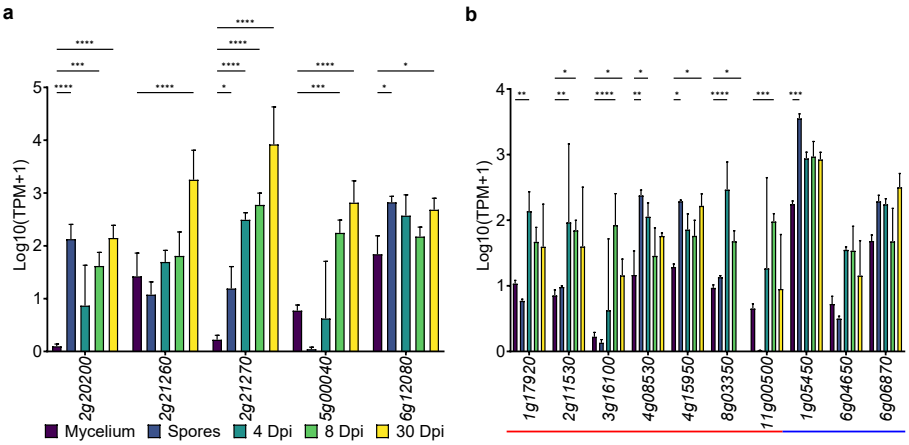


FIGURE S2 | Several core genome-encoded CAZymes, CFEM genes and effectors are upregulated during infection. a) Log_{10}(TPM+1) values for differentially expressed genes on the core genome regions encoding effectors of TR4 strain II5 during vegetative growth or infection of Cavendish banana plants. **b**) Log_{10}(TPM+1) values for differentially expressed CAZyme (red underlined) and CFEM (blue underlined) encoding genes on core chromosomes of TR4 strain II5 during vegetative growth or infection of Cavendish banana plants. For both **a**) and **b**) Asterisks indicate significant p values following Dunnett's test using mycelium TPM values as control. Error bars indicate SD. For significance, * P≤0.05, ** P≤0.01, *** P≤0.001, **** P≤0.0001.

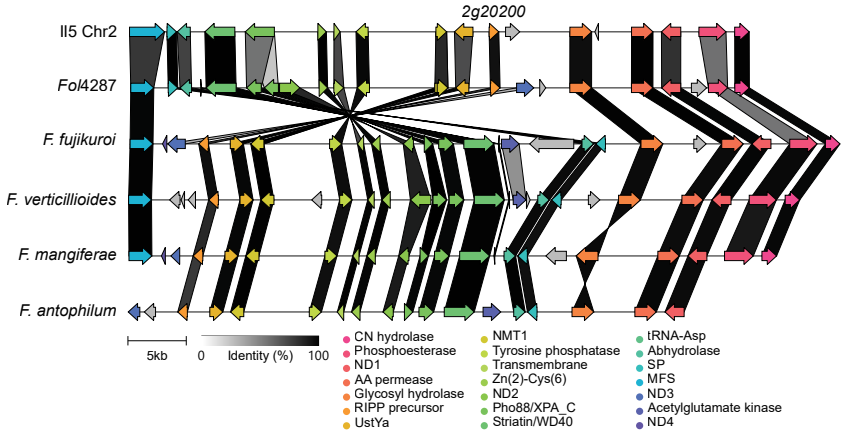


FIGURE S3 | *2g20200* is part of a conserved RiPP biosynthetic gene cluster. Alignment of RiPP biosynthetic gene cluster containing *2g20200* as precursor peptide between several *Fusarium* spp. ND indicates no detected domain.

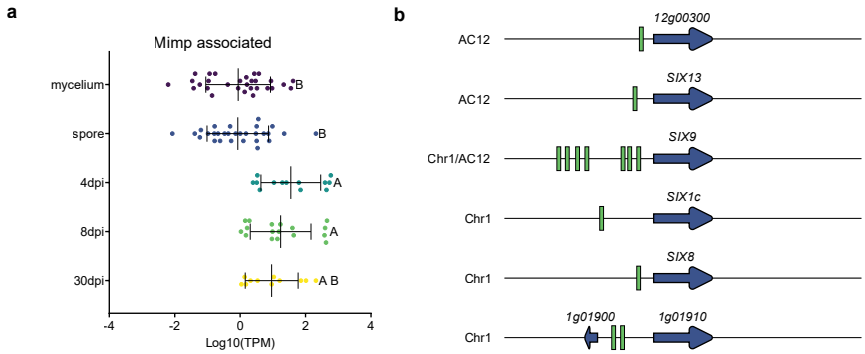


FIGURE S4 | Several effectors are associated with *mimps*. a) Scatterplot displaying average Log_{10}(TPM) expression levels of *mimp*-associated genes (*mimp* < 2.5 kb upstream) for TR4 strain II5 in mycelium, spores and 4-, 8- or 30-days post inoculation of Cavendish roots. Different letters indicate significant differences between treatments (Kruskal-Wallis test; P<0.05). Data are shown as mean ±SD. **b**) Schematic scale representation of known and novel effector candidates with a *mimp* TIR within 2 kb upstream.

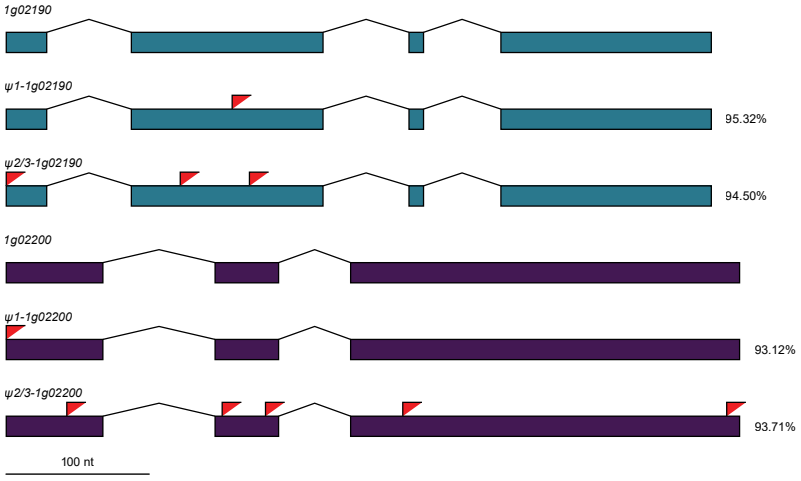


FIGURE S5 | Duplicated effector pair has additional pseudogenized copies. Schematic scale representation of effector genes *1g02190* and *1g02200* and their pseudogene copies. For both *1g02190* and *1g02200* pseudogene copies 2 and 3 are identical. Lacking start codons or premature stop codons are indicated by red markers. Nucleotide identity compared to the functional gene copies are indicated on the right. The scale denotes a length of 100 nucleotides.

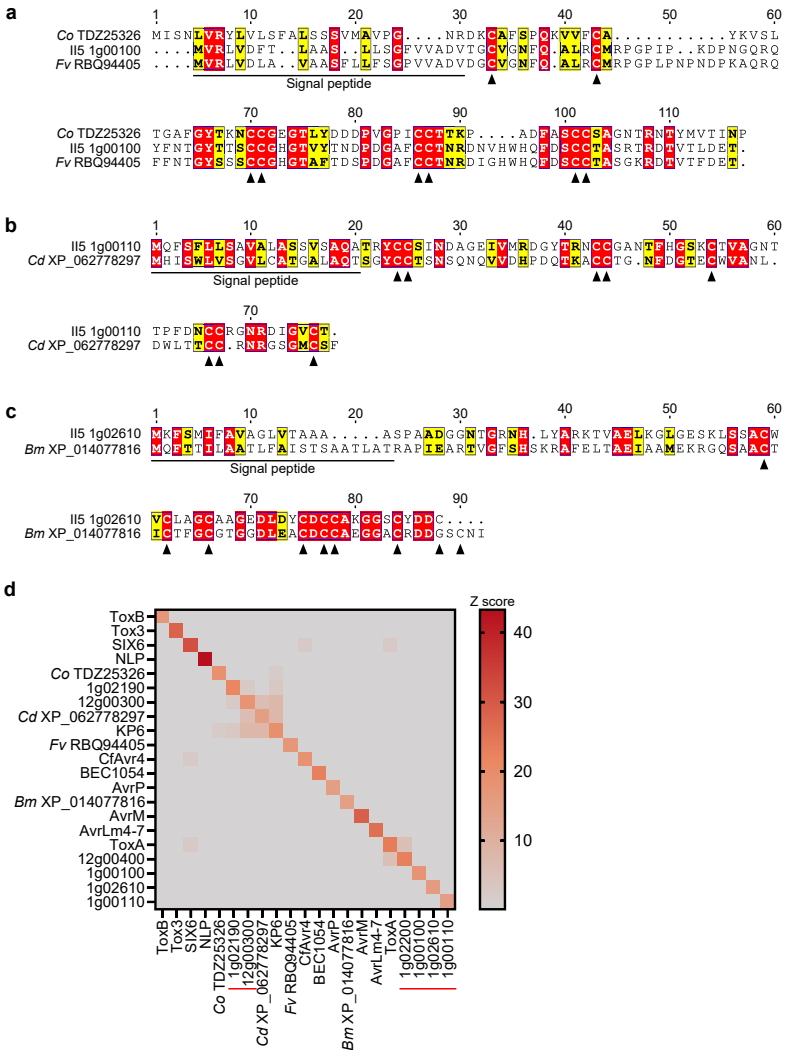


FIGURE S6 | Accessory genome-encoded effectors have low similarity to effectors in other fungal plant pathogens. a) Amino acid alignment of Il5 1g00100 and closest orthologs. Predicted signal peptide is underlined, and cysteine residues are indicated by black triangles. *Co, Colletotrichum obiculare; Fv, Fusarium verticillioides.* **b**) Amino acid alignment of Il5 1g00110 and closest ortholog. Predicted signal peptide is underlined, and cysteine residues are indicated by black triangles. *Cd, Colletotrichum destructivum.* **c**) Amino acid alignment of Il5 1g02610 and closest ortholog. Predicted signal peptide is underlined, and cysteine residues are indicated by black triangles. *Bm, Bipolaris maydis.* **d**) Heatmap depicting structural similarity between AlphaFold2 models of novel effector candidates (red underlined), selected orthologs, and crystal structures of characterized effectors using Dali pairwise comparison.

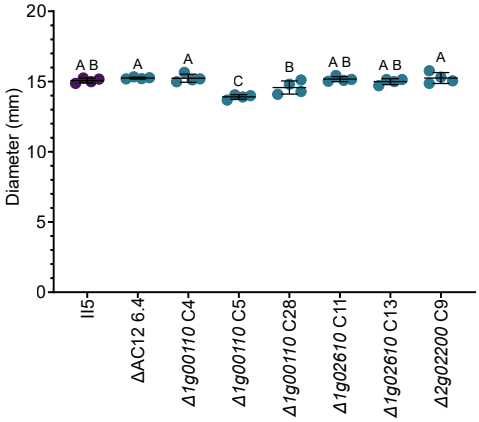


FIGURE S7 | Growth of effector knockouts. Colony diameter (mm) of TR4 strain II5 and mutant strains on PDA. Growth was quantified at 3 days post inoculation (dpi). Letters indicate significant differences between treatments (Tukey-Kramer test; P<0.05). Data are shown as mean ±SD (n=4).

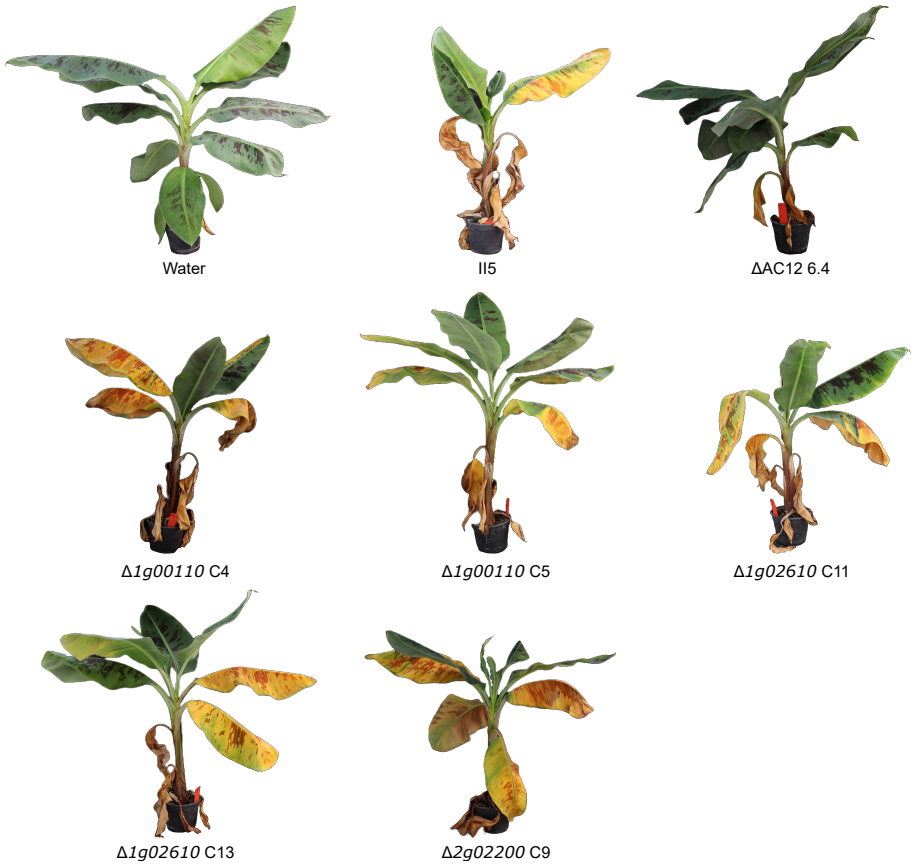


FIGURE S8 | Enlarged photos of external symptoms. Larger versions of the photos used in Fig. 4b.

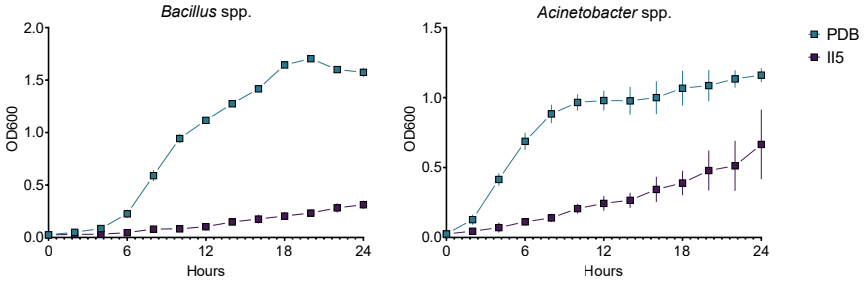


FIGURE S9 | Culture filtrate of TR4 strain II5 shows antimicrobial activity. Growth measurements (OD600) for a *Bacillus* and *Acinetobacter* isolate in LB supplemented with PDB (control) or culture filtrate obtained from a 7-day old II5 liquid culture. Bars represent ±SD (n=8).

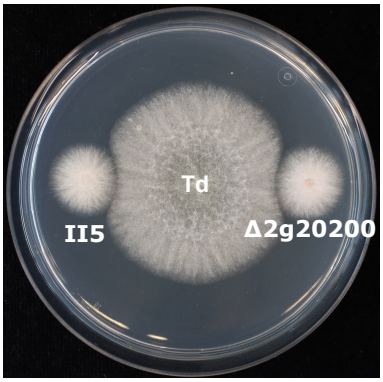


FIGURE S10 | Knockout of RiPP precursor gene does not affect antimicrobial activity against *Trichoderma* spp. PDA plate inoculated with wildtype TR4 strain II5, *Trichoderma* spp. and RiPP precursor gene knockout Δ*2g20200*. The photo was taken at 2 dpi.

TABLE S1 | Several accessory genome-encoded effectors have high predicted probability for antimicrobial activity. Table displaying the predicted local distance difference test value for local structural confidence of structure prediction (pLDDT) and AMP probability as predicted using AMAPEC on Alphafold2 generated protein structures for several accessory effectors.

Gene ID	pLDDT	AMP Probability	Prediction
1g00100/12g00320	39.187	0.831	Antimicrobial
1g00110	48.715	0.994	Antimicrobial
1g02190/12g00410	51.781	0.631	Antimicrobial
1g02200/12g00400	53.953	0.358	Non-antimicrobial
1g02610	58.729	0.850	Antimicrobial
12g00300	77.088	0.528	Antimicrobial
SIX6	74.169	0.298	Non-antimicrobial

TABLE S2 | Primers used in this study.

Primer name	Sequence 5′-3′	Purpose
II5_1g00110_9gRNA_F	CTCGTGAACGGAGCATAACATACCTCG	Cas9 plasmid
II5_1g00110_9gRNA_R	AAACCGAGGTATGTTATGCTCCGTTCA	-
II5_1g00110_9gRNA_F2	CTCGATTTATAGAGCAGCAATAACGCG	-
II5_1g00110_9gRNA_R2	AAACCGCGTTATTGCTGCTCTATAAAT	-
II5_1g02610_9gRNA_F	CTCGCTGGAAGAAATCACCTTTATGCA	-
II5_1g02610_9gRNA_R	AAACTGCATAAAGGTGATTTCTTCCAG	-
II5_1g02610_9gRNA_F2	CTCGAGGAAGACAGTTGCAGAGCTCAA	-
II5_1g02610_9gRNA_R2	AAACTTGAGCTCTGCAACTGTCTTCCT	-
II5_2g20200_9gRNA_F	CTCGTCCATAAGTAGTATATCCAGGAG	-
II5_2g20200_9gRNA_R	AAACCTCCTGGATATACTACTTATGGA	-
II5_2g20200_9gRNA_F2	CTCGAGCCAGAGTGAGGAGTGTAACAG	-
II5_2g20200_9gRNA_R2	AAACCTGTTACACTCCTCACTCTGGCT	-
1g00110up_F	AACCCGAAACTCTGCTTGCT	Donor template
1g00110up_R	cactagctccagccaagcccaaaaaAGGCAGCTGGAACACCTTAT	-
NatR_1g0110_F	ATAAGGTGTTCCAGCTGCCTtttttgggcttggctggagctagtg	-
NatR_1g0110_R	AGATTTACCACCTAAGATTGTTTGActcactgatacatctggcacctact	-
1g00110down_F	agtaggtgccagatgtatcagtgagTCAAACAATCTTAGGTGGTAAATCT	-
1g00110down_R	TTCCAAAGAGACCCACAGGA	-
1g02610up_F	TGCCGACAATACATACCGA	-
1g02610up_R	cactagctccagccaagcccaaaaaTTTCGTCGAGGTTATAGTAAGA	-
NatR_1g02610_F	TTACTATAACCTCGACGAAAttttttgggcttggctggagctagtg	-
NatR_1g02610_R	AGCCTCTTTGTCCCACTACActcactgatacatctggcacctact	-
1g02610down_F	gtgccagatgtatcagtgagTGTAGTGGGACAAAGAGGCT	-
1g02610down_R	GCGAAACTGCGTTGTCCTAAG	-
2g20200up_F	CAGAAAGCCACAATCACTACTGT	-
2g20200up_R	cactagctccagccaagcccaaaaaGACGCCTCTTAGATGTACAGAAA	-
NatR_2g20200_F	TTTCTGTACATCTAAGAGGCGTCtttttgggcttggctggagctagtg	-
NatR_2g20200_R	ATTGTTTCACCAGATTCTTAGctcactgatacatctggcacctact	-
2g20200down_F	agtaggtgccagatgtatcagtgagCTAAGAATCTGGTGAAACAAT	-
2g20200down_R	GTCTACGATGGCTTCAGTC	-
II5_1g00110screen_F	TAACCTCTTCTCCTCGCCCA	Screening
II5_1g00110screen_R	TCCGTAAGTTCCGAGAGTTGC	-
II5_1g00110genescreen_F	AATATCACGGTTACCCCGGC	-
II5_1g00110genescreen_R	CAGCTGTTGCTTTAGCCTCG	-
II5_1g00110screen_F2	GGCCCAACCTCCGTAAATCC	-
II5_1g00110screen_R2	CCCCTAGACAAGTCAAGATTTCCA	-
II5_1g02610screen_F	CTTTGCTGAGGAGGTTTGCC	-
II5_1g02610screen_R	ACCAACCACGACTACTGAGG	-
II5_2g20200_screen_F	AGCTGTGAGACTGATACGAGG	-
II5_2g20200_screen_R	GACATCGGAGAACAACCCCC	-
II5_2g20200_screen_F2	CGTGAGGCTGAGGTGAATCT	-
II5_2g20200_screen_R2	TCTCTCCGGGAGTAAAGCGA	-
II5_2g20200genescreen_F	ACCGCTGTTACACTCCTCAC	-
II5_2g20200genescreen_R	AACTCCTTGGCACGCTTGTA	-

Chapter 3

Extensive intrachromosomal duplications in a virulence-associated fungal accessory chromosome

Jelmer Dijkstra[1¶]
Anouk C. van Westerhoven[1,2¶]
Lucía Gómez-Gil[3]
Carolina Aguilera-Galvez[1,4]
Giuliana Nakasato-Tagami[1]
Sebastien D. Garnier[1]
Masaya Yamazaki[5,6]
Tsutomu Arie[6]
Takashi Kamakura[5]
Takayuki Arazoe[5]
Antonio Di Pietro[3]
Michael F. Seidl[2&]
Gert H.J. Kema[1&]

[1]Laboratory of Phytopathology, Wageningen University and Research, Wageningen, the Netherlands.
[2]Theoretical Biology & Bioinformatics Group, Department of Biology, Utrecht University, Utrecht, the Netherlands.
[3]Departamento de Genética, Facultad de Ciencias, Universidad de Córdoba, Campus de Excelencia Agroalimentario (ceiA3), Córdoba, Spain.
[4]Área de Sistemas Naturales y Sostenibilidad, Escuela de Ciencias Aplicadas e Ingeniería, Universidad EAFIT, Medellín, Colombia.
[5]Faculty of Science and Technology, Tokyo University of Science, Yamazaki, Noda, Chiba, Japan.
[6]Graduate school of Agriculture, Tokyo University of Agriculture and Technology (TUAT), Saiwai-cho, Fuchu, Tokyo, Japan.
[¶]These authors contributed equally to this work.
[&]These authors contributed equally to this work.

Abstract

Filamentous fungi have evolved compartmentalized genomes consisting of conserved core regions and dynamic accessory regions, which aid the adaptation to changing environments including the interaction with host organisms. In the *Fusarium oxysporum* species complex, accessory regions play an important role during infection and it has been reported that these regions undergo extensive duplications, however, it is currently unknown how such duplications shape accessory regions. Moreover, the function of accessory regions apart from encoding virulence effectors is not completely understood. Here we determined the karyotype of *F. oxysporum* Tropical Race 4 (TR4), which causes the ongoing pandemic of Fusarium wilt of banana (FWB). We show that the single accessory chromosome of TR4 isolate II5 has undergone extensive intrachromosomal duplications, resulting in triplication of the chromosome size compared to other closely related TR4 strains. By obtaining mutant strains that have lost the accessory chromosome, we demonstrate that this chromosome is dispensable for vegetative growth but is required for full virulence on banana. Lastly, we found that the loss of chromosome 12 co-occurs with structural rearrangements of core chromosomes, which are generally colinear between members of the *F. oxysporum* species complex. Together, our results provide new insights into the chromosome dynamics of the banana infecting TR4 lineage of the *F. oxysporum* species complex.

Introduction

Many filamentous pathogens have evolved compartmentalized genomes divided in conserved core regions and dynamic adaptive accessory regions (Croll & McDonald, 2012; Dong *et al.*, 2015; Bertazzoni *et al.*, 2018; Torres *et al.*, 2020; Wacker *et al.*, 2023). These accessory regions likely evolved to facilitate adaptation to changing environments and host interactions (Croll & McDonald, 2012; Yu, Houlin *et al.*, 2023). Accessory regions show distinct sequence characteristics compared to their core counterparts, including a higher sequence variation, abundance in transposable elements (TEs), different codon usage, and lower gene density (Coleman *et al.*, 2009; Seidl & Thomma, 2017; Bertazzoni *et al.*, 2018; Habig & Stukenbrock, 2020). Moreover, accessory regions are usually enriched for histone modifications associated with facultative heterochromatin (Connolly *et al.*, 2013; Schotanus *et al.*, 2015; Fokkens *et al.*, 2018; Cook *et al.*, 2020). Accessory regions can either be embedded in core chromosomes or comprise entire independent chromosomes (Ma *et al.*, 2010; van Westerhoven *et al.*, 2024a).

Although the function of accessory regions is not always clear (Möller *et al.*, 2018; Ayukawa *et al.*, 2021), many have been found to play an important role in the interaction between fungi and their hosts (Johnson *et al.*, 2001; Ma *et al.*, 2010; de Jonge *et al.*, 2013; Plaumann *et al.*, 2018; Ayukawa *et al.*, 2021; Sakane *et al.*, 2024; Wei *et al.*, 2024), often by encoding secreted effector proteins (Bertazzoni *et al.*, 2018; Yang, H *et al.*, 2020). The compartmentalization into accessory regions or chromosomes may also facilitate the horizontal transfer of beneficial traits, as natural populations of different fungal species bear signs of such events (Masel, 1996; Akagi *et al.*, 2009; Barragan *et al.*, 2024; Habig *et al.*, 2024). Moreover, experimental horizontal chromosome transfer has been achieved in several species (He *et al.*, 1998; Akagi *et al.*, 2009; Ma *et al.*, 2010; van Dam *et al.*, 2017; Li *et al.*, 2020b; Habig *et al.*, 2024). Despite these recent advances, many questions on the origin and evolution of accessory regions remain unanswered (Habig & Stukenbrock, 2020).

Members of the *Fusarium oxysporum* species complex are well-known fungal pathogens containing diverse sets of accessory chromosomes and regions (Yang, H *et al.*, 2020). The accessory regions found in *F. oxysporum* strains display characteristics common to analogous regions in other fungi (Yang, H *et al.*, 2020; van Westerhoven *et al.*, 2024a), including the presence of effector genes that play an important role in virulence (Ma *et al.*, 2010; Li *et al.*, 2020a; Li *et al.*, 2020b; Ayukawa *et al.*, 2021; Sakane *et al.*, 2024). Furthermore, horizontal acquisition of accessory chromosomes in a non-pathogenic strain can enable the recipient strain to infect a new plant species (Ma *et al.*, 2010). Importantly, accessory effector profiles are often shared between strains infecting the same or a similar host (van Dam *et al.*, 2016; Brenes Guallar *et al.*,

2022). Loss of accessory chromosomes has been experimentally induced in several *F. oxysporum* strains (van Dam *et al.*, 2017; Ayukawa *et al.*, 2021; Sakane *et al.*, 2024). For example, the induced loss of a small accessory chromosome in *F. oxysporum* f.sp. *radicis-cucuminerum* resulted in complete loss of virulence on cucurbit hosts (van Dam *et al.*, 2017).

Fusarium oxysporum strains infecting banana, the causal agents of Fusarium Wilt of Banana (FWB), are separated into three different races (race 1, race 2, and tropical race 4) based on their virulence profile against different banana cultivars (Ploetz, R. C., 2015), and contain a diverse set of accessory regions (van Westerhoven *et al.*, 2024a). The current FWB epidemic is caused by tropical race 4 (TR4) that can infect various banana varieties including Cavendish, which is widely used by the banana industry (Ordóñez *et al.*, 2015). TR4 isolates are highly similar and have recently been reclassified into the species *F. odoratissimum* (Maryani *et al.*, 2019). The TR4 reference strain II5 contains two large accessory regions: one is part of core chromosome 1 and the other is an independent accessory chromosome named AC12, which encodes various pathogenicity genes (van Westerhoven *et al.*, 2024a). Previous work discovered signs of large-scale duplications in the accessory genome of *F. oxysporum* strains, including a copy number increase in the AC12 sequence in a subset of sequenced TR4 strains (van Westerhoven *et al.*, 2024a). On the other hand, a recent independent study reported that the TR4 reference strain II5 lacks conventional accessory chromosomes and contains only accessory regions attached to core chromosomes (Zhang, Y *et al.*, 2024), which is in contrast to most thus far studied *F. oxysporum* isolates that can infect banana and other hosts (Ma *et al.*, 2010; van Dam *et al.*, 2017; Ayukawa *et al.*, 2021; Sakane *et al.*, 2024; van Westerhoven *et al.*, 2024a). Given the importance of TR4 for global banana production, these findings raise important questions about the karyotype of TR4 strain II5, the evolution of accessory chromosomes, and their roles in virulence. Here, we show that TR4 strains have an independent accessory chromosome named AC12. In the reference strain II5, AC12 is three times larger than previously reported (van Westerhoven *et al.*, 2024a) and has evolved through repeated intrachromosomal duplications. We further show that mutant strains without AC12 show attenuated virulence on banana plants as well as reduced abiotic stress responses.

Results

Intrachromosomal duplications cause size expansion of accessory chromosome 12 in a TR4 strain

Accessory chromosomes in *F. oxysporum* are known to encode many predicted secreted effector proteins, play a role in virulence, and evolve by segmental duplications (Ma *et al.*, 2010; Armitage *et al.*, 2018; Navasca *et al.*, 2024; van Westerhoven *et al.*, 2024a). The accessory chromosome AC12 of the TR4 reference strain II5 encodes 290 predicted genes. These include 13 putative secreted effectors such as the Secreted In Xylem (*SIX*) genes *SIX9* and *SIX13* (Schmidt *et al.*, 2013), suggesting a putative role of AC12 in pathogenicity on banana. Here we confirmed these results and found that AC12 also contains genes with predicted functions in high osmolarity and cell wall stress response (Fig. 1a). Chromosome alignments showed a high similarity between AC12 from the TR4 strains II5 and M1 (Fig. 1b), which were assembled into approximately the same size (1.11 Mb for strain II5; 1.08 Mb for strain M1). However, we previously noted that AC12 from II5 has a two-to-four-fold increase in copy number compared to the genome-wide average, which is absent in AC12 from M1 (Fig. 1b,(van Westerhoven *et al.*, 2024a)). Importantly, while AC12 is present in all 34 previously sequenced TR4 isolates (van Westerhoven *et al.*, 2024a), in most of them no copy number polymorphism was detected (Fig. 1c), but we observed a copy number increase similar to that of II5 in four TR4 isolates from the Middle East (Fig. 1c). However, these four isolates are not closely related to II5, based on single-nucleotide polymorphisms on the core chromosomes, suggesting that the copy number increase of AC12 has occurred independently multiple times (Fig. 1c).

The observed copy number increase of AC12 in II5 could be explained either by the presence of multiple separate copies of the AC12 chromosome (aneuploidy) or by large-scale internal duplications. To discriminate between these two hypotheses, we performed karyotyping of sequenced *F. oxysporum* strains using Contour-Clamped Homogeneous Electric Field (CHEF) gel electrophoresis (Fig. 1d). We included two TR4 strains, II5 showing a copy number increase, and M1 without a copy number increase (see Fig. 1b-c). We also included a banana pathogenic R1 strain CR1.1 carrying a 1.57 Mb accessory chromosome that is not homologous to AC12 (van Westerhoven *et al.*, 2024a). As a size standard, the well characterized tomato pathogenic isolate *Fol*4287(Ma *et al.*, 2010) was included. The CHEF gels showed the presence of a small chromosome (≤1.5 Mb) in both the M1 and CR1.1 strains, corresponding to the expected sizes of the small accessory chromosome assemblies (1.08 Mb for strain M1; 1.57 Mb for strain CR1.1; Fig. 1d). By contrast, II5 lacks a chromosome band at the position of the expected size for AC12 (1.1 Mb). Southern blot analysis using a probe

specific for AC12 showed a distinct hybridizing signal at the position coinciding with the smallest chromosome band of 1.08 Mb in M1, whereas in strain II5 the signal coincided with a chromosome band of a much larger size around 3.5 Mb (Fig. 1d). Importantly, the AC12-specific probe did not show a hybridization signal in R1 strain CR1.1, indicating that the signal is indeed specific for the TR4 accessory region (Fig. 1d). Thus, the size of AC12 in isolate II5 is approximately three times larger than in M1 (1.1 Mb). Together with the observed differences in chromosome coverage (van Westerhoven *et al.*, 2024a) (Fig. 1b), these findings demonstrate that AC12 has undergone extensive intrachromosomal duplications in strain II5.

It has recently been reported that TR4 strain II5 lacks conventional accessory chromosomes (Zhang, Y *et al.*, 2024), suggesting that the analyzed AC12 is not present as a separate chromosome. However, we do find a separate scaffold in the published TR4 genome assembly, which has been reported to lack accessory chromosomes (Zhang, Y *et al.*, 2024), that is homologous to AC12 in strain II5 and M1 (scaffold 101, Fig. S1). Additionally, the CHEF gel clearly demonstrates an independent accessory chromosome in TR4, either as the smallest chromosome (M1) or as a larger chromosome that underwent intrachromosomal duplications (II5). Thus we concluded that TR4 isolates carry conventional accessory chromosomes.

The fact that the intrachromosomal duplications are collapsed in the genome assembly (1.1 Mb in the assembly vs. ~3.5 Mb observed by CHEF analysis; Fig. 1b) indicates that these duplications are highly similar, thus preventing their separation during initial genome assembly. To unfold the assembly, we attempted to separate the duplicated reads but were unable to further improve the assembly due to the lack of sequence variation. The high similarity of the duplications strongly indicates that this evolutionary event occurred very recently. Moreover, the increase in chromosome size together with the 2x-4x increase is reminiscent of duplications caused by breakage-fusion-bridge cycles (BFB) (Croll *et al.*, 2013) (Fig. S2). Furthermore, the same duplications in AC12 were observed in three versions of the II5 isolate that are maintained independently for many years in three different laboratories (Fig. S3), showing that this chromosome duplication is stable.

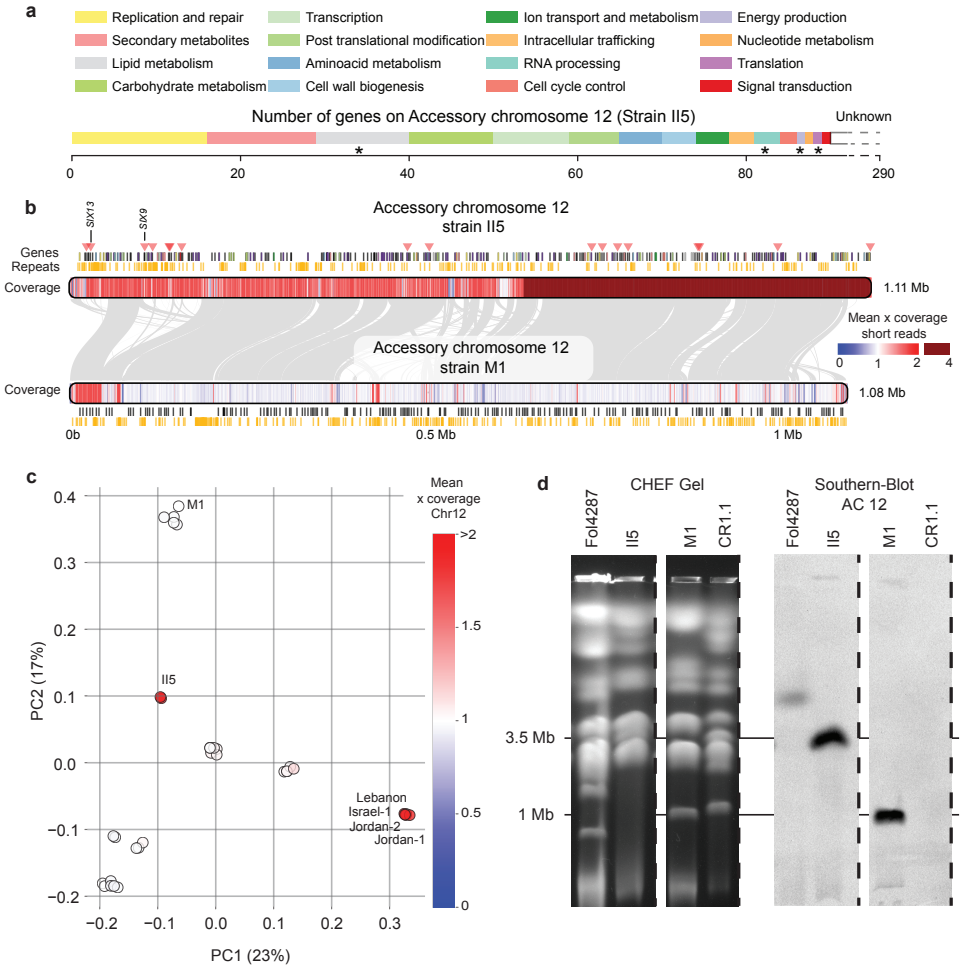


FIGURE 1 | Composition of accessory chromosome 12 (AC12) in the TR4 reference strain II5. a) Predicted functional categories of the genes located on AC12. Most of the genes (200) are of unknown function. Asterisks indicate gene categories significantly enriched on AC12 compared to the rest of the genome (Fisher-exact test, $P < 0.05$). **b**) Chromosome alignment of AC12 from isolates II5 and M1. Note that the accessory chromosomes of both strains are highly similar. Positions of predicted effector genes, including two Secreted In Xylem genes (*SIX9* and *SIX13*), are indicated by red triangles. The short-read coverage indicates a copy number increase (dark red) in II5, whereas one copy (white) is present in M1. **c**) Principal component analysis based on single-nucleotide polymorphisms (SNPs) located on the core genome of 35 TR4 strains. A copy-number increase of AC12 is found in strain II5 and in four strains from the Middle East (red dots), which are genetically different, suggesting that the event occurred independently multiple times. **d**) CHEF gel showing size-based chromosome separation of *Fusarium oxysporum* strains *Fol*4287, II5, M1, and CR1.1 and Southern blot of the separated chromosomes with a AC12 specific probe . Note that the chromosome band hybridizing to the AC12 probe is approximately 1 Mb in M1 whereas it is around 3.5 Mb in II5. Dashes indicate cropping of the gel image. The complete gel is depicted in Fig. S13.

Accessory chromosome 12 is dispensable for vegetative growth

To investigate the function of AC12, we obtained chromosome loss mutants of TR4 strain II5. A transformant of II5 carrying a hygromycin resistance cassette inserted in the *SIX13* gene located on AC12 (II5:Δ*SIX13*) was subjected to treatment with benomyl. Seven independent colonies that had lost hygromycin resistance were obtained, and loss of AC12 was initially confirmed by PCR with AC12-specific primers (Fig. S4). The putative mutants were then sequenced to corroborate the complete loss of AC12 and check for potential additional genomic changes. Mapping of the short reads to the II5 reference genome assembly confirmed the complete loss of AC12 in all seven mutants. Importantly, we did not observe other large-scale deletions after benomyl treatment (Fig. 2a), producing similar mapping as in the wild-type strain except for AC12 loss (Fig. S5). In addition, the loss of AC12 was independently confirmed for three of the mutants by CHEF electrophoresis revealing that all three had lost the chromosome band of approximately 3.5 Mb (Fig. 2b). The hybridization signal of the 3.5 Mb band was absent in the mutants in the Southern blots, further confirming the loss of AC12 in these strains. None of the chromosome loss mutants was affected in growth on PDA plates (Fig. S6), indicating that AC12 is dispensable for vegetative growth of isolate II5. Furthermore, loss of AC12 did not impair vegetative compatibility with II5 (Fig. S7). Although AC12 loss did not affect vegetative growth or vegetative compatibility, AC12 mutants were slightly affected in their tolerance to high salinity and cell wall related stress (Fig. S8).

Besides the loss of AC12, the CHEF gel revealed additional karyotypic differences, most notably in mutant 7.2 which showed a change in the core chromosome banding pattern (Fig. 2b). We hypothesized that the difference observed in this mutant could be the result of interchromosomal rearrangements, since sequencing did not detect loss of genetic material other than AC12 (Fig. 2a, Fig. S5). Further analysis of short-read genome assemblies uncovered several large-scale changes. Most structural variants were either deletions (6-12 deletions per mutant) or rearrangements (4-8 rearrangements per mutant) (Fig. S9). Most notably, five of the seven mutants showed interchromosomal rearrangements between chromosomes 7 and 8. Moreover, we detected rearrangements between chromosomes 1 and 2 in mutant 7.3 (Fig. S10a), between chromosomes 5 and 6 in mutant 7.2 (Fig. 2d), and between chromosomes 6 and 7 in mutant 10.1 (Fig. S10b). The rearrangement between chromosomes 5 and 6 in mutant 7.2 was independently confirmed by PCR (Fig. S11). None of the interchromosomal rearrangements between core chromosomes caused any detectable defects during vegetative growth on PDA plates (Fig. S6). In summary, these results suggest that benomyl treatment triggers interchromosomal rearrangements between core chromosomes in addition to loss of the accessory chromosome 12 in TR4 strain II5, and that none of these changes affects vegetative growth of the fungus.

Accessory chromosomes can be horizontally transferred between different *F. oxysporum* strains through vegetative hyphal fusion (Ma *et al.*, 2010; van Dam *et al.*, 2017; Ayukawa *et al.*, 2021). However, several attempts (30 plates) to transfer AC12 carrying the hygromycin resistance cassette from strain II5 to the R1 reference strain CR1.1 or to the non-pathogenic *F. oxysporum* strain *Fo*47 failed to provide any evidence for successful chromosome transfer.

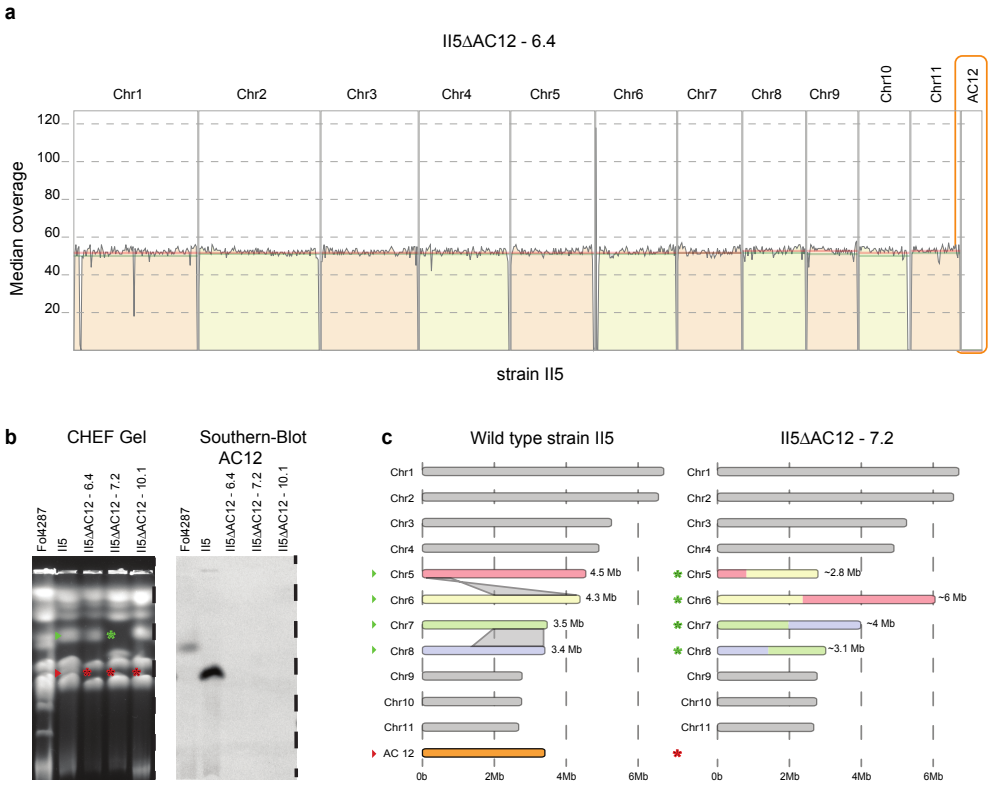


FIGURE 2 | Accessory chromosome 12 (AC12) is dispensable in strain II5. a) Mapping of Illumina short reads from the II5ΔAC12 mutant 6.4 to reference strain II5 demonstrates the specific loss of chromosome AC12. **b**) CHEF gel showing separation of chromosomes from *Fusarium oxysporum* strains *Fol*4287 and II5, and from three independent chromosome loss mutants II5ΔAC12 6.4, II5ΔAC12 7.2, and II5ΔAC12 10.1. Note the absence in the mutant lines of the AC12 chromosome band (left panel, red arrow and asterisks) and of the corresponding hybridization signal (right panel). Green arrow and asterisk indicate the position of a core chromosome that has undergone a rearrangement in mutant 7.2. The complete gel is depicted in Fig. S13. **c**) Schematic representation of the interchromosomal rearrangements observed in chromosome loss mutant II5ΔAC12 7.2. Translocations between chromosomes 5 and 6 and chromosomes 7 and 8 are highlighted by ribbons.

Accessory chromosome 12 is important for virulence of TR4 on banana plants

To determine the contribution of AC12 to virulence of TR4 on banana, plants of cultivar Cavendish were inoculated with strain II5 or with three mutants lacking AC12. Interestingly, the three mutants showed a strong reduction in corm necrosis levels, a well-established indicator for virulence (García-Bastidas *et al.*, 2019), when compared to the wild-type strain (Fig. 3a). Although the mutants were still able to infect Cavendish, the average severity of corm necrosis was 48.9% compared to 95% in the wild type. Importantly, benomyl treatment itself did not affect the virulence on Cavendish plants (Fig. S12).

Individual accessory effectors were previously shown to act as virulence factors of TR4 against banana (Widinugraheni *et al.*, 2018; An *et al.*, 2019). However, the study of some effectors has been difficult due to their duplication between the accessory region on chromosome 1 and the segmental duplications of AC12 (van Westerhoven *et al.*, 2024a). The availability of the AC12 loss mutants allows the genetic analysis of these effectors by simplifying knockout generation. To study the effect of effectors on Chr1, two independent knockout mutants of the gene *1g02190* located on the accessory region of chromosome 1, which encodes an *in planta* upregulated effector candidate, were obtained in the ΔAC12 background (ΔAC12Δ1g02190-1 and ΔAC12Δ1g02190-2). However, these effector knockout mutants did not show any additional reduction in virulence compared to the ΔAC12 mutant (Fig. 3b). By contrast, re-introducing the *12g0030*0 gene, which is unique to AC12 and encodes the only *in planta* upregulated effector, into an ΔAC12 mutant (strains ΔAC12::12g0300-1 and ΔAC12::12g0300-2), resulted in higher necrosis levels in some plants, although the difference was not significant compared with the ΔAC12 mutant. Finally, strains M1 and II5 were equally virulent, indicating that intrachromosomal duplications of AC12 do not affect virulence under greenhouse conditions. In general, external symptoms were also more severe and developed faster in the plants inoculated with the wild-type strains compared to the mutants (Fig. 3c).

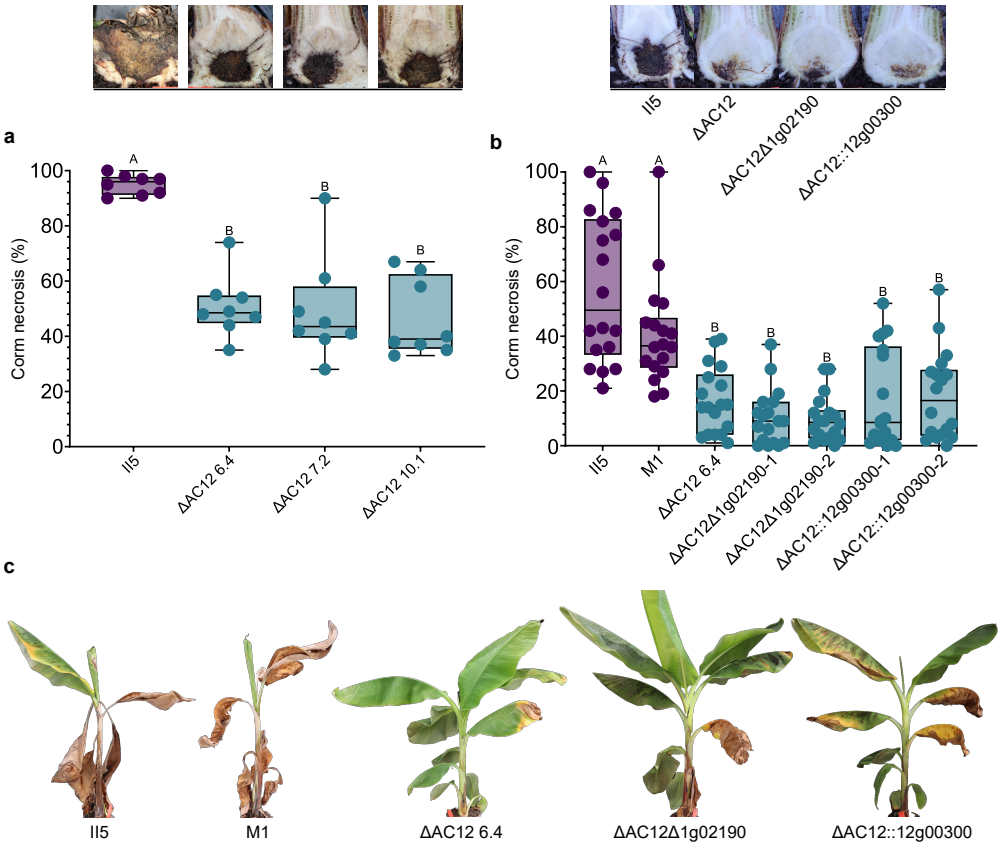


FIGURE 3 | Accessory chromosome 12 (AC12) is important for virulence of II5 on Cavendish plants. **a**) Percentage of corm necrosis of Cavendish 'Grand Naine' plants at 10 weeks post inoculation with reference strain II5 or with three independent AC12 loss mutants. Corm necrosis was quantified using ImageJ (n=8). Representative pictures of corms are displayed above. **b**) Percentage of corm necrosis of Cavendish 'Grand Naine' plants inoculated with TR4 wild type strains II5 or M1; with two independent knockout mutants in the effector gene *1g02190* obtained in the II5 ΔAC12 background (ΔAC12Δ1g02190-1 and ΔAC12Δ1g02190-2); or with two independent complemented strains where the *12g00300* gene encoding an AC12-specific effector candidate was re-introduced into an ΔAC12 background (ΔAC12::12g0300-1 and ΔAC12::12g0300-2) (n=18). Different letters indicate significant differences between treatments (Tukey-Kramer test; P<0.05). Representative pictures of corms are displayed above. **c**) Photos of external symptoms of plants analyzed in panel **b**.

Discussion

Genome compartmentalization occurs in many filamentous fungal pathogens (Dong *et al.*, 2015; Sánchez-Vallet *et al.*, 2018; Torres *et al.*, 2020; Wacker *et al.*, 2023). Accessory genomic regions show higher genetic variation compared to the core genome, which is thought to contribute to fast adaptation (Dong *et al.*, 2015; Torres *et al.*, 2020). Effector genes important for infection of the host are often located in such dynamic accessory regions (Sánchez-Vallet *et al.*, 2018). *Fusarium oxysporum* strains contain accessory regions either as independent chromosomes or as parts of core chromosomes (Ma *et al.*, 2010; van Westerhoven *et al.*, 2024a). These accessory regions play important roles in several *F. oxysporum* pathosystems (Ma *et al.*, 2010; van Dam *et al.*, 2017; Ayukawa *et al.*, 2021), exemplified by their ability to horizontally transfer pathogenicity on a given host plant from pathogenic to non-pathogenic isolates (Ma *et al.*, 2010; van Dam *et al.*, 2017; Li *et al.*, 2020b; Ayukawa *et al.*, 2021).

Here, we demonstrate the presence of an independent accessory chromosome in TR4 strain II5 and we show that a recently observed difference in copy-number of AC12 in the TR4 reference strain II5 (van Westerhoven *et al.*, 2024a) is the result of remarkably large intrachromosomal duplications causing an approximate triplication of the size of this accessory chromosome. Interestingly, a similar duplication event must have occurred at least twice independently in different isolates of the clonal TR4 lineage. Since these duplications were not observed in TR4 strains isolated from Taiwan (Boehm, 1994), the first known origin of TR4 (Su *et al.*, 1986), they appear to have occurred after the initial spread of these isolates. Moreover, the high similarity of the duplicated AC12 sequences in these different isolates indicates that these events occurred recently. Due to a lack of sequence variation between these intrachromosomal duplications, they initially resulted in the assembly of a single 1.1 Mb contig (van Westerhoven *et al.*, 2024a), instead of the 3.5 Mb chromosome detected by CHEF gel analysis. Although the initial assembly does not correctly represent the complete accessory chromosome, the assembled chromosome is highly similar to AC12 from strain M1 (van Westerhoven *et al.*, 2024a), as well as to a contig in the independently assembled UK0001 strain (Warmington *et al.*, 2019) and to scaffold101 in an independently acquired II5 genome assembly (Zhang, Y *et al.*, 2024). Importantly, our results clearly demonstrate the presence of an accessory chromosome in TR4 strains, contrasting a recent report concluding that TR4 strain II5 lacks separate accessory chromosomes (Zhang, Y *et al.*, 2024). Only VCG0121 strains do not carry any separate accessory chromosomes and lack AC12, as earlier reported for strain 36102 (van Westerhoven *et al.*, 2024a). Even though considered to be part of the same taxonomic lineage (van Westerhoven *et al.*, 2024a), VCG0121 strains are genetically different as indicated, amongst others, by their opposite

mating type (Zhang, Y *et al.*, 2024), different VCG, reduced virulence (Viljoen *et al.*, 2020; van Westerhoven *et al.*, 2024a) and different karyotype (Figs. S13-S14). Thus, this highlights that naturally occurring *F. oxysporum* strains that infect banana can lack accessory chromosomes, but this has only been observed for strains belonging to VCG0121. Therefore, how frequently this occurs in strains infecting banana or any other host remains an open question. Similar to our findings, a karyotype analysis of three decades ago also showed the presence of a 1.1-1.2 Mb chromosome in several TR4 strains, although at that time no accompanying genome assemblies were available for the strains in this early study (Boehm, 1994). The VCG0121 strains in this study exclusively contain chromosomes >2 Mb in size, indicating a lack of AC12 (Boehm, 1994). In addition to clarifying the karyotype of II5, we also show that AC12 is dispensable for vegetative growth on culture media, further underscoring its role as accessory chromosome. Taken together, these findings firmly establish the presence of independent accessory chromosomes in TR4 strains, including strain II5, similar to those found in the majority of the previously characterized *F. oxysporum* strains.

Intrachromosomal duplications were previously reported in *F. oxysporum* after experimental horizontal transfer of accessory chromosomes (van Dam *et al.*, 2017). It is therefore tempting to speculate that the duplications in AC12 also occurred after a horizontal transfer event. Although the mechanism driving these intrachromosomal duplications remains unknown, it could involve a process known as BFB cycles (Croll *et al.*, 2013). The duplications in AC12 could be explained by a different number of sequential perfect and/or complex BFB cycles, giving rise to a much larger accessory chromosome (Li *et al.*, 2023). To further study the formation of the observed duplications, an accurate assembly of the full length AC12 will be essential.

The viability of mutants lacking the complete AC12 chromosome proves that it is dispensable for vegetative growth, as previously reported for accessory chromosomes in *F. oxysporum* strains infecting different host plants (Ma *et al.*, 2010; van Dam *et al.*, 2017; Ayukawa *et al.*, 2021). However, we observed a significant reduction in disease severity on banana plants after inoculations with the AC12 loss mutants, suggesting an important role of this accessory chromosome in plant infection similar to reports for accessory chromosomes in *F. oxysporum* strains infecting different plant hosts (Li *et al.*, 2020a; Li *et al.*, 2020b; Ayukawa *et al.*, 2021; Sakane *et al.*, 2024). In addition, the growth of the AC12 loss mutants was slightly impaired under high salt and cell wall stress. Together with the putative functions of other AC12-encoded genes, the latter result suggests that this accessory chromosome likely has a wider role besides virulence. In contrast to previous observations (Ma *et al.*, 2010; van Dam *et al.*, 2017), the AC12 loss mutants were still able to infect the host plant and cause the typical FWB symptoms, albeit with reduced severity. This result could be explained by the presence of an additional accessory region on core chromosome 1 of isolate II5

(van Westerhoven *et al.*, 2024a), which encodes seven *SIX* homologs as well as 33 candidate effectors, suggesting an important role during infection (Widinugraheni *et al.*, 2018; An *et al.*, 2019). Moreover, the accessory region on chromosome 1 and AC12 share many duplications, including several putative effector genes (van Westerhoven *et al.*, 2024a). Because these duplications hamper the knockout analysis of effector candidates, the newly generated AC12 loss mutants represent a useful tool for determining the minimal set of effectors required to infect banana and facilitate the search for potential avirulence genes using resistant banana genotypes. Here we attempted to further quantify the relative contribution of AC12 and the accessory region of chromosome 1 to virulence, by generating two different effector mutants in the AC12 loss background. While knockout of an additional accessory effector gene on chromosome 1 did not further reduce virulence of the AC12 loss mutant, re-introduction into such a mutant of a single AC12-specific effector gene resulted in a slight, albeit not significant increase in virulence. Since complementation was done through ectopic integration with the native promoter, differences in gene expression might explain the partial phenotype of the complemented line. To better assess the contribution of this effector, a knockout mutant could be made in the M1 strain which lacks the duplicated copies. The contribution of AC12 to virulence of TR4 is remarkable considering the number of regions shared with the accessory region of chromosome 1 (van Westerhoven *et al.*, 2024a). Additional genes other than effectors located on AC12 might play a more prominent role in the virulence phenotype of the chromosome loss mutants than previously expected.

Besides loss of the accessory chromosome AC12, several mutant lines showed interchromosomal rearrangements of core chromosomes. These rearrangements are of interest considering the commonly observed high level of colinearity between core chromosomes of *F. oxysporum* strains (Armitage *et al.*, 2018; Kanapin *et al.*, 2020; Zhang *et al.*, 2020; van Westerhoven *et al.*, 2024a). Although chromosomal rearrangements can have a strong impact on different functions including plant pathogenicity (Forche *et al.*, 2009; Seidl & Thomma, 2014; Faino *et al.*, 2016; Mehrabi *et al.*, 2017; Olarte *et al.*, 2019), we observed no phenotypic differences in the mutants that could be associated with the core chromosome rearrangements.

Chromosome length polymorphisms have been observed for a long time in a wide array of fungi (Zolan, 1995), and large-scale duplications or aneuploidy have been linked to differential fitness (Wertheimer *et al.*, 2016; Vande Zande *et al.*, 2023). Gene copy number changes are often beneficial for growth in a specific (stressful) environmental condition (Hull *et al.*, 2017; Sanchez *et al.*, 2017; Yang *et al.*, 2019; Vande Zande *et al.*, 2023; Tralamazza *et al.*, 2024). On the other hand, aneuploidy can strongly affect transcription and, in some cases, lead to proteotoxic stress (Sheltzer *et al.*, 2012; Larrimore *et al.*, 2020). In yeast, smaller chromosomes with fewer genes are

more frequently duplicated, which might be a consequence of overexpression and proteotoxic stress (Kumaran *et al.*, 2013; Gilchrist & Stelkens, 2019). Similarly, in yeast, aneuploidy is a driver of further genomic instability (Sheltzer *et al.*, 2011). Less is known about these specific processes in filamentous fungi, despite the observed karyotype variability (Zolan, 1995; Mehrabi *et al.*, 2017). Our results showcase intrachromosomal duplication as another example of karyotype variability among field isolates of a filamentous plant pathogen. The intrachromosomal duplications appear relatively stable over time, and their independent occurrence in different isolates suggests a potential fitness benefit. It has been suggested that duplications of accessory chromosomes might be an important prelude to rapid sequence divergence and effector diversification (Seong & Krasileva, 2023). Nevertheless, a clear fitness benefit or detriment linked to these duplications remains to be discovered.

Together, our data demonstrate the occurrence of intrachromosomal duplications of AC12 in the TR4 reference strain II5 and a contribution of AC12 to different biological processes, particularly plant infection. The observed duplications and chromosomal rearrangements indicate a high degree of genome plasticity and highlights an important mechanism of accessory chromosome diversification in fungal plant pathogens. Further knowledge on the function and dynamics of accessory regions in the TR4 lineage will be crucial for combating this devastating banana pathogen.

Materials and methods

Fungal growth conditions and chromosome loss induction

Fusarium oxysporum Tropical Race 4 (TR4) strains II5 and M1 (van Westerhoven *et al.*, 2023; van Westerhoven *et al.*, 2024a) and newly generated II5 mutant strains were routinely cultured on PDA plates at 25 °C. Conidial suspensions of all strains were stored as glycerol stocks at –80 °C.

Chromosome loss was induced as described previously with slight modifications (Ayukawa *et al.*, 2021). II5:Δ*SIX13* was cultured in M100 medium supplemented with 25 µg/mL benomyl at 150 rpm 25 °C for 4 days. Conidia were obtained by filtering the culture through two layers of sterile cheesecloth. Conidia were plated on M100 plates supplemented with 0.04% Triton X-100. Plates were overlaid with a piece of sterile filter paper and incubated at 25 °C for 2-3 days. Subsequently, the filter paper was transferred to a PDA plate with 100 µg/mL hygromycin that was incubated at 25 °C for 1 day. Afterwards, the filter paper was removed, and colonies were selected for loss of hygromycin resistance by comparison to the original M100 plate. Putative chromosome loss mutants were transferred to separate PDA plates for further

validation. PCR genotyping was performed using the Phire Plant Direct PCR Master Mix (Thermo Scientific™, Waltham, Massachusetts USA). Chromosomal rearrangement between chromosomes 5 and 6 were validated using PCR as well. Primers are listed in Table S1.

Sequencing and sequence analysis

To validate that the mutants generated by benomyl treatment lost AC12 and analyze the effect of benomyl treatment on the presence of other genomic regions, seven chromosome 12 mutants were sequenced. The mutants were grown in PDB for 4 days at 150 rpm 25 °C to obtain mycelium. Cultures were centrifugated and mycelium was freeze-dried. DNA was extracted from freeze-dried mycelium using the Masterpure™ Yeast DNA Purification Kit (LGC Biosearch™ Technologies, Hoddesdon, United Kingdom). Extracted DNA was sent for Illumina whole-genome re-sequencing by Beijing Genomics Institute. The reads were mapped against the II5 reference genome assembly (van Westerhoven *et al.*, 2024a) using BWA mem version 0.7.17(Li & Durbin, 2009). The mapping was visualized using WGS coverage plotter from jvarkit version 589510ae3 (Lindenbaum, 2015).

Additionally, the short reads were assembled using SPAdes version 3.13.0 (Bankevich *et al.*, 2012). These assemblies were used to analyze structural variants, including chromosomal rearrangements, using mummer version 4(Marçais *et al.*, 2018) followed by MUMandCO version 3.8 (O'Donnell & Fischer, 2020).

To determine the putative function of the genes located on chromosome 12, we used eggnog mapper version 2.1.12 (Cantalapiedra *et al.*, 2021). Putative effector genes were identified using effectorP version 3 (Sperschneider & Dodds, 2022) on the secretome determined by signalP version 5(Almagro Armenteros *et al.*, 2019b). Secreted in Xylem (*SIX*) genes were identified based on homology searches of *SIX* genes from *Fol*4287 using blastP version 2.14.0 (Altschul *et al.*, 1990).

CHEF electrophoresis and Southern blotting

Chromosomes of all strains were separated by Contour-Clamped Homogeneous Electric Field (CHEF) electrophoresis. Protoplast preparation was performed as previously described (Powell & Kistler, 1990), with slight modifications: 5x108 fresh microconidia were germinated 14 hours at 28 °C in 200 ml of potato dextrose broth (PDB) medium, germlings were then transferred to a solution of 1.2M $MgSO_4$ pH 5.8, containing 5% (w/v) Extralyse® enzyme preparation (Laffort, Bordeaux, France) and incubated approximately 90 minutes at 30 °C and 60 rpm. Protoplasts were filtered through a double layer of Monodur mesh (pore size 10 µm), washed with ice-cold 1 M Sorbitol and harvested after 15 minutes of centrifugation at 2,500 rpm.

Subsequently, they were resuspended at a concentration of $8x10^8$/mL in STE solution (25 mM Tris-base, 50 mM EDTA, 1M Sorbitol; pH 7.5) containing 1 mg/mL proteinase K (Sigma-Aldrich, Madrid, Spain), mixed with an equal volume of 1.2% Low Melting agarose (NuSieveTM GTGTM, Lonza, Pontevedra, Spain), poured into plug casting molds (Bio-Rad, Madrid, Spain) and left to cool 15 minutes at 4 °C. These plugs were then transferred to a solution containing 1 mg/mL proteinase K in 100 mM Tris-base, 500 mM EDTA, 1% Lauryl sarcosine (w/v), pH 9.5 and incubated overnight at 50 °C and 60 rpm, and washed three times for 15 minutes in 50mM EDTA, pH 8.0 at room temperature and 60 rpm. For chromosome separation, the plugs were transferred to a 1% Certified Megabase agarose (Bio-Rad) gel in 0.5X TBE buffer (Fisher BioReagents™, Madrid, Spain) and subjected to electrophoresis in a CHEF-DR® III system (Bio-Rad) with the following settings: switching time 1,200–4,800 s, 1.6 V/cm, 120 angle, 700 ml/min flow, 8 °C and 255 hours. Gels were then stained for 30 minutes in GelRed® solution (3X final concentration in water; (Biotium, Fremont, California USA) and chromosomal bands were visualized on a GelDoc Go imaging system (Bio-Rad).

Southern blotting was performed as previously described (Sambrook, 1989). After the denaturing treatment, chromosomes were transferred from the CHEF gel onto a positively charged nylon membrane (Roche, Barcelona, Spain) and hybridized with digoxigenin-labelled DNA probes generated using the DIG DNA Labelling Mix (Roche). Detection was performed using an alkaline phosphatase kit and CDP-Star® chemiluminescent solution (Roche). Images were obtained with a chemiluminescence detection imager (LAS-3000 Fujifilm, Barcelona, Spain).

Stress tolerance tests

Based on the functional annotation different environmental stress factors were selected and the response of chromosome 12 mutants to these different environmental stress factors was determined. Strains II5, M1, and selected mutants were inoculated on PDA plates from glycerol stock. Afterwards, agar plugs from the border of the colony were placed on regular PDA plates, MMA plates (Puhalla, 1985) or MMA supplemented with either 0.8M NaCl, 1.2M glycerol, 10 µg/mL menadione or 40 µg/mL Congo Red. Colony diameter was measured at 3 dpi. Colonies were photographed at 5 dpi. VCG testing was also performed as described previously (Puhalla, 1985).

Fusarium transformation

Modified CRISPR-Cas9 vectors were used for transformation based on the plasmid previously described (Shinkado *et al.*, 2022). This plasmid (CRISPR/Cas9-FoU6-FoNLSx2) contains an additional H2B NLS and an optimized gRNA scaffold(Chen *et al.*, 2013). Cloning of the target sequence into the vector and generation of the

donor template were performed as previously described (Shinkado *et al.*, 2022). TR4 reference strain II5 and II5 ΔAC12 6.4 were transformed as described (Shinkado *et al.*, 2022) with modifications. Spores of II5 and II5 ΔAC12 6.4 were produced as described below. Subsequently, 500 µL of spore suspension was used to inoculate 50 mL of Fries medium and left to grow in the dark at 135 rpm 20 °C for 1 day. Newly formed mycelium was blended using an IKA® Ultra Turrax® Tube Drive P control (IKA, Staufen, Germany) for 10 seconds at 6000 rpm. All the blended mycelium was used to inoculate 200 mL of fresh Fries medium and incubated overnight in the dark at 135 rpm 20 °C. Overnight formed mycelium was filtered through a layer of nylon mesh (20 micron) and washed three times with 50 mL of KC solution (0.6 M KCl, 65 mM $CaCl_2$). Washed mycelium was collected and treated with 10 mL of the filter sterilized protoplasting enzyme mix consisting of 25 mg/ml Driselase from *Basidiomycetes* sp. (Sigma-Aldrich, St. Louis, Missouri USA), 5 mg/ml lysing enzyme from *Trichoderma harzianum* (Sigma-Aldrich, St. Louis, Missouri USA) and 100 µg/ml chitinase from *Trichoderma viride* (Sigma-Aldrich, St. Louis, Missouri USA) in KC. The enzyme mix was incubated at 28 °C with slow rocking movement for two hours. Protoplasts were separated from the mycelium by filtering through a layer of nylon mesh. Protoplasts were centrifuged at 1800g for 10 minutes at 4 °C and washed twice using ice cold STC (1.2 M Sorbitol, 10 mM Tris-HCL pH 8, 20 mM $CaCl_2$). After washing protoplasts were resuspended in 100 µL of STC per reaction. Protoplasts were then mixed with approximately 15 µg of Cas9 plasmid and 15 µg of donor template and 100 µL of 60% PEG solution (Polyethylene glycol 4000, dissolved in STC). Two different gRNA plasmids were combined for knockout of 1g02190. The mixture was left at room temperature for 20 minutes. Protoplasts were washed one last time with 1 mL of STC. Protoplasts were plated by mixing with cooled RM (34.2% sucrose, 0.1% yeast extract, 0.8% agar). After solidifying, a second layer of YG medium (2% glucose, 0.5% yeast extract, 1.5% agar) supplemented with 50 µg/ml nourseothricin was poured over the first agar layer. Resistant colonies were put on separate plates between 3-5 days and used for further genotyping by PCR and amplicon sequencing. Complementation of 12g00300 was performed with the same procedure without Cas9 for ectopic integration.

A II5:Δ*SIX13* mutant containing an hygromycin resistance cassette was generated by a protocol using Cas9 ribonucleoprotein gene editing as described (Wang *et al.*, 2018) with modifications. Specifically, the NLS of H2B was cloned from TR4 strain II5 and used to replace the SV40 NLS in the Cas9 plasmid pET-28b-Cas9-His (Gagnon *et al.*, 2014). A hygromycin cassette donor template with short 60 bp homologous overlap was used. Used primers are listed in Table S1. Coding sequences of the effectors are listed in Table S2.

Plant growth conditions and infection assays

Cavendish 'Grand Naine' plants were grown in the greenhouse at a day/night temperature of 25/23 °C and a day length of 16 hours with 80% relative humidity.

Infection assays of Cavendish 'Grand Naine' banana plants were performed as described previously (García-Bastidas *et al.*, 2019). In brief, strains II5, M1, and selected mutants were inoculated on PDA plates. Agar plugs from PDA plates were used to inoculate Erlenmeyer flasks containing mung bean broth. Flasks were cultivated in a rotary shaker at 150 rpm 25 °C for 5 days. Spores were collected by filtering the culture through two layers of sterile cheesecloth. Spores were subsequently diluted to $1x10^6$ spores per mL. Roots of the plants were injured prior to inoculation. Lastly, 200 mL of spore solution was poured directly on the soil for each plant. Corm necrosis was quantified at 8-10 weeks post inoculation using ImageJ.

Acknowledgements

The authors thank Li-Jun Ma, University of Massachusetts Amherst, for providing the US copy of TR4 strain II5. JD, ACW, CAG, GNT and GHJK were supported by the Bill and Melinda Gates Foundation, grant no.: AG – 4425. Banana research at Wageningen University has been supported by the Dutch Dioraphte Foundation, grant no.: 20 04 04 02. LGG was supported by grant PLEC2021-007777 from the Spanish AEI/10.13039/501100011033 and NextGenerationEU/PRTR.

Competing interests

None declared.

Author contributions

JD and ACW collected data and performed the analyses. LGG, CAG, GNT, SDG, MY, TA, TK, and TA contributed to data collection and experimental methods. JD and ACW wrote the manuscript with input from ADP, GHJK and MFS. All authors contributed to writing and editing the manuscript. GHJK and MFS conceived and supervised the project. JD and ACW, GHJK and MFS contributed equally to this work.

Data availability

The data that support the findings of this study are openly available in the Sequence Read Archive at https://www.ncbi.nlm.nih.gov/sra. The data sequenced in this study are available under accession no.: PRJNA1190342. All other data are available in the main text or in the supporting information (Figs S1-S14; Table S1-2).

Supplementary materials

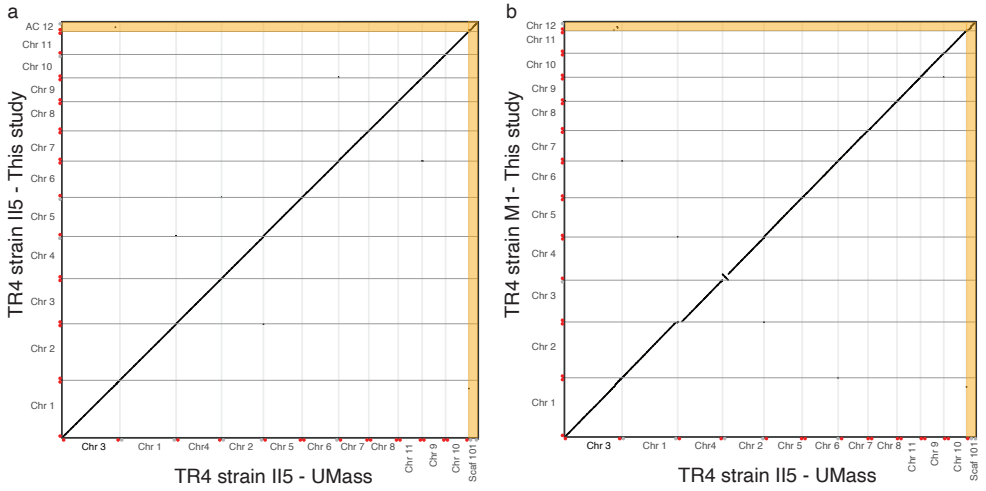


FIGURE S1 | Independently assembled TR4 strains are highly similar. Whole-genome comparison of TR4 strain II5 (a) and M1 (b) used in this study versus the TR4 strain II5 assembled by Zhang et al. (2024), which had been reported to lack conventional accessory chromosomes. The alignment shows that the assembly of strain II5 used in this study is highly similar to the strain II5 assembled by Zhang et al. (2024). Strain M1 shows a small inversion in chr 4 and a deletion in Chr 3, but furthermore is largely colinear to TR4 strain II5 assembled by Zhang et al. (2024). Importantly, Scaffold101 is homologous to AC12 in our study in both M1 and TR4 II5. Telomeres at chromosomal ends are indicated by red dots, grey dots indicate the absence of detectable telomeric repeats.

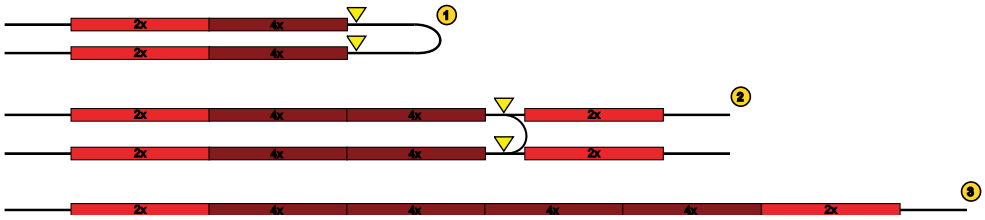


FIGURE S2 | Breakage-fusion-bridge cycles as a potential source of the intrachromosomal duplications of accessory chromosome 12 (AC12). Schematic representation of a possible mechanism for generation of large intrachromosomal duplications in AC12. Two separate sequential breakage-fusion-bridge events can lead to the displayed order of duplicated and quadruplicated sections of AC12, leading to a final chromosome with triplicate size. Yellow arrows indicate fold-back inversions of sister chromatids after loss of one telomere.

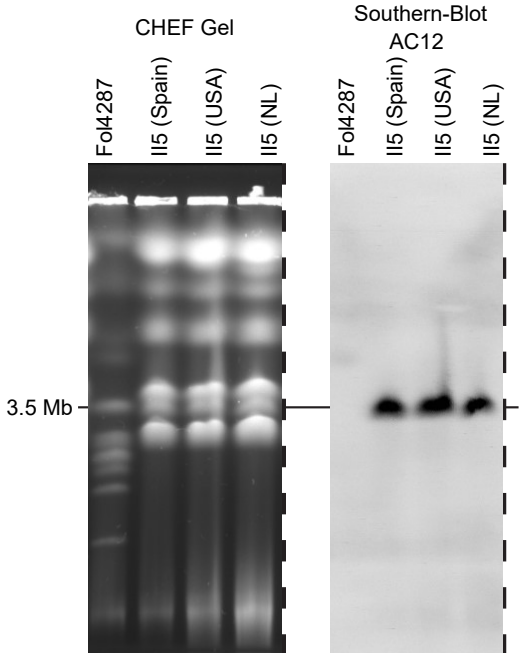


FIGURE S3 | The duplication of accessory chromosome 12 (AC12) in isolate II5 is stable across different laboratories. CHEF gel of two *Fusarium oxysporum* strains (*Fol*4287 and II5). Three independent copies of the TR4 reference isolate II5 maintained in different laboratories (Spain, USA, and NL) were tested. The same gel was used for a Southern Blot using an AC12 specific probe. Dashes indicate cropping from gel. Full gel depicted in Fig. S14.

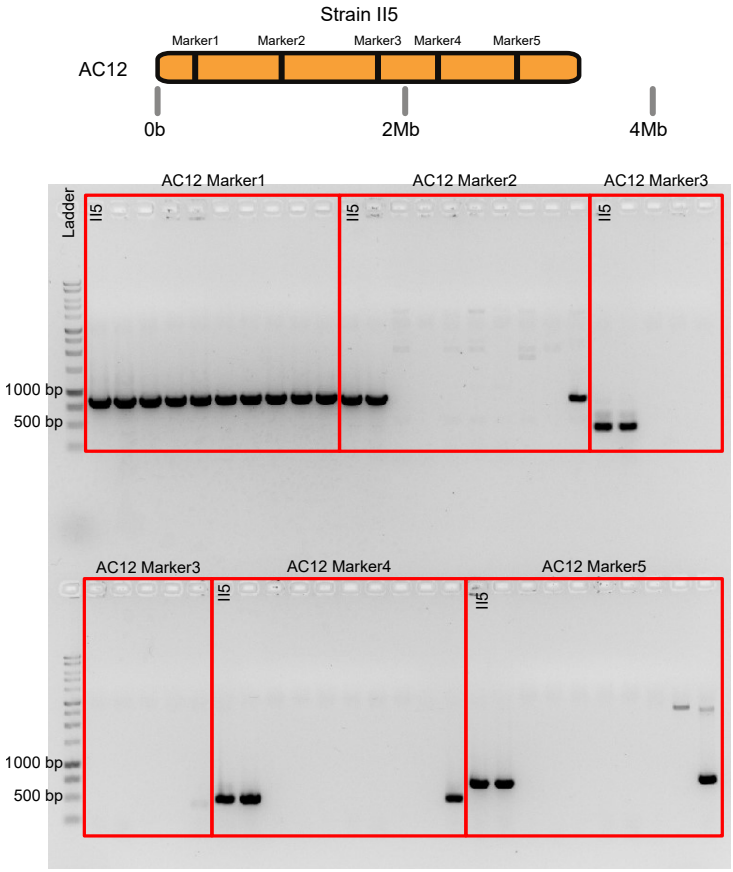


FIGURE S4 | PCR indicates loss of accessory chromosome 12 (AC12) after benomyl treatment. Schematic representation of primer locations on AC12 (black bands) and gel electrophoresis after PCR on strain II5 and putative AC12 mutants using five different AC12 PCR markers. Seven colonies did not give bands for markers 2-5. Note, marker 1 can also bind to the accessory region on chromosome 1, therefore giving a band for all colonies.

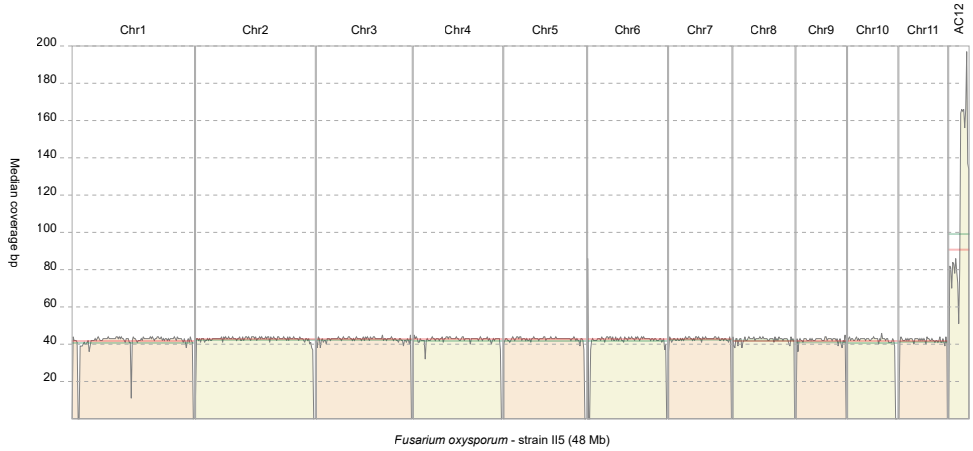


FIGURE S5 | Mapping of short reads to the II5 reference genome assembly. Mapping of Illumina reads from strain II5 to the II5 reference genome assembly shows higher coverage at accessory chromosome 12 (AC12).

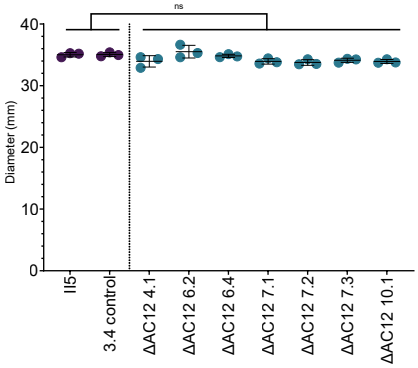


FIGURE S6 | Loss of accessory chromosome 12 (AC12) does not affect vegetative growth on PDA. Colony diameter (mm) of PDA plates inoculated with TR4 strain II5, benomyl treated control 3.4, and seven independent AC12 mutants. Growth was quantified at 6 dpi. Letters indicate significant differences between treatments (Tukey-Kramer test; $P<0.05$). Data are shown as mean ±SD (n=3).

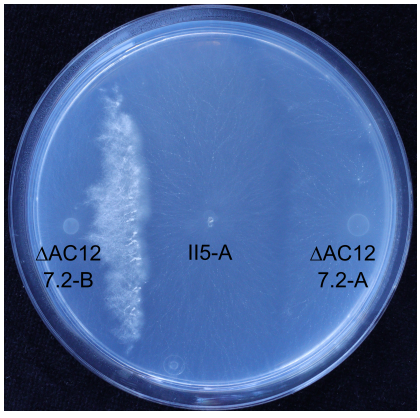


FIGURE S7 | Accessory chromosome 12 (AC12) mutant is vegetatively compatible with WT strain II5. MMA plate inoculated with *nit* mutant of II5 and II5ΔAC12 7.2. Dense hyphal growth at the colony contact points indicates vegetative compatibility.

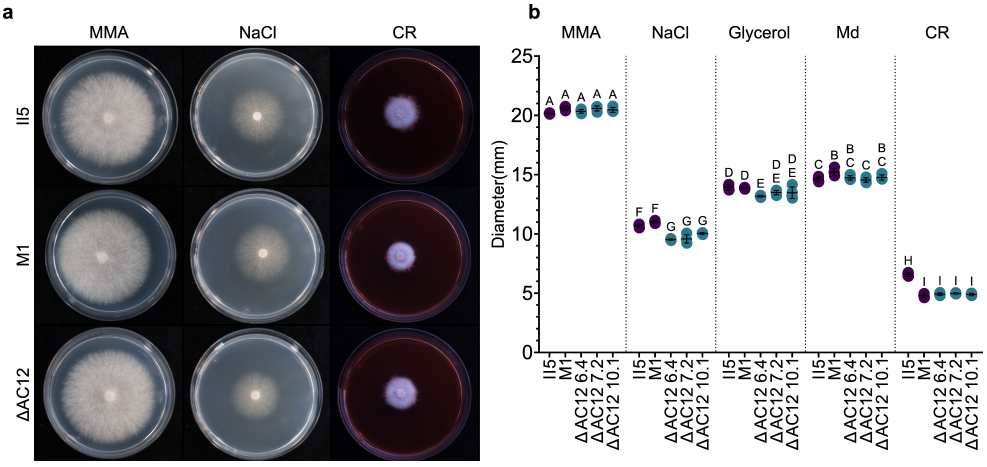


FIGURE S8 | Accessory chromosome 12 (AC12) plays a role in growth under different stress factors. **a**) MMA plates alone or supplemented with 0.8 M NaCl or 40 µg/mL Congo Red (CR) were inoculated with TR4 strains II5, M1, or II5ΔAC12 6.4 and photographed at 5 dpi. **b**) Colony diameter (mm) of MMA plates alone or supplemented with 0.8 M NaCl, 1.2 M glycerol, 10 µg/mL menadione (Md) or 40 µg/mL Congo Red (CR) inoculated with TR4 strains II5, M1 or three independent AC12 mutants. Colony growth was quantified at 3 dpi. Different letters indicate significant differences between treatments (Tukey-Kramer test; P<0.05). Data are shown as mean ±SD (n=4).

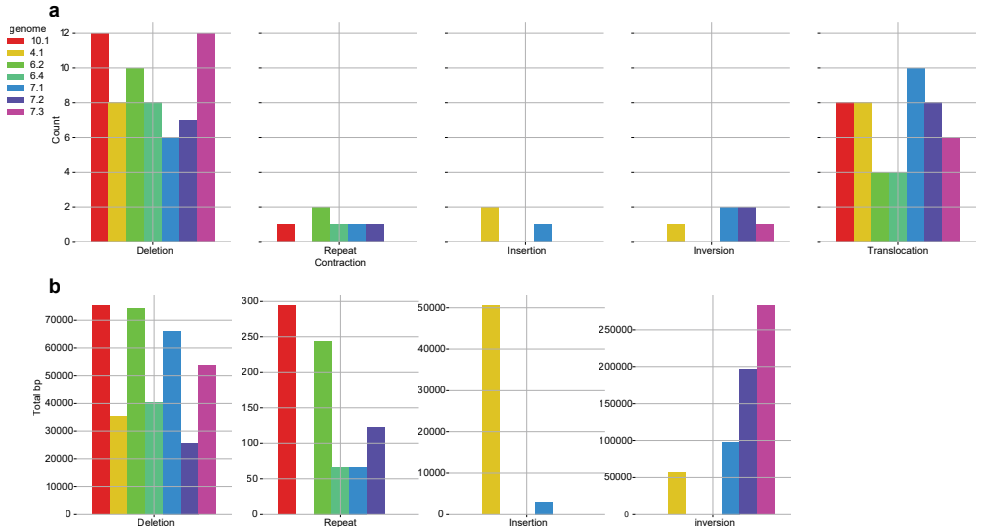


FIGURE S9 | Structural variants in the accessory chromosome 12 (AC12) deletion mutants. **a**) The number of structural variants per variant type is shown for all seven independent AC12 deletion mutants. **b**) Sizes (in bp) of the identified structural variants for all seven independent AC12 deletion mutants. Translocation sizes are not reported because the calculation is challenged by the fragmented short read assemblies.

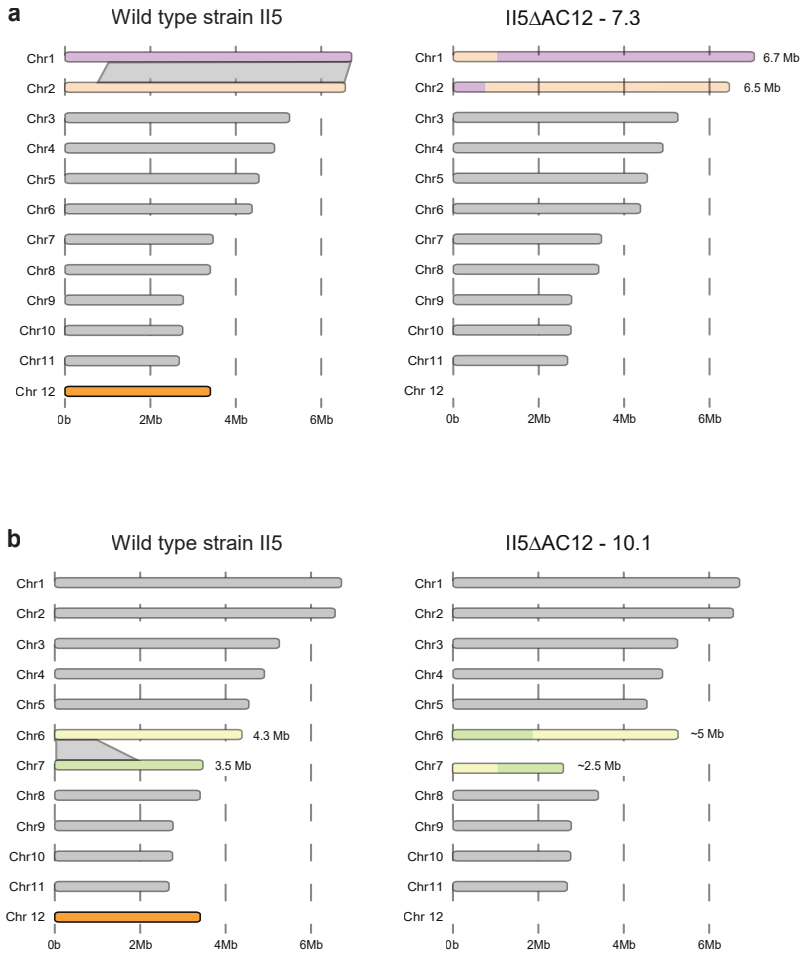


FIGURE S10 | Interchromosomal rearrangements of core chromosomes following benomyl treatment and accessory chromosome (AC12) loss. a) Schematic representation of the interchromosomal rearrangements that occurred in II5ΔAC12 - 7.3. Translocations between chromosomes 1 and 2 are highlighted by ribbons. **b**) Schematic representation of the interchromosomal rearrangements that occurred in II5ΔAC12 - 10.1. Translocations between chromosomes 6 and 7 are highlighted by ribbons.

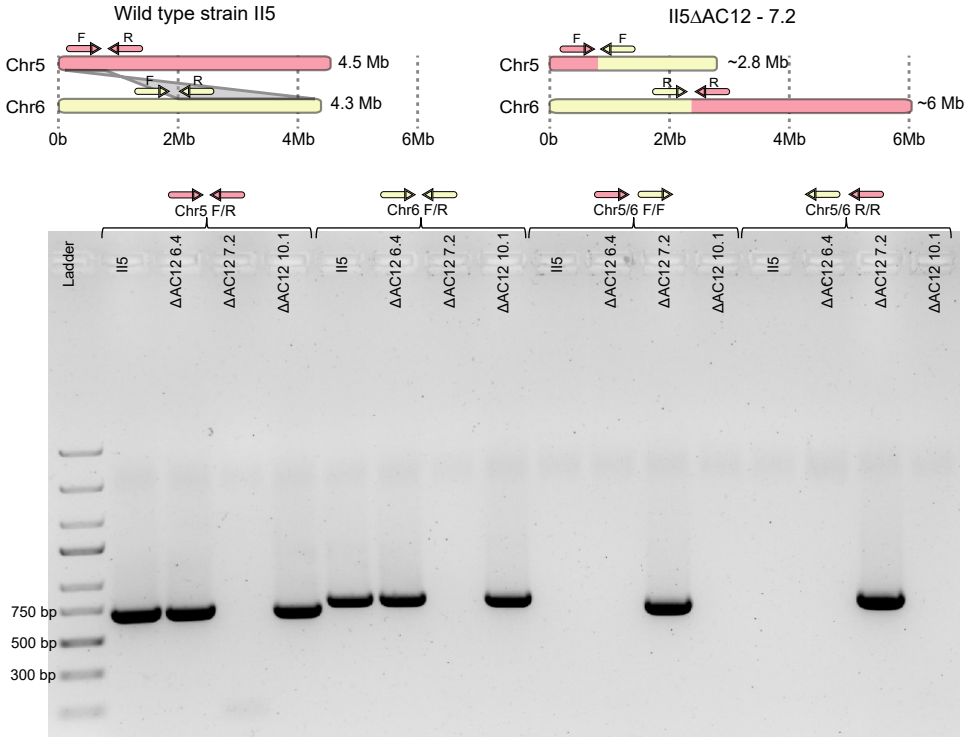


FIGURE S11 | Core chromosomal rearrangement in II5ΔAC12 - 7.2 is confirmed through PCR. Schematic representation of primer locations on chromosomes 5 and 6 in II5 and II5ΔAC12 - 7.2. Gel electrophoresis after PCR on II5 and three independent chromosome 12 mutants using chromosome 5 (F/R) and 6 (F/R) specific primers and the combinations thereof.

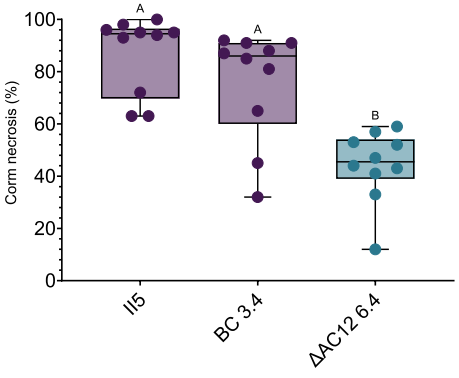


FIGURE S12 | Benomyl treatment does not affect virulence. Percentage of corm necrosis of Cavendish 'Grand Naine' plants inoculated with strain II5, benomyl treated control 3.4 and II5ΔAC12 6.4. Corm necrosis was quantified using ImageJ (n=10). Letters indicate significant differences between treatments (Tukey-Kramer test; P<0.05).

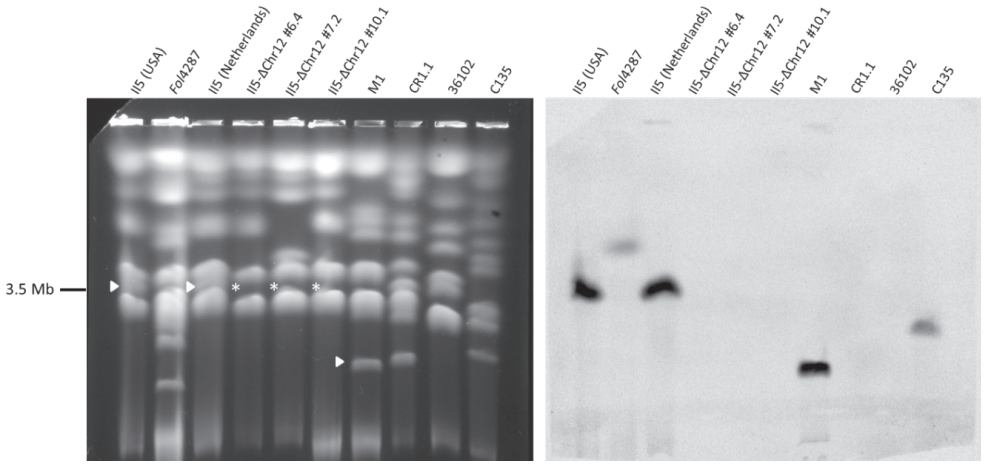


FIGURE S13 | Full uncropped CHEF gel and Southern blot used in Fig. 1 and 2.

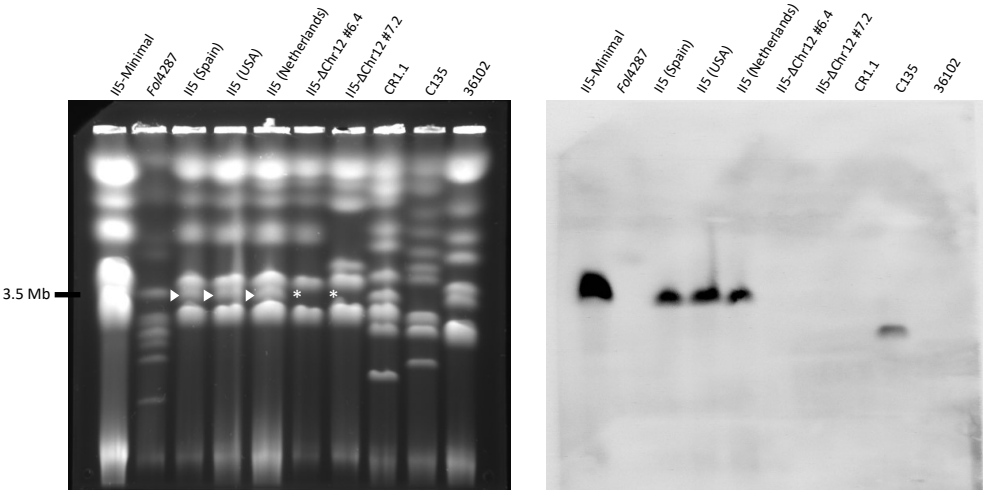


FIGURE S14 | Full uncropped CHEF gel and Southern blot used in Fig. S3. II5-Minimal concerns an isolate for an unrelated study.

TABLE S1 | Primers used in this study.

Primer name	Sequence 5′-3′	Purpose
H2B_sacII_F	CTGACCCGCGGATGGCTCCCAAGG	Cas9 RNP
H2B_speI_R	GTGCGGCCGCACTAGTCTTGTAGATGT	-
SIX13_dt_fwd1	ATCGGGATCAGGCCTTCAACGAAGAGGAGCTACTCAAAGTC GTGGACGAGCTCTCGGTAAtgctggccttttgctcacatgcatg	-
SIX13_dt_rv1	TCCGTTAGGGTATTGGTCGTTTTGACGCCTCTGTAGTGCT GCTTCCGAGACTAGGGCCCGatcgccggaaaggacccgcaaatg	-
SIX13_sgRNA1	AAGCTAATACGACTCACTATAGG AGCTAACAAACCATACG GAAGTTTTAGAGCTAGAAATAGCAAG	-
II5_1g02190_9gRNA_F	CTCGGGTTGACACGGGTAACGAACTGA	Cas9 plasmid
II5_1g02190_9gRNA_R	AAACTCAGTTCGTTACCCGTGTCAACC	-
II5_1g02190_9gRNA_F2	CTCGGCCTACATCAAGGAGGTTGACAC	-
II5_1g02190_9gRNA_R2	AAACGTGTCAACCTCCTTGATGTAGGC	-
1g02190up_F	TCCCACTTGTTAGTGCACCTG	Donor template
1g02190up_R	cactagctccagccaagcccaaaaaGCAGTCCCATGACAGCTTGA	-
NatR_1g02190_F	CAAGCTGTCATGGGACTGCAtttttgggcttggctggagctagtg	-
NatR_1g02190_R	ACTGATTATACCGACGAGTCCActcactgatacatctggcacctact	-
1g02190down_F	agtaggtgccagatgtatcagtgagTGGACTCGTCGGTATAATCAGT	-
1g02190down_R	TATCACAATACGCAAGTCTGGT	-
II5_1g02190screen_F	TGGGGCGGTCAGTATATGATAA	Screening
II5_1g02190screen_R	TTCAGTCACAAGGGGGAGGT	-
II5_1g02190genescreen_F	CCATCTGACGTCACCACCAC	-
II5_1g02190genescreen_R	CGGGCTATAGACGCAGGC	-
II5_12g00300screen_F	TAAGCGAATGCACCATCCTGT	-
II5_12g00300screen_R	AGCAAGTATACGCGGCCTTC	-
II5_12g00300_genescreen_F	GCCGCGTTGCAGAAACCATA	-
II5_12g00300_genescreen_R	GCCATTCACCACTTTGTCGG	-
II5_1g02190screen2_F	GACCGGCGCAAAATCTTTTCA	-
II5_1g02190screen2_R	TCATCCTCCTAAATCTTCTTTGCT	-
Six13_TR4_F	ACCATGACTCGGTTTCACCTTATCCT	-
Six13_TR4_R	TTACTCTAAAGTAACCTCCCACTGT	-
AC12mark1_F	ATCTGCTGCCGCTTTATCCT	-
AC12mark1_R	CCTCTTGTCGAGTTAGGCCC	-
AC12mark2_F	GAAAAGGTTTGTCGGGTTCGG	-
AC12mark2_R	CTTGTTTCGCTCAACGGCAA	-
AC12mark3_F	TCAAGCCTTTACACTATCCTCTGT	-
AC12mark3_R	GCACGCCTATTCATCCCCAT	-
AC12mark4_F	TTCCGTGTGGAAATGGCTCT	-
AC12mark4_R	CGGGCTTTGTTTATGGGGAGA	-
AC12mark5_F	CTTCGACTTGGGGTCGTCAA	-
AC12mark5_R	GCGAATGCAGTGATCGGAAC	-
12g00300up_F	GATCGCGTCTGTCCTGAGTG	Complementation
12g00300downNatR_R	cactagctccagccaagcccaaaaaATCAGCGACCTTATTTGCAGC	-
NatR_12g00300_F	GCTGCAAATAAGGTCGCTGATtttttgggcttggctggagctagtg	-
NatRfull_R	ctcactgatacatctggcacctact	-

Primer name	Sequence 5'-3'	Purpose
AC12 probe	TCCTCTGTCTCCCACTACTAAATACACCTCTATATCACATAG TAGAAAAACAAGTAAACGAGCTGCTAAGATTTTCAAAACGCT TAATTCTGCACTCTGTCGGCACCATCACTATCGTACGGC TCTTCCTCGGACTCGGAGGCGGACTCAGAGTCCGAAT CATACGCAGACATATCCCCATTCTCGCATTCATAAAG GTCCCATATATGACCGGCGTCCCTGCACTTTGCGCCGGCTCTA GAGCAAGACGAGCAAATGAGA	Southern blot
II5_Chr5mark_F	CTGAGGGGATGAGTTAGCGG	Rearrangement
II5_Chr5mark_R	GGGTCTCGTGTTATGCTCCG	-
II5_Chr6mark_F	TGCTCCCGCAAGGATTTGAT	-
II5_Chr6mark_R	TGCAGATCGTCGGTTGTGAA	-

TABLE S2 | Effector sequences.

Gene	CDS
1g02190	ATGAGGTTCTCCCTAACACAGATTGCACTCATTGGCCTTCTCGGGCTGGCTCATGCCGAGAATTGGGATTCAT-GCCATTGCATGCGGTATCCTGATACCCAGACGGCTAACTGGTGCGCAACCAATTTTGCTTGTGGCGATATGG GACCAGGCTATACCATCAAGCCCGGCGGCGATTGTTCTCGCCTGAACGGAAAATCGATCAGCGGACCGGAT TTCTATAATGTATGCCGGAAGCACGACCCCAATAACGGTGAAGCCGACAGCTGCTGCACTCGTTGGGTTGATG GCGTGGTGGTGACGTCAGATGGCTGTTTCAAGTAG
12g00300	ATGCAGCCATTCACCACTTTGTCGGTTATGCTCGTAGCAGTCATAAGCCCTGCTCTGATCAATGCCCAACTTAT AACTCATGCTATACGAGCAGACGCGGCCAATCCTCCCAACAGCAGTTCGACTAGTACTGTAACTGTTGTGACC ATGGCTCCACCTCCTCCCTCGGGAATGGGATGTGTCTGCATGGCACCAACCTCTTCCGGAAAAGATGAATCG ATGAGAGATCGTACACAGAATATTTGCCAGCAGCAAGGAGCCTTCTTGCGAGGTACTCTCGACTTTTACGG CAGGGGCAATTTCTATTGTAACTTTGTCAACGGTATCGATCCGGCTAAGTGGGACCAAAGCTGCCGTACGAT TTATGGTGATGGAACATATGGTTTCTGCAACGCGGCGAACTAA
SIX13	ATGACTCGGTTTCACCTTATCCTTTTACCATTACTTTTCTCCTGGTTCTCCTATTGTTTAGGGGAGTTAGAGGT GTCTGATTTGTCTGATCAGCCTCCTAGCGTCGAAAATACTTATCGGGATCAGGCCTTCAACGAAGAGGAGCTA CTCAAAGTCGTGGACGAGCTCTCGGTAAAGCTAACAAACCATACGGAACGGGCCCTAGTCTCGGAAGCAGC ACTACAGAGGCGTCAAAACGACCAATACCCTAACGGAGTTTGCCCGAGTGGAGGACGTTTTTATCTTGATG TAGATGAAGATAGGTCATGCAACAGTAAATGGGGAATTGCAACTCCCGACGAAACTAGAACGTTTGGCTCA ACTGGTTCGGTTTGCGCAGGCACGTTCAGGCGGATCACTTGCGCTTGCTGCTTTACAACGCACCCCATCA CGAATAATGATGCACCAAGAATGGACGGAATATATTGCCAAAAATGGGAGATCTGTAAGCAGGAACATGAACG ATGGAGTAAATGGGGAAAATTGGTACCCCATACATCATGTGTAAAGGCGAAGAAGCTCACCGAGATCTTCATC GCTACCAAAAAAGTCGTTAAAGAGTACTGTACTCCTAAGCGGTGGCTCCCATCAACTGGCAAGGGCAAAA ACGCAAAATTCCACGCCTGGGCATACAATTACAGCACGGGACAGTTTACAAAACTCAAGTGGATGTATTTGAA GTTGGATGGTCAATATGCTAAGTCAGCGCCAGGGATTTCGGAATGGGGACTCACCTACAGTGTCAATGAGCA TAACGCCATTGAATTATGTGGCTACCCCTCTGACGATATGCAAAAGAATTCCATCGATGCCGAGTTACAGTGGG AGGTTACTTTAGAGTAA

Chapter 4

Helitron activity in a plant pathogenic fungus caused large-scale deletions affecting secondary metabolism without attenuating pathogenicity

Jelmer Dijkstra[1]
Anouk C. van Westerhoven[1,2]
Yinping Li[1,3]
Carolina Aguilera-Galvez[1,4]
Giuliana Nakasato-Tagami[1]
Xiaoqian Shi-Kunne[1]
Desalegn W. Etalo[1]
Gert H.J. Kema[1]

[1]Laboratory of Phytopathology, Wageningen University and Research, Wageningen, the Netherlands.
[2]Theoretical Biology & Bioinformatics Group, Department of Biology, Utrecht University, Utrecht, the Netherlands.
[3]Institute of Pomology, Chinese Academy of Agricultural Sciences, Xingcheng, Liaoning Province, China
[4]Área de Sistemas Naturales y Sostenibilidad, Escuela de Ciencias Aplicadas e Ingeniería, Universidad EAFIT, Medellín, Colombia.

Abstract

Transposable elements (TEs) are significant drivers of genome evolution, influencing the genome dynamics of clonal fungal pathogens such as those in the *Fusarium oxysporum* species complex (FOSC), the cause of Fusarium wilt in over 100 plant hosts. Among these, Tropical Race 4 (TR4), a clonal lineage within the FOSC, poses a severe threat to global banana production. However, the role of TEs in shaping TR4's genome and adaptation remains underexplored. Here, we investigated Helitron-mediated structural variations in Mozambican TR4 strain (M1), revealing two large deletions on core chromosomes caused by a FoHeli1 Helitron transposon. One 464 kb deletion disrupted 158 genes, including the fusaric acid (FA) biosynthetic gene cluster (BGC), a conserved feature in many *Fusarium* species. Combining genomics, metabolomics, and pathogenicity assays, we demonstrate that these deletions abolishes FA production, and altered secondary metabolite profiles, and increases sensitivity to exogenous FA. Contrary to prevailing observations, infection assays with wildtype, mutant, knock-out, and complemented strains indicated that FA production does not significantly contribute to TR4 virulence in banana. These findings highlight the role of FoHeli1 in reshaping the genetic and metabolic landscape of TR4, challenging existing assumptions about the role of FA in pathogenicity. Our study underscores the broader impact of TEs on fungal genome evolution and adaptation, providing new insights into the mechanisms driving pathogenicity in clonal fungal lineages.

Introduction

Transposable elements (TEs) are powerful drivers of genome evolution, shaping genetic diversity and adaptation across the Tree of Life (Hayward & Gilbert, 2022). These mobile genetic elements can comprise substantial portions of the host genome (Wells & Feschotte, 2020) and influence critical processes, such as gene expression, splicing, deletion, recombination, and epigenetic regulation (Hirsch & Springer, 2017; Catlin & Josephs, 2022; Hayward & Gilbert, 2022). In plant-pathogenic fungi, TEs often associate closely with virulence-related genes and genomic compartments (Ma *et al.*, 2010; Rouxel *et al.*, 2011; Faino *et al.*, 2016; Bertazzoni *et al.*, 2018), playing a key role in adaptation and virulence evolution (Seidl & Thomma, 2017; Fouché *et al.*, 2022). This association is thought to facilitate fast adaptation in the arms race between pathogenic fungi and their hosts, particularly in clonal populations, by modulating gene stability and expression (Chuma *et al.*, 2011; de Jonge *et al.*, 2013; Möller & Stukenbrock, 2017; Fouché *et al.*, 2020; Torres *et al.*, 2020; Fouché *et al.*, 2022). However, while beneficial for short-term adaptation, the close association may have long-term negative fitness consequences due to TE accumulation, subsequent genome instability, and deleterious TE insertions (Fouché *et al.*, 2022).

The importance of TEs in fungal genome evolution is particularly evident in the *Fusarium oxysporum* species complex (FOSC). FOSC members can infect over 100 plant hosts (Dean *et al.*, 2012) and possess TE-enriched genome compartments that contribute to their adaptability and virulence (Ma *et al.*, 2010; Li *et al.*, 2020b; Ayukawa *et al.*, 2021; Dijkstra *et al.*, 2024; van Westerhoven *et al.*, 2024a). Among FOSC lineages, the clonal Tropical Race 4 (TR4) lineage poses a severe threat to global banana production, a crop crucial for food security and local economics (Frison, 2004; Ordóñez *et al.*, 2015; Ploetz *et al.*, 2015), particularly in regions such as the Great Lakes area of Eastern and Central Africa (Karamura, 1998; Karangwa *et al.*, 2016; van Westerhoven *et al.*, 2022). TR4 is pathogenic to most banana cultivars, including the dominant cultivar Cavendish (Ploetz, Randy C., 2015), while Race 1 and Race 2 strains continue to threaten locally produced banana varieties (Karangwa *et al.*, 2016; Martínez-de la Parte *et al.*, 2024). Despite the available genomic data on TR4, the impact TEs have on its genome evolution and adaptability have seen very limited investigation.

Helitrons, a distinct class of DNA transposons, are widespread across eukaryotic lineages and replicate via a rolling circle or peel-and-paste mechanism (Thomas & Pritham, 2015; Wells & Feschotte, 2020; Li, Z *et al.*, 2024). They have been extensively studied in plants (Du *et al.*, 2009; Hu *et al.*, 2019; Barro-Trastoy & Köhler, 2024) and animals (Grabundzija *et al.*, 2016; Barro-Trastoy & Köhler, 2024). Helitrons are also present in fungal genomes, but have seen less investigation compared to plants and animals (Castanera *et al.*, 2014; Castanera *et al.*, 2016; Chellapan *et al.*, 2016; Li, Z *et al.*,

2024). Here, we address this gap by investigating the recent activity and impact of Helitron element FoHeli1 in the M1 TR4 strain providing experimental evidence of large Helitron-driven structural variations.

We identified two major deletions on core chromosomes caused by FoHeli1 transposition, including a 464 kb deletion that eliminates the entire 12-gene biosynthetic gene cluster (BGC) for fusaric acid (FA) production (Niehaus *et al.*, 2014; Brown *et al.*, 2015; Studt *et al.*, 2016). As the first phytotoxin isolated from infected plants (Gaumann, 1957), FA has been implicated in virulence against tomato, banana and even mice (López-Díaz *et al.*, 2018; Liu *et al.*, 2020). Moreover, FA plays a role in the rhizosphere microbiome modulation in tomato (Jin *et al.*, 2024). However, its role in virulence appears context-dependent, as FA production is dispensable for *Fusarium verticillioides* during maize infection (Brown *et al.*, 2015).

Our study highlights the impact of Helitron activity on TR4 genome evolution, demonstrating their potential to reshape the genetic and metabolic landscape. We characterize FoHeli1 dynamics in the M1 strain and the reference TR4 strain II5, revealing extensive copy number variation across banana-infecting *Fusarium* strains. Furthermore, we assess the impact of the FA BGC loss on growth, metabolism, and pathogenicity, underscoring the broader implications of TE-mediated genomic changes on fungal biology and host-pathogen interactions.

Results

Helitron activity caused loss of the fusaric acid biosynthetic gene cluster in M1

TR4 has recently been shown to be spreading beyond its initial incursion point in Mozambique (van Westerhoven *et al.*, 2023). The TR4 strains from Mozambique were generally found to be highly similar to other globally occurring TR4 strains (van Westerhoven *et al.*, 2023). However, whole genome comparisons with the TR4 reference genome reveals two large scale deletions for strain M1, which was previously used for long-read whole genome sequencing (van Westerhoven *et al.*, 2023; van Westerhoven *et al.*, 2024a). These two large-scale deletions encompass 184 and 464 kb of the sub-telomeric regions of the M1 core chromosomes 2 and 3, respectively (Fig. 1a), representing approximately 1.25% of the 51 Mb sized genome of II5 (Dijkstra *et al.*, 2024), (Chapter 3). Together, the deleted regions comprise 210 putative genes, showing a significant loss of genetic material.

Prediction of BGCs in the reference genome of II5 indicates that the entire FA BGC is located within the borders of the deletion on chromosome 3 (Fig. 1b). Further genomic analysis, BGC prediction, and PCR confirmed that M1 had lost the 12 *fub* genes comprising the FA BGC and that the cluster was not translocated elsewhere

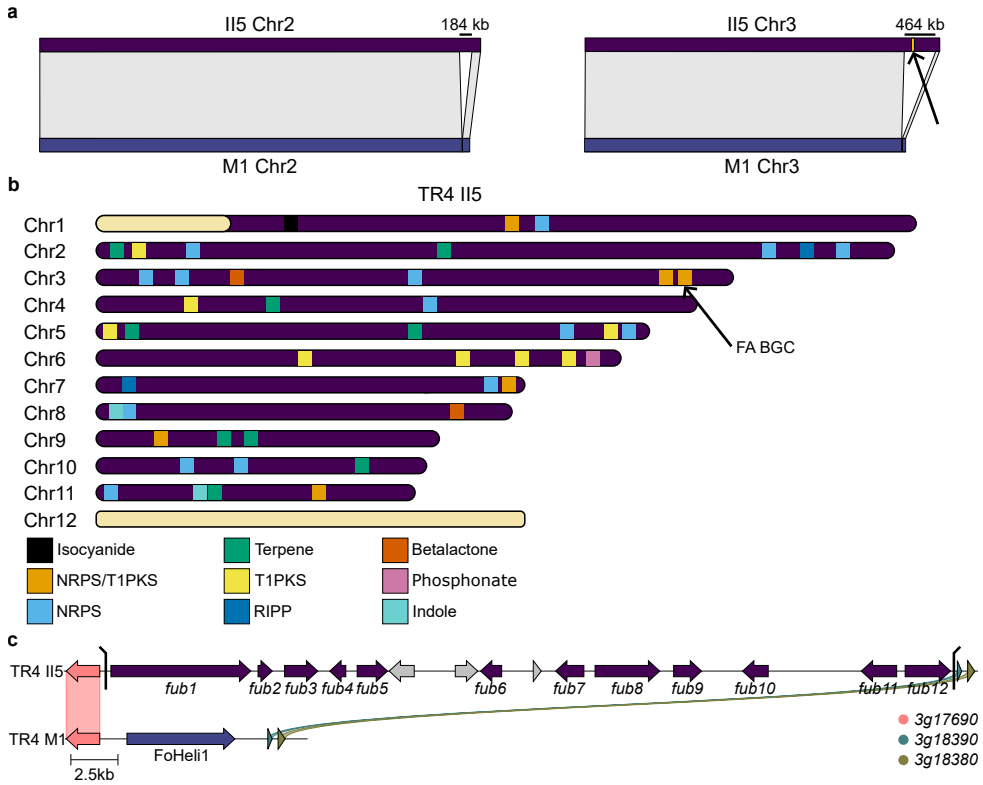


FIGURE 1 | Two large-scale deletions including the FA BGC on core chromosomes in TR4 strain M1. **a**) Alignment of core chromosomes 2 and 3 between TR4 strains II5 and M1. The approximate length of the deleted sequences compared to II5 is shown. The approximate location of the fusaric acid biosynthetic gene cluster (FA-BGC) is marked yellow on II5 chromosome 3 (black arrow). **b**) Schematic representation of the approximate locations of all predicted BGCs (46) and their types in TR4 strain II5. NRPS=Non ribosomal peptide synthase, T1PKS=Type I polyketide synthase, RIPP=Ribosomally synthesized and post-translationally modified peptide. The FA-BGC is located at the end of chromosome 3 (black arrow). **c**) Alignment of the FA-BGC regions in TR4 strains II5 and M1. For TR4 strain II5, the FA-BGC and its 12 genes are depicted, as well as the genes flanking the deletion. Black lines indicate the rest of the deleted sequence compared to II5. The entire FA-BGC of TR4 strain M1 is replaced by the ~6kb FoHeli1 TE.

in the genome (Fig. S1). To determine the potential cause of these large-scale deletions, we examined the deletion sites on chromosomes 2 and 3 and found that both deleted sequences were replaced by a short sequence of approximately 6 kb. Further BLAST analysis of this fragment indicated the presence of a FoHeli1 Helitron, a TE that replicates by a rolling-circle mechanism (Schmidt *et al.*, 2013; Chellapan *et*

al., 2016; Barro-Trastoy & Köhler, 2024). The FoHeli1 copy on chromosome 3 shares 98.6% identity with FoHeli1 in the tomato infecting strain *Fol*4287 (MF805714.1). We conclude that a total of 648 kb was lost in M1 because of FoHeli1 activity, including the full-length FA BGC (Fig. 1c).

To check whether loss of the FA BGC has occurred in other strains, we performed a blast analysis of the key biosynthesis gene *fub1* across a set of 35 publicly available *Fusarium oxysporum* genome assemblies (Meng *et al.*, 2024). This analysis shows the loss of the FA BGC in four additional strains that are pathogenic to common bean (Meng *et al.*, 2024). However, for these strains, no traces of FoHeli1 are present in the deleted region. Instead, a large 174 kb region is observed that is absent in II5 (Fig. S2a). Based on the large size of this fragment, in the otherwise conserved core chromosomes, we further analyzed the genes present in this region for strain F109. Based on the presence of several key genes, we conclude that this large section that is absent in II5 encompasses a Starship element (Fig.S2a-b) (Gluck-Thaler *et al.*, 2022). These results indicate that the FA BGC might be lost more commonly through different processes.

FoHeli1 activity in the TR4 lineage is recent and ongoing

The observed deletions indicate that Helitrons play an important role in the genome dynamics of *Fusarium oxysporum*. To further characterize FoHeli1 dynamics and search for additional copies, all TEs in the chromosomal assemblies of isolates II5 and M1 were predicted using Earl Grey (Baril *et al.*, 2024) (Fig. S3), which detected 15 and 16 copies of FoHeli1 TEs in II5 and M1, respectively. Most copies are full length (~6 kb), but both isolates contain a single copy of very short length corresponding to approximately the first 230 bases of the full-length FoHeli1 copies. This short length sequence might represent the remnants of a (non-autonomous) FoHeli1. Similarly, II5 and M1 contain one and two copies of FoHeli1, respectively, with a 5' truncation of several hundred bases, which may prevent further transposition. Transposable elements tend to accumulate mutations over time. By calculating the Kimura distance between TE sequences within the same family, we obtained a relative indication of when these elements last actively transposed (Chalopin *et al.*, 2015). FoHeli1 copies have the lowest average weighted Kimura distance in both II5 (0.04) and M1 (0.03) in comparison to all other predicted TEs which have a median average Kimura distance of 11.44 and 12.08 for II5 and M1, respectively, which suggests very recent activity (Fig. 2a – Fig. S4). To analyze the similarity of FoHeli1 copies in the strains, we compared the sequences of all individual copies. In general, the copies cluster at the strain level, except for two M1 derived copies that cluster along with the II5 derived copies (Fig. 2b). Interestingly, the FoHeli1 copies located on accessory chromosome

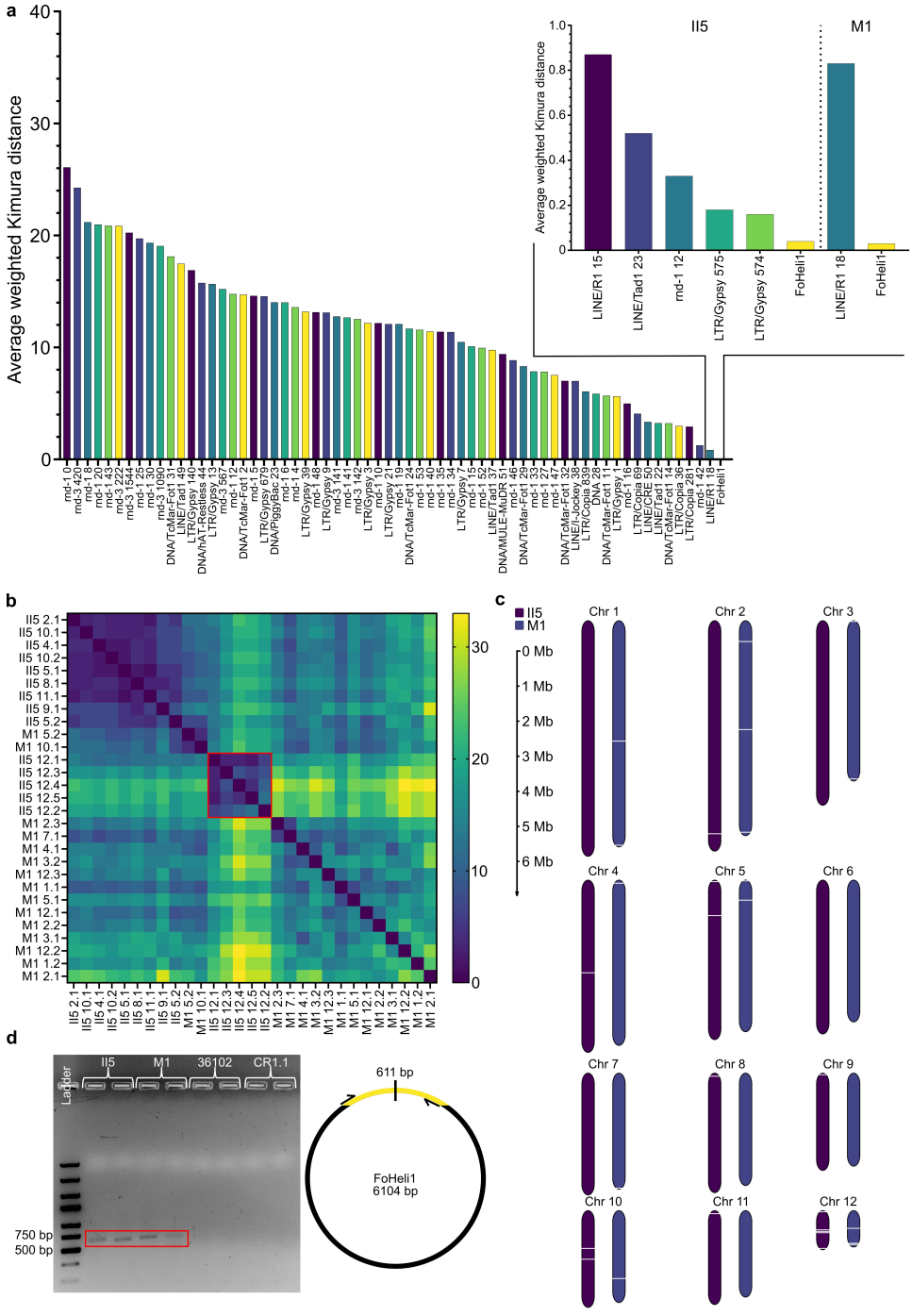


FIGURE 2 | Recent FoHeli1 activity in the TR4 lineage. a) Bar chart showing the average weighted Kimura distance of all TEs predicted and calculated by Earl Grey in TR4 strain M1. Inset shows TEs with

average weighted Kimura distance ≤1 in TR4 strains II5 and M1. **b**) Heatmap showing the number of SNPs between all long FoHeli1 copies in TR4 strains II5 and M1. **c**) Schematic representation of the location of all FoHeli1 copies per chromosome of TR4 strains II5 and M1. FoHeli1 locations are marked by white gaps. **d**) Gel electrophoresis of a PCR using FoHeli1 primers for a circular template (depicted right) on TR4 strains II5, M1, 36102 and Race 1 strain CR1.1. The expected band size is 611 bp.

12 of II5 formed a distinct cluster, suggesting intrachromosomal transpositions (Fig. 2b). Moreover, we observe that the vast majority of the FoHeli1 copies were found on different chromosomal locations between II5 and M1, further indicating recent activity of this TE (Fig. 2c). For both isolates, accessory chromosome 12 contains the most FoHeli1 copies in line with their generally higher TE density. Another way to determine FoHeli1 activity is to search for copies with multiple 5′ termini, which can arise from self-insertion events (Chellapan *et al.*, 2016). We used the previously determined FoHeli1 5′ terminal sequence (Chellapan *et al.*, 2016) and found that, of the 14 longer copies in II5, one copy contains two 5′ termini while another copy contains five 5′ termini. In M1, on the other hand, 5 out of 15 of the longer FoHeli1 copies contain two 5′ termini, while three copies contain three 5′ termini (Fig. S5). PCR further confirmed the presence of a circular intermediate of FoHeli1 in both TR4 isolates, while being absent in the other banana infecting *Fusarium* strains 36102 and CR1.1, which do not belong to the clonal TR4 lineage and lack any FoHeli1 copies (Fig. 2d). We also tested how recent FoHeli1 activity took place as well as its propensity to be involved in genomic changes in the TR4 lineage in strains UKTR4 and HN51, where FoHeli1 also had the lowest average weighted Kimura distance and was, in several cases, located at the border of rearrangements (Fig. S6), one of which was independently observed previously (Zhang, Y *et al.*, 2024). Taken together, we show that FoHeli1 activity in the TR4 lineage is very recent and most likely still ongoing.

FoHeli1 copy number is highly diverse in banana-infecting *Fusarium* strains

We used DeviaTE (Weilguny & Kofler, 2019) to estimate the FoHeli1 copy number of 58 Illumina sequenced banana infecting *Fusarium* strains (Martínez-de la Parte *et al.*, 2024; van Westerhoven *et al.*, 2024a). These estimates show that the copy number of FoHeli1 ranges between 9 and 36 in TR4 strains (Fig. 3a). Interestingly, the highest copy numbers (N=25-36) are observed in a set of TR4 strains which have intrachromosomal duplications of accessory chromosome 12 (Fig. 3a) (Dijkstra *et al.*, 2024), (Chapter 3). The copy number estimates for isolate II5 by DeviaTE are higher (N=25) than the copy number obtained from Earl Grey (N=15. This is caused by intrachromsomal duplications of chromosome 12, that is not resolved in the assembly (Dijkstra *et al.*, 2024), (Chapter 3). In contrast to TR4, Race 1 and Race 2 strains show a much wider range of FoHeli1 copy number than TR4 (Fig. 3b). Some of the analyzed Race 1 strains do not have any FoHeli1 copies, whereas all Race 2 strains contain a high number of FoHeli1 copies (N>50). It has previously been observed that Race 2 strains have

a larger genome size and contain more accessory material (van Westerhoven *et al.*, 2024a). Comparing the genome size of 47 banana-infecting *Fusarium* strains with their FoHeli1 copy number shows a moderate positive correlation between the two factors (Fig. S7). This indicates that the larger number of FoHeli1 elements in Race 2 strains is possibly caused by a larger accessory genome size (van Westerhoven *et al.*, 2024a). Helitrons are known to occasionally capture genes or gene fragments during transposition (Castanera *et al.*, 2014; Barro-Trastoy & Köhler, 2024). Hence, we searched for such events but identified only a single case in Race 2 strain C081 (Fig. 3c). However, such gene capture events are likely to be missed in Illumina sequenced strains due to the limitations of short-read sequencing for structural genomic analyses. Interestingly, FoHeli1 copies are present in all TR4 strains, which all contain chromosome 12, but FoHeli1 is absent in the most closely related strain 36102, which lacks this chromosome (van Westerhoven *et al.*, 2024a), thus raising questions on the origin of FoHeli1 within the TR4 lineage.

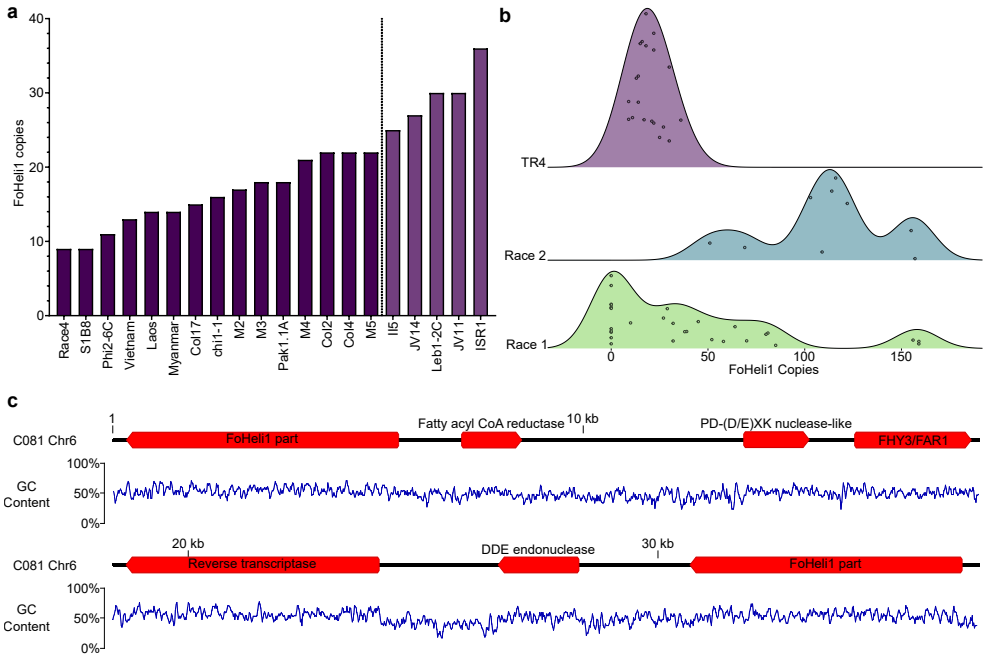


FIGURE 3 | FoHeli1 copy number is diverse in banana infecting *Fusarium* strains. a) Estimated FoHeli1 copy number in 20 Illumina sequenced TR4 strains based on DeviaTE. Strains with duplications within accessory chromosome 12 (Dijkstra *et al.*, 2024), (Chapter 3), are noted with a lighter shade and separated by a dotted line. **b**) Ridgeline plot of estimated FoHeli1 copy number in 58 Illumina sequenced banana infecting *Fusarium* strains based on DeviaTE. The plot separates Tropical Race 4 (TR4), Race 1 and Race 2 strains. Each dot represents one strain. The estimated copy number was cut off to the nearest full number for each strain. **c**) Fragment of the genomic sequence of Race 2 strain C081 (~38 kb) depicting a gene capture event by a FoHeli1 copy. Domains of the captured genes are noted. GC content is plotted below.

LC-MS analysis of M1 confirms the absence of fusaric acid

To investigate how the large-scale deletions on chromosomes 2 and 3 affect the overall metabolome, particularly FA biosynthesis, we performed untargeted metabolomics profiling on exometabolites of strains II5 and M1 following *in vitro* cultivation. Firstly, comparison to a commercial FA standard confirmed the presence of FA and the derivative dehydrofusaric acid in II5 and their absence in M1 (Fig. 4a). Thus, the deletion because of FoHeli1 activity abolished FA production in M1.

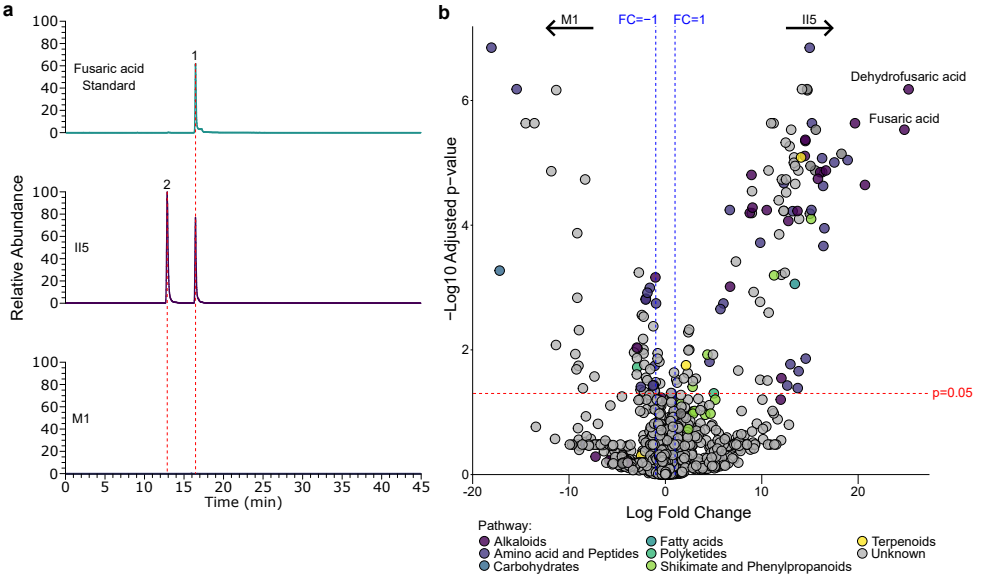


FIGURE 4 | TR4 strain M1 does not produce fusaric acid. a) LC-MS profile of commercial fusaric acid standard and liquid cultures of TR4 strains II5 and M1. Peak 1 corresponds to fusaric acid, and peak 2 corresponds to dehydrofusaric acid (red dotted lines). **b**) Volcano plot of metabolite features detected in TR4 strains II5 and M1. Blue threshold lines are shown at a log fold change (FC)>1 and FC<-1. The red threshold line indicates an adjusted p-value of 0.05. Negative fold change features are more abundant in M1; positive fold change features are more abundant in II5.

In total, 1594 metabolite features were detected in positive and negative ionization modes across the samples, including the growing medium (PDB) (Fig. 4b). We performed Principal Component Analysis (PCA) to examine the variation in the exometabolite profile among strains II5, M1 and M2 and the growing medium. The first and the second principal components explained 46.2% and 15.3% of the variability, respectively, accounting for a cumulative 61.5% of the total variability in the metabolite data (Fig. S8). The first principal component underscores the differences in metabolites between the growing medium and the fungal isolates, reflecting the metabolic activity of the fungi. In contrast, the second principal component depicts the variation in metabolite profiles between the three TR4 isolates. Additionally,

a pairwise comparison of the individual metabolite features between II5 and M1 revealed that 146 features exhibited significant variation (FC>1/FC<-1 and P <0.05), which included compounds from the alkaloids, amino acid and peptides, carbohydrates, fatty acids, polyketides, shikimate and phenylpropanoids, terpenoid pathways (Fig. 4b). In contrast, pairwise comparison between II5 and M2 showed 107 metabolite features with significant variation. M2 did not show significantly different FA production levels. In particular, comparative metabolomics of M1 with II5 showed either a complete absence or a significant reduction in metabolites belonging to the alkaloid pathway, including fusaric acid, dehydrofusaric acid, and other derivatives (Fig. 4b). Moreover, several metabolites associated with dipeptides showed a significantly higher abundance in II5.

Loss of the fusaric acid biosynthetic gene cluster impacts fungal development

FA has been shown previously to have an antimicrobial effect, including self-inhibition of the producing fungus (Crutcher *et al.*, 2015; Studt *et al.*, 2016). Normally, fungal self-protection against FA occurs by the cluster-specific transporter (*fub11*) and the regulation of derivatives with reduced toxicity (*fub12*) (Studt *et al.*, 2016). As M1 has lost the entire FA BGC, both functions should be disrupted. In turn, we observed an elevated sensitivity to exogenously applied FA in M1 compared to II5 (Fig. 5a-b). Similarly, FA production has been previously implicated with growth and biomass levels (Crutcher *et al.*, 2015; Studt *et al.*, 2016). To check for potential growth effects, we performed growth experiments using II5, M1, the *fub1* knock-out strain Δ*fub1*, and the complementation strain Δ*fub1*c. Growth on regular PDA or FA production promoting Czapek-Dox agar (CDA) showed no significant differences between all tested strains. Only M1 showed slightly higher growth rates on PDA plates similar to the experiment using exogenous FA application (Fig. 5c). Loss of FA production has been shown previously to affect the production of other secondary metabolites such as the pigment bikaverin (López-Díaz *et al.*, 2018; Phasha *et al.*, 2021). Similarly, we also observe more pigmentation of the M1 and Δ*fub1* colonies compared to II5 and Δ*fub1*^{c} (Fig. 5d).

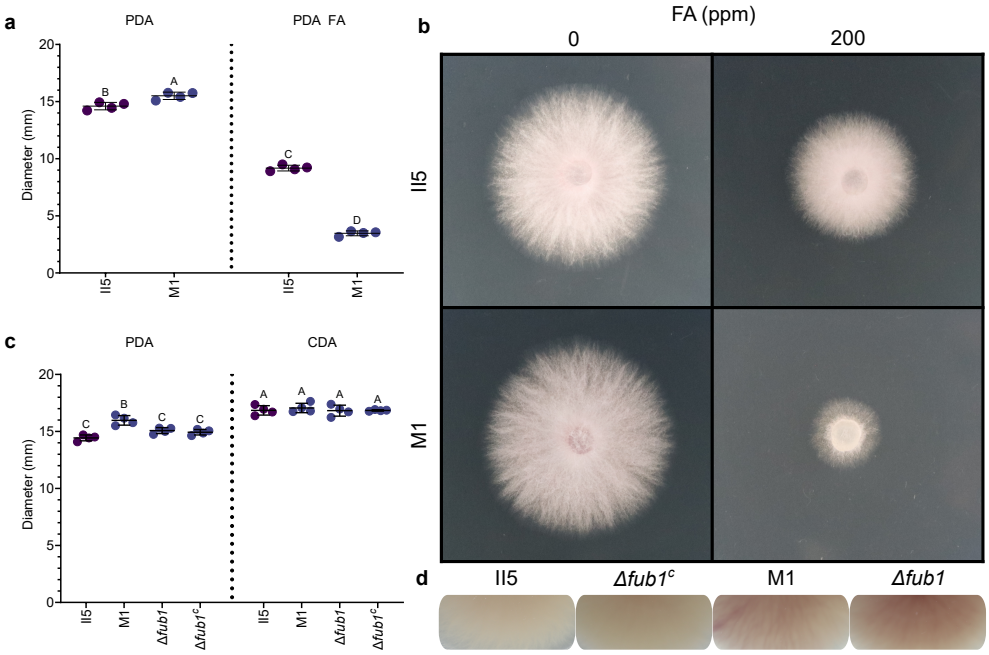


FIGURE 5 | Fusaric acid biosynthetic gene cluster loss affects different phenotypes. a) Colony diameter (mm) of TR4 strains II5 and M1 on PDA and PDA plates supplemented with 200 ppm fusaric acid. Growth was quantified at 3 days post inoculation (dpi). Letters indicate significant differences between treatments (Tukey-Kramer test; P<0.05). Data are shown as mean ±SD (n=4). **b**) PDA plates and PDA plates supplemented with 200 ppm fusaric acid inoculated with TR4 strains II5 or M1 photographed at 3 dpi. **c**) Colony diameter (mm) of PDA plates and CDA plates inoculated with TR4 strains II5, M1, Δ*fub1* mutant and complementation. Growth was quantified at 3 dpi. Letters indicate significant differences between treatments (Tukey-Kramer test; P<0.05). Data are shown as mean ±SD (n=4). **d**) Photos of the colony edge for strains II5, Δ*fub1c,* M1 and Δ*fub1* inoculated on PDA plates at 8 dpi. Photographed from the bottom of the plate.

Fusaric acid is not required for pathogenicity on banana

To test whether the large deletions affect M1 virulence and if FA contributes to banana infection, Cavendish plants were inoculated with wildtype strains II5 and M1, as well as the newly generated Δ*fub1* mutant and the complemented strain Δ*fub1*c. The results from the infection assays showed that isolates II5 and M1 caused similar disease severity irrespective of the used spore concentration (Fig. 6a). Similar results were obtained with the FA producing M2 strain (Fig. S9). Comparable to the M1 infection assay, no significant difference was observed between II5, the Δ*fub1* mutant, and the Δ*fub1*^{c} complementation line at the lower spore concentration (Fig. 6b). In general, a lower spore concentration leads to lower corm necrosis levels and reduced or delayed disease incidence and does not lead to significant differences between the different strains and mutants. No significant difference was observed

between II5 and the Δ*fub1* mutant at the regular spore concentration (10^6) either (Fig. S10). Together, these results indicate that the loss of the major toxin FA by FoHeli1 activity or CRISPR/Cas-9 mediated knockout of core enzyme *fub1* does not affect the overall virulence of TR4 on Cavendish plants.

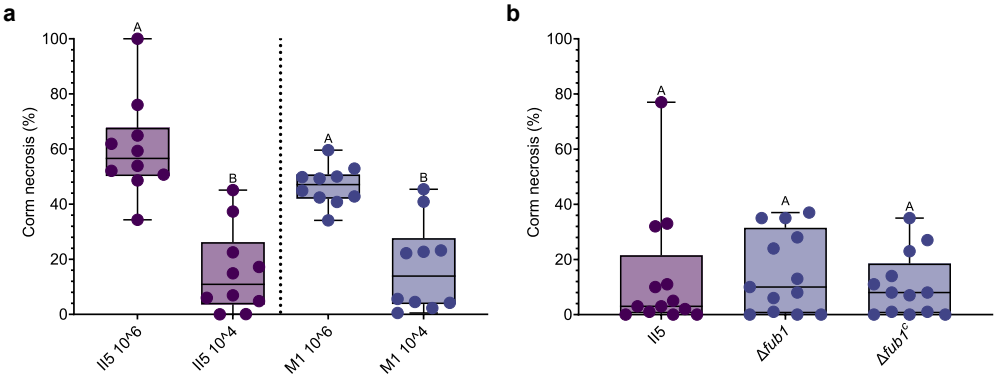


FIGURE 6 | Fusaric acid is not required for virulence on banana. a) Percentage of corm necrosis at 10 weeks post-inoculation of Cavendish 'Grand Naine' plants inoculated with the reference TR4 strain II5 or strain M1. Plants were inoculated with either 10^6 or 10^4 spores per mL. Corm necrosis was quantified using ImageJ (n=10). Letters indicate significant differences between treatments (Tukey-Kramer test; P<0.05). **b**) Percentage of corm necrosis at 10 weeks post-inoculation of Cavendish 'Grand Naine' plants inoculated with strain II5, Δ*fub1* mutant or the Δ*fub1*^{c} complementation strain. All plants were inoculated with 10^4 spores per mL. Corm necrosis was quantified using ImageJ (n=13). Letters indicate significant differences between treatments (Tukey-Kramer test; P<0.05).

Discussion

Our study reveals the genomic and metabolic dynamics driven by Helitron activity in the banana infecting clonal TR4 lineage. By characterizing large-scale deletions mediated by the transposon FoHeli1 through bioinformatic analysis, metabolomic profiling, growth and pathogenicity assays, our work underscores the significant impact of transposable elements on genome dynamics and the adaptive potential of fungal pathogens. These deletions, notably the loss of the fusaric acid biosynthetic gene cluster, provide new insight into understanding the evolutionary trade-offs inherent in TE-driven genome remodeling.

Helitrons have been implicated to play a role in genomic variation across diverse eukaryotes (Wells & Feschotte, 2020; Hayward & Gilbert, 2022; Barro-Trastoy & Köhler, 2024; Li, Z *et al.*, 2024). Although Helitrons have seen some investigation within fungi (Castanera *et al.*, 2014; Li, Z *et al.*, 2024; Oggenfuss *et al.*, 2024), including *Fusarium oxysporum* (Chellapan *et al.*, 2016) their impact on genome dynamics in fungal

pathogens has remained underexplored, particularly in banana-infecting *Fusarium*. The recent and likely ongoing activity of FoHeli1 underscores how transposable elements can generate genetic variation in clonally reproducing pathogens. The low sequence diversity among FoHeli1 copies in M1 and II5 strains, their occurrence in distinct loci between the two strains, and the detection of a putative circular intermediate suggest an active phase of transposition that continues to reshape the TR4 genome. This activity aligns with the prior observation of Helitron-mediated genomic changes in other *Fusarium* strains, such as the loss of an effector gene associated with host specificity (Biju *et al.*, 2017), further highlighting the evolutionary significance of these elements in host-pathogen interactions. Another indication of ongoing FoHeli1 activity within the TR4 lineage is our observation of multiple 5' termini in many M1 FoHeli1 copies, which are likely to arise following self-insertion events (Chellapan *et al.*, 2016). The presence of FoHeli1 copies at the border of genome rearrangements in additional TR4 strains suggest a broader TR4 wide impact of FoHeli1 activity. However, some investigated strains lack FoHeli1 entirely, such as the less virulent strain 36102, this strain is most closely related to the clonal TR4 lineage and lacks accessory chromosome 12 (van Westerhoven *et al.*, 2024a). This raises important questions around a potential horizontal transfer origin for FoHeli1 within the TR4 lineage.

Although Helitrons have also been implicated in the capture and transposition of adjacent genes (Castanera *et al.*, 2014; Barro-Trastoy & Köhler, 2024), we did not observe this within either II5 or M1. Putative captured genes, however, were observed for Race 2 strain C081. The availability of additional long-read genome assemblies could provide deeper insights into the frequency and mechanisms of gene capture by FoHeli1 and other Helitrons in banana-infecting *Fusarium*. Furthermore, such assemblies could improve understanding of FoHeli1-related structural genomic changes across the *Fusarium oxysporum* species complex (FOSC) and their evolutionary implications for host-pathogen interactions.

Further estimation of FoHeli1 copy number in 58 sequenced banana-infecting *Fusarium* strains indicates a large variation in copy number. TR4 strains recently shown to harbor intrachromosomal duplications of accessory chromosome 12 possess the highest number of FoHeli1 copies within the TR4 lineage (Dijkstra *et al.*, 2024), (Chapter 3). Interestingly, all FoHeli1 copies on chromosome 12 of II5 are highly similar to one another and distinct from those on core chromosomes. These findings indicate a recent local transposition burst, as these copies are not part of any larger segmental duplications. Compared to TR4, Race 1 and Race 2 strains show a much wider range of FoHeli1 copy number variation. Although generally thought to replicate via a peel-and-paste mechanism (Barro-Trastoy & Köhler, 2024), experimental evidence in maize suggests transposition by excision can occur as well (Li & Dooner, 2009). With the

occurrence of FoHeli1 in distinct loci in all investigated TR4 genome assemblies, the degree of copy number variation is more suggestive of predominant transposition by excision rather than a peel-and-paste mechanism.

The loss of the FA BGC challenges the prevailing view of FA as a critical virulence factor in the *Fusarium*-banana interaction (Li *et al.*, 2013; Liu *et al.*, 2020). While FA has been associated with phytotoxicity, self-toxicity, antimicrobial activity, and rhizosphere modulation (Bacon *et al.*, 2006; Son *et al.*, 2008; Crutcher *et al.*, 2015; Bohni *et al.*, 2016; Studt *et al.*, 2016; López-Díaz *et al.*, 2018; Jin *et al.*, 2024), our infection assays demonstrate that its absence does not compromise TR4 virulence in banana. These findings indicate that FA's role is context-dependent, potentially more significant in competitive microbial environments than in direct pathogenesis. Such flexibility highlights the adaptive resilience of TR4, which potentially compensates for FA loss through other genetic and metabolic pathways, for instance increased production of other antimicrobial compounds such as beauvericin, bikaverin, and equisetin to maintain ecological fitness (Spraker *et al.*, 2018; Xu *et al.*, 2023). Intriguingly, we also identified the loss of the FA BGC in another four *Fusarium* strains infecting common bean, suggesting that this cluster may be lost more frequently through diverse evolutionary mechanisms. Additionally, FA production has been shown to be dispensable for virulence in other pathosystems, such as the interaction between *F. verticillioides* and maize (Brown *et al.*, 2015). In general, the levels of FA production between different *Fusarium* strains can differ significantly, irrespective of virulence against a host (Notz *et al.*, 2002; Schouten *et al.*, 2004). Together, these findings indicate that FA's role in virulence is context-dependent, with its importance varying based on the host-pathogen system and environmental pressure.

Genomic variation because of TE activity, such as FoHeli1, may facilitate adaptation to environmental pressures, including host resistance and agricultural practices (Seidl & Thomma, 2017). This capacity for genomic remodeling, while beneficial for the pathogen, poses challenges for disease management, as it can lead to the emergence of new virulence traits or resistance mechanisms (Chuma *et al.*, 2011; Kashiwa *et al.*, 2016; Biju *et al.*, 2017; Zaccaron & Stergiopoulos, 2024). At the same time unrestricted TE activity and proliferation might have long term consequences for the pathogen (Fouché *et al.*, 2022). Expanding long-read genomic studies across the FOSC will allow for a better assessment of the impact of TEs on structural variation, gene loss and genome evolution.

Furthermore, the loss of FA production raises intriguing questions about the ecological trade-offs faced by TR4. The antimicrobial properties of FA likely confer advantages in niche competition (Notz *et al.*, 2002; Bacon *et al.*, 2006; Tung *et al.*, 2017; Jin *et al.*, 2024), yet its self-toxicity and energetic cost may render its production dispensable

under certain conditions. The toxicity of FA has been linked to its chelating capacity, modulating the availability of metal ions essential for microbial survival (Ruiz *et al.*, 2015; López-Díaz *et al.*, 2018). On the other hand, other microbes have developed several ways to withstand higher concentrations of FA, such as efflux transporters or the increased production of siderophores (Hu *et al.*, 2012; Ruiz *et al.*, 2015). Studies showing reduced phytotoxic and antimicrobial effects of FA in the presence of metals like copper, iron and zinc support this hypothesis (Ruiz *et al.*, 2015; López-Díaz *et al.*, 2018). This trade-off mirrors the broader evolutionary dynamics of secondary metabolites in fungal pathogens, where ecological versatility often necessitates balancing metabolic costs and adaptive benefits (Brakhage, 2013; Krishnan *et al.*, 2018; Abraham *et al.*, 2024).

In conclusion, this study highlights the dual role of TEs in generating novel genetic variation and affecting genomic instability. In addition, we show that the conserved FA-BGC can be lost in TR4 without affecting virulence on banana. The ongoing activity of FoHeli1 in TR4 exemplifies the dynamic interplay between TE activity, genome evolution and ecological adaptation in fungal pathogens. By elucidating the consequences of TE-mediated genomic changes, we advance our understanding of the impact of TEs on genome dynamics and secondary metabolism in a clonally reproducing pathogen.

Materials and methods

Fungal strains, growth conditions and transformation

Fusarium Tropical Race 4 reference strain II5, strains M1 and M2 isolated from Mozambique (van Westerhoven *et al.*, 2023; van Westerhoven *et al.*, 2024a) and newly generated *fub1* knockout strain *Δfub1* and *fub1*^{c} complementation mutants were used in this study. Strains were stored as conidial suspension stocks in 15% glycerol at -80 ˚C. General culturing of the fungal strains was performed using potato dextrose agar (PDA) at 25 ˚C.

The *Δfub1* mutant was generated in the II5 background as previously described (Dijkstra *et al.*, 2024), (Chapter 3). Complementation was performed using the same procedure instead using a DNA fragment containing the *fub1* gene and 1kb of upstream and downstream DNA fused with a hygromycin cassette by overlap extension PCR as donor fragment. Complementation was done by ectopic integration using the same procedure as in Dijkstra et al., (2024), (Chapter 3), in the absence of a Cas9 vector. Used primers are listed in Table S1.

Whole genome comparison

The previously published whole genome sequences of strains II5 and M1 were used for analysis (van Westerhoven *et al.*, 2024a). Putative biosynthetic gene clusters were predicted for the genomes of strains II5 and M1 using Antismash 7.1 with standard relaxed detection strictness (Blin *et al.*, 2023). The FA BGC cluster and Starship representation were made using Clinker (Gilchrist & Chooi, 2021). Chromosome alignments were made using syntenyPlotteR (Quigley *et al.*, 2023).

Transposable element analysis

Initial FoHeli1 identification was done using BLAST (Camacho *et al.*, 2009) and comparison to known FoHeli1 sequences (Chellapan *et al.*, 2016). TEs in long-read sequenced strains II5 and M1 were annotated and analyzed using Earl Grey using the standard parameters (Baril *et al.*, 2024). Full-length FoHeli1 copies were aligned using Clustal Omega to determine the number of SNPs between each copy (Sievers *et al.*, 2011). The FoHeli1 chromosomal location plot was made with the use of MG2C (Chao *et al.*, 2021). FoHeli1 copy numbers were further analyzed in 58 short-read sequenced *Fusarium* strains isolated from banana using DeviaTE (Weilguny & Kofler, 2019). The sequence of II5 translation elongation factor 1-alpha (EF-1 alpha) was used as single copy reference gene for copy number estimation. All used strains and their FoHeli1 copy number are noted in Table S2.

DNA from strains II5, M1, 36102, and CR1.1 was extracted from freeze-dried mycelium using the Masterpure™ Yeast DNA Purification Kit (LGC Biosearch™ Technologies, Hoddesdon, United Kingdom). Genomic DNA was used for PCR and subsequent gel electrophoresis to check for FoHeli1 circular intermediates. The primers used are listed in Table S1.

Exometabolite extraction

Strains II5, M1 and M2 were grown on PDA plates for 7 days. Five agar plugs were then used to inoculate flasks containing 100 ml PDB supplemented with 5% banana root exudate. Cultures were grown in triplicate at 25 ˚C and 150 rpm for 7 days. PDB with 5% banana root exudate without *Fusarium* was used as control. After growth the culture filtrates were obtained by filtering the medium through a 0.2 µm filter. Culture filtrates were freeze dried and afterwards dissolved in 4 mL ethyl acetate for one hour on a rolling shaker. Samples were subsequently dried with nitrogen and dissolved in 5 mL 75% MeOH, 0.1% formic acid. Afterwards samples were sonicated for one hour. Samples were further centrifuged twice at 13.000 rpm for 10 minutes. HPLC vials were filled with 250 µL supernatant for chromatographic analysis.

Exometabolite analysis

An UltiMate 3000 U-HPLC system (Dionex) was used to create a 45-minute linear gradient of 5-35% (v/v) acetonitrile in 0.1% (v/v) formic acid (FA) in water at a flow rate of 0.19 mL min^{-1}. 5 µL of each extract was injected, and compounds were separated on a Luna C18 column (2.0 x 150 mm, 3µm; Phenomenex, Torrance, California USA) maintained at 40 °C (De Vos *et al.*, 2007). The detection of compounds eluting from the column was performed with a Q-Exactive Plus Orbitrap FTMS mass spectrometer (Thermo Scientific™, Waltham, Massachusetts USA). Full scan MS data were generated with electrospray in switching positive/negative ionization mode at a mass resolution of 35,000 (FWHM at m/z 200) in a range of m/z 95-1350. Subsequent untargeted MS/MS analyses were performed with separate positive or negative electrospray ionization at a normalized collision energy of 27 and a mass resolution of 17,500. The ionization voltage was optimized at 3.5 kV for positive mode and 2.5 kV for negative mode; the capillary temperature was set at 250 °C; the auxiliary gas heater temperature was set to 220 °C; sheath gas, auxiliary gas, and the sweep gas flow were optimized at 36, 10 and 1 arbitrary units, respectively. Automatic gain control was set at 3e6 and the injection time at 100 ms. External mass calibration with formic acid clusters was performed in both positive and negative ionization modes before each sample series.

LCMS data preprocessing and analysis

Mass peak picking and alignment were performed using Metalign software (Lommen, 2009). Mass features in the resulting peak list were considered as a real signal if they were detected with an intensity of more than 3 times the noise value and in 2 out of the three biological replicates of at least one treatment. Mass features originating from the same metabolites were subsequently reconstituted based on their similar retention window and their intensity correlation across all measured samples, using MSClust software (Tikunov *et al.*, 2012). This resulted in the relative intensity of 725 putative mass features potentially representing individual metabolites across the samples. The raw data were processed using R (4.4.1 [2024-06-14]) for gap-filling and normalization. Average PDB intensities were calculated for each feature, and these were subtracted from the sample and QC intensities to correct for baseline signals. Negative values were replaced with small positive random values between 90 and 100 to avoid computational errors during subsequent analysis. Logarithmic transformation (log2) was applied to normalized intensities to stabilize variance and normalize distributions. Differentially abundant metabolites identified through statistical analyses were subjected to structural annotation. Representative samples from each treatment were analyzed using untargeted positive and negative ionization MS/MS, generating fragmentation spectra that were processed and exported as .mgf files in MZmine 4.3.0 (Schmid *et al.*, 2023). These spectra were processed using SIRIUS software for molecular formula prediction and compound annotation based on

fragmentation patterns (Dührkop *et al.*, 2019). MS/MS spectra were matched against public databases such as Biocyc, COCONUT, KEGG, KNApSAcK, LOTUS, GNPS, HMDB, and PubChem:bio and metabolites to enhance confidence in annotation. Annotation confidence levels were categorized following the Metabolomics Standards Initiative (MSI) guidelines, with Level 1 corresponding to confirmed identifications through reference standards (only for Fusaric acid) and Levels 2-4 representing varying degrees of confidence based on spectral similarity and predictive algorithms.

Principal Component Analysis (PCA)

Principal Component Analysis was conducted to visualize variance among the experimental groups. The normalized intensity data were transposed, and PCA was performed using the prcomp function in R with data scaling. The PCA results were visualized using fviz_pca_ind from the factoextra package. Two PCA analyses were performed, including all experimental groups and excluding PDB samples, to assess group-specific variation.

Differential Analysis

Differential metabolite abundance between experimental groups (M1 vs. M2, M1 vs. II5, and M2 vs. II5) was evaluated using the limma package in R. For each comparison, a linear model was fitted to the data, and empirical Bayes moderation was applied to improve robustness. The adjusted p-value threshold (false discovery rate, FDR) was set at 0.05. Fold changes greater than ±2 were considered biologically significant. All annotated features in the comparison between II5 and M1 are noted in Table S3. Annotated features in the comparison between II5 and M2 are noted in Table S4 (10.6084/m9.figshare.28607054).

Volcano Plot Visualization

Volcano plots were generated to highlight significant metabolites for each pairwise comparison. Log fold changes (logFC) and -log10 transformed adjusted p-values were plotted using ggplot2. Significant features were color-coded by pathway categories (e.g., alkaloids, carbohydrates, terpenoids) with a custom color palette. Threshold lines at logFC ±1 and p-value < 0.05 were annotated to demarcate significance criteria.

Growth assays

For the determination of colony growth, agar plugs were taken from glycerol stock inoculated PDA plates and put on fresh PDA, CDA or PDA plates supplemented with 200 ppm fusaric acid (Sigma-Aldrich, Saint Louis, USA). Colony diameter was measured at 3 days post inoculation (dpi). Colonies were photographed at 3 dpi. Photos for colony pigmentation were taken at 8 dpi.

Plant growth conditions and infection assays

Cavendish plants were inoculated as described previously (García-Bastidas *et al.*, 2019). In brief, conidia were produced by inoculating flasks of Mung bean medium with agar plugs of the different wild-type *Fusarium* strains and mutants. The flasks were incubated for 5 days at 150 rpm 25 °C. Conidia were collected by filtering the medium through two layers of sterile cheesecloth. The conidia were subsequently quantified and diluted to the desired concentration. Prior to inoculation, Cavendish plants were wounded in their roots twice and inoculated with 200 mL of either $1{\cdot}10^6$ or $1{\cdot}10^4$ conidia/ml by pouring. Plants were monitored and scored after 8-10 weeks post-inoculation. To assess virulence levels, plants were cut longitudinally at the corm, and pictures were taken. Finally, the percentage of necrosed corm tissue was determined using ImageJ.

Acknowledgements

JD, ACW, CAG, GNT and GHJK were supported by the Bill and Melinda Gates Foundation, grant no.: AG – 4425. Banana research at Wageningen University has been supported by the Dutch Dioraphte Foundation, grant no.: 20 04 04 02.

Competing interests

None declared.

Author contributions

JD conducted experiments and performed analyses. YL, CAG, and GNT conducted experiments. ACW, XSK and DWE contributed to the analyses. JD wrote the manuscript with input from GHJK and DWE. All authors contributed to writing and editing the manuscript. GHJK conceived and supervised the project.

Data availability

All data are available in the main text or in the supporting information (Figs S1-S10; Tables S1-S4).

Supplementary materials

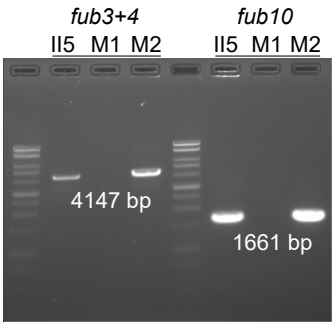


FIGURE S1 | PCR confirms loss of *fub* genes in TR4 strain M1. Gel electrophoresis after PCR using primers for fragments containing *fub* genes 3+4 or *fub10* in TR4 strains II5, M1, and M2.

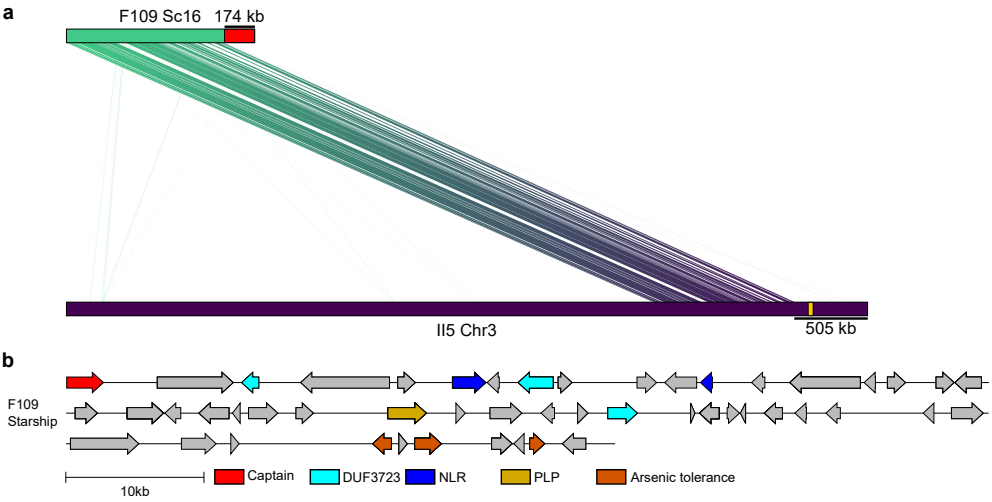


FIGURE S2 | Starship element in strain F109 caused fusaric acid BGC loss. a) Alignment between TR4 strain II5 chromosome 3 and F109 strain scaffold 16. The approximate length of absent sequences is shown. The approximate location of the fusaric acid biosynthetic gene cluster is noted on II5 chromosome 3 by a yellow marker. The Starship element is depicted by a red marker on scaffold 16 of F109. The fusaric acid biosynthetic gene cluster is similarly absent in F23, F79 and F105 (Meng *et al.*, 2024). **b**) Schematic representation of the 50 putative genes located on the Starship element on scaffold 16 of F109. Common Starship genes are noted (Captain=DUF3435, NLR=NOD-like receptor, PLP=patatin-like phospholipase). The scale bar depicts 10kb in length.

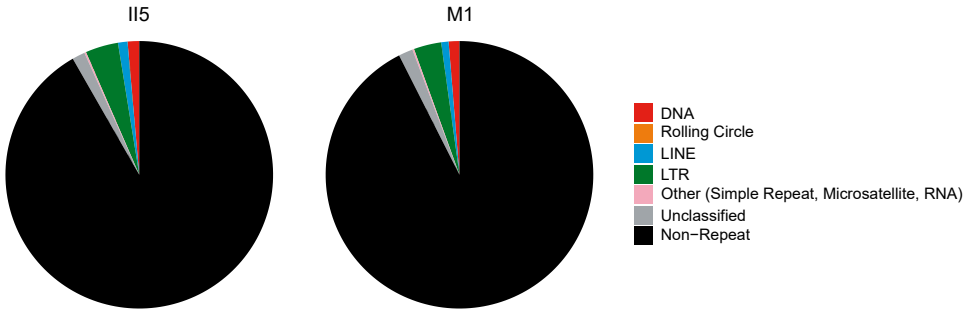


FIGURE S3 | Transposable element content of TR4 strains II5 and M1. Pie chart summary of all TEs predicted by Earl Grey and their contribution to the total genome size of TR4 strains II5 (8.2%) and M1 (7.4%). Note FoHeli1 is part of the unclassified section.

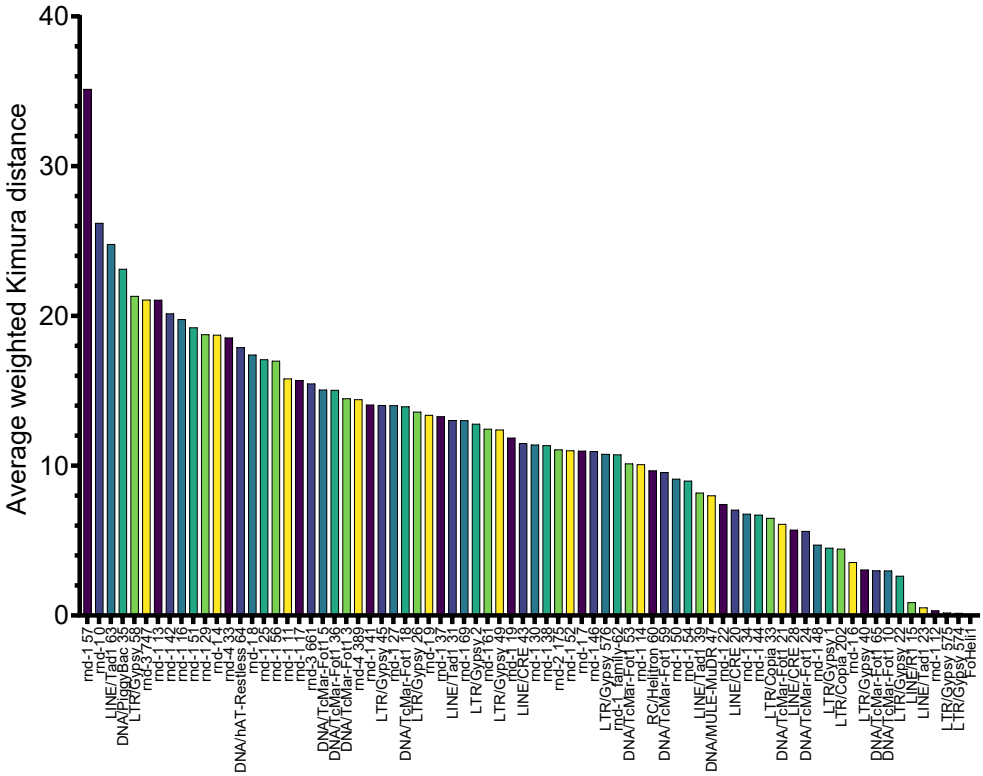


FIGURE S4 | Recent FoHeli1 activity in TR4 strain II5. Bar chart showing the average weighted Kimura distance of all TEs predicted and calculated by Earl Grey in TR4 strain II5.



FIGURE S5 | M1 FoHeli1 with multiple 5′ termini. First 100 bp of three FoHeli1 copies from TR4 strain M1 as predicted by Earl Grey. Colored markings indicate the 16 bp 5′ terminal sequence of FoHeli1 as described by Chellapan *et al.* (2016). FoHeli1 copies in M1 contain either one, two or three 5′ termini.

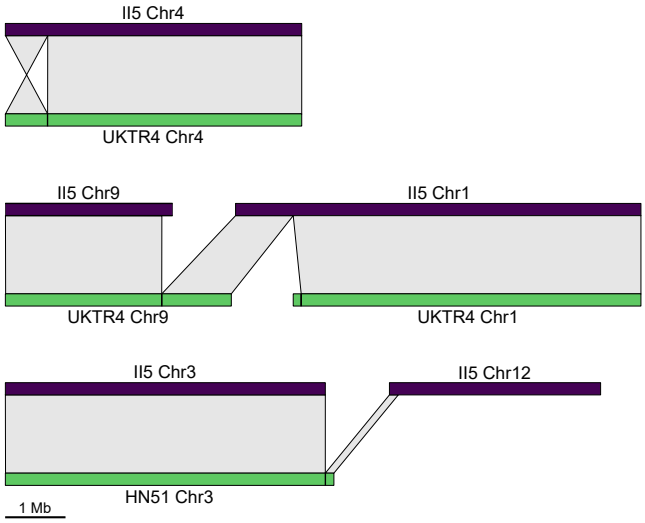


FIGURE S6 | FoHeli1 mediated genomic rearrangements in TR4 strains. Alignment between chromosomes of TR4 strain II5, UKTR4 and HN51 showing rearrangements at FoHeli1 loci.

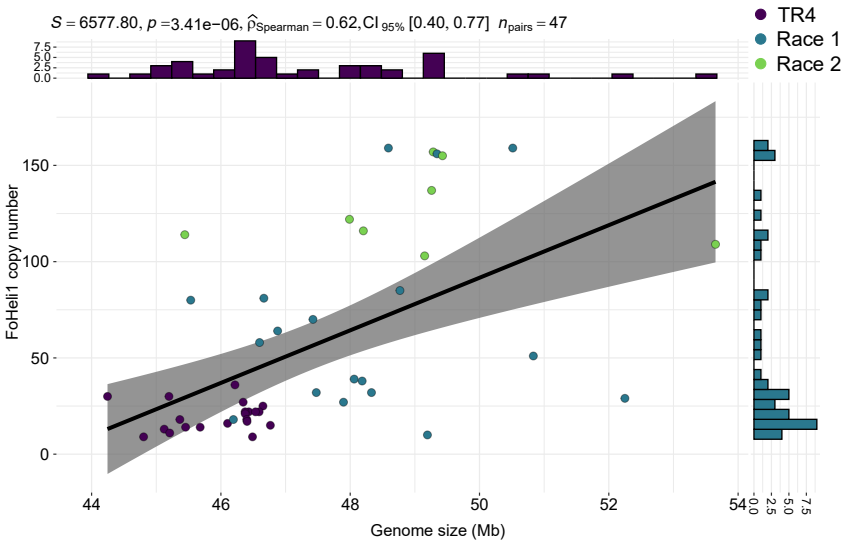


FIGURE S7 | Genome size shows moderate correlation with FoHeli1 copy number. Comparison between genome size in Mbp and estimated FoHeli1 copy number for 47 banana infecting *Fusarium* strains containing at least one copy. Spearman correlation coefficient ($\hat{P}$), p value and 95% confidence interval are noted above.

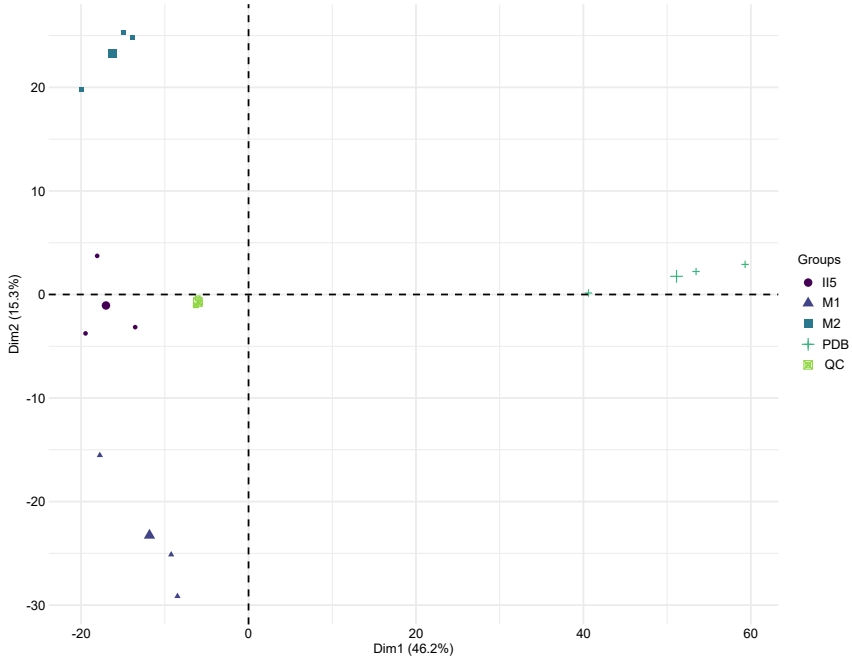


FIGURE S8 | TR4 strains II5, M1 and M2 show different exometabolite profiles. PCA of the exometabolite profiles of TR4 strains II5, M1 and M2 as well as medium without fungal growth (PDB) and quality control samples (QC).

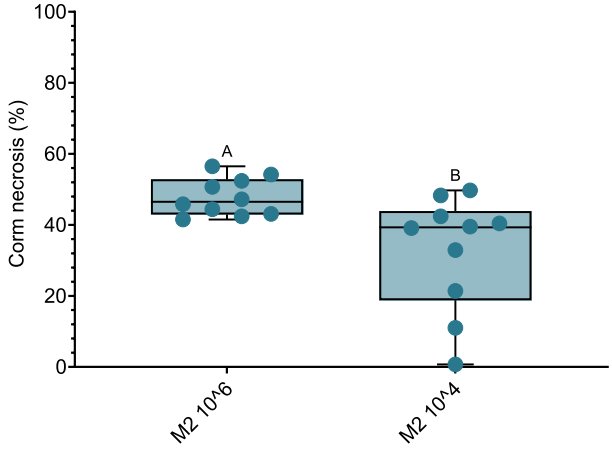


FIGURE S9 | M2 wilting severity is also affected by spore concentration. Percentage of corm necrosis at 10 weeks post-inoculation of Cavendish 'Grand Naine' plants inoculated with TR4 strain M2. Plants were inoculated with either 10^6 or 10^4 spores per mL. Corm necrosis was quantified using ImageJ (n=10). Letters indicate significant differences between treatments (t-test; P<0.05).

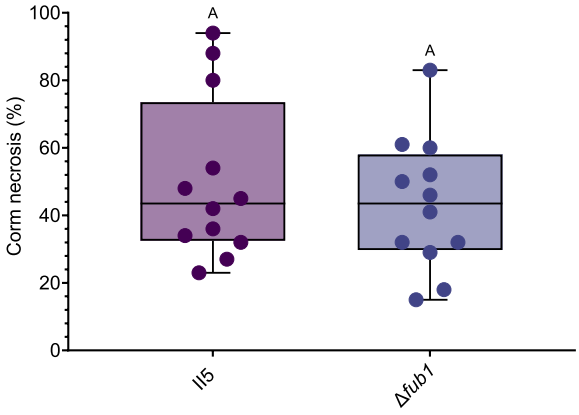


FIGURE S10 | Fusaric acid loss does not affect virulence at standard spore concentration. Percentage of corm necrosis at 10 weeks post- inoculation of Cavendish 'Grand Naine' plants inoculated with reference strain II5 or Δ*fub1* mutant. All plants were inoculated with 10^6 spores per mL. Corm necrosis was quantified using ImageJ (n=12). Letters indicate significant differences between treatments (t-test; P<0.05).

TABLE S1 | Primers used in this study.

Primer name	Sequence 5'-3'	Purpose
II5_Fub_9gRNA_F	CTCGAGTAGCTGGTCTCAAGATCGACG	Cas9 plasmid
II5_Fub_9gRNA_R	AAACCGTCGATCTTGAGACCAGCTACT	-
II5_Fub_9gRNA_F2	CTCGCCTCAAGGGCCATCACAACACCA	-
II5_Fub_9gRNA_R2	AAACTGGTGTTGTGATGGCCCTTGAGG	-
Fub1up_F	CTTCAGCTAGAGGGCAAGTCA	Donor template
Fub1up_R	cactagctccagccaagcccaaaaaAGGAAAAAGAGTCAGAAACAAAGGT	-
NatR_Fub1_F	TGTTTCTGACTCTTTTTCCTtttttgggcttggctggagctagtg	-
NatR_Fub1_R	GAGAGGCATAGTTTGAGGTTctcactgatacatctggcacctact	-
Fub1down_F	gtgccagatgtatcagtgagAACCTCAAACTATGCCTCTCTT	-
Fub1down_R	ACAAACAGACGCGTTCCTCT	-
II5_Fubscreen_F	TGCGCTTACACTGTGACCAT	Screening
II5_Fubscreen_R	GCTGAAGCATAAGTCGCACG	-
II5_Fub1fullscreen_F	TCCCCGGCTCGTTATCATTG	-
II5_Fub1fullscreen_R	GACCTTGAGAGGACGCCAAA	-
II5_Fub3_F	CACGCTGAGTGCTACCTGAA	-
II5_Fub4_R	GATTGACGGCTCTGGGAACA	-
II5_Fub10_F	CATCGTGGGAGATTTCGCCT	-
II5_Fub10_R	TCCACGACGATTCAGCCAAA	-
Fub1up_F	CTTCAGCTAGAGGGCAAGTCA	Complementation
Fub1downHyg_R	ACAGCTCATCTGCAATGCATTAacaaacagacgcgttcctct	-
HygR_Fub1_F	agaggaacgcgtctgtttgtTAATGCATTGCAGATGAGCTGT	-
Hygfull_R	GACTGCCTCAGGTGGG	-
FoHeli1C_F	TTGGATGCGCCATTTGATCG	FoHeli1 screening
FoHeli1C_R	TCGGGGTTGAGACCGAAATC	-

TABLE S2 | *Fusarium* strains and their estimated FoHeli1 copy number.

Strain	Race	FoHeli1 copies	Reference
ISR1	4	36	van Westerhoven *et al.* (2024a)
JV11	4	30	van Westerhoven *et al.* (2024a)
Race4	4	9	van Westerhoven *et al.* (2024a)
S1B8	4	9	van Westerhoven *et al.* (2024a)
Phi2-6C	4	11	van Westerhoven *et al.* (2024a)
Vietnam	4	13	van Westerhoven *et al.* (2024a)
Laos	4	14	van Westerhoven *et al.* (2024a)
Myanmar	4	14	van Westerhoven *et al.* (2024a)
Col17	4	15	van Westerhoven *et al.* (2024a)
chi1-1	4	16	van Westerhoven *et al.* (2024a)
M2	4	17	van Westerhoven *et al.* (2024a)
M3	4	18	van Westerhoven *et al.* (2024a)
Pak1.1A	4	18	van Westerhoven *et al.* (2024a)
M4	4	21	van Westerhoven *et al.* (2024a)
Col2	4	22	van Westerhoven *et al.* (2024a)
Col4	4	22	van Westerhoven *et al.* (2024a)
M5	4	22	van Westerhoven *et al.* (2024a)
TR4_II5	4	25	van Westerhoven *et al.* (2024a)

Strain	Race	FoHeli1 copies	Reference
JV14	4	27	van Westerhoven *et al.* (2024a)
Leb1-2C	4	30	van Westerhoven *et al.* (2024a)
CR1.1	1	0	van Westerhoven *et al.* (2024a)
Foc8	1	0	van Westerhoven *et al.* (2024a)
Foc16	1	0	van Westerhoven *et al.* (2024a)
FocP1	1	0	van Westerhoven *et al.* (2024a)
Indo110	1	0	van Westerhoven *et al.* (2024a)
NRRL36101	1	0	van Westerhoven *et al.* (2024a)
NRRL36107	1	0	van Westerhoven *et al.* (2024a)
P20a	1	0	van Westerhoven *et al.* (2024a)
P26c	1	0	van Westerhoven *et al.* (2024a)
P41b	1	0	van Westerhoven *et al.* (2024a)
Phi6.6a	1	0	van Westerhoven *et al.* (2024a)
NRRL36113	1	10	van Westerhoven *et al.* (2024a)
C176	1	27	van Westerhoven *et al.* (2024a)
R1B	1	29	van Westerhoven *et al.* (2024a)
C177	1	32	van Westerhoven *et al.* (2024a)
C187	1	32	van Westerhoven *et al.* (2024a)
Cub9	1	38	van Westerhoven *et al.* (2024a)
NRRL36118	1	39	van Westerhoven *et al.* (2024a)
NRRL36108	1	45	van Westerhoven *et al.* (2024a)
NRRL36116	1	52	van Westerhoven *et al.* (2024a)
NRRL36115	1	58	van Westerhoven *et al.* (2024a)
Mal43	1	64	van Westerhoven *et al.* (2024a)
NRRL36120	1	70	van Westerhoven *et al.* (2024a)
Race1	1	80	van Westerhoven *et al.* (2024a)
F9129	1	81	van Westerhoven *et al.* (2024a)
C192	1	85	van Westerhoven *et al.* (2024a)
C168	1	156	Martínez-de la Parte *et al.* (2024)
NRRL36117	1	159	van Westerhoven *et al.* (2024a)
C61	1	159	Martínez-de la Parte *et al.* (2024)
C081	2	51	van Westerhoven *et al.* (2024a)
C34	2	69	Martínez-de la Parte *et al.* (2024)
C172	2	103	Martínez-de la Parte *et al.* (2024)
C78	2	109	Martínez-de la Parte *et al.* (2024)
C142	2	114	Martínez-de la Parte *et al.* (2024)
C39	2	116	Martínez-de la Parte *et al.* (2024)
C161	2	122	Martínez-de la Parte *et al.* (2024)
C30	2	155	Martínez-de la Parte *et al.* (2024)
C170	2	157	Martínez-de la Parte *et al.* (2024)

Chapter 5

General discussion

Introduction

Fungi inhabit a wide range of ecological niches ranging from saprophytic growth and mycoparasitism to pathogens of insects and plants (Naranjo-Ortiz & Gabaldón, 2019). Within these interactions, fungi have likely already been associated with plants prior their terrestrialization, in which they are believed to have played a crucial role (Redecker *et al.*, 2000; Delaux *et al.*, 2015; Naranjo-Ortiz & Gabaldón, 2019). As a result, the interaction between plants and fungi is of an ancient origin. As part of this close and ancient association with plants, plant pathogenic fungi are believed to have been affecting agriculture since its origin (Stewart & Robertson, 1968; van Zeist & Palfenier-Vegter, 1981; Kislev, 1982; Dark & Gent, 2002; Iriti & Faoro, 2008; Zadoks, 2008). The domestication of wild plants for agriculture, in several cases, also resulted in divergence and changes in their respective pathogens leading to co-domestication (Stukenbrock & McDonald, 2008). The increasingly vast fields of genetically uniform host species that over time came along with crop domestication, and intensification during the rise of agriculture led to an entirely new environment that poses strong directional selection pressures on pathogens (Zhan *et al.*, 2015). These agricultural environments with low genetic diversity provide an enormous evolutionary potential for a successful pathogen (Fones *et al.*, 2020). Consequently, pests and diseases are a major source of crop losses (Flood, 2010; Savary *et al.*, 2019) and can severely threaten food security (Strange & Scott, 2005; Gurr *et al.*, 2011; Fones *et al.*, 2020). Moreover, they promote the emergence and rapid spread of new pathogens or virulent lineages (Fones *et al.*, 2020). The increased risks for plant disease pandemics, as a consequence of monocultures and their selection pressure, can be seen in recent examples such as the spread of the Ug99 lineage of *Puccinia graminis tritici* (Singh *et al.*, 2011) and the B71 lineage of *Magnaporthe oryzae* (Latorre *et al.*, 2023), causal agents of stem rust disease and wheat blast respectively.

Host plant and pathogen are in a co-evolutionary arms race based on their interactions involving host receptors to promote plant immunity and the pathogen's effector molecules to avoid recognition, suppress immunity and promote host colonization (Cook *et al.*, 2015; Sánchez-Vallet *et al.*, 2018). Therefore, the threat a plant pathogen poses to a given crop depends, in part, on their adaptability (McDonald & Linde, 2002). The higher this adaptability, the lower the potential durability of resistance, hence the more complex the essential agricultural process of resistance breeding (McDonald & Linde, 2002). Next to the impact on the durability of resistance through the co-evolutionary arms race, adaptability to environmental factors is another major factor in determining the threat a plant pathogen presents (Croll & McDonald, 2017). Consequently, it is essential to understand the processes that allow pathogens to adapt to their environment and host to aid in the search for sustainable control

methods. Understanding the adaptability of pathogenic fungi is further exemplified in the reoccurring threat posed by highly virulent lineages (Singh *et al.*, 2011; Ordóñez *et al.*, 2015; Latorre *et al.*, 2023).

Accessory chromosomes and their evolution

One major source of variation and adaptability of some pathogenic fungi is the presence of so-called accessory chromosomes. The organization of the genome in core- and accessory chromosomes is one of the various known forms of genome compartmentalization found in pathogenic fungi (Goodwin *et al.*, 2011; Croll & McDonald, 2012; Bertazzoni *et al.*, 2018; Sánchez-Vallet *et al.*, 2018; Torres *et al.*, 2020; Yang, H *et al.*, 2020). Accessory chromosomes are less conserved than core chromosomes, which together with their general sequence characteristics such as low gene density and enrichment in transposable elements (TEs), allows for their identification and distinction (Goodwin *et al.*, 2011; Schotanus *et al.*, 2015; Bertazzoni *et al.*, 2018; Fokkens *et al.*, 2018; Cook *et al.*, 2020; Habig & Stukenbrock, 2020; Habig *et al.*, 2021; Habig *et al.*, 2024).

Despite their prominent role as a source for adaptation (Croll & McDonald, 2012; Torres *et al.*, 2020), many questions remain unanswered on the origin and evolution of accessory chromosomes (Habig & Stukenbrock, 2020; Torres *et al.*, 2020). Two major processes have been proposed as potential 'origins' for accessory chromosomes in fungal genomes (Galazka & Freitag, 2014; Habig & Stukenbrock, 2020). Firstly, accessory chromosomes might have derived endogenously from core chromosomes (Galazka & Freitag, 2014; Habig & Stukenbrock, 2020). Observations in *Magnaporthe oryzae* and *Colletotrichum* spp. suggest specific core genomic rearrangements as a source for accessory chromosome (mini-chromosome) emergence (Langner *et al.*, 2021; Wang, H *et al.*, 2023). Additionally, a process known as breakage-fusion-bridge (BFB) cycles combined with general chromosome degeneration is further proposed to play a role in endogenous accessory chromosome generation (Croll *et al.*, 2013; Habig & Stukenbrock, 2020). Interestingly, sub-telomeric regions of core chromosomes often share some of the characteristics of accessory chromosomes such as their histone modifications or increased density of repetitive elements (Galazka & Freitag, 2014; Fokkens *et al.*, 2018; van Westerhoven *et al.*, 2024a). In addition, in both tomato and banana infecting *Fusarium* strains accessory regions can be the distal parts of larger core chromosomes (Ma *et al.*, 2010; van Westerhoven *et al.*, 2024a). As such, the generation of independent accessory chromosomes might be the result of specific core genomic rearrangements, potentially facilitated by the increased presence of repetitive elements (Langner *et al.*, 2021).

The second main proposed possibility for the emergence of specific accessory chromosomes in a fungal genome is horizontal transfer (Habig & Stukenbrock, 2020). Genomic studies of fungal populations (Henry *et al.*, 2021; Barragan *et al.*, 2024; Habig *et al.*, 2024), as well as experimental transfer (He *et al.*, 1998; Akagi *et al.*, 2009; Ma *et al.*, 2010; Habig *et al.*, 2024) show the propensity for horizontal transfer of accessory chromosomes. Although as of yet unconfirmed, the ability to be horizontally transferred might be aided by genes positioned on the accessory chromosomes (Habig *et al.*, 2024; Habig *et al.*, 2025). The lower levels of codon optimization observed for accessory chromosomes in fungi with known horizontal transfer events are seen as additional evidence for such events (Habig *et al.*, 2025).

In this thesis I describe several observations and explanations regarding accessory chromosome evolution. Firstly, we observe that genes encoded by the accessory regions of *Fusarium oxysporum* TR4 strain II5 show significantly lower relative synonymous codon usage (RSCU) levels compared to genes encoded by core genomic regions (Chapter 1). Presumably, horizontally transferred genes are unlikely to show high degrees of codon optimization due to their different evolutionary history (Wallau *et al.*, 2012). The exact origin of accessory chromosome 12 (AC12) of the TR4 lineage is unknown, but horizontal accessory chromosome transfer is known to play a significant role across the *Fusarium oxysporum* species complex (FOSC) (Fokkens *et al.*, 2018). Moreover, we observe a Helitron transposable element in the clonal TR4 lineage, which is absent in the most closely related strain 36102 that also lacks AC12 (Chapter 3). Although more detailed genomic analysis is required, one possible explanation for these observations is that AC12 was horizontally transferred prior to the global spread of the TR4 lineage and was the source for FoHeli1 into the TR4 lineage.

Secondly, we observe extensive intrachromosomal duplications for AC12 in strain II5 and several other TR4 strains from the Middle East (Chapter 2). Chromosome length polymorphisms are a commonly observed phenomenon in several fungi (Zolan, 1995; Croll *et al.*, 2013; Mehrabi *et al.*, 2017). The length polymorphism of AC12, however, is remarkable as it is neither the consequence of an insertion, deletion or rearrangement (Croll *et al.*, 2013; Liu *et al.*, 2024), nor the result from an experimental cross (Croll *et al.*, 2013). Instead, the length polymorphism is solely based on intrachromosomal duplications, that have likely occurred twice independently in nature (Chapter 2). In contrast to the copy number variation differences observed for mini-chromosomes in different *M. oryzae* strains (Liu *et al.*, 2024), we resolved the nature of the copy number variation to a chromosome length polymorphism rather than multiple AC12 copies. Intrachromosomal duplications were also observed previously in *F. oxysporum* following experimental horizontal transfer of accessory chromosomes (van Dam *et al.*, 2017). This would support a potential horizontal transfer 'origin' of AC12.

So far, due to the lack of sequence variation for the intrachromosomal duplications, the order of the duplicated regions cannot be determined. Nevertheless, the observed duplicated and quadruplicated sections could potentially be the result of sequential BFB cycles (Chapter 2). In this case, BFB cycles seem to contribute to variation in the dynamic genomes of fungi (Huang, J *et al.*, 2023) rather than facilitating the formation of accessory chromosomes. Although large scale duplications or aneuploidy have been linked to fitness effects in fungi (Garmaroodi & Taga, 2007; Wertheimer *et al.*, 2016; Vande Zande *et al.*, 2023), the consequence of the AC12 intrachromosomal duplications remains unknown (Chapter 2). As such, the observed chromosome length polymorphism raises questions on the evolutionary advantage and pressures resulting in such intrachromosomal duplications. One potential strategy to determine putative fitness effects of large accessory duplications is through artificial induction of duplications (Garmaroodi & Taga, 2007).

Although endogenous generation and horizontal transfer provide convincing explanations for the presence of accessory chromosomes within a fungal genome, they do not provide satisfactory explanations on the initial formation of the different accessory chromosome characteristics such as low gene density and high TE abundance. Additionally, neither of these processes provides any insights into the question why certain fungal lineages have evolved to contain such highly adaptive genomic compartments and others have not (Stam *et al.*, 2018; Frantzeskakis *et al.*, 2019; Torres *et al.*, 2020). Computational study suggests genome compartments enriched for TEs, and genes involved in the adaptation to a specific environment or host might form over time through selection for improved adaptability (Crombach & Hogeweg, 2007). However, unraveling these questions beyond models will require further research into the evolutionary impacts of TE proliferation and distribution in fungal genomes. Closer study of fungal pathogens with a lack of accessory chromosomes or clear genome compartmentalization might be one avenue in this regard (Stam *et al.*, 2018). Another option might be the experimental removal of all accessory genomic material (VanEtten *et al.*, 1998) and subsequent long-term genomic monitoring. Lastly, evolution experiments with different degrees of induced TE proliferation could contribute to a better understanding of TE activity and its effect on genome organization.

Accessory chromosomes and their function

Beyond their evolution, accessory chromosomes are mostly studied for their role in virulence. Their contribution to virulence has been shown for numerous fungi (Garmaroodi & Taga, 2007; Ma *et al.*, 2010; Balesdent *et al.*, 2013; Habig *et al.*, 2017; Plaumann *et al.*, 2018; Ayukawa *et al.*, 2021; Witte *et al.*, 2021; Habig *et al.*, 2024), and

is mostly attributed to their enrichment or association with effector genes (Ma *et al.*, 2010; Bertazzoni *et al.*, 2018; Sánchez-Vallet *et al.*, 2018; Langner *et al.*, 2021) or toxic secondary metabolites (Witte *et al.*, 2021). In this context, we also observe strong upregulation of accessory genes during infection of Cavendish bananas by TR4 strain II5, several of which encode for secreted proteins (Chapter 1). However, in contrast to tomato-infecting *Fusarium* (Ma *et al.*, 2010), the accessory regions of the TR4 reference strain II5 are neither specifically enriched for effectors nor contain any predicted biosynthetic gene clusters (BGC) (van Westerhoven *et al.*, 2024a), (Chapter 3). Nevertheless, several of the most highly upregulated accessory genes encode for putative effectors (Chapter 1).

In Chapter 2, we report on the contribution of AC12 to TR4 virulence on Cavendish bananas. Through the generation of AC12 loss mutants, we showed that this chromosome is (i) dispensable for vegetative growth, (ii) significantly contributes to virulence, but (iii) its loss does not abolish pathogenicity (Chapter 2). To our knowledge, this is the first example of partial pathogenicity contribution by an accessory chromosome across the FOSC. Loss of a particular accessory chromosome in *Fusarium* strains infecting other hosts has generally led to total loss of pathogenicity (van Dam *et al.*, 2017; Ayukawa *et al.*, 2021; Sakane *et al.*, 2024). We hypothesize the ability to infect Cavendish bananas is retained through genes encoded by the accessory region of chromosome 1. To continue determining the essential genes for pathogenicity on banana, the generated AC12 loss mutants should be used as a steppingstone in further knockout studies as was described in Chapter 2 of this thesis. In such follow-up studies, priority should be given to those effectors encoded by the accessory region of chromosome 1.

Despite the fact that accessory chromosome contribution to virulence is most often attributed to effector genes encoded by the accessory genome, several studies have highlighted more diverse functions for accessory genes such as degradation of antimicrobial compounds (Miao *et al.*, 1991; Covert *et al.*, 1996), spore formation (Möller *et al.*, 2018; Ayukawa *et al.*, 2021) and rhizosphere competition (Rodriguez-Carres *et al.*, 2008) (Fig. 1). Given the number of duplicated effectors and regions on both accessory regions of TR4 (van Westerhoven *et al.*, 2024a), (Chapters 1 & 2), the virulence contribution of AC12 could also be (partly) based on non-effector genes. The genes on AC12 encode a wide range of predicted functions. Moreover, although the effects are minor, initial experiments suggest a role for AC12 in tolerance to environmental stress factors such as high salt concentrations (Chapter 2). Lastly, it is important to note that non-pathogenic fungi can also contain accessory chromosomes (Pires *et al.*, 2015; Guo *et al.*, 2021). These observations point to potentially broader roles of accessory chromosomes beyond direct host adaptation, which could be tested by high throughput experiments using wide panels of phenotypes.

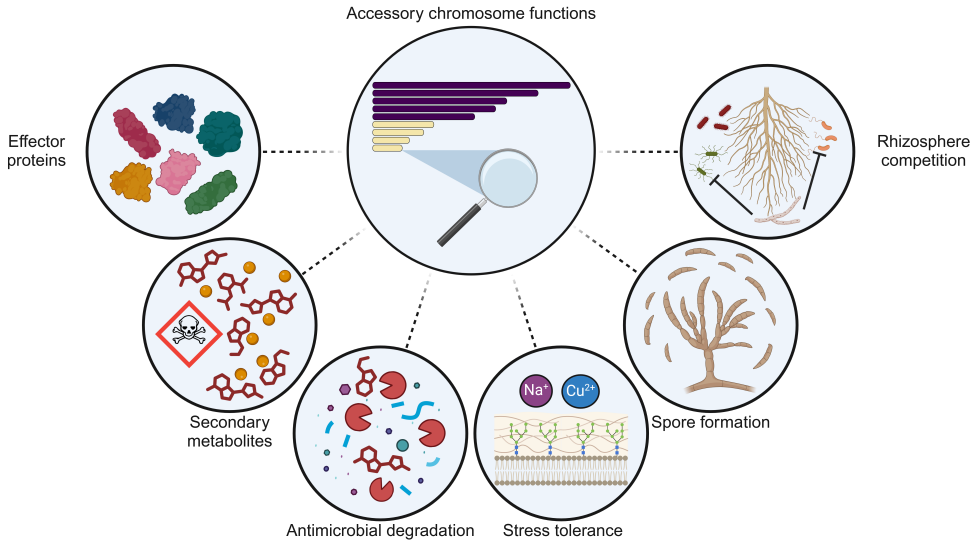


FIGURE 1 | Accessory chromosomes and their functions. Display of all functions, virulence related and others, for accessory chromosomes in fungi. Functions were identified in previous studies and experiments described in this thesis. Figure made using BioRender.

Transposable elements as drivers of genetic variation

The mechanisms through which TEs can affect genome evolution are intensely varied (Daboussi & Capy, 2003; Seidl & Thomma, 2017; Hayward & Gilbert, 2022; Barro-Trastoy & Köhler, 2024). Particularly because of their common association with accessory regions and effectors, TEs have gained an ever-wider interest in the study of fungal pathogens (Daboussi & Capy, 2003; Faino *et al.*, 2016; Seidl & Thomma, 2017; Bertazzoni *et al.*, 2018; Fouché *et al.*, 2022). Within this context, TEs are at times also seen as a double-edged sword, on one hand aiding increased adaptability, while on the other hand negatively affecting genome size and stability (Fouché *et al.*, 2022). For example, recent bursts of TE activity have resulted in significant genome expansion in several populations of the wheat pathogen *Zymoseptoria tritici* (Oggenfuss *et al.*, 2021).

Two of the major processes through which TEs can directly affect virulence are gene disruption (Wu *et al.*, 2015; Kashiwa *et al.*, 2016) and (large) chromosomal rearrangements (Biju *et al.*, 2017). In Chapter 3, we describe the recent activity of a Helitron TE, called FoHeli1, within the TR4 lineage. As a consequence of FoHeli1 transposition, a TR4 strain from Mozambique has lost two large sequence segments of core chromosomes 2 and 3. The sequence on chromosome 3 includes the BGC for fusaric acid production. This loss of more than 1% of the genome, compared to the

reference strain, showcases the significant impact TE activity can have on genome evolution and dynamics. Additionally, we observe FoHeli1 copies at the border of additional large chromosomal rearrangements, such as inversions and translocations, in other TR4 strains (Chapter 3). FoHeli1 stands out among all other TEs in the TR4 lineage by having the lowest average weighted Kimura distance, a proxy for dating TE activity (Chapter 3). This suggests that the activity of FoHeli1 across the TR4 lineage must have been very recent. The fact that the individual FoHeli1 copies are not part of larger segmental duplications underscores that the observed lack of sequence variation must have resulted from recent transposition events. Furthermore, based on a putative circular intermediate we hypothesize that FoHeli1 is still active in the TR4 lineage (Chapter 3).

We also observe several peculiar interchromosomal rearrangements following benomyl treatment and AC12 loss (Chapter 1). These rearrangements stand out as core chromosomes within the FOSC are generally colinear (Armitage *et al.*, 2018; Kanapin *et al.*, 2020; Zhang *et al.*, 2020; van Westerhoven *et al.*, 2024a). Some of these rearrangements are in repeat and TE-rich regions (van Westerhoven *et al.*, 2024a). The repetitive nature of these TE-rich regions might have played a role in the rearrangements, as was also suggested in other fungi (Faino *et al.*, 2016; Langner *et al.*, 2021).

Helitrons are most commonly referred to as copy-paste or more specifically rolling circle elements (Barro-Trastoy & Köhler, 2024). As long as a copy-paste element stays active, the copy number should naturally increase across the genome and the original template elements should remain intact (Barro-Trastoy & Köhler, 2024). However, we see relatively low levels of FoHeli1 copy number differences between TR4 strains (Chapter 3). Moreover, every observed FoHeli1 copy had distinct loci across the observed TR4 genomes (Chapter 3). These observations are not in line with the expectations for ongoing activity for a copy-paste element. Similarly, experiments in maize have shown that Helitrons sometimes transpose by excision instead of copy-paste (Li & Dooner, 2009). More detailed functional studies are required to determine the exact transposition mechanisms for Helitron elements in fungi and determine the balance between excision and copy-paste transposition.

As mentioned previously, the origin of FoHeli1 in the TR4 lineage could potentially be explained by its horizontal co-transfer with AC12. Both AC12 and FoHeli1 are absent in strain 36102 which is most closely related to the clonal TR4 lineage (van Westerhoven *et al.*, 2024a). After horizontal transfer, a transposon sometimes undergoes a transposition burst within the new genomic niche (Wallau *et al.*, 2012). Environmental stress factors or host infection can also lead to (temporary) increased TE activity (Daboussi & Capy, 2003; Fouché *et al.*, 2022). Such a transposition burst would

then have allowed for further FoHeli1 distribution across the genome, including the core chromosomes. Determining the origin of FoHeli1 in the TR4 lineage, if possible, will require (i) the sequencing of additional strains which are more closely related to strain 36102, such as those from the same vegetative compatibility group (VCG0121) (van Westerhoven *et al.*, 2024a) and (ii) the generation of more chromosome level assemblies of additional TR4 strains and other clade 1 FOSC members. Besides, the generation of additional chromosome level assemblies of TR4 strains would greatly aid in assessing the potential impact of other TEs on TR4 genome dynamics, some of which also show signs of recent activity (Chapter 3). Given the clonal nature and ongoing global spread of TR4, this lineage is ideal for investigating TE activity and its consequences on genome dynamics.

Effector proteins: functions, synergies and regulation

As a key component of the molecular battleground between host and pathogen, effector proteins have been scrutinized through a wide range of different lenses (Lo Presti *et al.*, 2015; Toruño *et al.*, 2016; Sánchez-Vallet *et al.*, 2018; He *et al.*, 2020; Rocafort *et al.*, 2020; Snelders *et al.*, 2022; Cai *et al.*, 2023; Lovelace *et al.*, 2023), primarily due to their ability to facilitate infection (He *et al.*, 2020) and their potential recognition by the plant's immune system (Cook *et al.*, 2015).

In Chapter 1, we identified several highly expressed genes encoding effectors in reference TR4 strain II5. Of particular interest were those located on the accessory regions of the genome, with few or no orthologs in *Fusarium* strains infecting other hosts as these might be host determinants. As part of our analysis, we first predicted their protein structures which is a rapidly developing component of effector analyses (Seong & Krasileva, 2023; Yu *et al.*, 2024). Structural analysis revealed that effectors 1g02190 and 12g00300 show similarity to KP6 from *Ustilago maydis* and effector 1g02200 is reminiscent to ToxA from *Pyrenophora tritici-repentis,* respectively. Both KP6 and ToxA exemplify characteristic structures of larger effector families (Yu *et al.*, 2024). The lack of sequence similarity for the other effectors is likely a consequence of the very limited number of crystal structures for effector proteins. With an increasing number of structurally analyzed effectors, more effector families will inevitably be discovered.

The effectors 1g02190 and 1g02200 do not just stand out for their individual structural similarity with other effectors, but also because KP6-like and ToxA-like effectors are paired in several other fungi (Talbi *et al.*, 2023) and their functioning is affected by their pairing and physical interaction (Ma *et al.*, 2015; Cao *et al.*, 2018; Ayukawa *et al.*, 2021; Blekemolen *et al.*, 2022; Talbi *et al.*, 2024). Specifically, SIX5 (KP6-like) and Avr2 (ToxA-

like) are required as a pair for I-2 mediated immunity in tomato (Ma *et al.*, 2015) and together alter the size exclusion limit of plasmodesmata (Cao *et al.*, 2018; Blekemolen *et al.*, 2022). This synergistic function can also affect the distribution of other effector proteins (Blekemolen *et al.*, 2022). The ability to affect cell-to-cell plasmodesmatal movement is also seen for another KP6-like and ToxA-like effector pair from the plant pathogen *Leptosphaeria maculans* (Talbi et al., 2024). The tomato infecting *Fusarium oxysporum* strain *Fol*4287 also contains two other effector pairs, SIX8/PSE1 and SIX8/PSL1 (Ayukawa *et al.*, 2021). Of these two pairs, SIX8 and PSL1 have also been shown to physically interact (Yu *et al.*, 2024). In contrast to the SIX5/Avr2 pair, the SIX8/PSE1 effector pair is implicated in the suppression of secondary metabolite-dependent immunity during infection of *Arabidopsis thaliana* (Ayukawa *et al.*, 2021). Based on these observations, it is tempting to assume that the 1g02190/1g02200 effector pair in the banana infecting TR4 strains might serve a similar synergistic function. The SIX5/Avr2 pair is absent in the TR4 lineage and the SIX8/PSE1 pair is incomplete, as such it remains unknown if the 1g02190/1g02200 effector pair serves a similar or unique function to aid infection of the host. Functional studies should confirm whether or not the 1g02190 and 1g02200 proteins physically interact and determine their function for virulence. Moreover, searches for additional head-to-head oriented effector pairs could lead to further insights into the synergistic functions and regulation of novel effectors.

We also observe the presence of *1g02200* orthologs (ToxA/Avr2-like) in *Fusarium xylarioides* and *Verticillium dahliae* (Chapter 1). The presence of *1g02200* orthologs in the absence of a paired effector might be explained by the independent virulence functions observed for Avr2 (SIX3) (Di *et al.*, 2017). Several cases of the absence of paired effectors (Chapter 1), (Ayukawa *et al.*, 2021), suggests that the individual genes might still provide a fitness benefit (Di *et al.*, 2017; Ayukawa *et al.*, 2021; Li *et al.*, 2022). The presence of *1g02200* orthologs in the more distantly related plant pathogens *F. xylarioides* and *V. dahliae* is highly suggestive of horizontal transfer (Chapter 1). A recent study of *F. xylarioides* showed strong signs of multiple horizontal transfers of regions from FOSC-member accessory chromosomes, supporting our observation (Peck *et al.*, 2024). The *1g02200* ortholog in *V. dahliae* is called TOM and is essential for infection of tomato plants (Li et al., 2022), and interacts with the host' auxin response factors (Li *et al.*, 2022). Given the newly available high quality Cavendish genome (Li, X *et al.*, 2024), effort should be made to determine whether 1g02200 interacts with banana auxin response factors.

Lastly, in Chapter 1 we address the potential experimental complexity of effector redundancy. Numerous studies, in both fungal and bacterial plant pathogens, have shown that knockouts of single effectors does not always lead to significantly reduced virulence levels (Kvitko *et al.*, 2009; Pliego *et al.*, 2013; Ali *et al.*, 2014; Brefort *et al.*, 2014).

Effector redundancy, promoting virulence by targeting the same host target or the same process is one explanation for this common observation. Although effector redundancy is a plausible and convenient explanation, other more subtle virulence attenuations could easily be overlooked. For example, the virulence contribution of accessory chromosomes and their associated (effector) genes in *Z. tritici* is dependent on the tested host genotype (Habig *et al.*, 2017). Similarly, some effectors can promote virulence by affecting the hosts' microbiome (Snelders *et al.*, 2020; Snelders *et al.*, 2023). Hence, the virulence contribution of an effector can also depend on the microbial composition of the soil. Despite generating several effector knockout mutants, we do not observe any significant virulence reductions except when AC12 is removed (Chapters 1 & 2). Given the other ways by which effectors might contribute to virulence, future studies should include additional (resistant) banana genotypes for phenotyping effector mutants. Furthermore, several TR4 effectors have high levels of predicted antimicrobial activity (Chapter 1). Knockout mutants of these effector genes might therefore benefit from phenotyping with different (synthetic) microbial communities.

Another important component to consider is how the regulation of effectors contributes to virulence and general fitness benefits. For *F. oxysporum*, effector expression can be regulated by transcription factors encoded both by the core- and the accessory chromosomes (van der Does *et al.*, 2016). Moreover, several transcription factor families are expanded in copy number across the FOSC, and this is, in part, a consequence of increased copy numbers of accessory encoded transcription factors (Yu, H. *et al.*, 2023). In total, more than 25 transcription factors, primarily core genome-encoded, have been functionally analyzed regarding virulence (Zuriegat *et al.*, 2021). This number is very low compared to the total number of predicted transcription factors (N=1149) in TR4 II5 (Yu, H. *et al.*, 2023). Several of these transcription factors are encoded by the accessory genome, some of which are unique, while others are orthologs of transcription factors involved in virulence (Yu, H. *et al.*, 2023) (Table 1). The exact impact and role of almost all of these accessory genome-encoded transcription factors remain unknown. Most of the studied transcription factors encoded by the accessory genome show a certain degree of functional redundancy to those encoded by the core genome (Jonkers *et al.*, 2014; Niño-Sánchez *et al.*, 2016; van der Does *et al.*, 2016). Nevertheless, small functional differences and dosage effects might underlie the evolution of these copies encoded by the accessory regions (de Vega-Bartol *et al.*, 2011; van der Does *et al.*, 2016). Moreover, strain-specific contributions of transcription factors might muddle characterization attempts (Yu, H. *et al.*, 2023). The transcription factors encoded by the accessory genome (Table 1) and their potential regulation of effectors or other virulence factors might be another reason why AC12-loss mutants show reduced virulence (Chapter 2). Further insight into the interplay between

transcription factors encoded by the core- and accessory genomes is essential for our understanding of pathogens with compartmentalized genomes. Additionally, important regulators of virulence are interesting targets for control, for example through host-induced gene silencing (Ghag *et al.*, 2014).

TABLE 1 | Virulence associated transcription factor orthologs encoded by the accessory regions of TR4 strain II5.

Transcription factor representative	Gene family	Gene ID	Function of representative
FvFug1	GATA	1g00200	Virulence/Sexual Development/Fumonisin biosynthesis
Ftf1/Ftf2	Zn2-C6	1g00460	Virulence
Ftf1/Ftf2	Zn2-C6	1g00490	Virulence
Ftf1/Ftf2	Zn2-C6	1g00590	Virulence
Ftf1/Ftf2	Zn2-C6	1g00820	Virulence
Ren1	disordered	1g02140	Toxin Synthesis/Reproduction
Ftf1/Ftf2	Zn2-C6	12g00440	Virulence
FvFug1	GATA	12g01140	Virulence/Sexual Development/Fumonisin biosynthesis
Ebr1/Ebr2	Zn2-C6	12g01210	Virulence

Secondary metabolites in a plant pathogen context

The broadest definition of effector as any secreted molecule facilitating host colonization (General Introduction) also includes secondary metabolites, which are sometimes referred to as component of non-proteinaceous effectors (Collemare *et al.*, 2019). In the context of plant pathogens, secondary metabolites are mostly studied for their roles as host-specific or nonhost-specific toxins (Pusztahelyi *et al.*, 2015; Collemare *et al.*, 2019). The presence or absence of such toxins, especially host-specific toxins, can strongly affect the outcome of the interaction with the host (Masunaka *et al.*, 2005; Condon *et al.*, 2013; Kessler *et al.*, 2020). Although the study of toxic secondary metabolites prevails, expression studies of plant pathogen genes during biotrophic growth suggest a role for many secondary metabolites beyond direct toxicity (Collemare *et al.*, 2008a; Harris *et al.*, 2016; Brown, NA *et al.*, 2017; Dallery *et al.*, 2017). Nontoxic functions of secondary metabolites that affect plant pathogens in their interaction with the host include, amongst others, the production of pigments (Chumley & Valent, 1990), plant hormones (Bömke & Tudzynski, 2009; Patkar *et al.*, 2015), iron chelating siderophores (Oide *et al.*, 2014), and antimicrobial compounds (Spraker *et al.*, 2018; Jin *et al.*, 2024). In rare occasions, secondary metabolites can even act as avirulence determinants, similar to many proteinaceous effectors (Collemare *et al.*, 2008b).

The capacity of fungi to produce a wide range of secondary metabolites is also observed in TR4 strains. In reference strain II5 we identified 46 BGCs for the production

of different classes of secondary metabolites (Chapter 3). For the vast majority of these clusters the product or their function remains unknown. Amongst these BGCs is the cluster for the production of the relatively well studied secondary metabolite fusaric acid. Despite its purported role in virulence and high degree of conservation across several *Fusarium* spp. (Brown *et al.*, 2015; Studt *et al.*, 2016; Liu *et al.*, 2020), we discovered a natural mutant in fusaric acid production (Chapter 3). Through the use of the natural mutant strain M1 as well as a newly generated mutant of the key biosynthesis gene *fub1,* we showcase that the loss of fusaric acid production does not affect TR4 virulence on banana. This observation is in contrast to observations made by Liu *et al.* (2020), who state that fusaric acid production is important for the infection of banana by TR4, but this observation was only made using lower spore concentrations of the inoculum (Liu *et al.*, 2020). However, despite our efforts using various inoculum concentrations, we were unable to reproduce these results (Chapter 3).

Based on the recent shift towards the importance of the holobiont view in plant pathology (Snelders *et al.*, 2022) and the studies of fusaric acid as antimicrobial compound (Bacon *et al.*, 2006; Son *et al.*, 2008; Studt *et al.*, 2016; Jin *et al.*, 2024), we hypothesize a context dependent role for fusaric acid (Chapter 3). In this role, the contribution of fusaric acid is based on the composition of the present microbiome. Importantly, the loss of the fusaric acid BGC in a natural environment suggests that it is dispensable under certain conditions. Fusaric acid also causes self-toxicity (Chapter 3) and as one of the most produced secondary metabolites might impose a significant energetic cost. Therefore, in an environment with low levels of microbial competition, or a high number of fusaric acid tolerant microbes (Hu *et al.*, 2012; Ruiz *et al.*, 2015), fusaric acid might not provide a fitness benefit or even be mildly detrimental. This context-dependent role could help explain the extreme range in observed fusaric acid production levels (Notz *et al.*, 2002; Schouten *et al.*, 2004). Moreover, our discovery of several other *F. oxysporum* strains that have lost the fusaric acid BGC suggests this might be a more common phenomenon (Chapter 3). A similar situational trade-off for production of a secondary metabolite was hypothesized for melanin production levels in *Z. tritici* (Krishnan et al., 2018). Furthermore, the antimicrobial role of fusaric acid might be supplemented through higher production levels of products with lower self-toxicity. Both effector proteins and other secondary metabolites might fulfill this function (Chapter 1), (Spraker *et al.*, 2018; Xu *et al.*, 2023).

As mentioned previously, accessory chromosomes can play a major role in virulence. This is mostly attributed to accessory genome-encoded proteinaceous effectors; however, an increasing number of studies are addressing the role of accessory chromosome-acquired secondary metabolism (Witte *et al.*, 2021). Especially in the fungal *Alternaria* genus, host-specific toxins are commonly encoded by genes on

the accessory chromosomes (Johnson *et al.*, 2001; Hatta *et al.*, 2002; Masunaka *et al.*, 2005; Akagi *et al.*, 2009). However, bioinformatic analysis suggests that accessory genome-encoded BGCs are present, and perhaps even common, in several other fungal taxa including *Fusarium* (Witte *et al.*, 2021). Although TR4 strain II5 does not contain any predicted BGCs on its accessory regions, these regions are enriched for genes involved in secondary metabolism (van Westerhoven *et al.*, 2024a). Moreover, TR4 strain M1 as well as several Race 2 strains do contain accessory chromosomes encoding predicted BGCs. A proper assessment of the impact and role of secondary metabolites for *Fusarium* spp. and other pathogens will first and foremost require the linking of the many uncharacterized BGCs to their respective products. Similar to effector proteins, the role of secondary metabolites should be addressed within the wide range of potential functions besides direct toxicity.

Banana breeding in the age of genomics

Despite the importance of banana for food security and as a cash crop, banana research and breeding efforts are arguably still decades behind other crops. Investments in banana breeding have generally been lackluster and there is an overall lack of willingness for increased genetic diversification (Drenth & Kema, 2021). Consequently, banana breeding needs to play catch up to truly be capable of addressing the challenges that global banana production faces, especially in the form of TR4-driven Fusarium wilt and black leaf streak disease caused by *Pseudocercospora fijiensis*. Banana breeding should try to emulate and draw inspiration from the herculean efforts made in the improvement of other crops, especially cereals by organizations such as CIMMYT and IRRI (Borlaug, 2002). Such initiatives have already started, for example, through the breeding better bananas program spearheaded by IITA, which funded this thesis project, and the private breeding efforts by Yelloway.

To date only a single resistance gene has been cloned in banana (Peraza-Echeverria *et al.*, 2008a; Peraza-Echeverria *et al.*, 2008b), despite a relative abundance of potential resistance sources (Li *et al.*, 2015; Zuo *et al.*, 2018; García-Bastidas *et al.*, 2019; Zhan *et al.*, 2022). This gene called resistance gene analog 2 (RGA2), identified in the TR4-resistant subspecies *Musa acuminata* ssp. *malaccensis* (Peraza-Echeverria *et al.*, 2008a; Peraza-Echeverria *et al.*, 2008b), has been successfully used to generate TR4-resistant Cavendish banana plants (Dale *et al.*, 2017). Although the gene provides robust resistance to TR4, these plants were generated through cisgenesis (transgenesis according to the authors) and, therefore, international regulation and consumer acceptance remain questionable. Moreover, the corresponding avirulence determinant in TR4 remains unknown, limiting proper assessment on the long-term applicability of this resistance

gene. Similarly, to the RGA2 study, several more studies have shown the possibility for the generation of resistant banana plants through other transgenic approaches (Paul *et al.*, 2011; Ghag *et al.*, 2014; Dou *et al.*, 2020).

To successfully employ the wider genetic diversity of cultivated bananas and wild *Musa* (sub)species for resistance breeding the number and quality of sequenced genomes will have to increase drastically. The publication of the high-quality chromosome level genome assemblies of the Cavendish and Gros Michel cultivars is an important advancement in this regard (Li, X *et al.*, 2024). Likewise, the increasing number of sequenced wild (sub)species (D'Hont *et al.*, 2012; Wu *et al.*, 2016; Wang *et al.*, 2019; Belser *et al.*, 2021; Wang, ZF *et al.*, 2022; Martin *et al.*, 2025) will greatly benefit banana breeding efforts. The study of the Cavendish and Gros Michel genomes (Li, X *et al.*, 2024), together with an earlier genetic mapping study in *Musa acuminata* ssp. *malaccensis* (Ahmad et al., 2020) has already narrowed down the search for the genetic basis of Race 1 resistance. Interestingly, some of the resistance genes found in banana show similarities to previously characterized Fusarium wilt resistance genes in other hosts (Peraza-Echeverria *et al.*, 2008a; Álvarez-López *et al.*, 2022). As such, these genes are promising candidates for further characterization in the search for the genetic basis of resistance to both Race 1 and TR4.

The resistance of Cavendish to Race 1 strains is remarkably durable and robust when compared to other pathosystems, where in some cases resistance might be lost in a matter of a few years (McDonald & Linde, 2002). Cavendish's Race 1 resistance is even more peculiar since TR4 strains, that can infect Cavendish, form a separate lineage (van Westerhoven *et al.*, 2024a). This contrasts the situation in tomato where *Fusarium oxysporum* races 1, 2, and 3 have emerged several times independently in different clonal lineages through loss of function of avirulence genes (Biju *et al.*, 2017). Although classified by McDonald & Linde (2002) as a lower risk pathogen for circumventing resistance, due to a lack of (observed) sexual reproduction and limited gene flow, these observations seem to suggest that this is not necessarily the case given a sufficient selection pressure. Why there have been no similar instances of loss of resistance in the case of Cavendish and Race 1 strains remains unknown. Similarly, it is still unclear whether the ability for TR4 strains to infect Cavendish is based on the presence of a unique immune suppressing effector, the absence of an avirulence factor or on an entirely different factor. Potentially, Cavendish resistance to Race 1 strains is more robust if the avirulence gene in Race 1 is an important effector with a strong fitness benefit (Brown, 2015). Given its uncommon robustness, determining both the specific gene responsible for Race 1 resistance in Cavendish and the corresponding avirulence gene in Race 1 would be a great boon for banana resistance breeding and resistance breeding in general.

Although this thesis is about Fusarium wilt and focused on strains belonging to the TR4 lineage, I want to highlight another key component in banana breeding that needs to be addressed to truly propel it forward. Banana breeding suffers from a major hurdle, that I would like to refer to as the 'seed paradox'. On the one hand, the accurate mapping of traits of interest often requires the screening of large populations for obtaining as many recombinants as possible for rare crossover events (Wijnker & de Jong, 2008). On the other hand, the final product of banana breeding needs to be sterile for seedless edible fruit, as are all other cultivated varieties (Drenth & Kema, 2021). These two requirements for banana breeding severely hamper its progress. As an example, after hand pollinating 20,000 Cavendish bunches only 40 viable embryos were able to be rescued (Aguilar Morán, 2013). For this reason, the molecular mechanism of parthenocarpy in banana is of strong interest, but so far, the exact genes involved remain unknown (Backiyarani *et al.*, 2021). Currently, conventional banana breeding is still reliant on cumbersome breeding schemes in a process that can take up to 15 years (Fig. 2) (Brown, A *et al.*, 2017; Nyine *et al.*, 2017), but the development of increasing numbers of markers and other molecular tools are improving the efficiency of banana breeding (Ortiz & Swennen, 2014). Similarly, improved genetic engineering techniques will enable accelerated improvement of banana (Ortiz & Swennen, 2014).

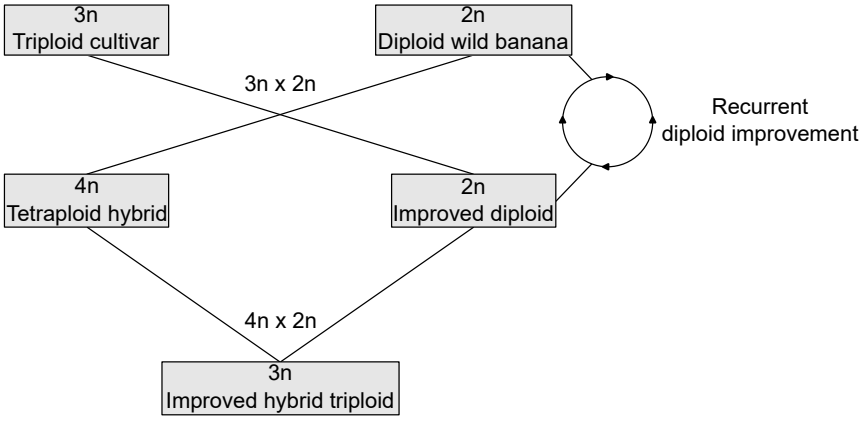


FIGURE 2 | Breeding scheme for generation of improved hybrid triploids. Banana breeding can make use of several different breeding schemes depending on fertility levels, ploidy issues and the desired end product (Ortiz *et al.*, 1995). This scheme displays a breeding strategy used for the generation of improved hybrid triploids, while trying to accelerate the process by optimal use of the generally more fertile diploid plants. Initial crosses using a triploid cultivar (e. g. Cavendish) and a diploid wild banana species with a desired trait e.g. resistance to a pathogen result in predominantly tetraploid and diploid progeny. Improved diploids can be used for recurrent diploid improvement to generate improved diploid germplasm for further breeding. Moreover, improved diploid progeny can be used in secondary crosses with tetraploid hybrids to finally generate improved hybrid triploids with the desired trait(s). Breeding scheme based on (Vuylsteke *et al.*, 1992; Tenkouano & Swennen, 2004; Dochez *et al.*, 2005; Brown, A *et al.*, 2017).

One of the major modern tools in resistance breeding is the use of pathogen effectors to aid in the identification and characterization of resistance genes (Vleeshouwers & Oliver, 2014). Despite significant efforts by myself and others, banana still lacks a high throughput transient expression system. The development of such a tool will be crucial for efficient screening of the response to a wide range of banana pathogen effectors. For the time being, knockout mutants of single or multiple effectors can give some first insights into their potential role in resistance. For this thesis several individual effector mutants have been generated as well as mutants lacking a virulence associated chromosome (Chapters 1 & 2). Although the individual effector mutants did not show significant differences compared to the wildtype during infection on Cavendish, they should still be tested on resistant wild (sub)species. Similarly, the chromosome mutants should be tested on resistant germplasm. Both the effectors and accessory genome-encoded genes could still play a role in the immunity of TR4 resistant plants. In the end, to catapult banana breeding and research forward and bring it up to par with other crops will require a concerted long-term effort, significant development of molecular tools and large continued investments and interest as seen in the Yelloway and IITA breeding programs.

Finally, to conclude, there are several key points that I think should be used as a guide for future studies on banana and its interaction with *Fusarium* spp. Expanding on the building leads (Ahmad *et al.*, 2020; Li, X *et al.*, 2024), the exact genetic basis for Race 1 resistance in Cavendish should be determined. The Race 1 resistance gene or the TR4 resistance gene RGA2 (Dale *et al.*, 2017), could allow for the establishment of the first effector-receptor interaction for *Fusarium* and banana. As the origin of the TR4 lineage does not lie in a simple mutation of a Race 1 strain, resolving the determining difference between Race 1 and TR4 strains will strongly benefit our understanding of resistance and its durability. Lastly, determining the minimum required effector repertoire in TR4 for banana infection will be relevant in directing breeding efforts. Addressing these goals will ultimately aid in the modernization and rationalization of banana breeding.

References

Abraham LN, Oggenfuss U, Croll D. 2024. Population-level transposable element expression dynamics influence trait evolution in a fungal crop pathogen. *mBio* **15**(3): e0284023.

Aguilar Morán JF. 2013. Improvement of Cavendish Banana Cultivars through Conventional Breeding. *Acta Horticulturae*(986): 205-208.

Ahmad F, Martawi NM, Poerba YS, de Jong H, Schouten H, Kema GHJ. 2020. Genetic mapping of Fusarium wilt resistance in a wild banana *Musa acuminata* ssp. *malaccensis* accession. *Theor Appl Genet* **133**(12): 3409-3418.

Akagi Y, Akamatsu H, Otani H, Kodama M. 2009. Horizontal chromosome transfer, a mechanism for the evolution and differentiation of a plant-pathogenic fungus. *Eukaryot Cell* **8**(11): 1732-1738.

Ali S, Laurie JD, Linning R, Cervantes-Chavez JA, Gaudet D, Bakkeren G. 2014. An immunity-triggering effector from the Barley smut fungus *Ustilago hordei* resides in an *Ustilaginaceae*-specific cluster bearing signs of transposable element-assisted evolution. *PLoS Pathog* **10**(7): e1004223.

Almagro Armenteros JJ, Salvatore M, Emanuelsson O, Winther O, von Heijne G, Elofsson A, Nielsen H. 2019a. Detecting sequence signals in targeting peptides using deep learning. *Life Sci Alliance* **2**(5).

Almagro Armenteros JJ, Tsirigos KD, Sonderby CK, Petersen TN, Winther O, Brunak S, von Heijne G, Nielsen H. 2019b. SignalP 5.0 improves signal peptide predictions using deep neural networks. *Nat Biotechnol* **37**(4): 420-423.

Altschul SF, Gish W, Miller W, Myers EW, Lipman DJ. 1990. Basic local alignment search tool. *J Mol Biol* **215**(3): 403-410.

Álvarez-López D, Herrera-Valencia VA, Góngora-Castillo E, García-Laynes S, Puch-Hau C, López-Ochoa LA, Lizama-Uc G, Peraza-Echeverria S. 2022. Genome-Wide Analysis of the LRR-RLP Gene Family in a Wild Banana (*Musa acuminata* ssp. *malaccensis*) Uncovers Multiple Fusarium Wilt Resistance Gene Candidates. *Genes (Basel)* **13**(4).

Amezrou R, Audéon C, Compain J, Gélisse S, Ducasse A, Saintenac C, Lapalu N, Louet C, Orford S, Croll D, et al. 2023. A secreted protease-like protein in *Zymoseptoria tritici* is responsible for avirulence on *Stb9* resistance gene in wheat. *PLoS Pathog* **19**(5): e1011376.

An B, Hou X, Guo Y, Zhao S, Luo H, He C, Wang Q. 2019. The effector SIX8 is required for virulence of Fusarium oxysporum f.sp. cubense tropical race 4 to Cavendish banana. *Fungal Biol* **123**(5): 423-430.

Aoki T, O'Donnell K, Geiser DM. 2014. Systematics of key phytopathogenic *Fusarium* species: current status and future challenges. *Journal of General Plant Pathology* **80**(3): 189-201.

Arie T, Kaneko I, Yoshida T, Noguchi M, Nomura Y, Yamaguchi I. 2000. Mating-type genes from asexual phytopathogenic ascomycetes *Fusarium oxysporum* and *Alternaria alternata*. *Mol Plant Microbe Interact* **13**(12): 1330-1339.

Armitage AD, Taylor A, Sobczyk MK, Baxter L, Greenfield BPJ, Bates HJ, Wilson F, Jackson AC, Ott S, Harrison RJ, et al. 2018. Characterisation of pathogen-specific regions and novel effector candidates in *Fusarium oxysporum* f. sp. *cepae*. *Sci Rep* **8**(1): 13530.

Ayukawa Y, Asai S, Gan P, Tsushima A, Ichihashi Y, Shibata A, Komatsu K, Houterman PM, Rep M, Shirasu K, et al. 2021. A pair of effectors encoded on a conditionally dispensable chromosome of *Fusarium oxysporum* suppress host-specific immunity. *Commun Biol* **4**(1): 707.

Backiyarani S, Sasikala R, Sharmiladevi S, Uma S. 2021. Decoding the molecular mechanism of parthenocarpy in *Musa* spp. through protein-protein interaction network. *Sci Rep* **11**(1): 14592.

Bacon CW, Hinton DM, Hinton A, Jr. 2006. Growth-inhibiting effects of concentrations of fusaric acid on the growth of *Bacillus mojavensis* and other biocontrol *Bacillus* species. *J Appl Microbiol* **100**(1): 185-194.

Balesdent MH, Fudal I, Ollivier B, Bally P, Grandaubert J, Eber F, Chevre AM, Leflon M, Rouxel T. 2013. The dispensable chromosome of *Leptosphaeria maculans* shelters an effector gene conferring avirulence towards *Brassica rapa*. *New Phytol* **198**(3): 887-898.

Balter M. 2007. Plant science. Seeking agriculture's ancient roots. *Science* **316**(5833): 1830-1835.

Bankevich A, Nurk S, Antipov D, Gurevich AA, Dvorkin M, Kulikov AS, Lesin VM, Nikolenko SI, Pham S, Prjibelski AD, et al. 2012. SPAdes: a new genome assembly algorithm and its applications to single-cell sequencing. *J Comput Biol* **19**(5): 455-477.

Baril T, Galbraith J, Hayward A. 2024. Earl Grey: A Fully Automated User-Friendly Transposable Element Annotation and Analysis Pipeline. *Mol Biol Evol* **41**(4).

Baroncelli R, Amby DB, Zapparata A, Sarrocco S, Vannacci G, Le Floch G, Harrison RJ, Holub E, Sukno SA, Sreenivasaprasad S, et al. 2016. Gene family expansions and contractions are associated with host range in plant pathogens of the genus *Colletotrichum*. *BMC Genomics* **17**: 555.

Barragan AC, Latorre SM, Malmgren A, Harant A, Win J, Sugihara Y, Burbano HA, Kamoun S, Langner T. 2024. Multiple Horizontal Mini-chromosome Transfers Drive Genome Evolution of Clonal Blast Fungus Lineages. *Mol Biol Evol* **41**(8): 2024.2002.2013.580079.

Barro-Trastoy D, Köhler C. 2024. Helitrons: genomic parasites that generate developmental novelties. *Trends Genet* **40**(5): 437-448.

Belser C, Baurens FC, Noel B, Martin G, Cruaud C, Istace B, Yahiaoui N, Labadie K, Hribova E, Dolezel J, et al. 2021. Telomere-to-telomere gapless chromosomes of banana using nanopore sequencing. *Commun Biol* **4**(1): 1047.

Bertazzoni S, Williams AH, Jones DA, Syme RA, Tan KC, Hane JK. 2018. Accessories Make the Outfit: Accessory Chromosomes and Other Dispensable DNA Regions in Plant-Pathogenic Fungi. *Mol Plant Microbe Interact* **31**(8): 779-788.

Biju VC, Fokkens L, Houterman PM, Rep M, Cornelissen BJC. 2017. Multiple Evolutionary Trajectories Have Led to the Emergence of Races in *Fusarium oxysporum* f. sp. *lycopersici*. *Appl Environ Microbiol* **83**(4).

Blekemolen MC, Cao L, Tintor N, de Groot T, Papp D, Faulkner C, Takken FLW. 2022. The primary function of Six5 of *Fusarium oxysporum* is to facilitate Avr2 activity by together manipulating the size exclusion limit of plasmodesmata. *Front Plant Sci* **13**: 910594.

Blin K, Shaw S, Augustijn HE, Reitz ZL, Biermann F, Alanjary M, Fetter A, Terlouw BR, Metcalf WW, Helfrich EJN, et al. 2023. antiSMASH 7.0: new and improved predictions for detection, regulation, chemical structures and visualisation. *Nucleic Acids Res* **51**(W1): W46-W50.

Boehm EWA. 1994. Statistical Analysis of Electrophoretic Karyotype Variation Among Vegetative Compatibility Groups of *Fusarium oxysporum* f. sp. *cubense*. *Molecular Plant-Microbe Interactions* **7**(2).

Bohni N, Hofstetter V, Gindro K, Buyck B, Schumpp O, Bertrand S, Monod M, Wolfender JL. 2016. Production of Fusaric Acid by *Fusarium* spp. in Pure Culture and in Solid Medium Co-Cultures. *Molecules* **21**(3): 370.

Bömke C, Tudzynski B. 2009. Diversity, regulation, and evolution of the gibberellin biosynthetic pathway in fungi compared to plants and bacteria. *Phytochemistry* **70**(15-16): 1876-1893.

Borlaug NE. 2002. The Green Revolution Revisited and the Road Ahead.

Brakhage AA. 2013. Regulation of fungal secondary metabolism. *Nat Rev Microbiol* **11**(1): 21-32.

Brankovics B, van Dam P, Rep M, de Hoog GS, TA JvdL, Waalwijk C, van Diepeningen AD. 2017. Mitochondrial genomes reveal recombination in the presumed asexual *Fusarium oxysporum* species complex. *BMC Genomics* **18**(1): 735.

Bray NL, Pimentel H, Melsted P, Pachter L. 2016. Near-optimal probabilistic RNA-seq quantification. *Nat Biotechnol* **34**(5): 525-527.

Brefort T, Tanaka S, Neidig N, Doehlemann G, Vincon V, Kahmann R. 2014. Characterization of the largest effector gene cluster of *Ustilago maydis*. *PLoS Pathog* **10**(7): e1003866.

Brenes Guallar MA, Fokkens L, Rep M, Berke L, van Dam P. 2022. *Fusarium oxysporum* effector clustering version 2: An updated pipeline to infer host range. *Front Plant Sci* **13**: 1012688.

Brown A, Tumuhimbise R, Amah D, Uwimana B, Nyine M, Mduma H, Talengera D, Karamura D, Kuriba J, Swennen R 2017. Bananas and Plantains (*Musa* spp.). In: Campos H, Caligari PDS eds. *Genetic Improvement of Tropical Crops*. Cham: Springer International Publishing, 219-240.

Brown DW, Lee SH, Kim LH, Ryu JG, Lee S, Seo Y, Kim YH, Busman M, Yun SH, Proctor RH, et al. 2015. Identification of a 12-gene Fusaric Acid Biosynthetic Gene Cluster in *Fusarium* Species Through Comparative and Functional Genomics. *Mol Plant Microbe Interact* **28**(3): 319-332.

Brown JK. 2015. Durable resistance of crops to disease: a Darwinian perspective. *Annu Rev Phytopathol* **53**: 513-539.

Brown NA, Evans J, Mead A, Hammond-Kosack KE. 2017. A spatial temporal analysis of the *Fusarium graminearum* transcriptome during symptomless and symptomatic wheat infection. *Mol Plant Pathol* **18**(9): 1295-1312.

Cai J, Jiang Y, Ritchie ES, Macho AP, Yu F, Wu D. 2023. Manipulation of plant metabolism by pathogen effectors: more than just food. *FEMS Microbiol Rev* **47**(2).

Camacho C, Coulouris G, Avagyan V, Ma N, Papadopoulos J, Bealer K, Madden TL. 2009. BLAST+: architecture and applications. *BMC Bioinformatics* **10**: 421.

Cantalapiedra CP, Hernandez-Plaza A, Letunic I, Bork P, Huerta-Cepas J. 2021. eggNOG-mapper v2: Functional Annotation, Orthology Assignments, and Domain Prediction at the Metagenomic Scale. *Mol Biol Evol* **38**(12): 5825-5829.

Cantu D, Vicente AR, Labavitch JM, Bennett AB, Powell AL. 2008. Strangers in the matrix: plant cell walls and pathogen susceptibility. *Trends Plant Sci* **13**(11): 610-617.

Cao L, Blekemolen MC, Tintor N, Cornelissen BJC, Takken FLW. 2018. The *Fusarium oxysporum* Avr2-Six5 Effector Pair Alters Plasmodesmatal Exclusion Selectivity to Facilitate Cell-to-Cell Movement of Avr2. *Mol Plant* **11**(5): 691-705.

Castanera R, Lopez-Varas L, Borgognone A, LaButti K, Lapidus A, Schmutz J, Grimwood J, Perez G, Pisabarro AG, Grigoriev IV, et al. 2016. Transposable Elements versus the Fungal Genome: Impact on Whole-Genome Architecture and Transcriptional Profiles. *PLoS Genet* **12**(6): e1006108.

Castanera R, Perez G, Lopez L, Sancho R, Santoyo F, Alfaro M, Gabaldon T, Pisabarro AG, Oguiza JA, Ramirez L. 2014. Highly expressed captured genes and cross-kingdom domains present in Helitrons create novel diversity in *Pleurotus ostreatus* and other fungi. *BMC Genomics* **15**(1): 1071.

Catlin NS, Josephs EB. 2022. The important contribution of transposable elements to phenotypic variation and evolution. *Curr Opin Plant Biol* **65**: 102140.

Chaloner TM, Gurr SJ, Bebber DP. 2021. Plant pathogen infection risk tracks global crop yields under climate change. *Nature Climate Change* **11**(8): 710-715.

Chalopin D, Naville M, Plard F, Galiana D, Volff JN. 2015. Comparative analysis of transposable elements highlights mobilome diversity and evolution in vertebrates. *Genome Biol Evol* **7**(2): 567-580.

Chang HX, Noel ZA, Chilvers MI. 2021. A beta-lactamase gene of *Fusarium oxysporum* alters the rhizosphere microbiota of soybean. *Plant J* **106**(6): 1588-1604.

Chang W, Li H, Chen H, Qiao F, Zeng H. 2020. Identification of *mimp*-associated effector genes in *Fusarium oxysporum* f. sp. *cubense* race 1 and race 4 and virulence confirmation of a candidate effector gene. *Microbiol Res* **232**: 126375.

Chao J, Li Z, Sun Y, Aluko OO, Wu X, Wang Q, Liu G. 2021. MG2C: a user-friendly online tool for drawing genetic maps. *Mol Hortic* **1**(1): 16.

Chellapan BV, van Dam P, Rep M, Cornelissen BJ, Fokkens L. 2016. Non-canonical Helitrons in *Fusarium oxysporum*. *Mob DNA* **7**: 27.

Chen B, Gilbert LA, Cimini BA, Schnitzbauer J, Zhang W, Li GW, Park J, Blackburn EH, Weissman JS, Qi LS, et al. 2013. Dynamic imaging of genomic loci in living human cells by an optimized CRISPR/Cas system. *Cell* **155**(7): 1479-1491.

Chong P, Essoh JN, Arango Isaza RE, Keizer P, Stergiopoulos I, Seidl MF, Guzman M, Sandoval J, Verweij PE, Scalliet G, et al. 2021. A world-wide analysis of reduced sensitivity to DMI fungicides in the banana pathogen *Pseudocercospora fijiensis*. *Pest Manag Sci* **77**(7): 3273-3288.

Chuma I, Isobe C, Hotta Y, Ibaragi K, Futamata N, Kusaba M, Yoshida K, Terauchi R, Fujita Y, Nakayashiki H, et al. 2011. Multiple translocation of the AVR-Pita effector gene among chromosomes of the rice blast fungus *Magnaporthe oryzae* and related species. *PLoS Pathog* **7**(7): e1002147.

Chumley FG, Valent B. 1990. Genetic Analysis of Melanin-Deficient, Nonpathogenic Mutants of *Magnaporthe grisea*. *Molecular Plant-Microbe Interactions* **3**(3).

Coleman JJ, Rounsley SD, Rodriguez-Carres M, Kuo A, Wasmann CC, Grimwood J, Schmutz J, Taga M, White GJ, Zhou S, et al. 2009. The genome of *Nectria haematococca*: contribution of supernumerary chromosomes to gene expansion. *PLoS Genet* **5**(8): e1000618.

Collemare J, Billard A, Bohnert HU, Lebrun MH. 2008a. Biosynthesis of secondary metabolites in the rice blast fungus *Magnaporthe grisea*: the role of hybrid PKS-NRPS in pathogenicity. *Mycol Res* **112**(Pt 2): 207-215.

Collemare J, O'Connell R, Lebrun MH. 2019. Nonproteinaceous effectors: the terra incognita of plant-fungal interactions. *New Phytol* **223**(2): 590-596.

Collemare J, Pianfetti M, Houlle AE, Morin D, Camborde L, Gagey MJ, Barbisan C, Fudal I, Lebrun MH, Böhnert HU. 2008b. *Magnaporthe grisea* avirulence gene ACE1 belongs to an infection-specific gene cluster involved in secondary metabolism. *New Phytol* **179**(1): 196-208.

Condon BJ, Leng Y, Wu D, Bushley KE, Ohm RA, Otillar R, Martin J, Schackwitz W, Grimwood J, MohdZainudin N, et al. 2013. Comparative genome structure, secondary metabolite, and effector coding capacity across *Cochliobolus* pathogens. *PLoS Genet* **9**(1): e1003233.

Connolly LR, Smith KM, Freitag M. 2013. The *Fusarium graminearum* histone H3 K27 methyltransferase KMT6 regulates development and expression of secondary metabolite gene clusters. *PLoS Genet* **9**(10): e1003916.

Cook DE, Kramer HM, Torres DE, Seidl MF, Thomma B. 2020. A unique chromatin profile defines adaptive genomic regions in a fungal plant pathogen. *Elife* **9**.

Cook DE, Mesarich CH, Thomma BP. 2015. Understanding plant immunity as a surveillance system to detect invasion. *Annu Rev Phytopathol* **53**: 541-563.

Covert SF, Enkerli J, Miao VP, VanEtten HD. 1996. A gene for maackiain detoxification from a dispensable chromosome of *Nectria haematococca*. *Mol Gen Genet* **251**(4): 397-406.

Croll D, McDonald BA. 2012. The accessory genome as a cradle for adaptive evolution in pathogens. *PLoS Pathog* **8**(4): e1002608.

Croll D, McDonald BA. 2017. The genetic basis of local adaptation for pathogenic fungi in agricultural ecosystems. *Mol Ecol* **26**(7): 2027-2040.

Croll D, Zala M, McDonald BA. 2013. Breakage-fusion-bridge cycles and large insertions contribute to the rapid evolution of accessory chromosomes in a fungal pathogen. *PLoS Genet* **9**(6): e1003567.

Crombach A, Hogeweg P. 2007. Chromosome rearrangements and the evolution of genome structuring and adaptability. *Mol Biol Evol* **24**(5): 1130-1139.

Crutcher FK, Liu J, Puckhaber LS, Stipanovic RD, Bell AA, Nichols RL. 2015. FUBT, a putative MFS transporter, promotes secretion of fusaric acid in the cotton pathogen *Fusarium oxysporum* f. sp. *vasinfectum*. *Microbiology (Reading)* **161**(Pt 4): 875-883.

Cui H, Tsuda K, Parker JE. 2015. Effector-triggered immunity: from pathogen perception to robust defense. *Annu Rev Plant Biol* **66**: 487-511.

Czymmek KJ, Fogg M, Powell DH, Sweigard J, Park SY, Kang S. 2007. In vivo time-lapse documentation using confocal and multi-photon microscopy reveals the mechanisms of invasion into the Arabidopsis root vascular system by *Fusarium oxysporum*. *Fungal Genet Biol* **44**(10): 1011-1023.

D'Hont A, Denoeud F, Aury JM, Baurens FC, Carreel F, Garsmeur O, Noel B, Bocs S, Droc G, Rouard M, et al. 2012. The banana (*Musa acuminata*) genome and the evolution of monocotyledonous plants. *Nature* **488**(7410): 213-217.

Daboussi MJ, Capy P. 2003. Transposable elements in filamentous fungi. *Annu Rev Microbiol* **57**: 275-299.

Dale J, James A, Paul JY, Khanna H, Smith M, Peraza-Echeverria S, García-Bastidas F, Kema G, Waterhouse P, Mengersen K, et al. 2017. Transgenic Cavendish bananas with resistance to Fusarium wilt tropical race 4. *Nat Commun* **8**(1): 1496.

Dallery JF, Lapalu N, Zampounis A, Pigne S, Luyten I, Amselem J, Wittenberg AHJ, Zhou S, de Queiroz MV, Robin GP, et al. 2017. Gapless genome assembly of *Colletotrichum higginsianum* reveals chromosome structure and association of transposable elements with secondary metabolite gene clusters. *BMC Genomics* **18**(1): 667.

Dark P, Gent H. 2002. Pests and Diseases of Prehistoric Crops: A Yield 'Honeymoon' for Early Grain Crops in Europe? *Oxford Journal of Archaeology* **20**(1): 59-78.

de Guillen K, Mammri L, Gracy J, Padilla A, Barthe P, Hoh F, Lahfa M, Rouffet J, Petit-Houdenot Y, Kroj T, et al. 2024. *Zymoseptoria tritici* effectors structurally related to killer proteins UmV-KP4 and UmV-KP6 are toxic to fungi, and define extended protein families in fungi. *bioRxiv*: 2024.2010.2014.618152.

de Guillen K, Ortiz-Vallejo D, Gracy J, Fournier E, Kroj T, Padilla A. 2015. Structure Analysis Uncovers a Highly Diverse but Structurally Conserved Effector Family in Phytopathogenic Fungi. *PLoS Pathog* **11**(10): e1005228.

de Jonge R, Bolton MD, Kombrink A, van den Berg GC, Yadeta KA, Thomma BP. 2013. Extensive chromosomal reshuffling drives evolution of virulence in an asexual pathogen. *Genome Res* **23**(8): 1271-1282.

de Jonge R, van Esse HP, Maruthachalam K, Bolton MD, Santhanam P, Saber MK, Zhang Z, Usami T, Lievens B, Subbarao KV, et al. 2012. Tomato immune receptor Ve1 recognizes effector of multiple fungal pathogens uncovered by genome and RNA sequencing. *Proc Natl Acad Sci U S A* **109**(13): 5110-5115.

De Langhe E, Vrydaghs L, de Maret P, Perrier X, Denham T. 2009. Why Bananas Matter: An introduction to the history of banana domestication. *Ethnobotany Research and Applications* **7**(0): 165-177.

de Vega-Bartol JJ, Martín-Dominguez R, Ramos B, García-Sánchez MA, Díaz-Mínguez JM. 2011. New virulence groups in *Fusarium oxysporum* f. sp. *phaseoli*: the expression of the gene coding for the transcription factor ftf1 correlates with virulence. *Phytopathology* **101**(4): 470-479.

De Vos RC, Moco S, Lommen A, Keurentjes JJ, Bino RJ, Hall RD. 2007. Untargeted large-scale plant metabolomics using liquid chromatography coupled to mass spectrometry. *Nat Protoc* **2**(4): 778-791.

Dean R, Van Kan JA, Pretorius ZA, Hammond-Kosack KE, Di Pietro A, Spanu PD, Rudd JJ, Dickman M, Kahmann R, Ellis J, et al. 2012. The Top 10 fungal pathogens in molecular plant pathology. *Mol Plant Pathol* **13**(4): 414-430.

Delaux PM, Radhakrishnan GV, Jayaraman D, Cheema J, Malbreil M, Volkening JD, Sekimoto H, Nishiyama T, Melkonian M, Pokorny L, et al. 2015. Algal ancestor of land plants was preadapted for symbiosis. *Proc Natl Acad Sci U S A* **112**(43): 13390-13395.

Di X, Cao L, Hughes RK, Tintor N, Banfield MJ, Takken FLW. 2017. Structure-function analysis of the *Fusarium oxysporum* Avr2 effector allows uncoupling of its immune-suppressing activity from recognition. *New Phytol* **216**(3): 897-914.

Dijkstra J, van Westerhoven AC, Gómez-Gil L, Aguilera-Galvez C, Nakasato-Tagami G, Garnier SD, Yamazaki M, Arie T, Kamakura T, Arazoe T, et al. 2024. Extensive intrachromosomal duplications in a virulence-associated fungal accessory chromosome. *bioRxiv*: 2024.2009.2016.611982.

Dita M, Barquero M, Heck D, Mizubuti ESG, Staver CP. 2018. Fusarium Wilt of Banana: Current Knowledge on Epidemiology and Research Needs Toward Sustainable Disease Management. *Front Plant Sci* **9**: 1468.

Dochez C, Whyte J, Tenkouano A, Ortiz R, De Waele D. 2005. Response of East African highland bananas and hybrids to *Radopholus similis*. *Nematology* **7**(5): 655-666.

Dong H, Fan H, Lei Z, Wu C, Zhou D, Li H. 2019. Histological and Gene Expression Analyses in Banana Reveals the Pathogenic Differences between Races 1 and 4 of Banana Fusarium Wilt Pathogen. *Phytopathology* **109**(6): 1029-1042.

Dong S, Raffaele S, Kamoun S. 2015. The two-speed genomes of filamentous pathogens: waltz with plants. *Curr Opin Genet Dev* **35**: 57-65.

Dou T, Shao X, Hu C, Liu S, Sheng O, Bi F, Deng G, Ding L, Li C, Dong T, et al. 2020. Host-induced gene silencing of *Foc* TR4 *ERG6/11* genes exhibits superior resistance to Fusarium wilt of banana. *Plant Biotechnol J* **18**(1): 11-13.

Drenth A, Kema G. 2021. The Vulnerability of Bananas to Globally Emerging Disease Threats. *Phytopathology®* **111**(12): 2146-2161.

Du C, Fefelova N, Caronna J, He L, Dooner HK. 2009. The polychromatic Helitron landscape of the maize genome. *Proc Natl Acad Sci U S A* **106**(47): 19916-19921.

Dührkop K, Fleischauer M, Ludwig M, Aksenov AA, Melnik AV, Meusel M, Dorrestein PC, Rousu J, Bocker S. 2019. SIRIUS 4: a rapid tool for turning tandem mass spectra into metabolite structure information. *Nat Methods* **16**(4): 299-302.

Dulal N, Wilson RA. 2024. Paths of Least Resistance: Unconventional Effector Secretion by Fungal and Oomycete Plant Pathogens. *Mol Plant Microbe Interact* **37**(9): 653-661.

Dutheil JY, Mannhaupt G, Schweizer G, C MKS, Munsterkotter M, Guldener U, Schirawski J, Kahmann R. 2016. A Tale of Genome Compartmentalization: The Evolution of Virulence Clusters in Smut Fungi. *Genome Biol Evol* **8**(3): 681-704.

Dyer PS, Kück U. 2017. Sex and the Imperfect Fungi. *Microbiol Spectr* **5**(3).

Faino L, Seidl MF, Shi-Kunne X, Pauper M, van den Berg GC, Wittenberg AH, Thomma BP. 2016. Transposons passively and actively contribute to evolution of the two-speed genome of a fungal pathogen. *Genome Res* **26**(8): 1091-1100.

Fang X, Kuo J, You MP, Finnegan PM, Barbetti MJ. 2012. Comparative root colonisation of strawberry cultivars Camarosa and Festival by *Fusarium oxysporum* f. sp. *fragariae*. *Plant and Soil* **358**(1-2): 75-89.

FAO. 2020. *Fruit and vegetables – your dietary essentials. The International Year of Fruits and Vegetables, 2021, background paper.* Rome.

Faris JD, Friesen TL. 2020. Plant genes hijacked by necrotrophic fungal pathogens. *Curr Opin Plant Biol* **56**: 74-80.

Fayyaz A, Robinson G, Chang PL, Bekele D, Yimer S, Carrasquilla-Garcia N, Negash K, Surendrarao A, von Wettberg EJB, Kemal SA, et al. 2023. Hiding in plain sight: Genome-wide recombination and a dynamic accessory genome drive diversity in *Fusarium oxysporum* f.sp. *ciceris*. *Proc Natl Acad Sci U S A* **120**(27): e2220570120.

Fisher MC, Henk DA, Briggs CJ, Brownstein JS, Madoff LC, McCraw SL, Gurr SJ. 2012. Emerging fungal threats to animal, plant and ecosystem health. *Nature* **484**(7393): 186-194.

Flood J. 2010. The importance of plant health to food security. *Food Security* **2**(3): 215-231.

Fokkens L, Rep M. 2023. Population genomics reveals meiotic recombination in *Fusarium oxysporum*. *Proc Natl Acad Sci U S A* **120**(30): e2309677120.

Fokkens L, Shahi S, Connolly LR, Stam R, Schmidt SM, Smith KM, Freitag M, Rep M. 2018. The multi-speed genome of *Fusarium oxysporum* reveals association of histone modifications with sequence divergence and footprints of past horizontal chromosome transfer events. *bioRxiv*: 465070.

Fones HN, Bebber DP, Chaloner TM, Kay WT, Steinberg G, Gurr SJ. 2020. Threats to global food security from emerging fungal and oomycete crop pathogens. *Nat Food* **1**(6): 332-342.

Forche A, Magee PT, Selmecki A, Berman J, May G. 2009. Evolution in *Candida albicans* populations during a single passage through a mouse host. *Genetics* **182**(3): 799-811.

Fouché S, Badet T, Oggenfuss U, Plissonneau C, Francisco CS, Croll D. 2020. Stress-Driven Transposable Element De-repression Dynamics and Virulence Evolution in a Fungal Pathogen. *Mol Biol Evol* **37**(1): 221-239.

Fouché S, Oggenfuss U, Chanclud E, Croll D. 2022. A devil's bargain with transposable elements in plant pathogens. *Trends Genet* **38**(3): 222-230.

Frantzeskakis L, Kusch S, Panstruga R. 2019. The need for speed: compartmentalized genome evolution in filamentous phytopathogens. *Mol Plant Pathol* **20**(1): 3-7.

Frison EA, Escalant, J. V., Sharrock, S., Jain, S. M., & Swennen, R. . 2004. *The global Musa genomic consortium: a boost for banana improvement.*

Gagnon JA, Valen E, Thyme SB, Huang P, Akhmetova L, Pauli A, Montague TG, Zimmerman S, Richter C, Schier AF. 2014. Efficient mutagenesis by Cas9 protein-mediated oligonucleotide insertion and large-scale assessment of single-guide RNAs. *PLoS One* **9**(5): e98186.

Galazka JM, Freitag M. 2014. Variability of chromosome structure in pathogenic fungi--of 'ends and odds'. *Curr Opin Microbiol* **20**: 19-26.

Gan P, Ikeda K, Irieda H, Narusaka M, O'Connell RJ, Narusaka Y, Takano Y, Kubo Y, Shirasu K. 2013. Comparative genomic and transcriptomic analyses reveal the hemibiotrophic stage shift of *Colletotrichum* fungi. *New Phytol* **197**(4): 1236-1249.

García-Bastidas FA, Arango-Isaza R, Rodriguez-Cabal HA, Seidl MF, Cappadona G, Segura R, Salacinas M, Kema GHJ. 2022. Induced resistance to Fusarium wilt of banana caused by Tropical Race 4 in Cavendish cv Grand Naine bananas after challenging with avirulent *Fusarium* spp. *PLoS One* **17**(9): e0273335.

García-Bastidas FA, Van der Veen AJT, Nakasato-Tagami G, Meijer HJG, Arango-Isaza RE, Kema GHJ. 2019. An Improved Phenotyping Protocol for Panama Disease in Banana. *Front Plant Sci* **10**: 1006.

Garmaroodi HS, Taga M. 2007. Duplication of a conditionally dispensable chromosome carrying pea pathogenicity (PEP) gene clusters in *Nectria haematococca*. *Mol Plant Microbe Interact* **20**(12): 1495-1504.

Gaumann E. 1957. Fusaric acid as a wilt toxin. *Phytopathology* **47**(6): 342–357 pp.

Geiser DM, Al-Hatmi AMS, Aoki T, Arie T, Balmas V, Barnes I, Bergstrom GC, Bhattacharyya MK, Blomquist CL, Bowden RL, et al. 2021. Phylogenomic Analysis of a 55.1-kb 19-Gene Dataset Resolves a Monophyletic *Fusarium* that Includes the *Fusarium solani* Species Complex. *Phytopathology* **111**(7): 1064-1079.

Ghag SB, Shekhawat UK, Ganapathi TR. 2014. Host-induced post-transcriptional hairpin RNA-mediated gene silencing of vital fungal genes confers efficient resistance against Fusarium wilt in banana. *Plant Biotechnol J* **12**(5): 541-553.

Gilchrist C, Stelkens R. 2019. Aneuploidy in yeast: Segregation error or adaptation mechanism? *Yeast* **36**(9): 525-539.

Gilchrist CLM, Booth TJ, van Wersch B, van Grieken L, Medema MH, Chooi YH. 2021. cblaster: a remote search tool for rapid identification and visualization of homologous gene clusters. *Bioinform Adv* **1**(1): vbab016.

Gilchrist CLM, Chooi YH. 2021. clinker & clustermap.js: automatic generation of gene cluster comparison figures. *Bioinformatics* **37**(16): 2473-2475.

Gíslason MH, Nielsen H, Almagro Armenteros JJ, Johansen AR. 2021. Prediction of GPI-anchored proteins with pointer neural networks. *Current Research in Biotechnology* **3**: 6-13.

Gluck-Thaler E, Ralston T, Konkel Z, Ocampos CG, Ganeshan VD, Dorrance AE, Niblack TL, Wood CW, Slot JC, Lopez-Nicora HD, et al. 2022. Giant Starship Elements Mobilize Accessory Genes in Fungal Genomes. *Mol Biol Evol* **39**(5).

Godfray HC, Beddington JR, Crute IR, Haddad L, Lawrence D, Muir JF, Pretty J, Robinson S, Thomas SM, Toulmin C. 2010. Food security: the challenge of feeding 9 billion people. *Science* **327**(5967): 812-818.

Godfrey D, Böhlenius H, Pedersen C, Zhang Z, Emmersen J, Thordal-Christensen H. 2010. Powdery mildew fungal effector candidates share N-terminal Y/F/WxC-motif. *BMC Genomics* **11**: 317.

Goodwin SB, M'Barek S B, Dhillon B, Wittenberg AH, Crane CF, Hane JK, Foster AJ, Van der Lee TA, Grimwood J, Aerts A, et al. 2011. Finished genome of the fungal wheat pathogen Mycosphaerella graminicola reveals dispensome structure, chromosome plasticity, and stealth pathogenesis. *PLoS Genet* **7**(6): e1002070.

Gordon TR. 2017. *Fusarium oxysporum* and the *Fusarium* Wilt Syndrome. *Annu Rev Phytopathol* **55**: 23-39.

Grabundzija I, Messing SA, Thomas J, Cosby RL, Bilic I, Miskey C, Gogol-Doring A, Kapitonov V, Diem T, Dalda A, et al. 2016. A Helitron transposon reconstructed from bats reveals a novel mechanism of genome shuffling in eukaryotes. *Nat Commun* **7**: 10716.

Guo L, Wang J, Liang C, Yang L, Zhou Y, Liu L, Huang J. 2022. Fosp9, a Novel Secreted Protein, Is Essential for the Full Virulence of *Fusarium oxysporum* f. sp. *cubense* on Banana (*Musa* spp.). *Appl Environ Microbiol* **88**(6): e0060421.

Guo L, Yu H, Wang B, Vescio K, Delulio GA, Yang H, Berg A, Zhang L, Edel-Hermann V, Steinberg C, et al. 2021. Metatranscriptomic Comparison of Endophytic and Pathogenic *Fusarium*-Arabidopsis Interactions Reveals Plant Transcriptional Plasticity. *Mol Plant Microbe Interact* **34**(9): 1071-1083.

Gurr S, Samalova M, Fisher M. 2011. The rise and rise of emerging infectious fungi challenges food security and ecosystem health. *Fungal Biology Reviews* **25**(4): 181-188.

Habig M, Grasse AV, Muller J, Stukenbrock EH, Leitner H, Cremer S. 2024. Frequent horizontal chromosome transfer between asexual fungal insect pathogens. *Proc Natl Acad Sci U S A* **121**(11): e2316284121.

Habig M, Kema GH, Holtgrewe Stukenbrock E. 2018. Meiotic drive of female-inherited supernumerary chromosomes in a pathogenic fungus. *Elife* **7**.

Habig M, Lorrain C, Feurtey A, Komluski J, Stukenbrock EH. 2021. Epigenetic modifications affect the rate of spontaneous mutations in a pathogenic fungus. *Nat Commun* **12**(1): 5869.

Habig M, Patneedi SK, Stam R, De Fine Licht HH. 2025. Horizontal transfer of accessory chromosomes in fungi – a regulated process for exchange of genetic material? *Heredity*.

Habig M, Quade J, Stukenbrock EH. 2017. Forward Genetics Approach Reveals Host Genotype-Dependent Importance of Accessory Chromosomes in the Fungal Wheat Pathogen *Zymoseptoria tritici*. *mBio* **8**(6).

Habig M, Stukenbrock EH 2020. Origin, Function, and Transmission of Accessory Chromosomes. In: Benz JP, Schipper K eds. *Genetics and Biotechnology*. Cham: Springer International Publishing, 25-47.

Harris LJ, Balcerzak M, Johnston A, Schneiderman D, Ouellet T. 2016. Host-preferential *Fusarium graminearum* gene expression during infection of wheat, barley, and maize. *Fungal Biol* **120**(1): 111-123.

Hatta R, Ito K, Hosaki Y, Tanaka T, Tanaka A, Yamamoto M, Akimitsu K, Tsuge T. 2002. A conditionally dispensable chromosome controls host-specific pathogenicity in the fungal plant pathogen *Alternaria alternata*. *Genetics* **161**(1): 59-70.

Hayward A, Gilbert C. 2022. Transposable elements. *Curr Biol* **32**(17): R904-R909.

He C, Rusu AG, Poplawski AM, Irwin JA, Manners JM. 1998. Transfer of a supernumerary chromosome between vegetatively incompatible biotypes of the fungus *Colletotrichum gloeosporioides*. *Genetics* **150**(4): 1459-1466.

He Q, McLellan H, Boevink PC, Birch PRJ. 2020. All Roads Lead to Susceptibility: The Many Modes of Action of Fungal and Oomycete Intracellular Effectors. *Plant Commun* **1**(4): 100050.

Henry PM, Pincot DDA, Jenner BN, Borrero C, Aviles M, Nam MH, Epstein L, Knapp SJ, Gordon TR. 2021. Horizontal chromosome transfer and independent evolution drive diversification in *Fusarium oxysporum* f. sp. *fragariae*. *New Phytol* **230**(1): 327-340.

Hirsch CD, Springer NM. 2017. Transposable element influences on gene expression in plants. *Biochim Biophys Acta Gene Regul Mech* **1860**(1): 157-165.

Holm L. 2022. Dali server: structural unification of protein families. *Nucleic Acids Res* **50**(W1): W210-W215.

Houterman PM, Ma L, van Ooijen G, de Vroomen MJ, Cornelissen BJ, Takken FL, Rep M. 2009. The effector protein Avr2 of the xylem-colonizing fungus *Fusarium oxysporum* activates the tomato resistance protein I-2 intracellularly. *Plant J* **58**(6): 970-978.

Hu K, Xu K, Wen J, Yi B, Shen J, Ma C, Fu T, Ouyang Y, Tu J. 2019. Helitron distribution in *Brassicaceae* and whole Genome Helitron density as a character for distinguishing plant species. *BMC Bioinformatics* **20**(1): 354.

Hu RM, Liao ST, Huang CC, Huang YW, Yang TC. 2012. An inducible fusaric acid tripartite efflux pump contributes to the fusaric acid resistance in *Stenotrophomonas maltophilia*. *PLoS One* **7**(12): e51053.

Huang HR, Liu X, Arshad R, Wang X, Li WM, Zhou Y, Ge XJ. 2023. Telomere-to-telomere haplotype-resolved reference genome reveals subgenome divergence and disease resistance in triploid Cavendish banana. *Hortic Res* **10**(9): uhad153.

Huang J, Liu S, Cook DE. 2023. Dynamic Genomes - Mechanisms and consequences of genomic diversity impacting plant-fungal interactions. *Physiological and Molecular Plant Pathology* **125**.

Huang WRH, Joosten M. 2025. Immune signaling: receptor-like proteins make the difference. *Trends Plant Sci* **30**(1): 54-68.

Hull RM, Cruz C, Jack CV, Houseley J. 2017. Environmental change drives accelerated adaptation through stimulated copy number variation. *PLoS Biol* **15**(6): e2001333.

Iriti M, Faoro F. 2008. Ancient plant diseases in Roman Age. *Acta Phytopathologica et Entomologica Hungarica* **43**(1): 15-21.

Jin X, Jia H, Ran L, Wu F, Liu J, Schlaeppi K, Dini-Andreote F, Wei Z, Zhou X. 2024. Fusaric acid mediates the assembly of disease-suppressive rhizosphere microbiota via induced shifts in plant root exudates. *Nat Commun* **15**(1): 5125.

Johnson LJ, Johnson RD, Akamatsu H, Salamiah A, Otani H, Kohmoto K, Kodama M. 2001. Spontaneous loss of a conditionally dispensable chromosome from the *Alternaria alternata* apple pathotype leads to loss of toxin production and pathogenicity. *Curr Genet* **40**(1): 65-72.

Jonkers W, Xayamongkhon H, Haas M, Olivain C, van der Does HC, Broz K, Rep M, Alabouvette C, Steinberg C, Kistler HC. 2014. *EBR1* genomic expansion and its role in virulence of *Fusarium* species. *Environ Microbiol* **16**(7): 1982-2003.

Jumper J, Evans R, Pritzel A, Green T, Figurnov M, Ronneberger O, Tunyasuvunakool K, Bates R, Zidek A, Potapenko A, et al. 2021. Highly accurate protein structure prediction with AlphaFold. *Nature* **596**(7873): 583-589.

Kanapin A, Samsonova A, Rozhmina T, Bankin M, Logachev A, Samsonova M. 2020. The Genome Sequence of Five Highly Pathogenic Isolates of *Fusarium oxysporum* f. sp. *lini*. *Mol Plant Microbe Interact* **33**(9): 1112-1115.

Kanja C, Hammond-Kosack KE. 2020. Proteinaceous effector discovery and characterization in filamentous plant pathogens. *Mol Plant Pathol* **21**(10): 1353-1376.

Karamura E, Frison, E., Karamura, D. A., & Sharrock, S. . 1998. *Banana production systems in eastern and southern Africa*.

Karangwa P, Blomme G, Beed F, Niyongere C, Viljoen A. 2016. The distribution and incidence of banana Fusarium wilt in subsistence farming systems in east and central Africa. *Crop Protection* **84**: 132-140.

Kashiwa T, Suzuki T, Sato A, Akai K, Teraoka T, Komatsu K, Arie T. 2016. A new biotype of *Fusarium oxysporum* f. sp. *lycopersici* race 2 emerged by a transposon-driven mutation of avirulence gene *AVR1*. *FEMS Microbiol Lett* **363**(14).

Kelley BS, Lee SJ, Damasceno CM, Chakravarthy S, Kim BD, Martin GB, Rose JK. 2010. A secreted effector protein (SNE1) from *Phytophthora infestans* is a broadly acting suppressor of programmed cell death. *Plant J* **62**(3): 357-366.

Kessler SC, Zhang X, McDonald MC, Gilchrist CLM, Lin Z, Rightmyer A, Solomon PS, Turgeon BG, Chooi YH. 2020. Victorin, the host-selective cyclic peptide toxin from the oat pathogen *Cochliobolus victoriae*, is ribosomally encoded. *Proc Natl Acad Sci U S A* **117**(39): 24243-24250.

Kislev ME. 1982. Stem rust of wheat 3300 years old found in Israel. *Science* **216**(4549): 993-994.

Kom Ad. 1971. *Wij slaven van Suriname*. Amsterdam,: Contact.

Komluski J, Stukenbrock EH, Habig M. 2022. Non-Mendelian transmission of accessory chromosomes in fungi. *Chromosome Res* **30**(2-3): 241-253.

Krishnan P, Meile L, Plissonneau C, Ma X, Hartmann FE, Croll D, McDonald BA, Sanchez-Vallet A. 2018. Transposable element insertions shape gene regulation and melanin production in a fungal pathogen of wheat. *BMC Biol* **16**(1): 78.

Kubiriba J, Ssali RT, Barekye A, Akankwasa K, Tushemereirwe WK, Batte M, Karamura EB, Karamura D. 2016. The performance of East African highland bananas released in farmers' fields and the need for their further improvement. *Acta Horticulturae*(1114): 231-238.

Kumaran R, Yang SY, Leu JY. 2013. Characterization of chromosome stability in diploid, polyploid and hybrid yeast cells. *PLoS One* **8**(7): e68094.

Kvitko BH, Park DH, Velasquez AC, Wei CF, Russell AB, Martin GB, Schneider DJ, Collmer A. 2009. Deletions in the repertoire of *Pseudomonas syringae* pv. *tomato* DC3000 type III secretion effector genes reveal functional overlap among effectors. *PLoS Pathog* **5**(4): e1000388.

LaBella AL, Opulente DA, Steenwyk JL, Hittinger CT, Rokas A. 2021. Signatures of optimal codon usage in metabolic genes inform budding yeast ecology. *PLoS Biol* **19**(4): e3001185.

Lagopodi AL, Ram AF, Lamers GE, Punt PJ, Van den Hondel CA, Lugtenberg BJ, Bloemberg GV. 2002. Novel aspects of tomato root colonization and infection by *Fusarium oxysporum* f. sp. *radicis-lycopersici* revealed by confocal laser scanning microscopic analysis using the green fluorescent protein as a marker. *Mol Plant Microbe Interact* **15**(2): 172-179.

Langley LD. 2002. *The banana wars : United States intervention in the Caribbean, 1898-1934*. Wilmington, Del.: SR Books.

Langley LD, Schoonover TD. 1995. *The banana men : American mercenaries and entrepreneurs in Central America, 1880-1930*. Lexington, Ky.: University Press of Kentucky.

Langner T, Harant A, Gomez-Luciano LB, Shrestha RK, Malmgren A, Latorre SM, Burbano HA, Win J, Kamoun S. 2021. Genomic rearrangements generate hypervariable mini-chromosomes in host-specific isolates of the blast fungus. *PLoS Genet* **17**(2): e1009386.

Larmarange J 2025. ggstats: Extension to 'ggplot2' for Plotting Stats.

Larrimore KE, Barattin-Voynova NS, Reid DW, Ng DTW. 2020. Aneuploidy-induced proteotoxic stress can be effectively tolerated without dosage compensation, genetic mutations, or stress responses. *BMC Biol* **18**(1): 117.

Latorre SM, Were VM, Foster AJ, Langner T, Malmgren A, Harant A, Asuke S, Reyes-Avila S, Gupta DR, Jensen C, et al. 2023. Genomic surveillance uncovers a pandemic clonal lineage of the wheat blast fungus. *PLoS Biol* **21**(4): e3002052.

Laurence MH, Summerell BA, Burgess LW, Liew EC. 2014. Genealogical concordance phylogenetic species recognition in the *Fusarium oxysporum* species complex. *Fungal Biol* **118**(4): 374-384.

Leclair S, Ansan-Melayah D, Rouxel T, Balesdent M. 1996. Meiotic behaviour of the minichromosome in the phytopathogenic ascomycete *Leptosphaeria maculans*. *Curr Genet* **30**(6): 541-548.

Lee E, Helt GA, Reese JT, Munoz-Torres MC, Childers CP, Buels RM, Stein L, Holmes IH, Elsik CG, Lewis SE. 2013. Web Apollo: a web-based genomic annotation editing platform. *Genome Biol* **14**(8): R93.

Li C, Chen L, Pan G, Zhang W, Li SC. 2023. Deciphering complex breakage-fusion-bridge genome rearrangements with Ambigram. *Nat Commun* **14**(1): 5528.

Li C, Chen S, Zuo C, Sun Q, Ye Q, Yi G, Huang B. 2011. The use of GFP-transformed isolates to study infection of banana with *Fusarium oxysporum* f. sp. *cubense* race 4. *European Journal of Plant Pathology* **131**(2): 327-340.

Li C, Yang J, Li W, Sun J, Peng M. 2017. Direct Root Penetration and Rhizome Vascular Colonization by *Fusarium oxysporum* f. sp. *cubense* are the Key Steps in the Successful Infection of Brazil Cavendish. *Plant Dis* **101**(12): 2073-2078.

Li C, Zuo C, Deng G, Kuang R, Yang Q, Hu C, Sheng O, Zhang S, Ma L, Wei Y, et al. 2013. Contamination of bananas with beauvericin and fusaric acid produced by *Fusarium oxysporum* f. sp. *cubense*. *PLoS One* **8**(7): e70226.

Li H, Durbin R. 2009. Fast and accurate short read alignment with Burrows-Wheeler transform. *Bioinformatics* **25**(14): 1754-1760.

Li J, Faino L, Fiorin GL, Bashyal S, Schaveling A, van den Berg GCM, Seidl MF, Thomma BPHJ. 2022. A single *Verticillium dahliae* effector determines pathogenicity on tomato by targeting auxin response factors. *bioRxiv*: 2022.2011.2022.517554.

Li J, Fokkens L, Conneely LJ, Rep M. 2020a. Partial pathogenicity chromosomes in *Fusarium oxysporum* are sufficient to cause disease and can be horizontally transferred. *Environ Microbiol* **22**(12): 4985-5004.

Li J, Fokkens L, van Dam P, Rep M. 2020b. Related mobile pathogenicity chromosomes in *Fusarium oxysporum* determine host range on cucurbits. *Mol Plant Pathol* **21**(6): 761-776.

Li WM, Dita M, Wu W, Hu GB, Xie JH, Ge XJ. 2015. Resistance sources to *Fusarium oxysporum* f. sp. *cubense* tropical race 4 in banana wild relatives. *Plant Pathology* **64**(5): 1061-1067.

Li X, Yu S, Cheng Z, Chang X, Yun Y, Jiang M, Chen X, Wen X, Li H, Zhu W, et al. 2024. Origin and evolution of the triploid cultivated banana genome. *Nat Genet* **56**(1): 136-142.

Li Y, Dooner HK. 2009. Excision of Helitron transposons in maize. *Genetics* **182**(1): 399-402.

Li Z, Gilbert C, Peng H, Pollet N. 2024. Discovery of numerous novel Helitron-like elements in eukaryote genomes using HELIANO. *Nucleic Acids Res* **52**(17): e79.

Lindenbaum P. 2015. JVarkit: java-based utilities for Bioinformatics.

Liu S, Li J, Zhang Y, Liu N, Viljoen A, Mostert D, Zuo C, Hu C, Bi F, Gao H, et al. 2020. Fusaric acid instigates the invasion of banana by *Fusarium oxysporum* f. sp. *cubense* TR4. *New Phytol* **225**(2): 913-929.

Liu S, Lin G, Ramachandran SR, Daza LC, Cruppe G, Tembo B, Singh PK, Cook D, Pedley KF, Valent B. 2024. Rapid mini-chromosome divergence among fungal isolates causing wheat blast outbreaks in Bangladesh and Zambia. *New Phytol* **241**(3): 1266-1276.

Lo Presti L, Lanver D, Schweizer G, Tanaka S, Liang L, Tollot M, Zuccaro A, Reissmann S, Kahmann R. 2015. Fungal effectors and plant susceptibility. *Annu Rev Plant Biol* **66**: 513-545.

Lommen A. 2009. MetAlign: interface-driven, versatile metabolomics tool for hyphenated full-scan mass spectrometry data preprocessing. *Anal Chem* **81**(8): 3079-3086.

López-Díaz C, Rahjoo V, Sulyok M, Ghionna V, Martin-Vicente A, Capilla J, Di Pietro A, Lopez-Berges MS. 2018. Fusaric acid contributes to virulence of *Fusarium oxysporum* on plant and mammalian hosts. *Mol Plant Pathol* **19**(2): 440-453.

Lovelace AH, Dorhmi S, Hulin MT, Li Y, Mansfield JW, Ma W. 2023. Effector Identification in Plant Pathogens. *Phytopathology* **113**(4): 637-650.

Ma L, Houterman PM, Gawehns F, Cao L, Sillo F, Richter H, Clavijo-Ortiz MJ, Schmidt SM, Boeren S, Vervoort J, et al. 2015. The *AVR2-SIX5* gene pair is required to activate *I-2*-mediated immunity in tomato. *New Phytol* **208**(2): 507-518.

Ma LJ. 2014. Horizontal chromosome transfer and rational strategies to manage Fusarium vascular wilt diseases. *Mol Plant Pathol* **15**(8): 763-766.

Ma LJ, Geiser DM, Proctor RH, Rooney AP, O'Donnell K, Trail F, Gardiner DM, Manners JM, Kazan K. 2013. *Fusarium* pathogenomics. *Annu Rev Microbiol* **67**: 399-416.

Ma LJ, van der Does HC, Borkovich KA, Coleman JJ, Daboussi MJ, Di Pietro A, Dufresne M, Freitag M, Grabherr M, Henrissat B, et al. 2010. Comparative genomics reveals mobile pathogenicity chromosomes in *Fusarium*. *Nature* **464**(7287): 367-373.

Mapuranga J, Zhang N, Zhang L, Chang J, Yang W. 2022. Infection Strategies and Pathogenicity of Biotrophic Plant Fungal Pathogens. *Front Microbiol* **13**: 799396.

Marçais G, Delcher AL, Phillippy AM, Coston R, Salzberg SL, Zimin A. 2018. MUMmer4: A fast and versatile genome alignment system. *PLoS Comput Biol* **14**(1): e1005944.

Marquardt S. 2001. "Green Havoc": Panama Disease, Environmental Change, and Labor Process in the Central American Banana Industry. *The American Historical Review* **106**(1).

Marquardt S. 2002. Pesticides, Parakeets, and Unions in the Costa Rican Banana Industry, 1938-1962. *Latin American Research Review* **37**(2): 3-36.

Marshall B, Newton AC, Zhan J. 2009. Quantitative evolution of aggressiveness of powdery mildew under two-cultivar barley mixtures. *Plant Pathology* **58**(2): 378-388.

Martin G, Istace B, Baurens FC, Belser C, Hervouet C, Labadie K, Cruaud C, Noel B, Guiougou C, Salmon F, et al. 2025. Unravelling genomic drivers of speciation in *Musa* through genome assemblies of wild banana ancestors. *Nat Commun* **16**(1): 961.

Martínez-de la Parte E, Perez-Vicente L, Torres DE, van Westerhoven A, Meijer HJG, Seidl MF, Kema GHJ. 2024. Genetic diversity of the banana Fusarium wilt pathogen in Cuba and across Latin America and the Caribbean. *Environ Microbiol* **26**(5): e16636.

Martínez-Soto D, Yu H, Allen KS, Ma LJ. 2023. Differential Colonization of the Plant Vasculature Between Endophytic Versus Pathogenic *Fusarium oxysporum* Strains. *Mol Plant Microbe Interact* **36**(1): 4-13.

Maryani N, Lombard L, Poerba YS, Subandiyah S, Crous PW, Kema GHJ. 2019. Phylogeny and genetic diversity of the banana Fusarium wilt pathogen *Fusarium oxysporum* f. sp. *cubense* in the Indonesian centre of origin. *Stud Mycol* **92**: 155-194.

Masel AM. 1996. Molecular Evidence for Chromosome Transfer Between Biotypes of *Colletotrichum gloeosporioides*. *Molecular Plant-Microbe Interactions* **9**(5).

Masunaka A, Ohtani K, Peever TL, Timmer LW, Tsuge T, Yamamoto M, Yamamoto H, Akimitsu K. 2005. An Isolate of *Alternaria alternata* That Is Pathogenic to Both Tangerines and Rough Lemon and Produces Two Host-Selective Toxins, ACT- and ACR-Toxins. *Phytopathology* **95**(3): 241-247.

McDonald BA, Linde C. 2002. Pathogen population genetics, evolutionary potential, and durable resistance. *Annu Rev Phytopathol* **40**: 349-379.

McDonald MC, Renkin M, Spackman M, Orchard B, Croll D, Solomon PS, Milgate A. 2019. Rapid Parallel Evolution of Azole Fungicide Resistance in Australian Populations of the Wheat Pathogen *Zymoseptoria tritici*. *Appl Environ Microbiol* **85**(4).

McTaggart AR, James TY, Shivas RG, Drenth A, Wingfield BD, Summerell BA, Duong TA. 2021. Population genomics reveals historical and ongoing recombination in the *Fusarium oxysporum* species complex. *Stud Mycol* **99**: 100132.

Mehrabi R, Mirzadi Gohari A, Kema GHJ. 2017. Karyotype Variability in Plant-Pathogenic Fungi. *Annu Rev Phytopathol* **55**: 483-503.

Mejías Herrera R, Hernández Y, Magdama F, Mostert D, Bothma S, Paredes Salgado EM, Teran D, González E, Angulo R, Angel L, et al. 2023. First report of Fusarium wilt of Cavendish bananas caused by *Fusarium oxysporum* f. sp. *cubense* Tropical Race 4 in Venezuela. *Plant Dis*.

Meng EC, Goddard TD, Pettersen EF, Couch GS, Pearson ZJ, Morris JH, Ferrin TE. 2023. UCSF ChimeraX: Tools for structure building and analysis. *Protein Sci* **32**(11): e4792.

Meng T, Jiao H, Zhang Y, Zhou Y, Chen S, Wang X, Yang B, Sun J, Geng X, Ayhan DH, et al. 2024. FoPGDB: a pangenome database of *Fusarium oxysporum*, a cross-kingdom fungal pathogen. *Database (Oxford)* **2024**.

Merril TL, ed. 1995. *Honduras, a country study*. Area handbook series: Library of Congress.

Mesarich CH, Griffiths SA, van der Burgt A, Okmen B, Beenen HG, Etalo DW, Joosten MH, de Wit PJ. 2014. Transcriptome sequencing uncovers the *Avr5* avirulence gene of the tomato leaf mold pathogen *Cladosporium fulvum*. *Mol Plant Microbe Interact* **27**(8): 846-857.

Mesny F, Thomma BPHJ. 2024. AMAPEC: accurate antimicrobial activity prediction for fungal effector proteins. *bioRxiv*: 2024.2001.2004.574150.

Miao VP, Matthews DE, VanEtten HD. 1991. Identification and chromosomal locations of a family of cytochrome P-450 genes for pisatin detoxification in the fungus *Nectria haematococca*. *Mol Gen Genet* **226**(1-2): 214-223.

Michielse CB, Rep M. 2009. Pathogen profile update: *Fusarium oxysporum*. *Mol Plant Pathol* **10**(3): 311-324.

Misas Villamil JC, Mueller AN, Demir F, Meyer U, Okmen B, Schulze Huynck J, Breuer M, Dauben H, Win J, Huesgen PF, et al. 2019. A fungal substrate mimicking molecule suppresses plant immunity via an inter-kingdom conserved motif. *Nat Commun* **10**(1): 1576.

Möller M, Habig M, Freitag M, Stukenbrock EH. 2018. Extraordinary Genome Instability and Widespread Chromosome Rearrangements During Vegetative Growth. *Genetics* **210**(2): 517-529.

Möller M, Stukenbrock EH. 2017. Evolution and genome architecture in fungal plant pathogens. *Nat Rev Microbiol* **15**(12): 756-771.

Morgan W, Kamoun S. 2007. RXLR effectors of plant pathogenic oomycetes. *Curr Opin Microbiol* **10**(4): 332-338.

Naranjo-Ortiz MA, Gabaldón T. 2019. Fungal evolution: diversity, taxonomy and phylogeny of the Fungi. *Biol Rev Camb Philos Soc* **94**(6): 2101-2137.

Navasca A, Singh J, Rivera-Varas V, Gill U, Secor G, Baldwin T. 2024. Dispensable genome and segmental duplications drive the genome plasticity in *Fusarium solani*. *bioRxiv*: 2024.2006.2005.597655.

Neruda P. 1966. The United Fruit Co. *Monthly Review* **18**(4).

Niehaus EM, von Bargen KW, Espino JJ, Pfannmuller A, Humpf HU, Tudzynski B. 2014. Characterization of the fusaric acid gene cluster in *Fusarium fujikuroi*. *Appl Microbiol Biotechnol* **98**(4): 1749-1762.

Niño-Sánchez J, Casado-Del Castillo V, Tello V, De Vega-Bartol JJ, Ramos B, Sukno SA, Diaz Minguez JM. 2016. The *FTF* gene family regulates virulence and expression of SIX effectors in *Fusarium oxysporum*. *Mol Plant Pathol* **17**(7): 1124-1139.

Notz R, Maurhofer M, Dubach H, Haas D, Defago G. 2002. Fusaric acid-producing strains of *Fusarium oxysporum* alter 2,4-diacetylphloroglucinol biosynthetic gene expression in *Pseudomonas fluorescens* CHA0 in vitro and in the rhizosphere of wheat. *Appl Environ Microbiol* **68**(5): 2229-2235.

Nyine M, Uwimana B, Swennen R, Batte M, Brown A, Christelová P, Hřibová E, Lorenzen J, Doležel J. 2017. Trait variation and genetic diversity in a banana genomic selection training population. *PLoS One* **12**(6): e0178734.

O'Donnell K, Kistler HC, Cigelnik E, Ploetz RC. 1998. Multiple evolutionary origins of the fungus causing Panama disease of banana: concordant evidence from nuclear and mitochondrial gene genealogies. *Proc Natl Acad Sci U S A* **95**(5): 2044-2049.

O'Donnell K, Whitaker BK, Laraba I, Proctor RH, Brown DW, Broders K, Kim HS, McCormick SP, Busman M, Aoki T, et al. 2022. DNA Sequence-Based Identification of *Fusarium*: A Work in Progress. *Plant Dis* **106**(6): 1597-1609.

O'Donnell S, Fischer G. 2020. MUM&Co: accurate detection of all SV types through whole-genome alignment. *Bioinformatics* **36**(10): 3242-3243.

Oggenfuss U, Badet T, Croll D. 2024. A systematic screen for co-option of transposable elements across the fungal kingdom. *Mob DNA* **15**(1): 2.

Oggenfuss U, Badet T, Wicker T, Hartmann FE, Singh NK, Abraham L, Karisto P, Vonlanthen T, Mundt C, McDonald BA, et al. 2021. A population-level invasion by transposable elements triggers genome expansion in a fungal pathogen. *Elife* **10**.

Ohara T, Inoue I, Namiki F, Kunoh H, Tsuge T. 2004. REN1 is required for development of microconidia and macroconidia, but not of chlamydospores, in the plant pathogenic fungus *Fusarium oxysporum*. *Genetics* **166**(1): 113-124.

Oide S, Berthiller F, Wiesenberger G, Adam G, Turgeon BG. 2014. Individual and combined roles of malonichrome, ferricrocin, and TAFC siderophores in *Fusarium graminearum* pathogenic and sexual development. *Front Microbiol* **5**: 759.

Olarte RA, Menke J, Zhang Y, Sullivan S, Slot JC, Huang Y, Badalamenti JP, Quandt AC, Spatafora JW, Bushley KE. 2019. Chromosome rearrangements shape the diversification of secondary metabolism in the cyclosporin producing fungus *Tolypocladium inflatum*. *BMC Genomics* **20**(1): 120.

Olivain C, Humbert C, Nahalkova J, Fatehi J, L'Haridon F, Alabouvette C. 2006. Colonization of tomato root by pathogenic and nonpathogenic *Fusarium oxysporum* strains inoculated together and separately into the soil. *Appl Environ Microbiol* **72**(2): 1523-1531.

Orbach MJ. 1996. Electrophoretic Karyotypes of *Magnaporthe grisea* Pathogens of Diverse Grasses. *Molecular Plant-Microbe Interactions* **9**(4).

Ordóñez N, Seidl MF, Waalwijk C, Drenth A, Kilian A, Thomma BP, Ploetz RC, Kema GH. 2015. Worse Comes to Worst: Bananas and Panama Disease--When Plant and Pathogen Clones Meet. *PLoS Pathog* **11**(11): e1005197.

Ortiz R, Ferris R, Vuylsteke D 1995. Banana and plantain breeding. *Bananas and plantains*: Springer, 110-146.

Ortiz R, Swennen R. 2014. From crossbreeding to biotechnology-facilitated improvement of banana and plantain. *Biotechnol Adv* **32**(1): 158-169.

Palmer JM, Stajich J 2020. Funannotate v1.8.1: Eukaryotic genome annotation (v1.8.1): Zenodo.

Park CH, Shirsekar G, Bellizzi M, Chen S, Songkumarn P, Xie X, Shi X, Ning Y, Zhou B, Suttiviriya P, et al. 2016. The E3 Ligase APIP10 Connects the Effector AvrPiz-t to the NLR Receptor Piz-t in Rice. *PLoS Pathog* **12**(3): e1005529.

Patkar RN, Benke PI, Qu Z, Chen YY, Yang F, Swarup S, Naqvi NI. 2015. A fungal monooxygenase-derived jasmonate attenuates host innate immunity. *Nat Chem Biol* **11**(9): 733-740.

Paul JY, Becker DK, Dickman MB, Harding RM, Khanna HK, Dale JL. 2011. Apoptosis-related genes confer resistance to Fusarium wilt in transgenic 'Lady Finger' bananas. *Plant Biotechnol J* **9**(9): 1141-1148.

Peck LD, Llewellyn T, Bennetot B, O'Donnell S, Nowell RW, Ryan MJ, Flood J, Rodriguez de la Vega RC, Ropars J, Giraud T, et al. 2024. Horizontal transfers between fungal *Fusarium* species contributed to successive outbreaks of coffee wilt disease. *PLoS Biol* **22**(12): e3002480.

Peraza-Echeverria S, Dale JL, Harding RM, Collet C. 2008a. Molecular cloning and in silico analysis of potential *Fusarium* resistance genes in banana. *Molecular Breeding* **23**(3): 431-443.

Peraza-Echeverria S, Dale JL, Harding RM, Smith MK, Collet C. 2008b. Characterization of disease resistance gene candidates of the nucleotide binding site (NBS) type from banana and correlation of a transcriptional polymorphism with resistance to *Fusarium oxysporum* f.sp. *cubense* race 4. *Molecular Breeding* **22**(4): 565-579.

Perrier X, De Langhe E, Donohue M, Lentfer C, Vrydaghs L, Bakry F, Carreel F, Hippolyte I, Horry JP, Jenny C, et al. 2011. Multidisciplinary perspectives on banana (*Musa* spp.) domestication. *Proc Natl Acad Sci U S A* **108**(28): 11311-11318.

Peters Haugrud AR, Zhang Z, Richards JK, Friesen TL, Faris JD. 2019. Genetics of Variable Disease Expression Conferred by Inverse Gene-For-Gene Interactions in the Wheat-*Parastagonospora nodorum* Pathosystem. *Plant Physiol* **180**(1): 420-434.

Phasha MM, Wingfield BD, Wingfield MJ, Coetzee MPA, Hammerbacher A, Steenkamp ET. 2021. Deciphering the effect of FUB1 disruption on fusaric acid production and pathogenicity in *Fusarium circinatum*. *Fungal Biol* **125**(12): 1036-1047.

Pillay M, Tripathi L 2007. Banana. *Fruits and nuts*: Springer, 281-301.

Pimentel H, Bray NL, Puente S, Melsted P, Pachter L. 2017. Differential analysis of RNA-seq incorporating quantification uncertainty. *Nat Methods* **14**(7): 687-690.

Pingali PL. 2012. Green Revolution: Impacts, limits, and the path ahead. *Proceedings of the National Academy of Sciences* **109**(31): 12302-12308.

Pires AS, Azinheira HG, Cabral A, Tavares S, Tavares D, Castro M, Várzea V, Silva MC, Abranches R, Loureiro J, et al. 2015. Cytogenomic characterization of *Colletotrichum kahawae*, the causal agent of coffee berry disease, reveals diversity in minichromosome profiles and genome size expansion. *Plant Pathology* **65**(6): 968-977.

Plaumann PL, Schmidpeter J, Dahl M, Taher L, Koch C. 2018. A Dispensable Chromosome Is Required for Virulence in the Hemibiotrophic Plant Pathogen *Colletotrichum higginsianum*. *Front Microbiol* **9**: 1005.

Plett JM, Plett KL, Wong-Bajracharya J, de Freitas Pereira M, Costa MD, Kohler A, Martin F, Anderson IC. 2020. Mycorrhizal effector PaMiSSP10b alters polyamine biosynthesis in *Eucalyptus* root cells and promotes root colonization. *New Phytol* **228**(2): 712-727.

Pliego C, Nowara D, Bonciani G, Gheorghe DM, Xu R, Surana P, Whigham E, Nettleton D, Bogdanove AJ, Wise RP, et al. 2013. Host-induced gene silencing in barley powdery mildew reveals a class of ribonuclease-like effectors. *Mol Plant Microbe Interact* **26**(6): 633-642.

Ploetz RC. 2009. Assessing Threats Posed by Destructive Banana Pathogens. *Acta Horticulturae*(828): 245-252.

Ploetz RC. 2015. Fusarium Wilt of Banana. *Phytopathology* **105**(12): 1512-1521.

Ploetz RC. 2015. Management of Fusarium wilt of banana: A review with special reference to tropical race 4. *Crop Protection* **73**: 7-15.

Ploetz RC, Kema GHJ, Ma L-J. 2015. Impact of Diseases on Export and Smallholder Production of Banana. *Annual Review of Phytopathology* **53**(1): 269-288.

Powell WA, Kistler HC. 1990. In vivo rearrangement of foreign DNA by *Fusarium oxysporum* produces linear self-replicating plasmids. *J Bacteriol* **172**(6): 3163-3171.

Puhalla JE. 1985. Classification of strains of *Fusarium oxysporum* on the basis of vegetative compatibility. *Canadian Journal of Botany* **63**(2): 179-183.

Pusztahelyi T, Holb IJ, Pocsi I. 2015. Secondary metabolites in fungus-plant interactions. *Front Plant Sci* **6**: 573.

Quigley S, Damas J, Larkin DM, Farre M. 2023. syntenyPlotteR: a user-friendly R package to visualize genome synteny, ideal for both experienced and novice bioinformaticians. *Bioinform Adv* **3**(1): vbad161.

Rajaram S. 2011. Norman Borlaug: the man I worked with and knew. *Annu Rev Phytopathol* **49**: 17-30.

Redecker D, Kodner R, Graham LE. 2000. Glomalean fungi from the Ordovician. *Science* **289**(5486): 1920-1921.

Redkar A, Sabale M, Schudoma C, Zechmann B, Gupta YK, López-Berges MS, Venturini G, Gimenez-Ibanez S, Turrà D, Solano R, et al. 2022. Conserved secreted effectors contribute to endophytic growth and multihost plant compatibility in a vascular wilt fungus. *Plant Cell* **34**(9): 3214-3232.

Robert X, Gouet P. 2014. Deciphering key features in protein structures with the new ENDscript server. *Nucleic Acids Res* **42**(Web Server issue): W320-324.

Rocafort M, Bowen JK, Hassing B, Cox MP, McGreal B, de la Rosa S, Plummer KM, Bradshaw RE, Mesarich CH. 2022. The *Venturia inaequalis* effector repertoire is dominated by expanded families with predicted structural similarity, but unrelated sequence, to avirulence proteins from other plant-pathogenic fungi. *BMC Biol* **20**(1): 246.

Rocafort M, Fudal I, Mesarich CH. 2020. Apoplastic effector proteins of plant-associated fungi and oomycetes. *Curr Opin Plant Biol* **56**: 9-19.

Rodriguez-Carres M, White G, Tsuchiya D, Taga M, VanEtten HD. 2008. The supernumerary chromosome of *Nectria haematococca* that carries pea-pathogenicity-related genes also carries a trait for pea rhizosphere competitiveness. *Appl Environ Microbiol* **74**(12): 3849-3856.

Rouard M, Droc G, Martin G, Sardos J, Hueber Y, Guignon V, Cenci A, Geigle B, Hibbins MS, Yahiaoui N, et al. 2018. Three New Genome Assemblies Support a Rapid Radiation in *Musa acuminata* (Wild Banana). *Genome Biol Evol* **10**(12): 3129-3140.

Rouxel T, Grandaubert J, Hane JK, Hoede C, van de Wouw AP, Couloux A, Dominguez V, Anthouard V, Bally P, Bourras S, et al. 2011. Effector diversification within compartments of the *Leptosphaeria maculans* genome affected by Repeat-Induced Point mutations. *Nat Commun* **2**: 202.

Ruiz JA, Bernar EM, Jung K. 2015. Production of siderophores increases resistance to fusaric acid in *Pseudomonas protegens* Pf-5. *PLoS One* **10**(1): e0117040.

Sakane K, Akiyama M, Jogaiah S, Ito SI, Sasaki K. 2024. Pathogenicity chromosome of *Fusarium oxysporum* f. sp. *cepae*. *Fungal Genet Biol* **170**: 103860.

Sambrook J, Fritsch, EF., Maniatis, T. 1989. *Molecular Cloning: A Laboratory Manual (2nd ed.)*. Cold Spring Harbor: Cold Spring Harbor Laboratory Press.

Sánchez-Vallet A, Fouche S, Fudal I, Hartmann FE, Soyer JL, Tellier A, Croll D. 2018. The Genome Biology of Effector Gene Evolution in Filamentous Plant Pathogens. *Annu Rev Phytopathol* **56**: 21-40.

Sanchez MR, Miller AW, Liachko I, Sunshine AB, Lynch B, Huang M, Alcantara E, DeSevo CG, Pai DA, Tucker CM, et al. 2017. Differential paralog divergence modulates genome evolution across yeast species. *PLoS Genet* **13**(2): e1006585.

Savary S, Willocquet L, Pethybridge SJ, Esker P, McRoberts N, Nelson A. 2019. The global burden of pathogens and pests on major food crops. *Nat Ecol Evol* **3**(3): 430-439.

Schebesta H, Bernaz N, Macchi C. 2020. The European union farm to fork strategy. *European food and feed law review* **15**(5): 420-427.

Schmid R, Heuckeroth S, Korf A, Smirnov A, Myers O, Dyrlund TS, Bushuiev R, Murray KJ, Hoffmann N, Lu M, et al. 2023. Integrative analysis of multimodal mass spectrometry data in MZmine 3. *Nat Biotechnol* **41**(4): 447-449.

Schmidt SM, Houterman PM, Schreiver I, Ma L, Amyotte S, Chellappan B, Boeren S, Takken FL, Rep M. 2013. MITEs in the promoters of effector genes allow prediction of novel virulence genes in *Fusarium oxysporum*. *BMC Genomics* **14**: 119.

Schotanus K, Soyer JL, Connolly LR, Grandaubert J, Happel P, Smith KM, Freitag M, Stukenbrock EH. 2015. Histone modifications rather than the novel regional centromeres of *Zymoseptoria tritici* distinguish core and accessory chromosomes. *Epigenetics Chromatin* **8**: 41.

Schouten A, van den Berg G, Edel-Hermann V, Steinberg C, Gautheron N, Alabouvette C, de Vos CH, Lemanceau P, Raaijmakers JM. 2004. Defense responses of *Fusarium oxysporum* to 2,4-diacetylphloroglucinol, a broad-spectrum antibiotic produced by *Pseudomonas fluorescens*. *Mol Plant Microbe Interact* **17**(11): 1201-1211.

Seidl MF, Thomma B. 2017. Transposable Elements Direct The Coevolution between Plants and Microbes. *Trends Genet* **33**(11): 842-851.

Seidl MF, Thomma BP. 2014. Sex or no sex: evolutionary adaptation occurs regardless. *Bioessays* **36**(4): 335-345.

Seong K, Krasileva KV. 2021. Computational Structural Genomics Unravels Common Folds and Novel Families in the Secretome of Fungal Phytopathogen *Magnaporthe oryzae*. *Mol Plant Microbe Interact* **34**(11): 1267-1280.

Seong K, Krasileva KV. 2023. Prediction of effector protein structures from fungal phytopathogens enables evolutionary analyses. *Nat Microbiol* **8**(1): 174-187.

Sheltzer JM, Blank HM, Pfau SJ, Tange Y, George BM, Humpton TJ, Brito IL, Hiraoka Y, Niwa O, Amon A. 2011. Aneuploidy drives genomic instability in yeast. *Science* **333**(6045): 1026-1030.

Sheltzer JM, Torres EM, Dunham MJ, Amon A. 2012. Transcriptional consequences of aneuploidy. *Proc Natl Acad Sci U S A* **109**(31): 12644-12649.

Shi G, Zhang Z, Friesen TL, Raats D, Fahima T, Brueggeman RS, Lu S, Trick HN, Liu Z, Chao W, et al. 2016. The hijacking of a receptor kinase-driven pathway by a wheat fungal pathogen leads to disease. *Sci Adv* **2**(10): e1600822.

Shinkado S, Saito H, Yamazaki M, Kotera S, Arazoe T, Arie T, Kamakura T. 2022. Genome editing using a versatile vector-based CRISPR/Cas9 system in *Fusarium* species. *Sci Rep* **12**(1): 16243.

Sievers F, Wilm A, Dineen D, Gibson TJ, Karplus K, Li W, Lopez R, McWilliam H, Remmert M, Söding J, et al. 2011. Fast, scalable generation of high-quality protein multiple sequence alignments using Clustal Omega. *Mol Syst Biol* **7**: 539.

Singh RP, Hodson DP, Huerta-Espino J, Jin Y, Bhavani S, Njau P, Herrera-Foessel S, Singh PK, Singh S, Govindan V. 2011. The emergence of Ug99 races of the stem rust fungus is a threat to world wheat production. *Annu Rev Phytopathol* **49**: 465-481.

Smillie C, Garcillan-Barcia MP, Francia MV, Rocha EP, de la Cruz F. 2010. Mobility of plasmids. *Microbiol Mol Biol Rev* **74**(3): 434-452.

Snelders NC, Boshoven JC, Song Y, Schmitz N, Fiorin GL, Rovenich H, van den Berg GCM, Torres DE, Petti GC, Prockl Z, et al. 2023. A highly polymorphic effector protein promotes fungal virulence through suppression of plant-associated Actinobacteria. *New Phytol* **237**(3): 944-958.

Snelders NC, Petti GC, van den Berg GCM, Seidl MF, Thomma B. 2021. An ancient antimicrobial protein co-opted by a fungal plant pathogen for in planta mycobiome manipulation. *Proc Natl Acad Sci U S A* **118**(49).

Snelders NC, Rovenich H, Petti GC, Rocafort M, van den Berg GCM, Vorholt JA, Mesters JR, Seidl MF, Nijland R, Thomma B. 2020. Microbiome manipulation by a soil-borne fungal plant pathogen using effector proteins. *Nat Plants* **6**(11): 1365-1374.

Snelders NC, Rovenich H, Thomma B. 2022. Microbiota manipulation through the secretion of effector proteins is fundamental to the wealth of lifestyles in the fungal kingdom. *FEMS Microbiol Rev* **46**(5).

Sommerhalder RJ, McDonald BA, Mascher F, Zhan J. 2011. Effect of hosts on competition among clones and evidence of differential selection between pathogenic and saprophytic phases in experimental populations of the wheat pathogen *Phaeosphaeria nodorum*. *BMC Evol Biol* **11**: 188.

Son SW, Kim HY, Choi GJ, Lim HK, Jang KS, Lee SO, Lee S, Sung ND, Kim JC. 2008. Bikaverin and fusaric acid from *Fusarium oxysporum* show antioomycete activity against *Phytophthora infestans*. *J Appl Microbiol* **104**(3): 692-698.

Sperschneider J, Dodds PN. 2022. EffectorP 3.0: Prediction of Apoplastic and Cytoplasmic Effectors in Fungi and Oomycetes. *Mol Plant Microbe Interact* **35**(2): 146-156.

Spraker JE, Wiemann P, Baccile JA, Venkatesh N, Schumacher J, Schroeder FC, Sanchez LM, Keller NP. 2018. Conserved Responses in a War of Small Molecules between a Plant-Pathogenic Bacterium and Fungi. *mBio* **9**(3).

Srivastava V, Patra K, Pai H, Aguilar-Pontes MV, Berasategui A, Kamble A, Di Pietro A, Redkar A. 2024. Molecular Dialogue During Host Manipulation by the Vascular Wilt Fungus *Fusarium oxysporum*. *Annu Rev Phytopathol*.

Stam R, Munsterkotter M, Pophaly SD, Fokkens L, Sghyer H, Guldener U, Huckelhoven R, Hess M. 2018. A New Reference Genome Shows the One-Speed Genome Structure of the Barley Pathogen *Ramularia collo-cygni*. *Genome Biol Evol* **10**(12): 3243-3249.

Steenwyk JL, Buida TJ, Goncalves C, Goltz DC, Morales G, Mead ME, LaBella AL, Chavez CM, Schmitz JE, Hadjifrangiskou M, et al. 2022. BioKIT: a versatile toolkit for processing and analyzing diverse types of sequence data. *Genetics* **221**(3).

Stergiopoulos I, de Wit PJ. 2009. Fungal effector proteins. *Annu Rev Phytopathol* **47**: 233-263.

Stewart RB, Robertson W. 1968. Fungus Spores from Prehistoric Potsherds. *Mycologia* **60**(3): 701-704.

Strange RN, Scott PR. 2005. Plant disease: a threat to global food security. *Annu Rev Phytopathol* **43**: 83-116.

Studt L, Janevska S, Niehaus EM, Burkhardt I, Arndt B, Sieber CM, Humpf HU, Dickschat JS, Tudzynski B. 2016. Two separate key enzymes and two pathway-specific transcription factors are involved in fusaric acid biosynthesis in *Fusarium fujikuroi*. *Environ Microbiol* **18**(3): 936-956.

Stukenbrock EH, McDonald BA. 2008. The origins of plant pathogens in agro-ecosystems. *Annu Rev Phytopathol* **46**: 75-100.

Su H-j, Hwang S, Ko W. 1986. Fusarial wilt of Cavendish bananas in Taiwan. *Plant Dis* **70**(9): 814-818.

Summerell BA, Laurence MH, Liew ECY, Leslie JF. 2010. Biogeography and phylogeography of *Fusarium*: a review. *Fungal Diversity* **44**(1): 3-13.

Talbi N, Blekemolen MC, Janevska S, Zendler D, van Tilbeurgh H, Fudal I, Takken FLW. 2024. Facilitation of Symplastic Effector Protein Mobility by Paired Effectors Is Conserved in Different Classes of Fungal Pathogens. *Mol Plant Microbe Interact* **37**(3): 304-314.

Talbi N, Fokkens L, Audran C, Petit-Houdenot Y, Pouzet C, Blaise F, Gay EJ, Rouxel T, Balesdent MH, Rep M, et al. 2023. The neighbouring genes *AvrLm10A* and *AvrLm10B* are part of a large multigene family of cooperating effector genes conserved in Dothideomycetes and Sordariomycetes. *Mol Plant Pathol* **24**(8): 914-931.

Tao J, Ginsberg I, Banerjee N, Held W, Koltin Y, Bruenn JA. 1990. *Ustilago maydis* KP6 killer toxin: structure, expression in *Saccharomyces cerevisiae*, and relationship to other cellular toxins. *Mol Cell Biol* **10**(4): 1373-1381.

Tenkouano A, Swennen R. 2004. Plantains and banana: progress in breeding and delivering improved plantain and banana to African farmers *Chronica Horticulturae* **44 (1)**: 9-15.

Teufel F, Almagro Armenteros JJ, Johansen AR, Gislason MH, Pihl SI, Tsirigos KD, Winther O, Brunak S, von Heijne G, Nielsen H. 2022. SignalP 6.0 predicts all five types of signal peptides using protein language models. *Nat Biotechnol* **40**(7): 1023-1025.

Teulet A, Quan C, Evangelisti E, Wanke A, Yang W, Schornack S. 2023. A pathogen effector FOLD diversified in symbiotic fungi. *New Phytol* **239**(3): 1127-1139.

Thomas J, Pritham EJ. 2015. Helitrons, the Eukaryotic Rolling-circle Transposable Elements. *Microbiol Spectr* **3**(4).

Tikunov YM, Laptenok S, Hall RD, Bovy A, de Vos RC. 2012. MSClust: a tool for unsupervised mass spectra extraction of chromatography-mass spectrometry ion-wise aligned data. *Metabolomics* **8**(4): 714-718.

Torres Bedoya E, Bebber DP, Studholme DJ. 2021. Taxonomic Revision of the Banana Fusarium Wilt TR4 Pathogen Is Premature. *Phytopathology* **111**(12): 2141-2145.

Torres DE, Oggenfuss U, Croll D, Seidl MF. 2020. Genome evolution in fungal plant pathogens: looking beyond the two-speed genome model. *Fungal Biology Reviews* **34**(3): 136-143.

Toruño TY, Stergiopoulos I, Coaker G. 2016. Plant-Pathogen Effectors: Cellular Probes Interfering with Plant Defenses in Spatial and Temporal Manners. *Annu Rev Phytopathol* **54**: 419-441.

Tralamazza SM, Gluck-Thaler E, Feurtey A, Croll D. 2024. Copy number variation introduced by a massive mobile element facilitates global thermal adaptation in a fungal wheat pathogen. *Nat Commun* **15**(1): 5728.

Troisi M, Gullino ML, Garibaldi A. 2010. *Gerbera jamesonii*, a New Host of *Fusarium oxysporum* f.sp. *tracheiphilum*. *Journal of Phytopathology* **158**(1): 8-14.

Tung TT, Jakobsen TH, Dao TT, Fuglsang AT, Givskov M, Christensen SB, Nielsen J. 2017. Fusaric acid and analogues as Gram-negative bacterial quorum sensing inhibitors. *Eur J Med Chem* **126**: 1011-1020.

Tzeng TH, Lyngholm LK, Ford CF, Bronson CR. 1992. A restriction fragment length polymorphism map and electrophoretic karyotype of the fungal maize pathogen *Cochliobolus heterostrophus*. *Genetics* **130**(1): 81-96.

van Dam P, Fokkens L, Ayukawa Y, van der Gragt M, Ter Horst A, Brankovics B, Houterman PM, Arie T, Rep M. 2017. A mobile pathogenicity chromosome in *Fusarium oxysporum* for infection of multiple cucurbit species. *Sci Rep* **7**(1): 9042.

van Dam P, Fokkens L, Schmidt SM, Linmans JHJ, Kistler HC, Ma L-J, Rep M. 2016. Effector profiles distinguish *formae speciales* of *Fusarium oxysporum*. *Environmental Microbiology* **18**(11): 4087-4102.

van Dam P, Rep M. 2017. The Distribution of *Miniature Impala* Elements and *SIX* Genes in the *Fusarium* Genus is Suggestive of Horizontal Gene Transfer. *J Mol Evol* **85**(1-2): 14-25.

van der Burgh AM, Joosten MHAJ. 2019. Plant Immunity: Thinking Outside and Inside the Box. *Trends Plant Sci* **24**(7): 587-601.

van der Does HC, Constantin ME, Houterman PM, Takken FLW, Cornelissen BJC, Haring MA, van den Burg HA, Rep M. 2018. *Fusarium oxysporum* colonizes the stem of resistant tomato plants, the extent varying with the R-gene present. *European Journal of Plant Pathology* **154**(1): 55-65.

van der Does HC, Fokkens L, Yang A, Schmidt SM, Langereis L, Lukasiewicz JM, Hughes TR, Rep M. 2016. Transcription Factors Encoded on Core and Accessory Chromosomes of *Fusarium oxysporum* Induce Expression of Effector Genes. *PLoS Genet* **12**(11): e1006401.

van Schie CC, Takken FL. 2014. Susceptibility genes 101: how to be a good host. *Annu Rev Phytopathol* **52**: 551-581.

van Westerhoven AC, Aguilera-Galvez C, Nakasato-Tagami G, Shi-Kunne X, Martinez de la Parte E, Chavarro-Carrero E, Meijer HJG, Feurtey A, Maryani N, Ordóñez N, et al. 2024a. Segmental duplications drive the evolution of accessory regions in a major crop pathogen. *New Phytol* **242**(2): 610-625.

van Westerhoven AC, Dijkstra J, Aznar Palop JL, Wissink K, Bell J, Kema GHJ, Seidl MF. 2024b. Frequent genetic exchanges revealed by a pan-mitogenome graph of a fungal plant pathogen. *mBio* **15**(12): e0275824.

van Westerhoven AC, Meijer HJG, Houdijk J, Martinez de la Parte E, Matabuana EL, Seidl MF, Kema GHJ. 2023. Dissemination of Fusarium Wilt of Banana in Mozambique Caused by *Fusarium odoratissimum* Tropical Race 4. *Plant Dis* **107**(3): 628-632.

van Westerhoven AC, Meijer HJG, Seidl MF, Kema GHJ. 2022. Uncontained spread of Fusarium wilt of banana threatens African food security. *PLoS Pathog* **18**(9): e1010769.

van Zeist W, Palfenier-Vegter RM. 1981. Seeds and fruits from the Swifterbant S3 site. Final reports on Swifterbant IV. *Palaeohistoria*: 105-168.

Vande Zande P, Zhou X, Selmecki A. 2023. The Dynamic Fungal Genome: Polyploidy, Aneuploidy and Copy Number Variation in Response to Stress. *Annu Rev Microbiol* **77**: 341-361.

VanEtten H, Jorgensen S, Enkerli J, Covert SF. 1998. Inducing the loss of conditionally dispensable chromosomes in *Nectria haematococca* during vegetative growth. *Curr Genet* **33**(4): 299-303.

Viljoen A, Ma L-J, Molina AB 2020. CHAPTER 8: Fusarium Wilt (Panama Disease) and Monoculture in Banana Production: Resurgence of a Century-Old Disease. *Emerging Plant Diseases and Global Food Security*: The American Phytopathological Society, 159-184.

Vitale S, Di Pietro A, Turra D. 2019. Autocrine pheromone signalling regulates community behaviour in the fungal pathogen *Fusarium oxysporum*. *Nat Microbiol* **4**(9): 1443-1449.

Vlaardingerbroek I, Beerens B, Rose L, Fokkens L, Cornelissen BJ, Rep M. 2016. Exchange of core chromosomes and horizontal transfer of lineage-specific chromosomes in *Fusarium oxysporum*. *Environ Microbiol* **18**(11): 3702-3713.

Vleeshouwers VG, Oliver RP. 2014. Effectors as tools in disease resistance breeding against biotrophic, hemibiotrophic, and necrotrophic plant pathogens. *Mol Plant Microbe Interact* **27**(3): 196-206.

Vogan AA, Ament-Velasquez SL, Granger-Farbos A, Svedberg J, Bastiaans E, Debets AJ, Coustou V, Yvanne H, Clave C, Saupe SJ, et al. 2019. Combinations of Spok genes create multiple meiotic drivers in *Podospora*. *Elife* **8**.

Vuylsteke DR, Swennen RL, Ortiz R. 1992. Development and performance of balck sigatoka-resistant tetraploid hybrids of plantain (*Musa* spp., AAB group). *Euphytica* **65**(1): 33-42.

Wacker T, Helmstetter N, Wilson D, Fisher MC, Studholme DJ, Farrer RA. 2023. Two-speed genome evolution drives pathogenicity in fungal pathogens of animals. *Proc Natl Acad Sci U S A* **120**(2): e2212633120.

Wallau GL, Ortiz MF, Loreto EL. 2012. Horizontal transposon transfer in eukarya: detection, bias, and perspectives. *Genome Biol Evol* **4**(8): 689-699.

Wang H, Huang R, Ren J, Tang L, Huang S, Chen X, Fan J, Li B, Wang Q, Hsiang T, et al. 2023. The evolution of mini-chromosomes in the fungal genus *Colletotrichum*. *mBio* **14**(4): e0062923.

Wang Q, Cobine PA, Coleman JJ. 2018. Efficient genome editing in *Fusarium oxysporum* based on CRISPR/Cas9 ribonucleoprotein complexes. *Fungal Genet Biol* **117**: 21-29.

Wang T, Xu Y, Zhao Y, Liang X, Liu S, Zhang Y, Kang Z, Chen D, Zheng L. 2023. Systemic screening of *Fusarium oxysporum* candidate effectors reveals FoSSP17 that suppresses plant immunity and contributes to virulence. *Phytopathology Research* **5**(1).

Wang X, Jiang N, Liu J, Liu W, Wang GL. 2014. The role of effectors and host immunity in plant-necrotrophic fungal interactions. *Virulence* **5**(7): 722-732.

Wang Y, Pruitt RN, Nurnberger T, Wang Y. 2022. Evasion of plant immunity by microbial pathogens. *Nat Rev Microbiol* **20**(8): 449-464.

Wang Z, Miao H, Liu J, Xu B, Yao X, Xu C, Zhao S, Fang X, Jia C, Wang J, et al. 2019. *Musa balbisiana* genome reveals subgenome evolution and functional divergence. *Nat Plants* **5**(8): 810-821.

Wang ZF, Rouard M, Droc G, Heslop-Harrison PJS, Ge XJ. 2022. Genome assembly of *Musa beccarii* shows extensive chromosomal rearrangements and genome expansion during evolution of Musaceae genomes. *Gigascience* **12**.

Warman NM, Aitken EAB. 2018. The Movement of *Fusarium oxysporum* f.sp. *cubense* (Sub-Tropical Race 4) in Susceptible Cultivars of Banana. *Front Plant Sci* **9**: 1748.

Warmington RJ, Kay W, Jeffries A, O'Neill P, Farbos A, Moore K, Bebber DP, Studholme DJ. 2019. High-Quality Draft Genome Sequence of the Causal Agent of the Current Panama Disease Epidemic. *Microbiol Resour Announc* **8**(36).

Wei H, Zhong Z, Li Z, Zhang Y, Stukenbrock EH, Tang B, Yang N, Baroncelli R, Peng L, Liu Z, et al. 2024. Loss of the accessory chromosome converts a pathogenic tree-root fungus into a mutualistic endophyte. *Plant Commun* **5**(1): 100672.

Weilguny L, Kofler R. 2019. DeviaTE: Assembly-free analysis and visualization of mobile genetic element composition. *Mol Ecol Resour* **19**(5): 1346-1354.

Wells JN, Feschotte C. 2020. A Field Guide to Eukaryotic Transposable Elements. *Annu Rev Genet* **54**: 539-561.

Wertheimer NB, Stone N, Berman J. 2016. Ploidy dynamics and evolvability in fungi. *Philos Trans R Soc Lond B Biol Sci* **371**(1709).

WHO. 2022. *WHO fungal priority pathogens list to guide research, development and public health action*: World Health Organization.

Widinugraheni S, Nino-Sanchez J, van der Does HC, van Dam P, García-Bastidas FA, Subandiyah S, Meijer HJG, Kistler HC, Kema GHJ, Rep M. 2018. A SIX1 homolog in Fusarium oxysporum f.sp. cubense tropical race 4 contributes to virulence towards Cavendish banana. *PLoS One* **13**(10): e0205896.

Wijnker E, de Jong H. 2008. Managing meiotic recombination in plant breeding. *Trends Plant Sci* **13**(12): 640-646.

Wisecaver JH, Slot JC, Rokas A. 2014. The evolution of fungal metabolic pathways. *PLoS Genet* **10**(12): e1004816.

Witte TE, Villeneuve N, Boddy CN, Overy DP. 2021. Accessory Chromosome-Acquired Secondary Metabolism in Plant Pathogenic Fungi: The Evolution of Biotrophs Into Host-Specific Pathogens. *Front Microbiol* **12**: 664276.

Wittenberg AH, van der Lee TA, Ben M'barek S, Ware SB, Goodwin SB, Kilian A, Visser RG, Kema GH, Schouten HJ. 2009. Meiosis drives extraordinary genome plasticity in the haploid fungal plant pathogen *Mycosphaerella graminicola*. *PLoS One* **4**(6): e5863.

Wu J, Kou Y, Bao J, Li Y, Tang M, Zhu X, Ponaya A, Xiao G, Li J, Li C, et al. 2015. Comparative genomics identifies the *Magnaporthe oryzae* avirulence effector *AvrPi9* that triggers *Pi9*-mediated blast resistance in rice. *New Phytol* **206**(4): 1463-1475.

Wu W, Yang YL, He WM, Rouard M, Li WM, Xu M, Roux N, Ge XJ. 2016. Whole genome sequencing of a banana wild relative *Musa itinerans* provides insights into lineage-specific diversification of the *Musa* genus. *Sci Rep* **6**: 31586.

Xu M, Huang Z, Zhu W, Liu Y, Bai X, Zhang H. 2023. *Fusarium*-Derived Secondary Metabolites with Antimicrobial Effects. *Molecules* **28**(8).

Yan X, Tang B, Ryder LS, MacLean D, Were VM, Eseola AB, Cruz-Mireles N, Ma W, Foster AJ, Oses-Ruiz M, et al. 2023. The transcriptional landscape of plant infection by the rice blast fungus *Magnaporthe oryzae* reveals distinct families of temporally co-regulated and structurally conserved effectors. *Plant Cell* **35**(5): 1360-1385.

Yang F, Teoh F, Tan ASM, Cao Y, Pavelka N, Berman J. 2019. Aneuploidy Enables Cross-Adaptation to Unrelated Drugs. *Mol Biol Evol* **36**(8): 1768-1782.

Yang H, Yu H, Ma LJ. 2020. Accessory Chromosomes in *Fusarium oxysporum*. *Phytopathology* **110**(9): 1488-1496.

Yang Q, Huai B, Lu Y, Cai K, Guo J, Zhu X, Kang Z, Guo J. 2020. A stripe rust effector Pst18363 targets and stabilises TaNUDX23 that promotes stripe rust disease. *New Phytol* **225**(2): 880-895.

Yang Y, Tilman D, Jin Z, Smith P, Barrett CB, Zhu YG, Burney J, D'Odorico P, Fantke P, Fargione J, et al. 2024. Climate change exacerbates the environmental impacts of agriculture. *Science* **385**(6713): eadn3747.

Yu DS, Outram MA, Smith A, McCombe CL, Khambalkar PB, Rima SA, Sun X, Ma L, Ericsson DJ, Jones DA, et al. 2024. The structural repertoire of *Fusarium oxysporum* f. sp. *lycopersici* effectors revealed by experimental and computational studies. *Elife* **12**.

Yu H, Ayhan DH, Martínez-Soto D, Cochavi SM, Ma L-J 2023. Accessory Chromosomes of the *Fusarium oxysporum* Species Complex and Their Contribution to Host Niche Adaptation. In: Scott B, Mesarich C eds. *Plant Relationships: Fungal-Plant Interactions*. Cham: Springer International Publishing, 371-388.

Yu H, Yang H, Haridas S, Hayes RD, Lynch H, Andersen S, Newman M, Li G, Martinez-Soto D, Milo-Cochavi S, et al. 2023. Conservation and Expansion of Transcriptional Factor Repertoire in the *Fusarium oxysporum* Species Complex. *J Fungi (Basel)* **9**(3).

Zaccaron AZ, Stergiopoulos I. 2024. Analysis of five near-complete genome assemblies of the tomato pathogen *Cladosporium fulvum* uncovers additional accessory chromosomes and structural variations induced by transposable elements effecting the loss of avirulence genes. *BMC Biol* **22**(1): 25.

Zadoks JC. 2008. *On the political economy of plant disease epidemics: capita selecta in historical epidemiology*. Wageningen, The Netherlands: Wageningen Academic Publishers.

Zhan J, Thrall PH, Papaïx J, Xie L, Burdon JJ. 2015. Playing on a pathogen's weakness: using evolution to guide sustainable plant disease control strategies. *Annu Rev Phytopathol* **53**: 19-43.

Zhan N, Kuang M, He W, Deng G, Liu S, Li C, Roux N, Dita M, Yi G, Sheng O. 2022. Evaluation of Resistance of Banana Genotypes with AAB Genome to Fusarium Wilt Tropical Race 4 in China. *J Fungi (Basel)* **8**(12).

Zhang J 2022. ClusterGVis: One-step to Cluster and Visualize Gene Expression Matrix.

Zhang M, Xu JH, Liu G, Yao XF, Li PF, Yang XP. 2015. Characterization of the watermelon seedling infection process by *Fusarium oxysporum* f. sp. *niveum*. *Plant Pathology* **64**(5): 1076-1084.

Zhang X, Huang H, Wu B, Xie J, Viljoen A, Wang W, Mostert D, Xie Y, Fu G, Xiang D, et al. 2021. The M35 Metalloprotease Effector FocM35_1 Is Required for Full Virulence of *Fusarium oxysporum* f. sp. *cubense* Tropical Race 4. *Pathogens* **10**(6).

Zhang Y, Liu S, Mostert D, Yu H, Zhuo M, Li G, Zuo C, Haridas S, Webster K, Li M, et al. 2024. Virulence of banana wilt-causing fungal pathogen *Fusarium oxysporum* tropical race 4 is mediated by nitric oxide biosynthesis and accessory genes. *Nat Microbiol*.

Zhang Y, Yang H, Turra D, Zhou S, Ayhan DH, Delulio GA, Guo L, Broz K, Wiederhold N, Coleman JJ, et al. 2020. The genome of opportunistic fungal pathogen *Fusarium oxysporum* carries a unique set of lineage-specific chromosomes. *Commun Biol* **3**(1): 50.

Zhang YD, Ji XB, Zong J, Dai XF, Klosterman SJ, Subbarao KV, Zhang DD, Chen JY. 2024. Functional analysis of the mating type genes in *Verticillium dahliae*. *BMC Biol* **22**(1): 108.

Zhong Z, Marcel TC, Hartmann FE, Ma X, Plissonneau C, Zala M, Ducasse A, Confais J, Compain J, Lapalu N, et al. 2017. A small secreted protein in *Zymoseptoria tritici* is responsible for avirulence on wheat cultivars carrying the Stb6 resistance gene. *New Phytol* **214**(2): 619-631.

Zolan ME. 1995. Chromosome-length polymorphism in fungi. *Microbiol Rev* **59**(4): 686-698.

Zuo C, Deng G, Li B, Huo H, Li C, Hu C, Kuang R, Yang Q, Dong T, Sheng O, et al. 2018. Germplasm screening of *Musa* spp. for resistance to *Fusarium oxysporum* f. sp. *cubense* tropical race 4 (Foc TR4). *European Journal of Plant Pathology* **151**(3): 723-734.

Zuriegat Q, Zheng Y, Liu H, Wang Z, Yun Y. 2021. Current progress on pathogenicity-related transcription factors in *Fusarium oxysporum*. *Mol Plant Pathol* **22**(7): 882-895.

Summary

Plant diseases and pests are a major problem in agriculture and can cause very significant yield losses. Moreover, the problems posed by diseases and pests are expected to worsen with the changing climate, especially for lower income countries and regions. Banana is one of many crops suffering from significant plant diseases. Fusarium wilt of banana (FWB) is a major threat to global banana production and is caused by fungi belonging to the *Fusarium oxysporum* species complex (FOSC). These soilborne fungi infect banana roots and further colonization in susceptible plants causes the characteristic wilting symptoms. The disease can destroy entire plantations and cause havoc across the industry and small subsistence farms alike. In **chapter 1**, I describe the importance of banana as a staple crop and discuss the troubled modern history of banana cultivation. Additionally, I illustrate how the modern history of banana production is intertwined with two major fungal pathogens. Especially the lineage described as *Fusarium* Tropical Race 4 (TR4) is currently causing severe problems for banana growers worldwide, primarily due to a lack of resistance in the predominantly cultivated banana varieties. Moreover, I discuss some of the common shared characteristics in fungal plant pathogens that aid in their rapid adaptation and facilitate their colonization of a host plant. One such characteristic, present in many fungal pathogens, is the compartmentalization of the genome in conserved core regions and more dynamic accessory regions. Accessory genomic regions have likely evolved to facilitate adaptation to changing environments and host interactions. In this thesis project, I studied several aspects of the interaction between banana and its Fusarium wilt pathogens. The aim of this project was to gain further insights into the molecular aspects of this interaction and determine the fungal components that facilitate the infection of the host plant. Further research into the different aspects governing the interaction between banana and the Fusarium wilt pathogens is essential to transform the current fragile banana industry, that largely depends on a few very susceptible banana varieties, into a sustainable agricultural production environment.

One approach to start determining important factors of TR4 that allow it to infect banana plants, is through gene expression analysis. In **chapter 2**, we analyze the expression of all genes of TR4 during growth on media and during banana colonization. The expression data show that many genes are upregulated during host colonization, especially those encoding for secreted proteins or effectors. Two of these genes show a specific structural organization in the genome, similar to synergizing effectors in other plant pathogens. However, the functional analyses of two other genes encoding effectors, with high expression levels, did not affect the pathogenicity of these mutant strains. Analyses of several secreted proteins from TR4

indicate their potential role in microbiome modulation, which is an indirect effect in the Fusarium-banana interaction.

In **chapter 3**, we investigate the variation and function of accessory chromosome 12 in the TR4 lineage. Based on a recent study of a fellow PhD candidate, we hypothesized the presence of sequence length variations for chromosome 12 across this lineage. By generating chromosome 12 loss mutants and the analysis of several wildtype strains, we prove that chromosome 12 underwent several large intrachromosomal duplications in some strains, but not in others. Moreover, we show that chromosome 12 is important for pathogenicity towards banana. Chromosome 12 loss mutants did, however, not lose all their pathogenic capabilities.

Transposable elements can strongly affect the genome of an organism, by disrupting genes or facilitating larger structural changes. In **chapter 4**, we aimed to investigate the role of transposable elements in the TR4 lineage. We showed that in a TR4 strain isolated from Mozambique, a transposable element caused two large-scale deletions. We show that this same transposable element is also active in other strains and that its activity is correlated with other large genomic modifications. As a consequence of these deletions this strain from Mozambique lost a gene cluster for the production of the secondary metabolite fusaric acid. The aforementioned deletions abolished the protection against fusaric acid self-toxicity. However, they did not impact pathogenicity, which shows that this secondary metabolite is not required to infect banana plants. We hypothesize on a fine lined context-dependent role of fusaric acid in the banana-*Fusarium* interaction based on the broader composition of the soil microbiome.

In **chapter 5**, I synthesize an overall assessment of the different aspects and components studied in this thesis project. I describe how my observations relate to prevailing views on the evolution and roles of accessory chromosomes. Additionally, I discuss the impact of transposable element activity in the TR4 lineage. Next, I embed my observations on different virulence factors, proteins or secondary metabolites in an overarching pathosystem and relate this to their functions in other plant pathogens. Lastly, I underscore the importance of further fundamental insights into both the genetics of banana and its pathogens. From there, I develop and explain my view on the needs for banana breeding and how this will contribute to be in par with contemporary breeding practices of other crops.

Acknowledgements

As for any PhD or long-term project it was a journey with its ups and downs, but one for which I am also very grateful. In large part, this journey was much more enjoyable because of all the people involved in one way or another, throughout the entirety of it, or parts.

First and foremost, I would like to express my appreciation to **Gert**. I really appreciate your role as promotor and mentor. Thank you for your time and dedication to the project and the advancement of banana research as a whole. Perhaps most of all I appreciate your willingness to support me in my ideas and provide ample opportunity to broaden my horizons. I also enjoyed our more general discussions on broader scientific or historical topics. Thank you for all of it.

Thank you, **Carolina**, for introducing me to all the basics of working with *Fusarium* and banana in the lab. Your experience formed a great foundation for the rest of the experimental work in my PhD. Thanks also for your mentoring role and all the discussions we had on how to tackle specific questions for the project.

I would also like to thank **Lotje**. I appreciate you stepping in as co-promotor for my PhD and all the suggestions and advice. I would also like to say thanks for the great *Fusarium* research you have performed over the years, which those paying attention will notice is cited at many points throughout my thesis.

Of course I would like to express my thanks to current and former members of the Wageningen **Banana Team** for all the support and discussions on our research. **Giuliana**, thanks for keeping the lab and greenhouse running as smoothly as possible. **Harold, Einar, Sen, Lisanne, Desalegn, Rahim, Diego,** thanks for the help and input on experiments and understanding the struggles of working with banana. Special thanks to **Anouk**, it was great to work together within the same project for our PhDs. Thanks for all your input and contributions, seeing some of our work come together was a very nice experience.

Xiaoqian, thanks for all your help and valuable input on many of the analyses in my thesis. More than that thanks for being a listening ear to some of the general frustrations that come with a PhD project. The dinner evenings at your place were a comfortable respite to the regular working days. **Maikel,** thank you for your great and seemingly always positive and helpful attitude. I really enjoyed sharing the lab together for such a long time. Your long-time experience meant I could often rely on you for questions on all the small things that come along with a PhD. Thanks to the both of you for being my paranymphs.

Thanks to all the MSc students that I supervised and contributed to my PhD trajectory, **Emma, Liz and Sebastien**. At times it probably was as much a learning experience for me as it was for you.

In actuality, my journey in phytopathological research started with a different fungus. **Jan**, I would like to thank you for being my main introduction to research with plant pathogens and the Phytopathology lab in Wageningen specifically. Your enthusiasm for fungal research is inspiring and infectious. Thank you for often posing insightful questions and providing valuable feedback. **Si**, thank you for being the other person to get me acquainted with phytopathological research. My enjoyment during my MSc thesis played a significant factor in my desire to continue for a PhD.

Of course I would like to thank all current and former members of the **Laboratory of Phytopathology**. Being a part of the group made my PhD a much more enjoyable experience. Thanks for all the suggestions, interesting discussions and fun activities. **Michiel,** thank you for your enthusiasm and drive to do something together every once in a while as PhDs, whether it was actually science related, or just to have some drinks, they were welcome distractions from the average day. I would also say the Asilomar fungal genetics conference, my first international conference, that we went to together was one of the highlights of my PhD. **Dian,** I greatly enjoyed being desk neighbors for the last years of my PhD and brainstorming some ideas to explain the often curious results in research. **Suraj,** thank you for our discussions on shared scientific interests. Moreover, my second Asilomar conference with you and Maikel, as well as the days prior that we spent together in San Francisco were a lot of fun. Thanks also to **Frank, Sen and Chris** and others mentioned before for some of the scientific discussions or just general banter along with a drink. You all helped breaking the, at times, monotonous grind of a PhD.

Thanks to my friends and family for their support, although I did not often talk about my research. Disconnecting from work and the general PhD pressures every once in a while was important. **Kelvin, Ruben, Frederike,** bedankt voor de ondertussen al vele jaren aan vriendschap en alle afleiding van de wetenschap en alles eromheen. **Marijke, Esger,** bedankt voor al jullie steun, aanmoediging, interesse. Ik besef me dat ik erg weinig details van mijn onderzoek heb gedeeld, maar dan zien jullie nu toch eindelijk het eindproduct. **Rien,** ik had dit graag nog met je gedeeld. Bedankt dat je in mij het verlangen hebt gewekt om de wereld te leren kennen en te begrijpen. **Mengyu,** thank you for everything, your unconditional support, love and patience. Although perhaps it might have seemed strange to you at times, thank you for trying to understand my interest for fungal research. I look forward to all our future adventures.

Unfortunately, I can not thank everyone individually, but hereby, thanks also to everyone I interacted with at one point or another such as during the (international) conferences. All of these interactions enriched my PhD and opened up to me all the fascinating aspects of biological research.

About the author



Jelmer Dijkstra was born on November 21st, 1996 in Utrecht, the Netherlands. After completing VWO at the Montessori Lyceum Herman Jordan in Zeist, he started his BSc studies Biology at Utrecht University. During his BSc he quickly gained a strong interest for the molecular and microbial world, following courses focused on plant-, cell- and microbiology. After completion of his BSc, Jelmer continued with a MSc program in Plant Science at Wageningen University. In line with the prior acquired interests, he chose for the specialization of phytopathology. After his thesis on the fungal pathogen *Botrytis cinerea* at the Laboratory of Phytopathology, he got the opportunity to continue on a new PhD project at the same laboratory, working with a different fungus, under the supervision of Dr Gert Kema. During his PhD, he focused on several aspects related to virulence and genome dynamics in the causal agents of Fusarium wilt of banana. The results of these studies are described in this thesis.

List of publications

Dijkstra J, van Westerhoven AC, Gómez-Gil L, Aguilera-Galvez C, Nakasato-Tagami G, Garnier SD, Yamazaki M, Arie T, Kamakura T, Arazoe T, et al. 2024. Extensive intrachromosomal duplications in a virulence-associated fungal accessory chromosome. *bioRxiv*: 2024.09.16.611982.

Dijkstra J, van Westerhoven AC, Gómez-Gil L, Aguilera-Galvez C, Nakasato-Tagami G, Garnier SD, Yamazaki M, Arie T, Kamakura T, Arazoe T, et al. The banana wilt pathogen Fusarium Tropical Race 4 carries independent accessory chromosomes. Submitted.

Dijkstra J, van Westerhoven AC, Li Y, Aguilera-Galvez C, Nakasato-Tagami G, Shi-Kunne X, Etalo DW, Kema GHJ. 2025. Transposon activity eliminates a crucial fungal secondary metabolite cluster while preserving pathogenicity. *bioRxiv*: 2025.05.14.653967.

van Westerhoven AC, **Dijkstra J**, Aznar Palop JL, Wissink K, Bell J, Kema GHJ, Seidl MF. 2024b. Frequent genetic exchanges revealed by a pan-mitogenome graph of a fungal plant pathogen. *mBio* 15(12): e0275824.

The research described in this thesis was financially supported by the Bill and Melinda Gates Foundation, grant no.: AG - 4425.

Financial support from Wageningen University for printing this thesis is gratefully acknowledged.

Cover & layout design: Iliana Boshoven-Gkini | Agilecolor.com
Printed: Ridderprint | Ridderprint.nl

